

**GOLD CATALYSIS: DEVELOPMENT OF RELAY CATALYTIC BRANCHING
CASCADES AND CHEMOSENSORS FOR DETECTION OF GOLD IONS**

**A THESIS
SUBMITTED TO AcSIR FOR THE AWARD OF
DEGREE OF
DOCTOR OF PHILOSOPHY
IN CHEMISTRY**



BY

VALMIK S. SHINDE

AcSIR Enrollment No. 10CC11J26135

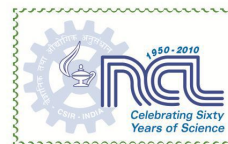
Under the guidance of

Dr. Nitin T. Patil

**ORGANIC CHEMISTRY DIVISION
CSIR-NATIONAL CHEMICAL LABORATORY
PUNE – 411 008, INDIA
OCTOBER – 2014**



राष्ट्रीय रासायनिक प्रयोगशाला
(वैज्ञानिक तथा औद्योगिक अनुसंधान परिषद)
डॉ. होमी भाभा रोड, पुणे - 411 008. भारत
NATIONAL CHEMICAL LABORATORY
(Council of Scientific & Industrial Research)
Dr. Homi Bhabha Road, Pune - 411008. India




THESIS CERTIFICATE

This is to certify that the work incorporated in this Ph.D. thesis entitled “*Gold Catalysis: Development of Relay Catalytic Branching Cascades and Chemosensors for Detection of Gold Ions*” is a bonafide research work, carried out by Mr. **VALMIK S. SHINDE** under my supervision in the Organic Chemistry Division, CSIR–National Chemical Laboratory, Pune for the award of Doctor of Philosophy in Chemical Sciences. The contents of this thesis, in full or in parts, have not been submitted to any other academy, university or institute for the award of any degree or diploma.

Oct 2014
Pune

Dr. NITIN T. PATIL
(Research Supervisor)

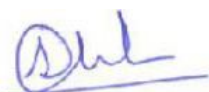
Communications Channels  +91 20 25902000
+91 20 25893300
+91 20 25893400

Fax +91 20 25902601 (Director)
+91 20 25902660 (Admin.)
+91 20 25902639 (Business Development)

URL : www.ncl-india.org

CANDIDATE'S DECLARATION

I hereby declare that the original research work embodied in this thesis entitled, "***Gold Catalysis: Development of Relay Catalytic Branching Cascades and Chemosensors for Detection of Gold Ions***" submitted to Academy of Scientific and Innovative Research for the award of degree of Doctor of Philosophy (Ph.D.) is the outcome of experimental investigations carried out by me under the supervision of **Dr. Nitin T. Patil**, Senior Scientist, Organic Chemistry Division, CSIR–National Chemical Laboratory, Pune. I affirm that the work incorporated is original and has not been submitted to any other academy, university or institute for the award of any degree or diploma.



Mr. VALMIK S. SHINDE
(Research student)
Organic Chemistry Division,
CSIR-National Chemical Laboratory,
Pune 411 008.

October 2014,
Pune.

Acknowledgments

First and foremost, I would like to express my sincere gratitude and thanks to my research advisor **Dr. Nitin T. Patil** for all his guidance, support, enthusiasm, and motivation for my research studies. He is a fantastic mentor who was influential for my interest, and my ability to grasp the essence of organic chemistry. He taught me everything he knows and always encourages me to think creatively and be prepared to learn new things. I am grateful to him for all the ways in which he has prepared me to move forward in my career and life. I truly feel lucky to have been able to be a part of NTP group. I am also indebted to Mrs. Nilima Patil (Madam) and their daughter Neha for their warmth and hospitality. Although I am sad to be leaving, I am looking forward to the future and will enjoy watching the lab develop during the upcoming years.

Over the last five years, I have had the privilege of studying with an extraordinary group of Ph.D. students and project trainees. These individuals have made PhD research truly collaborative and rewarding experience for me and the work described in this thesis would not be possible without all of their efforts. In particular I would like to thank, Dr. Vivek Raut, Dr. Rahul Kavthe, Dr. Ashok Konala, Dr. Vipender Singh, Dr. Anil Mutyala, P. G. V. V. Lakshmi, Rajshekhar Reddy. I also extend my sincere thanks to Dr. Suleman Inamdar, Avinash Bansode, Aslam Shaikh, Amol Gade, Pradip Bagale, Popat Shinde, Somsuvra Banerjee, Manjur Oyasim Akram, Indradweep Chakrabarty, and Prakash Jadhav. A special thank goes to past members Milind Thakare, Dr. Gouri Shankar Aland, Dr. Dhanaji Jawale, Chitra Juneja, Suchand Basuli, Gowri Payasam, N. Jagdeesh, A. Ramesh, Lalit Bade, Jesuraj Ravichandran, Dr. Murali Krishna and Mahesh Thoke for their help and friendship.

I would also like to thank the Doctoral Advisory Committee (DAC) members, Dr. A. Sudalai, Dr. Santosh Mhaske and Dr. Benudhar Punji for accepting to judge my work.

I am grateful to Prof. V. Jayathirtha Rao, (HOD), Dr. V. V. Narayana Reddy and Dr. B. B. Gawali (former HODs) and for their kind help and providing excellent facilities and infrastructure at CSIR-IICT for the research work. I also would like to thank Dr. J. S. Yadav, Dr. Ahmad Kamal, Dr. M. Lakshmi Kantam, Dr. Rajesh Chandra and Dr. G. Sudhakar who have always been encouraging with their kind words and deeds.

I thank to my friends with whom I enjoyed the atmosphere, their friendship, and their support, *viz.* Vikas Gore, Vijay Kale, Sambhaji Godse, Dr. Prasad Wakchaure, Dr. Umesh Kshirsagar, Dr. Rajeev Sawant, Dr. Sanjay Borhade, Dr. Sudhir Arbuj, Pankaj Daramwar, Dr. Aditi Patil, Dr. Arvind Jagannathan, Dr. Swati Kolet, Dr. Prajakta Naik, Dr. Brinda Prasad, Dr. Nilesh Dumare, Santosh Dumbre, Kamlakar Nandre, Vilas Kadam, Dr. Hanmant Gaikwad, Dr. Digambar Shinde, Dr. Nagesh Khupse, Sachin Wadavrao, Ramesh Ghogare, Ganesh Shitre,

Namdeo Ghule, Manjusha Karkhelikar, Ajit Singh, Shruthi Bayya, Janardhan Reddy, Ravi Kiran, Venkat Reddy, Shiva Reddy, Dr. Shivshankar Mane, Dr. Prakash Chavan, Chandrakant Mali, Shruti Vandana K., Nivedita Patil, Atul More, Majid Tamboli, Dr. Deepak Jadhav, Dnyaneshwar Garad, Chinmay Nardele, Dr. Kiran Patil, Rohan Erande, Gorakh Jachak, Dinesh Kalbhor, Kailas Pawar, Dr. Prashant Deore, Sachin Bhojgude, Vijay Koshti, Ramesh Batwal, Satish Malwal, Brijesh Sharma, Kumodini Yadav, Vikas Kamble, Yogesh Pawar, Sonia Verma, Lavanya George, Nikita Parekh Farauk Shaikh, Gangadhar Kamble, Samir Pawar, Dr. Suman Ralhan, Dr. Varma, Dr. G. P. Singh, Dr. Rajesh Vyas, Dr. Rajesh Thaper, Dr. Manoj Prabhavat and Dr. Bipin Nerurkar.

I am also thankful to all my institute's staff members whose names not mentioned here, but have allways been ready to understand my problem and helped me in all possible manners. The assistance rendered by NMR, Mass, IR, X-ray, other analytical divisions, administration and library staff is gratefully acknowledged.

I am highly obliged to my teachers and mentors, who have been a tremendous source of inspiration. The people who helped me achieve my goals and shape my career: Prof. Dhavale, Dr. Waghmode, Prof. Wadia, Prof. Kusurkar, Dr. (Mrs.) Shinde, Aware Sir, Darkunde Sir, Kadam Sir, I thank them for their magnificent teaching and sharing of knowledge.

Completion of doctoral degree would not have been possible without my family and friends supporting me along the way. My parents have always been enthusiastic about my education, even when they didn't understand what exactly I was doing. I am forever grateful to my parents for giving me the freedom to find my own interests and goals and for supporting me with so much love and in so many ways in attaining them. I extend heartiest thanks to my dear wife Snehal for her love and of course an ever-lasting support.

Finally, I dedicate this thesis to the people who mean the most to me, my dear respected parents, grandmother, uncles, aunts, brothers, sisters, relatives and all my well-wishers whose continuous encouragement and support have been a source of inspiration in completion of this task.

Financial assistance from the University Grant Commission (UGC)-New Delhi and CSIR-IICT, Hyderabad and CSIR-NCL in the form of fellowship is gratefully acknowledged.

With many thanks,
Valmik S. Shinde

Note: *Research work presented in this thesis, in part, has been carried out at CSIR-IICT, Hyderabad during June 2009–July 2013. Rest of the research work was carried out at CSIR–National Chemical Laboratory (Organic Chemistry Division), Pune during August–2013 to September–2014.*



***Dedicated to
My Beloved Parents***

Content

List of Abbreviations	i
Instrumentation and General Remarks	iii
Abstract	v
List of Publications	x

Chapter 1: Gold Catalysis: An Overview

1.1	Introduction	2
1.2	Lewis Acidity of Gold - Relativistic Effects	3
1.3	Gold Catalyzed Organic Transformations	4
1.3.1	Addition reactions of Alkynes	4
1.3.1A	Addition of O-H Bond	5
1.3.1B:	Addition of N-H Bond	8
1.3.1C:	Addition of S-H Bond	11
1.3.1D:	Addition of C-H bond	11
1.3.1E:	Addition of X-Y Bond	15
1.3.2	Cycloaddition Reactions	17
1.3.3	Enyne Cycloisomerization	19
1.3.4	Rearrangement of Propargylic Carboxylates	21
1.3.5	Reactivities of Gold Carbenoids	24
1.3.6	Oxidative Cross-coupling Reactions	26
1.3.7	C-H Functionalization Reactions	27
1.3.8	Application in Total Synthesis	29
1.4	Conclusion	35
1.5	References	36

Chapter 2: Relay Catalytic Branching Cascade: A Technique to Access Diverse Molecular Scaffolds

2.1	Introduction	42
2.2	Hypothesis	46
	One Pot Catalysis: A Strategic Classification	47
2.3	Results and Discussion	49
2.3.1	Substrate Scope	49
2.3.2	Mechanistic Studies	53
2.4	Polyheterocyclic Scaffolds Accessed Through RCBC–Literature Known Synthesis and Their Applications	54
2.5	Conclusion	62
2.6	Experimental Procedures and Characterization Data	63
2.7	Spectra	95
2.8	References	119

Chapter 3: Enantioselective Relay Catalytic Branching Cascade: The Importance of Merging Gold(I) with Chiral Brønsted Acid Catalysis

3.1	Introduction	124
3.2	Hypothesis	133
3.3	Results and Discussion	134
3.3.1	Optimization of Reaction Conditions	134
3.3.2	Scope and Generality Studies	138
3.3.3	Control Experiments	143
3.4	Computational Studies	144
3.5	Conclusion	146
3.6	Experimental Procedures	146
3.7	Characterization Data of Starting Materials and Products	150
3.8	¹ H NMR and ¹³ C NMR Spectra	175
3.9	HPLC Chromatograms	191
3.10	References	203

**Chapter 4: Development of Highly Selective Fluorescent Probe
(Chemosensor) for Detection of Gold Ions**

4.1	Introduction	207
4.2	Hypothesis	213
4.3	Results and Discussion	214
4.3.1	Studies of UV-Visible Absorption Changes	216
4.3.2	Studies of Fluorescence Spectrophotometric Changes	217
4.3.2	Studies of Specificity and Selectivity of Probe	219
4.4	Bioimaging Studies Using A549 Lung Cancer Cells	221
4.5	Conclusion	223
4.6	Experimental Procedures and Characterization Data	223
4.7	Spectra	229
4.8	References	232

List of Abbreviations

Units:

°C	Degree centigrade
mg	Milligram
hr	Hour
Hz	Hertz
mL	Millilitre
MHz	Megahertz
mmol	Millimol
nm	nanometre
ppm	Parts per million

Chemical Groups:

Aq.	Aqueous
Ac	Acetyl
Bn	Benzyl
Bu	Butyl
CDCl ₃	Deuterated chloroform
DCE	1, 2-Dichloroethane
DCM	Dichloromethane
DME	1, 2-Dimethoxyethane
DMF	Dimethylformamide
DMSO- <i>d</i> ₆	Deuterated dimethyl sulphoxide
Et	Ethyl
BH	Brønsted acid
Me	Methyl
Tf	Trifluoromethanesulfonyl
Ph	Phenyl
<i>p</i> -TSA	<i>p</i> -Toluensulphonic acid
THF	Tetrahydrofuran
TMS	Trimethylsilyl

Other Notations:

Cat	Catalytic
calcd	Calculated
d	Doublet
δ	Chemical shift
Eq.	Equation
equiv	Equivalent
e.g.	<u>exempli grātiā</u>
HRMS	High resolution mass spectrometry
HEPES	4-(2-hydroxyethyl)-1-piperazineethanesulfonic acid
IR	Infrared
J	Coupling constant in NMR
m.p.	Melting point
MS	Mass spectrometry
M.S.	Molecular sieves
M.W.	Molecular weight
MW	Microwave
NMR	Nuclear magnetic resonance
%	Percentage
PBS	Phosphate –buffered saline
rt	Room temperature
TLC	Thin layer chromatography

Instrumentation and General Remarks

Thin Layer Chromatography (TLC)

TLC was performed on pre-coated silica gel plates. After elution, plate was visualized under UV illumination at 254 nm for UV active materials. Further visualization was achieved by staining KMnO_4 and charring on a hot plate.

Column Chromatography

Column chromatography was performed using silica gel (100-200 and/or 200-400 mesh) and neutral aluminum oxide. The solvents used for column chromatography were distilled prior to use.

IR Spectroscopy

Infrared spectra were recorded on Perkin-Elmer infrared spectrophotometer. Spectra were calibrated against the polystyrene absorption at 1610 cm^{-1} . Samples were scanned either in KBr or in thin film.

NMR Spectroscopy

^1H and ^{13}C NMR spectra were recorded on Bruker AV, 200/300/400/500, JEOL 400 MHz, and INOVA 500 MHz spectrometers in appropriate solvents using TMS as internal standard or the solvent signals as secondary standards and the chemical shifts are shown in δ scales. Multiplicities of NMR signals are designated as s (singlet), d (doublet), t (triplet), q (quartet), br (broad), m (multiplet, for unresolved lines) etc.

Mass Spectrometry

High resolution mass spectra were obtained by using ESI-QTOF mass spectrometry. The measurements were performed in EtOAc, MeOH, and Acetonitrile solvents.

Polarimeter

Optical rotation measured with a JASCO P 2000 digital polarimeter at rt using 50 mm cell of 1 mL capacity.

High Performance Liquid Chromatography (HPLC)

HPLC analysis was performed on SHIMADZU HPLC system, Class-VP V6.12 SP5 with UV detector. The compounds were separated on various columns such as Chiralcel OJ-H,

Chiralcel OD-H, Kromacil-5 Amycoat, CHIRALPAK IF. The HPLC grade solvents were purchased from MERCK and used as received.

General Remarks:

Unless otherwise specified, all reactions were carried out in oven dried vials or reaction vessels with magnetic stirring under argon atmosphere. Dried solvents and liquid reagents were transferred by oven-dried syringes or hypodermic syringe cooled to ambient temperature in a desiccators. All experiments were monitored by analytical thin layer chromatography (TLC). TLC was performed on pre-coated silica gel plates. After elution, plate was visualized under UV illumination at 254 nm for UV active materials. Further visualization was achieved by staining KMnO_4 and charring on a hot plate. Combined organic layers after extraction were dried over anhydrous sodium sulfate. Solvents were removed in vacuo and heated with a water bath at 35-45 °C. Silica gel finer than 100-200 or 200-400 mesh was used for flash column chromatography. Columns were packed as slurry of silica gel in hexane or petroleum ether and equilibrated with the appropriate solvent mixture prior to use. The compounds were loaded neat or as a concentrated solution using the appropriate solvent system. The elution was assisted by applying pressure with an air pump.

The compounds, schemes and reference numbers given in each chapter refers to that particular chapter only.

Abstract

Thesis Title: “Gold Catalysis: Development of Relay Catalytic Branching Cascades and Chemosensors for Detection of Gold Ions”

The present thesis deals with the development of relay catalytic branching cascades in diversity oriented synthesis and design of chemosensors for the detection of Au-ions. The work presented herein delineates the importance of carbophilic activation chemistry in diversity oriented synthesis and sensing of metal ions. The work also describes the importance of Au(I)/chiral Brønsted acid binary catalytic systems to enable an enantioselective transformation in one-pot that cannot be achieved by gold catalysts alone.

Chapter 1: Gold Catalysis: An Overview

The homogeneous gold catalysis is a fascinating field of chemistry that underwent a tremendous development in the last years, a true "golden era". This chapter is intended to give a brief overview of this exceptional subject and to identify some of the most important applications of homogeneous gold catalysts in organic synthesis.

A great number of novel transformations have appeared during the last decade based on the gold-catalyzed activation of C-C multiple bonds. Generally, this type of activation relies on interaction of the metal catalyst with the C-C multiple bonds. This superior activity of gold complexes compared to other transition metals could be due to maximum relativistic effects exhibited by them. A historical retrospect on the progress in this area reveals that gold chemistry is based on: 1) addition reactions, 2) substitution reactions, 3) rearrangement reactions, 4) C-H functionalization reaction, 5) cross-coupling reactions...etc. In recent years, a number of reports appeared on the back bonding of Au-complexes leading to the formation of highly reactive gold carbenoid species which can exhibit a plethora of reactivities. The application of gold chemistry has also been found in the total syntheses of architecturally challenging natural products. Many of the above reactivities have been reviewed in the literature. This chapter gives a brief overview of this enticing subject and identifies some of the most important aspects of homogeneous gold catalysis in organic synthesis. While it is beyond the scope of this chapter to comprehensively describe the literature, we have endeavored to describe very selected examples on each category with appropriate citations.

Chapter 2: Relay Catalytic Branching Cascade: A Technique to Access Diverse Molecular Scaffolds

This chapter describes the design and development relay catalytic branching cascade as a new technique in "Diversity Oriented Synthesis" to access a series of multifunctional polyheterocyclic scaffolds in an efficient manner.

Diversity Oriented Synthesis (DOS) is considered as one of the techniques for identifying the biologically relevant chemical space. In recent years, branching cascade technique has been proposed as a new form of DOS. The technique is very promising due to its ability to transform a common type of starting material into diverse and distinct molecular frameworks under the influence of either reagents or conditions. Although there exists quite a few reports on branching cascades, there were no reports on a catalytic branching cascade that generates large scaffold diversity. Scaffold diversity is very important in DOS, because it is used to populate chemical space efficiently. Therefore, we wondered whether it would be possible to develop a catalytic branching-cascade technique - a process that would allow the rapid synthesis of several multifunctional polyheterocyclic scaffolds.

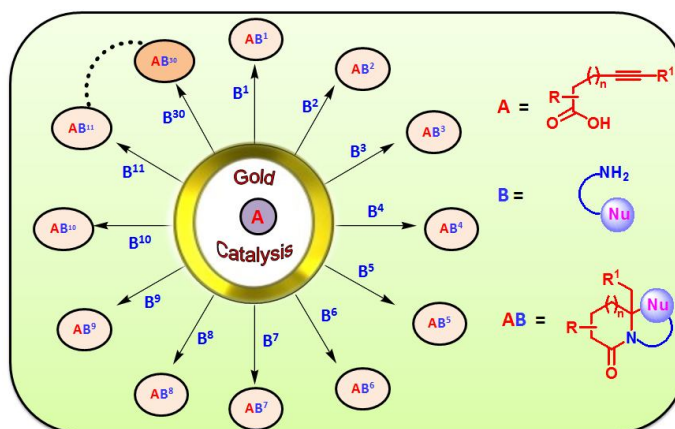


Figure 1: Concept of relay catalytic branching cascade.

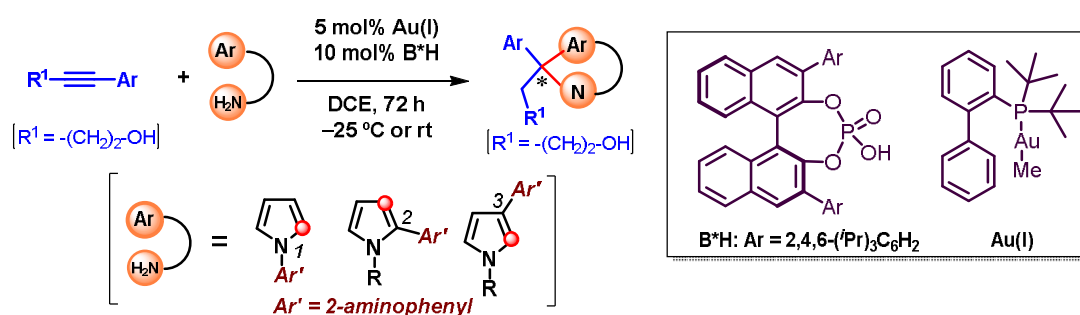
In this chapter, the development of relay catalytic branching cascade has been described. The reaction of alkynoic acid **A** (common type of substrate) with several scaffold-building agents **B** (SBAs; variables) in the presence of gold catalyst leads to the formation of various heterocyclic scaffolds **AB** (Fig 1). The method worked well over a range of 30 SBAs and provided an access to series of multifunctional polyheterocyclic scaffolds in an efficient manner. The key feature of this approach is its extraordinary scope, because it allows the preparation of a library of compounds with a high skeletal diversity and a broad scope for

further diversification. The great importance of the technique and the utility of scaffolds accessed through this chemistry is highlighted in this chapter.

Chapter 3: Enantioselective Relay Catalytic Branching Cascade: The Importance of Merging Gold(I) with Chiral Brønsted Acid Catalysis

This chapter describes the efforts in the realization of enantioselective relay catalytic branching cascade for accessing enantiopure aza-heterocyclic scaffolds utilizing gold(I) with chiral Brønsted acid binary catalytic system.

In continuation of the work presented in chapter 2, it is envisaged that the common type of substrate might react with various scaffold-building agents in the presence of appropriate chiral catalyst leading to the formation of various heterocyclic scaffolds in enantio-pure form. The technique could be referred as enantioselective relay catalytic branching cascade and suppose to be valuable as one can access the library of enantiopure scaffolds efficiently. In order to validate this hypothesis, the investigation was focused on the enantioselective hydroamination/hydroarylation of Alkynes - the racemic version of the reaction which has already been reported by our group.



Scheme 2: Concept of enantioselective relay catalytic branching cascade.

In this chapter, our successful efforts on the development of enantioselective relay catalytic branching cascade has been described. The reaction of alkynols with pyrrole-based SBAs in the presence of $(R_3P)\text{-Au-Me}$ and $(S)\text{-TRIP}$ binary catalytic system afforded pyrrole containing aza-heterocyclic scaffolds bearing quaternary carbon center. It was discovered that the $-OH$ group in the alkyne tether is essential to obtain the products in high yields and enantioselectivities. The scope and limitation of the reaction and the role of tethered hydroxyl group in the alkynes has been investigated with experiments and DFT calculations.

Chapter 4: Development of Highly Selective Fluorescent Probe (Chemosensor) for Detection of Gold Ions

The chapter documents the design and development of new approach; namely, "anchoring-unanchoring of fluorophores" for the selective detection gold ions.

Though gold in elemental form is inert, its salt exhibits some biological effects. For instance, gold ions have anti-inflammatory properties and are used as pharmaceuticals in the treatment of anticancer, arthritis and tuberculosis. In addition, it is well established that gold ions are known as inhibitors of macrophages and polymorphonuclear leucocytes. However, gold species may tightly bind to biomolecules such as enzymes and DNA, leading to toxicity to humans. Similarly, certain gold salts such as gold chloride are known to cause damage to the liver, kidneys, and the peripheral nervous system. Therefore, it is essential to develop a chemosensor to monitor the presence of gold species both in the environment and under physiological conditions. Literature reports revealed that the development of chemosensor for the detection of gold is based on two approaches. The first one is the complexation based approach wherein the nonfluorescent probe, containing a fluorophore and a gold ion receptor, binds with Au ions triggering change in the fluorescence intensity (Fig 2A). Another approach involves a nonfluorescent probe consisting of a fluorophore and organic molecule which on reaction with gold species generates new structure resulting in a change in the fluorescence intensity (functional group manipulation approach, Fig 2B).

A rational design of the chemosensors, their synthesis and their performance on the sensing of gold ions has been discussed in this chapter. The technique involves the anchoring-unanchoring of the fluorophore (Fig 2C). It can be judged from Figure 1C, the fluorescence of fluorophore is turned off by anchoring with organic substrate. Once the gold ions have been sensed, the probe would liberate highly fluorescent fluorophore with formation of organic product (Fig 3). The fluorescent probe was found to be highly selective for sensing gold species in the presence of several other metal ions. A successful application to bioimaging has also been demonstrated with A549 lung cancer cells.

Figure 2: Approaches for detection of gold ions (literature and work presented in chapter 4).

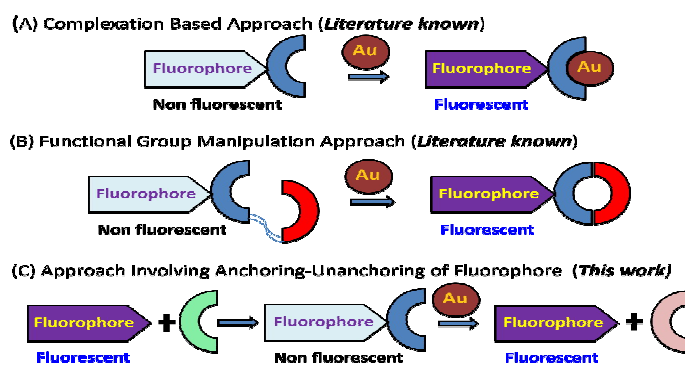
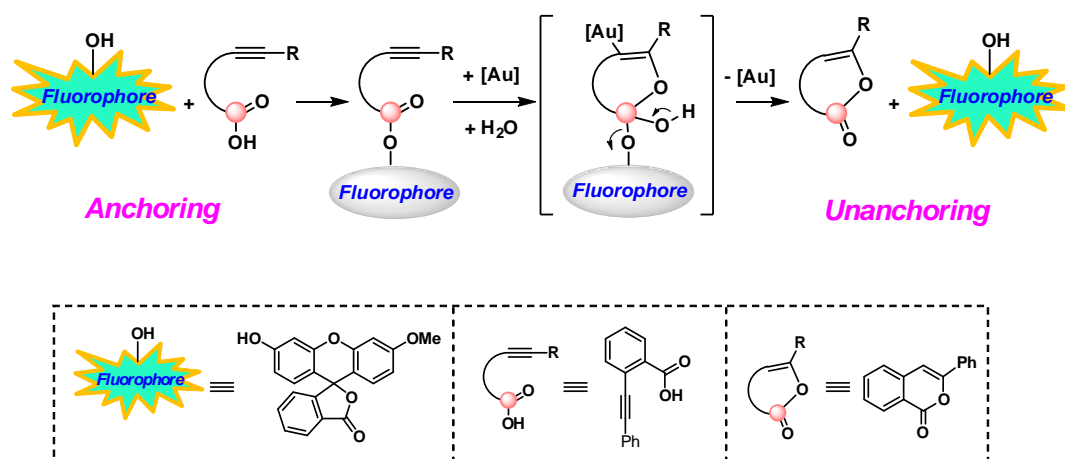


Figure 3: Chemosensor for gold ions - A concept based on π -activation.



List of Publications

1. Robustness Screen in Enantioselective Catalysis Enabled Generation of Enantioenriched Heterocyclic Scaffolds in One Pot
Pradip N. Bagle, **Valmik S. Shinde**, Nitin T. Patil *Chem. Eur. J.* **2015**, *21*, (accepted article) DOI: 10.1002/chem.201406045.
2. Au(I)/Bronsted acid Catalyzed Asymmetric Hydroamination-Hydroarylation of Alkynes: Effect of Remote Hydroxyl Group in the Reactivity and Enantioselectivity.
Valmik S. Shinde, Manoj V. Mane, Kumar Vanka, Arijit Mallick, Nitin T. Patil *Chem. Eur. J.* **2015**, *21*, 975 – 979.
3. Relay Catalytic Branching Cascade: A Technique to Access Diverse Molecular Scaffolds.
Nitin T. Patil, **Valmik S. Shinde**, B. Sridhar *Angew. Chem. Int. Ed.* **2013**, *52*, 2251–2255. (Selected as “Hot paper”)
4. Exploiting the higher alkynophilicity of Au-species: development of a highly selective fluorescent probe for gold ions.
Nitin T. Patil, **Valmik S. Shinde**, Milind S. Thakare, P. Hemant Kumar, Prakriti R. Bangal, Ayan K. Barui, Chitta R. Patra *Chem. Commun.* **2012**, *48*, 11229–11231.
5. Gold(I)-Catalyzed Unprecedented Rearrangement Reaction Between 2-Aminobenzaldehydes with Propargyl Amines: An Expedient Route to 3-Aminoquinolines.
Nitin T. Patil, Vivek S. Raut, **Valmik S. Shinde**, Gaddamanugu Gayatri, G. Narahari Sastry *Chem. Eur. J.* **2012**, *18*, 5530–5535.
6. Pt(IV)-Catalyzed Hydroamination Triggered Cyclization: A Strategy to Fused Pyrrolo[1,2-a]quinoxalines, Indolo[1,2-a]quinoxalines, and Indolo[3,2-c]quinolines.
Nitin T. Patil, Rahul D. Kavthe, **Valmik S. Shinde**, Balasubramanian Sridhar *J. Org. Chem.* **2010**, *75*, 3371–3380.

7. Gold- and Platinum-Catalyzed Formal Markownikoff's Double Hydroamination of Alkynes: A Rapid Access to Tetrahydroquinazolinones and Angularly-Fused Analogues Thereof.

Nitin T. Patil, Rahul D. Kavthe, Vivek S. Raut, **Valmik S. Shinde**, Balasubramanian Sridhar *J. Org. Chem.* **2010**, *75*, 1277–1280.

Reviews

1. A one-pot catalysis: the strategic classification with some recent examples.
Nitin T. Patil, **Valmik S. Shinde**, Balakrishna Gajula *Org. Biomol. Chem.* **2012**, *10*, 211–224. (Selected as “Hot paper” and “top ten accessed” in November 2011)
2. Transition metal-catalyzed addition of C-, N- and O-nucleophiles to unactivated C–C multiple bonds.
Nitin T. Patil, Rahul D. Kavthe, **Valmik S. Shinde** *Tetrahedron* **2012**, *68*, 8079–8146.

Table of Contents

1.1	Introduction.....	2
1.2	Lewis Acidity of Gold - Relativistic Effects	3
1.3	Gold Catalyzed Organic Transformations	4
1.3.1	Addition reactions of Alkynes	4
1.3.1A:	Addition of O-H Bond	5
1.3.1B:	Addition of N-H Bond	8
1.3.1C:	Addition of S-H Bond.....	11
1.3.1D:	Addition of C-H bond.....	11
1.3.1E:	Addition of X-Y Bond	15
1.3.2	Cycloaddition Reactions	17
1.3.3	Enyne Cycloisomerization.....	19
1.3.4	Rearrangement of Propargylic Carboxylates.....	21
1.3.5	Reactivities of Gold Carbenoids.....	24
1.3.6	Oxidative Cross-coupling Reactions.....	26
1.3.7	C-H Functionalization Reactions	27
1.3.8	Application in Total Synthesis	29
1.4	Conclusion	35
1.5	References.....	36

1.1 Introduction

Gold has been present in the collective conscience of mankind since the beginning of known history. It always exerted a deep fascination, being associated with beauty, wealth and authority probably due to its collective and unique properties such as high density, softness, malleability, ductility and most aesthetically pleasing property such as glittery. Gold in free elemental form does not get oxidized by air or water as evident by its occurrence as nuggets or grains in rocks, in veins and in alluvial deposits.¹ Such high stability of gold in the nature might have created the misconceptions amongst the scientific community that the metal is extremely inert and therefore its salts could not be used as catalysts for organic reactions. This could be the reason why gold has lived in the shadow of other metals for a long time.

In the beginning of the 1970's several examples in the area of heterogeneous catalysis have appeared.² Some of the great examples of industrial importance include hydrochlorination of ethyne to vinyl chloride³ and the low temperature oxidation of CO to CO₂.⁴ Similarly, gold nano particles played an important role in the development of this discipline.⁵ Homogeneous gold catalysis have several advantages over the heterogeneous catalysis in terms of many aspects such as yields, enantioselectivity, much better substrate tolerance and most importantly the use of low temperature and pressure which makes reaction to be conducted under mild conditions. The main benefit of the homogeneous gold catalysis is that the specific modification of the catalyst structure may influence the reaction paths in a controlled and predictable manner. In recent years, homogeneous gold catalysis has attracted much attention and a lot of powerful new reaction cascades for the rapid construction of molecular complexity, starting from simple key precursors, have been explored.⁶ An early example of enantioselective gold catalyzed reaction is the Aldol reaction of isocyano acetates/amides with aldehydes.⁷ In fact, this is one of the rarest phenomenons in organic chemistry; wherein the enantioselective reaction was discovered first before the discovery of relatively simple reactions took place.

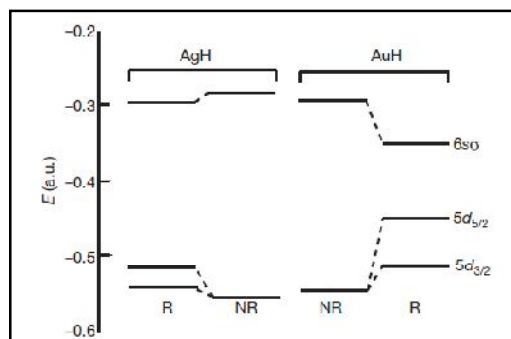
A great number of novel transformations have appeared during the last decade based on the gold-catalyzed activation of C-C multiple bonds. Generally, this type of activation relies on interaction of the metal catalyst with the C-C multiple bonds. This superior activity of gold complexes compared to other transition metals could be due to maximum relativistic effects (vide infra) exhibited by them. A historical retrospect on the progress in this area reveals that gold chemistry is based on: 1) addition reactions, 2) substitution reactions, 3) rearrangement

reactions, 4) C-H functionalization reaction, 5) cross-coupling reactions...etc. In recent years, a number of reports appeared on the back bonding of Au-complexes leading to the formation of highly reactive gold carbenoid species which can exhibit a plethora of reactivities. The application of gold chemistry has also been found in the total syntheses of architecturally challenging natural products. Many of the above reactivities have been reviewed in the literature.⁸ This chapter gives a brief overview of this enticing subject and identifies some of the most important aspects of homogeneous gold catalysis in organic synthesis.

1.2 Lewis Acidity of Gold - Relativistic Effects

Gold has an electronic configuration of $[\text{Xe}] 4f^{14} 5d^{10} 6s^1 6p^0$. The oxidation states of gold range from -1 to $+5$, but Au(I) and Au(III) complexes dominate the chemistry. These cationic gold complexes are exceptionally potent and superior Lewis acids that have a high affinity for π bonds of alkenes, alkynes and allenes. The unusual catalytic properties and reactivity of gold catalysts can be rationalized in terms of relativistic effects.⁹ The strong relativistic contractions of the $6s$ and $6p$ orbitals (LUMO) makes the electrons closer to the nucleus.¹⁰ This contraction explains the increased ionization energy of Au when compared to other group 11 elements, Cu and Ag, or Pt (group 10) (Figure 1.1), this ultimately accounts for a greater Lewis acidity of Au(I) cationic complexes. This conclusion also correlates with the strong electronegativity of gold (2.4 for Au, compared to Ag 1.9). Thus relativistic effects can also explain the expansion of d and f orbitals, being electrons occupying the outer orbitals of $5d$ and $4f$ orbitals (HOMO) are better shielded by the electrons in the contracted s and p orbitals. Hence there will be a weaker nuclear attraction for $5d$ and $4f$ orbitals, which results in the soft Lewis acidic nature of gold(I) species reacting preferentially with "soft" species (such as π -systems) and being less oxophilic. Thus relativistic effects are particularly helpful in explaining the reactivity and reactive pathways of the gold.

Figure 1.1: The relativistic (R) and nonrelativistic (NR) orbital energies of [AgH] and [AuH] molecules (*figure is taken from reference 10b*)



1.3 Gold Catalyzed Organic Transformations

This part describes a selection of most representative examples which show the diversity of the gold catalyzed homogenous transformations utilizing alkynes as starting materials. While it is beyond the scope of this chapter to comprehensively describe the literature, we have endeavoured to describe only selected examples on each category with appropriate citations. This categorization has been done on the basis of types of reactions and mechanism involved therein.

1.3.1 Addition reactions of Alkynes

The addition of X–H (X = O, N, C) bonds to C–C multiple bonds represents one of the most important fundamental reactions in gold catalysis, which features diverse functional group tolerance and the easy formation of carbon–carbon and carbon–heteroatom bonds.¹¹ Furthermore, the rapid growing area of tandem reactions has allowed chemists to assemble diverse complex molecular frameworks more conveniently. Alkynes are more reactive than allenes or alkenes when activated by a gold catalyst, and have thus been the most studied of the three. One of the early reactions in this rapidly developing field was the gold-catalyzed addition of water and alcohols to alkynes, a reaction previously dominated by mercury(II) and strongly acidic conditions or, direct nucleophilic addition of alcohols to alkynes under strongly basic conditions.¹² This reaction not only showed the benefits of gold catalysis, it has also guided the

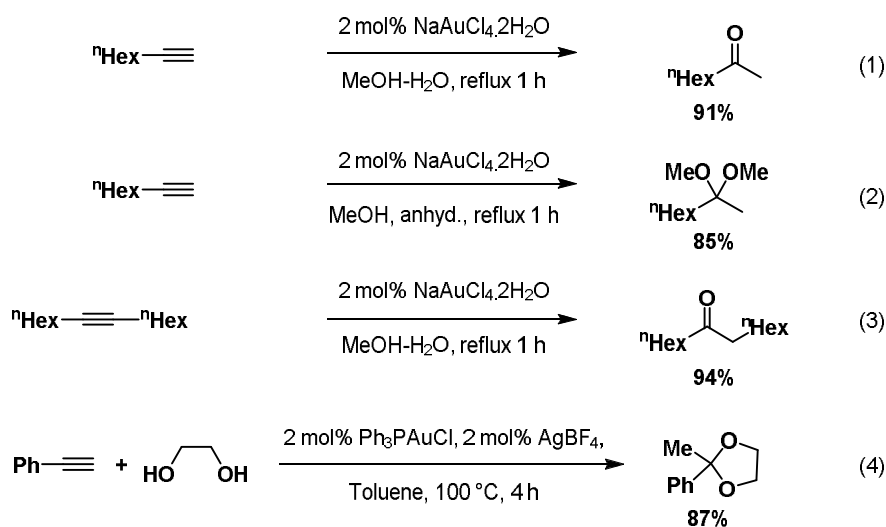
selection of the reaction types to be covered in this section, namely the addition of an X–H bond to a C–C multiple bond, with X being an electronegative heteroatom.

1.3.1A: Addition of O–H Bond

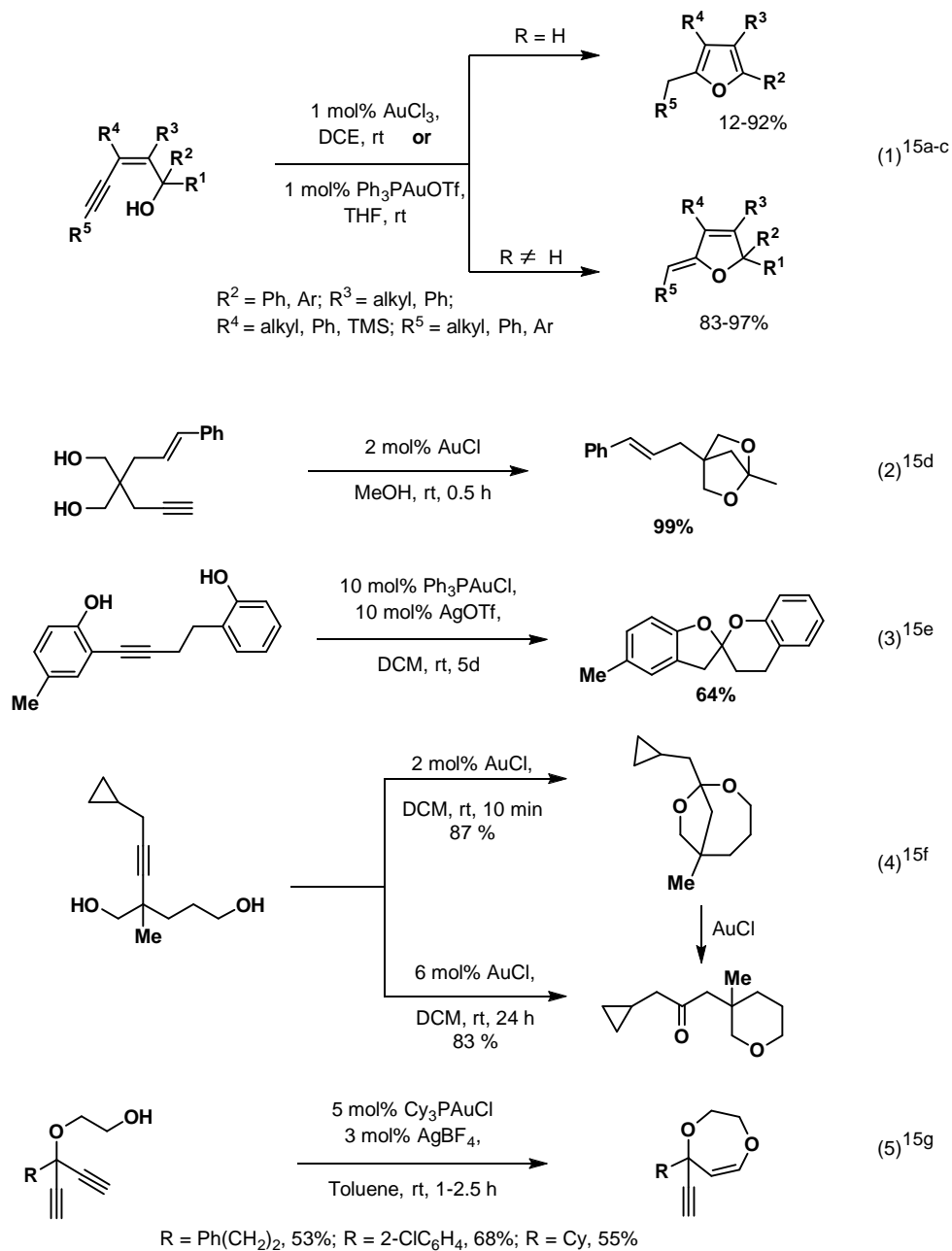
The pioneering work by Utimoto and co-workers observed a Markovnikov addition to the alkyne: with terminal alkynes, water delivered methyl ketones while methanol gave ketals (Scheme 1.1, Eq. 1, 2 and 3).¹³ The regioselectivity in the case of internal alkynes was found to be poor, and, therefore, symmetrical alkynes had to be employed to obtain a single adduct. When ethylene glycol reacted with phenylacetylene, the cyclic ketals are formed. (Scheme 1.1, Eq. 4).¹⁴

Apart from the intermolecular reaction, intramolecular examples have been reported. The alkyne functionality could be transformed to various functional groups including ketones, acetals, enol ethers and spiroketals. The mild conditions involved make these reactions attractive alternatives over the use of organolanthanides, alkali metals, or inherently less tolerant transition metals. Low catalyst loadings (0.5–1 mol%) usually suffice to obtain nearly quantitative yields which has been reported in numerous cases. In contrast to most other catalysts used for similar purposes, no external base is necessary to promote the reaction. The representative examples of gold catalyzed intramolecular hydroalkoxylation reactions are listed in Scheme 1.2.¹⁵

Scheme 1.1: Gold-catalyzed intermolecular hydration/hydroalkoxylation of alkynes



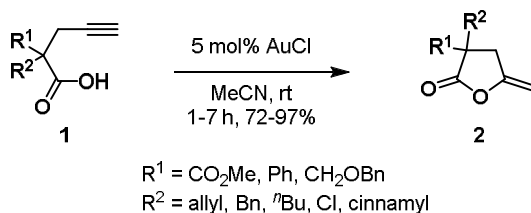
Scheme 1.2: Gold-catalyzed intramolecular hydroalkoxylation and double hydroalkoxylation of alkynes



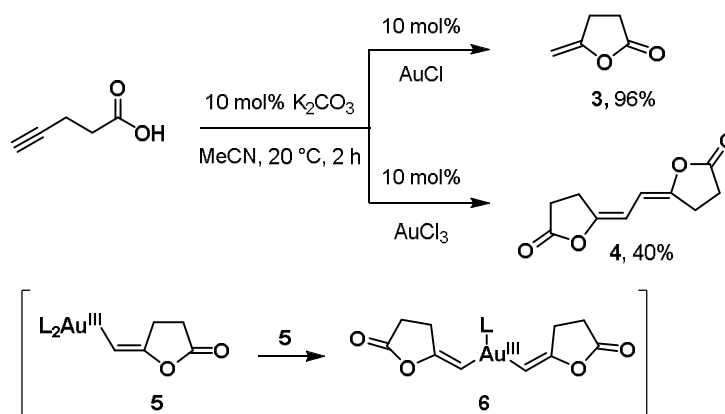
The addition of -COOH across alkyne is known as hydrocarboxylation. The alkynylsubstituted acids **1** were efficiently cyclized to the corresponding lactones **2** with 5 mol% AuCl in acetonitrile at rt (Scheme 1.3).¹⁶ A Thorpe-Ingold effect in the hydrocarboxylation of alkynes catalyzed by AuCl was observed. A striking dimerization reaction was observed while

examining the reactivity of 4-pentynoic acid with Au-catalysts by Pale and coworkers.¹⁷ Generally, AuCl₃ led to a higher selectivity for the lactone dimerization product **4** (cf. **5** and **6**), while the use of AuCl provided larger quantities of the expected lactone **3** (Scheme 1.4).

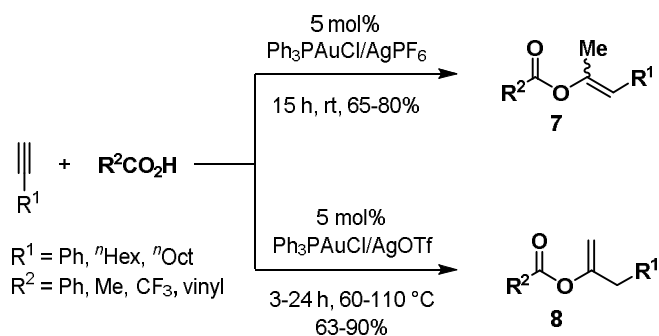
Scheme 1.3: Gold-catalyzed intramolecular hydrocarboxylation of alkynes



Scheme 1.4: Au(I)/Au(II)-catalyzed intramolecular hydrocarboxylation of 4-pentynoic acid

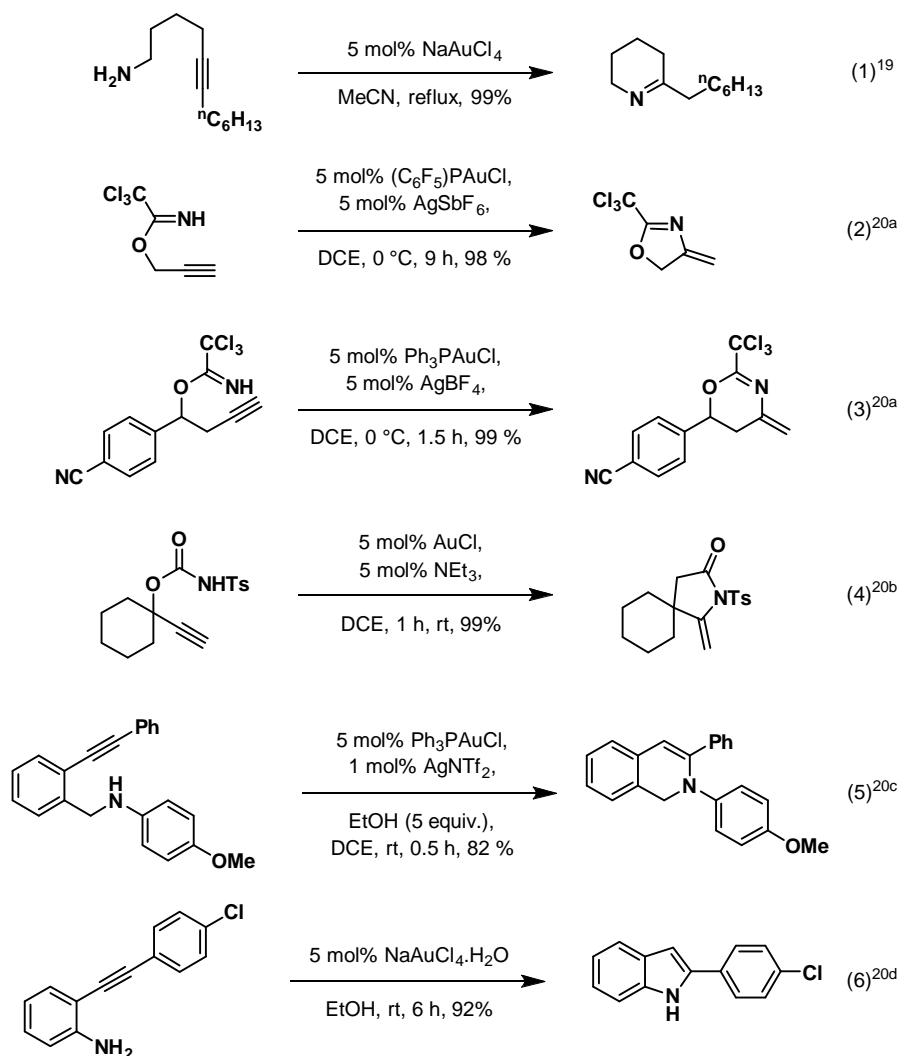
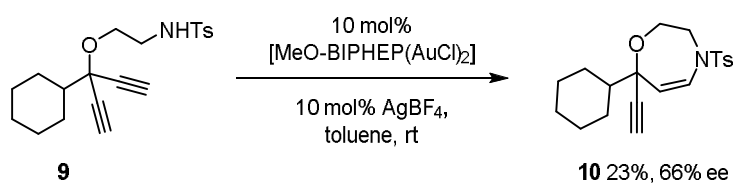


Au(I)-catalyzed intermolecular addition of carboxylic acids to alkynes led to the formation of enol esters. For instance, the Ph₃PAuCl/AgPF₆ catalyst afforded the Markovnikov addition products **7**, whereas Ph₃PAuCl/AgOTf gave the more stable isomerized anti-Markovnikov addition products **8** (Scheme 1.5).¹⁸

Scheme 1.5: Au(I)-catalyzed intermolecular hydrocarboxylation of alkynes**1.3.1B: Addition of N-H Bond**

Fukuda and Utimoto reported one of the first examples of gold catalyzed intramolecular N-H addition to alkynes (Scheme 1.6, Eq. 1).¹⁹ Because of the high functional-group tolerance observed in gold catalysis, oxygen and moisture do not have to be excluded from the reaction medium, especially in Au(I) catalysis. Selective intramolecular monohydroamination is observed in a number of cases, in which the initially formed enamine cannot isomerize to the corresponding imine. Imidates, carbamates, secondary amines, and even primary amines exhibited this reactivity pattern and gave rise to a number of useful heterocyclic enamines (Scheme 1.6, Eq. 2-6).²⁰

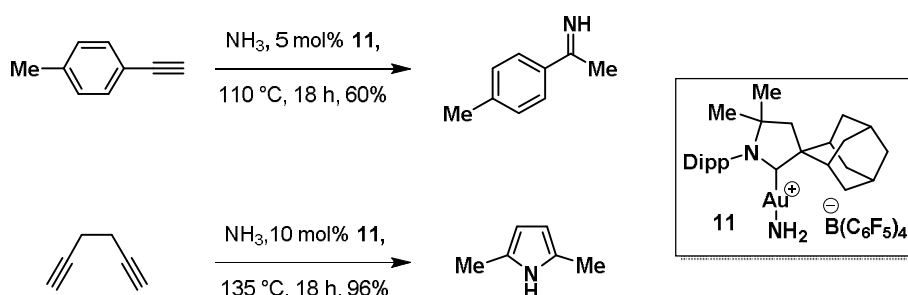
In 2012, Czekelius and coworkers reported an entirely different approach based on the desymmetrization triggered by hydroamination reaction. When 1,4-diyamide **9** was treated with chiral gold-catalyst, tetrahydrooxazepines derivative **10** was obtained in only 23% yield with 66% ee (Scheme 1.7).²¹ In order to improve reactions efficiency, the same authors explored the potential application of gold complexes bearing chiral phosphate counterion for desymmetrization of diyanamides.²²

Scheme 1.6: Au-catalyzed intramolecular hydroamination of alkynes**Scheme 1.7:** Au-catalyzed enantioselective intramolecular hydroamination of 1,4-diynamide

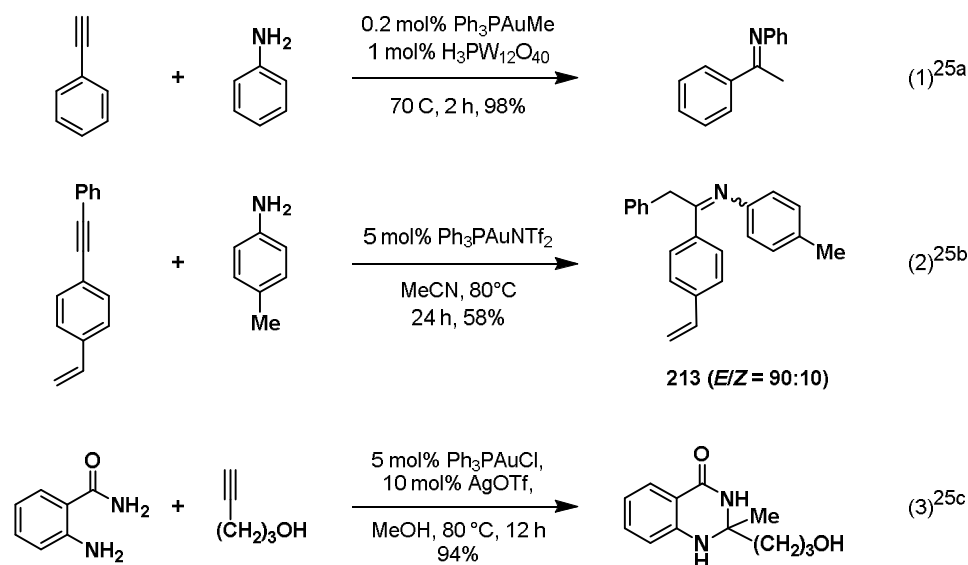
In case of intermolecular of hydroamination reactions one of the major breakthroughs in this area has appeared from Bertrand's group when they reported the catalytic hydroamination of

alkynes with ammonia (Scheme 1.8).²³ None of the literature methods were reported to be effective with ammonia as the nitrogen nucleophile before this work. A cationic gold(I) complex supported by a cyclic (alkyl)aminocarbene (CAAC) ligand **11** readily catalyzes the addition of ammonia to various unactivated alkynes to provide linear and cyclic nitrogen-containing compounds with Markovnikov selectivity. Subsequently, they explored the use of the complex [(CAAC)AuCl] for the addition of primary and secondary amines to terminal and internal alkynes.²⁴

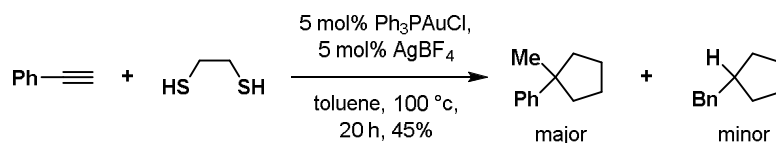
Scheme 1.8: Gold-catalyzed direct addition of ammonia onto alkynes



In 2003, Tanaka and coworkers reported an acid promoted Au(I) catalyzed intermolecular hydroamination of alkynes to give imines (Scheme 1.9, Eq. 1).²⁵ Leyva and Corma have shown that (SPhos)AuNTf₂ and Ph₃PAuNTf₂ are active catalysts for regioselective intermolecular N-H bond addition to alkynes as exemplified by the Eq. 2 in scheme 1.9. The main features of this protocol are that the Au(I) complexes operated without the exclusion of air, no acidic promoters were required and, most importantly, the catalysts can be recovered when used under solvent-free conditions and reused just by simple precipitation in hexane. Our research group reported the reaction of 4-pentyn-1-ol with 2-aminobenzamide as bis-nucleophiles in the presence of 5 mol % of Ph₃PAuCl/AgOTf catalysts in methanol (Scheme 1.9, Eq. 3). This led to development of reaction involving efficient Markownikoff's double hydroamination of alkynes to deliver the tetrahydroquinazolinone in 91% yield.

Scheme 1.9: Au-catalyzed intermolecular hydroamination and double hydroamination of alkynes**1.3.1C: Addition of S-H Bond**

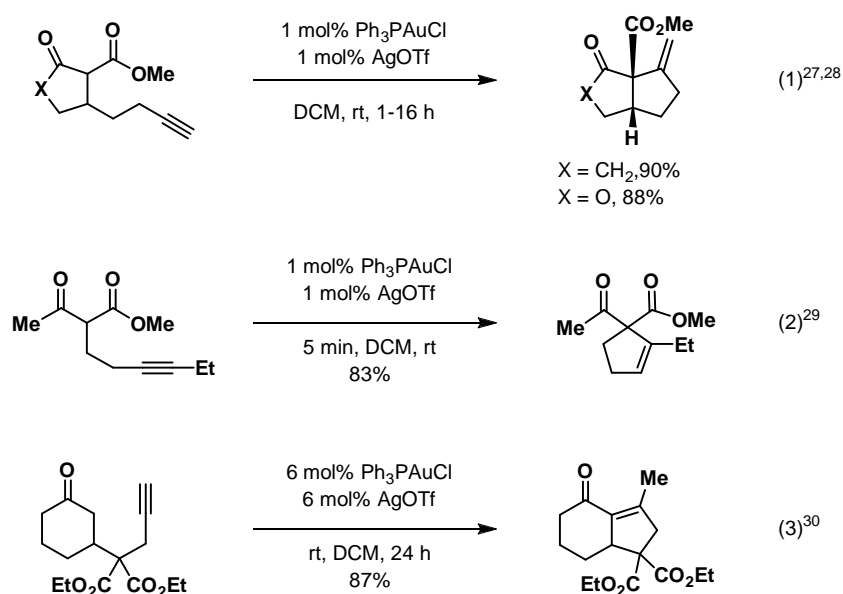
The addition of sulfur nucleophiles to alkynes is relatively less investigated, probably due to the assumption that thiol moiety coordinates to the metal centre causing catalyst poisoning. Very interestingly, the two-fold addition of ethylenedithiol to phenylacetylene delivers the corresponding dithioketals in 45% yields (Scheme 1.10).¹⁴

Scheme 1.10: Au(I)-catalyzed intermolecular double addition of thiols to alkyne**1.3.1D: Addition of C-H bond****(a) Conia-ene Reactions**

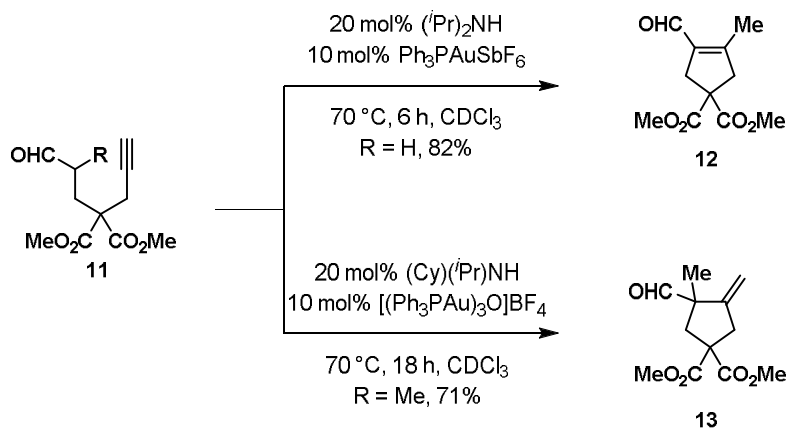
The addition of stabilized carbon nucleophiles onto alkyne is known as Conia-ene reaction.²⁶ The gold catalysis represents a potential approach for this reaction to occur under relatively mild conditions. Toste and coworkers developed Au(I)-catalyzed Conia-ene reaction of alkynyl β -ketoester that proceeds at rt (Scheme 1.11, Eq. 1).²⁷ This method provides an

efficient means for the synthesis of *exo*-methylenecycloalkanes with high diastereoselectivities. The exclusive formation of five membered cyclic products via *5-exo-dig* cyclization was observed. Later, Gagosz's research group found that 0.1 mol% of $\text{Ph}_3\text{PAuNTf}_2$ efficiently also catalyzes this transformation.²⁸ The Toste's research group further extended their work to internal alkynes. Using similar reaction conditions *5-endo-dig* cycloisomerization of alkynyl β -ketoester **3** took place to give cyclopentenes (Scheme 1.11, Eq. 2).²⁹ Similarly, Davies and Detty-Mambo³⁰ demonstrated the cycloisomerization of keto-alkyne to give bicyclic compound at rt under gold catalysis (Scheme 1.11, Eq. 3)

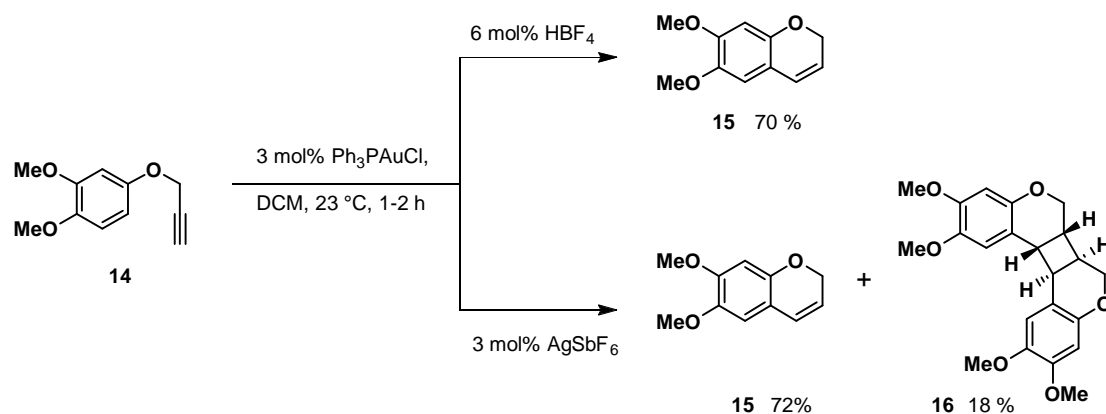
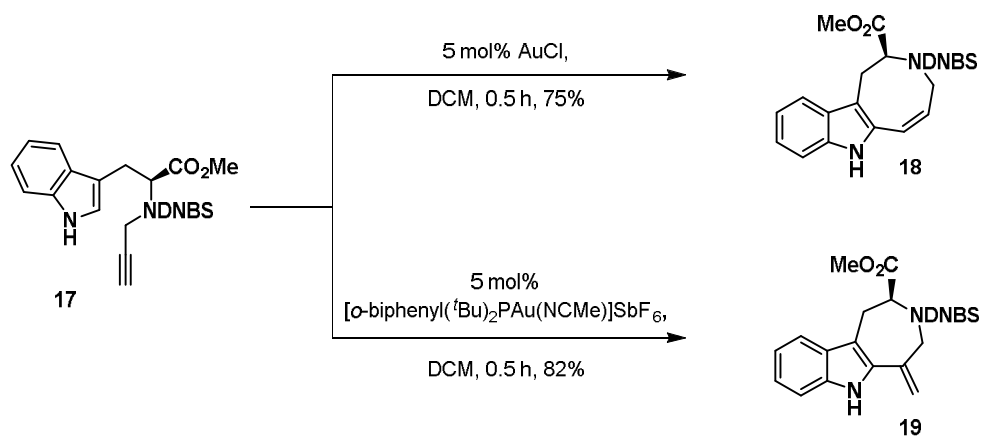
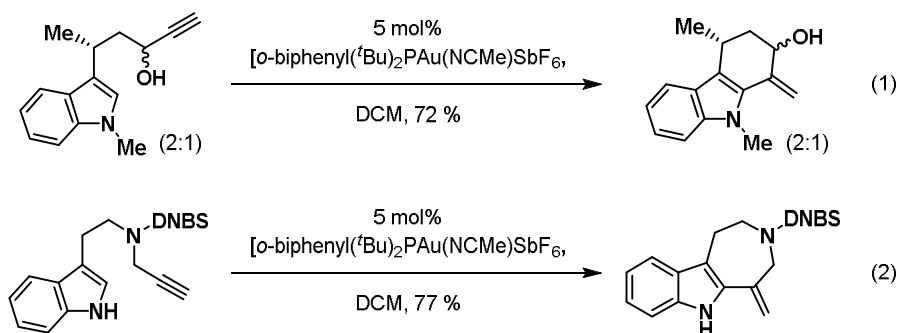
Scheme 1.11: Gold-catalyzed Conia-ene reactions



In an another report, the principle of mutual cooperativity between Au(I) complexes and secondary amine was used for direct intramolecular C-C bond formation using alkynals **11** by Kirsch *et al.* (cf. **12/13**) (Scheme 1.12).³¹ In this case, catalyst dependent product selectivity was observed.

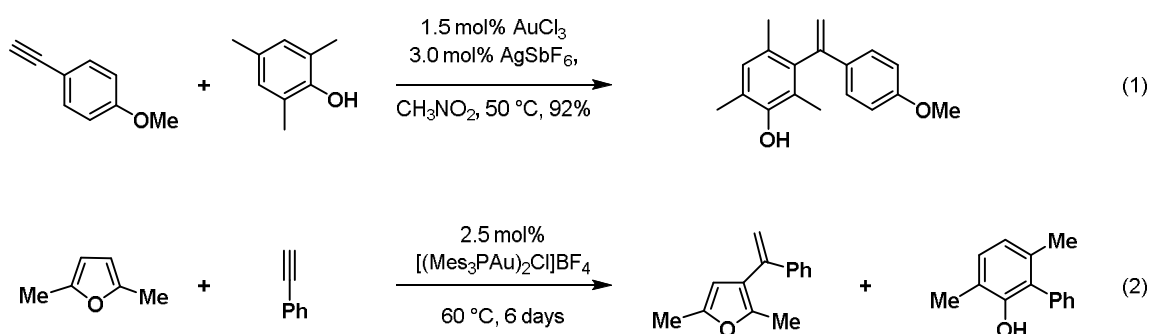
Scheme 1.12: Au(I)/secondary amine catalyzed Conia-ene reaction**(b) Hydroarylation Reactions**

The direct addition of electron rich arenes to unactivated multiple bonds such as alkynes commonly referred to as the hydroarylation, represents an attractive tool for the construction of new C–C bonds. In 2003, Echavarren and coworkers³² reported the intramolecular hydroarylation of alkynes **14** in presence of 5 mol% of Ph₃PAuCl using HBF₄ as a cocatalyst (Scheme 1.13). Interestingly, when AgSbF₆ was used as a cocatalyst a mixture of 2*H*-chromones **15** and cyclobutane **16** was obtained. The same group further extended the hydroarylation strategy to substrate of type **17** and observed an interesting catalyst dependent selectivity (Scheme 1.14).³³ The use of [*o*-biphenyl(*t*Bu)PAuNCMe]SbF₆) catalyst gave azepino [4,5-*b*] indole **19**; whereas, AuCl₃ as a catalyst gave indoloazocine **18**. The scheme 15 represents some other intramolecular hydroarylation reactions catalyzed by gold catalysts.³⁴

Scheme 1.13: Au(I)-catalyzed intramolecular hydroarylation**Scheme 1.14:** Catalyst dependent selectivity in gold catalyzed intramolecular hydroarylation**Scheme 1.15:** Gold catalyzed intramolecular addition of indoles to alkynes

Reetz *et al.*³⁵ demonstrated that the cationic Au(I) and Au(III) complexes catalyze the intermolecular hydroarylation of alkynes. Aryl substituted terminal alkynes were reacted with electron rich arenes in the presence of 1.5 mol% AuCl₃ and 3 mol% of AgSbF₆ in CH₃NO₂ to yield the 1,1-disubstituted alkenes (Scheme 1.16, Eq. 1). Later, in 2006, Hashmi *et al.* also investigated the intermolecular reaction of phenyl acetylene and 2,5-dimethylfuran in presence of Au(I)-catalyst to afford hydroarylation product along with phenol (Scheme 1.16, Eq. 2).³⁶

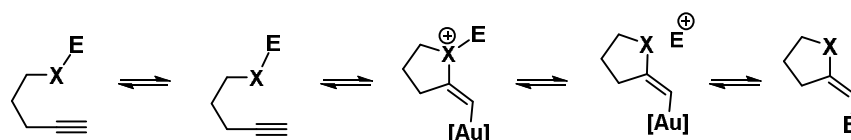
Scheme 1.16: Au(I)-catalyzed intermolecular hydroarylation of alkynes



1.3.1E: Addition of X-Y Bond

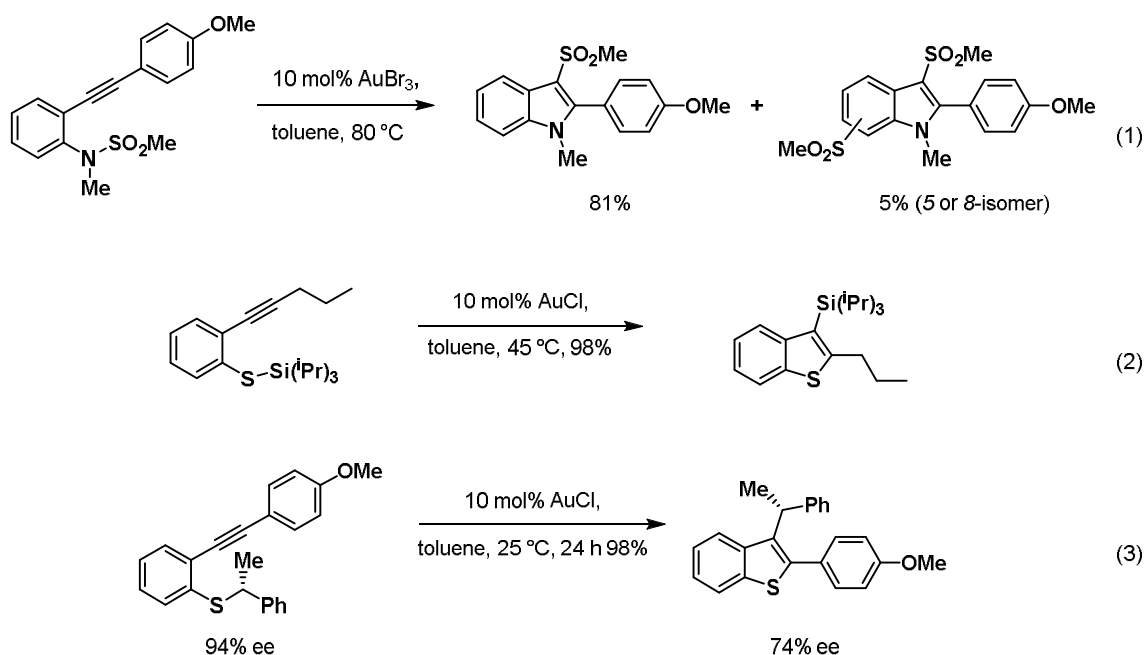
Recently, gold-catalyzed cyclizations of alkynes bearing X–Y (X = heteroatom; Y = migratory group) functionality in the proximity have been reported. The migratory group includes allyl, propargyl, acyl, (α -alkoxy alkyl), (*p*-methoxyphenyl)methyl, etc.⁶ As shown in scheme 1.17, an onium complex is formed after the nucleophilic attack of heteroatom to the gold-coordinated alkyne. One of the substituents gets transferred to the metallated position resulting in overall X \rightarrow C shift. It should be noted that the substituent best-able to stabilize a developing positive charge undergoes the shift.

Scheme 1.17: General addition pattern of X–Y bonds to alkyne



In early 2007, Yamamoto *et al.* have shown that gold-catalyzed intramolecular aminosulfonylation of 2-alkynyl-*N*-sulfonylanilines produces 3-sulfonylindoles in good to high yields (Scheme 1.18, Eq. 1).³⁷ They further extended the protocol for the synthesis of 3-silylbenzo[*b*]thiophenes from (ortho-alkynylphenylthio)silanes (Scheme 1.18, Eq. 2).³⁸ In another interesting example, Yamamoto *et al.* have observed the chirality transfer in gold-catalyzed carbothiolations of *o*-alkynylphenyl-1-arylethyl sulfides proceeded with retention of the configuration at the 1-arylethyl group (Scheme 1.18, Eq. 3).³⁹ As suggested by the authors, the retention of the stereocenter is via [1,3] migration of the *R*-phenethyl group that took place through generation of the contact ion pair followed by C-C bond formation before racemization of the stereocenter takes place. Mechanistic study also supports the generation of a contact ion pair prior to C-C bond formation.

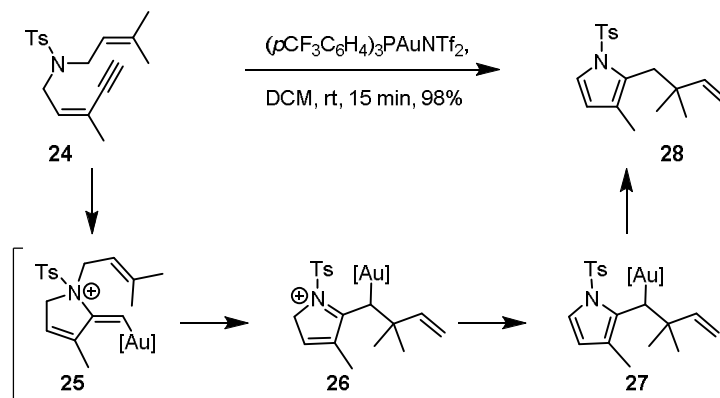
Scheme 1.18: Au-catalyzed intramolecular N-S, S-Si and C-S addition to alkynes



Based on similar reactivity, Gagosz and co-workers developed a gold(I)-catalyzed cyclization of pentenynyl allyl tosylamide **24** that allows the rapid construction of functionalized pyrroles **28** (Scheme 1.19).⁴⁰ The activation of C-C triple bond by the gold(I) catalyst in **24** triggered the intramolecular nucleophilic attack of the tethered nitrogen functionality to form the vinyl gold intermediate **25**. A subsequent aza-Claisen-type rearrangement furnishes intermediate

26 which after aromatization forms intermediate **27** that subsequently formed pyrrole **28**. The proposed concerted aza-Claisen-type mechanism was also supported by cross-over experiments.

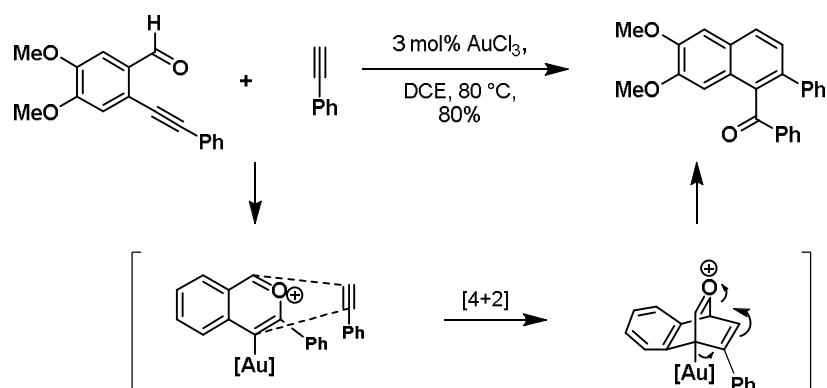
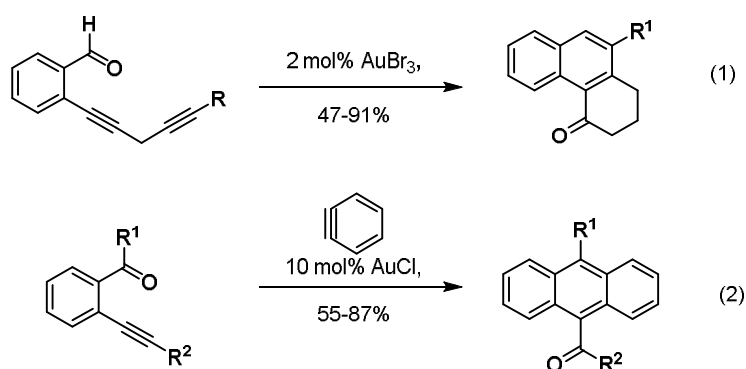
Scheme 1.19: Au(I)-catalyzed aza-Claisen type rearrangement



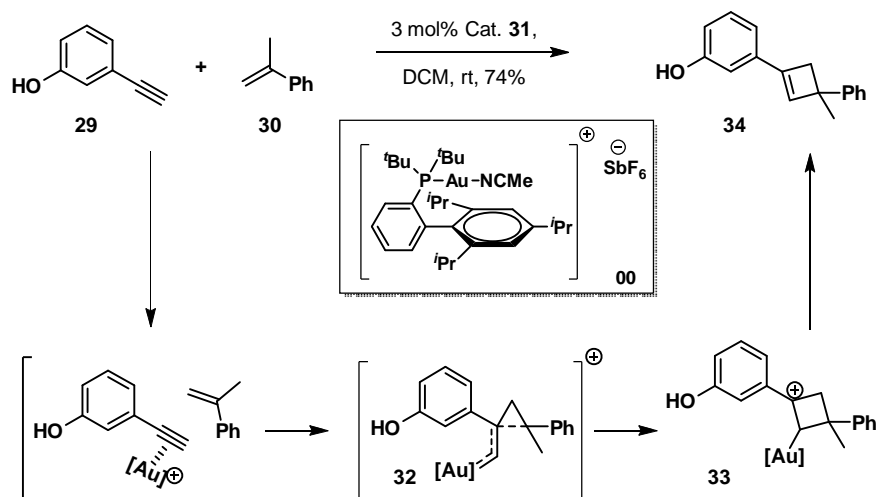
1.3.2 Cycloaddition Reactions

Gold catalyzed cycloadditions and cyclizations involving 1,n dipoles as well as 1,n-zwitterionic intermediates have become a rapidly developing field. These processes enable the construction of polycyclic motifs in a highly regio- and stereocontrolled manner from simple starting materials under mild reaction conditions. A particular case is the use of *o*-alkynylated benzaldehyde derivatives which upon activation with a π -acid affords benzopyrylium ions with 1,3- or 1,4-dipole that subsequently undergoes [3+2] or [4+2] cycloaddition reactions giving rise to polysubstituted aromatic systems.

By making the use of this reactivity, Yamamoto *et al.* discovered the $AuCl_3$ -catalyzed formal [4+2] benzannulation between *o*-alkynylbenzaldehydes with alkynes to produce naphthyl ketones in good yields (Scheme 1.20).⁴¹ The reaction proceeds through the formation of the benzopyrylium intermediate followed by the cycloaddition with phenyl acetylene and the subsequent rearrangement resulted in the formation naphthyl ketones.⁴² The same group extended the protocol to intramolecular [4+2] cycloaddition that afforded functionalized polycyclic hydrocarbons (Scheme 1.21, Eq. 1).⁴³ Also on the basis of this idea, the group of Sato reported [4+2] benzannulation reaction using benzyne as one of the partner which was in situ generated from the corresponding benzenediazonium 2-carboxylate precursor (Scheme 1.21, Eq. 2).⁴⁴

Scheme 1.20: Gold catalyzed [4+2] cycloaddition of alkyne**Scheme 1.21:** Reactivities of benzopyrylium 1,4-dipole

In 2010, Echavarren and co-workers reported the first example of gold(I)-catalyzed intermolecular [2+2] cycloaddition of terminal alkynes such as **29** with alkenes **30** that leads to regioselective formation of substituted cyclobutenes **34** (Scheme 1.22). Key for the success of this cycloaddition reaction is the use of gold(I) complexes with bulky ligands that selectively activate alkynes in the presence of alkenes. The authors suggested that [2+2] cycloaddition proceeded stepwise through cyclopropane intermediates **32** which subsequently undergo ring expansion to cyclobutane intermediate **33** that led to the formation of cyclobutenes **34** with regeneration of gold catalyst.

Scheme 1.22: Gold(I)-catalyzed intermolecular (2 + 2) cycloaddition of alkynes with alkenes

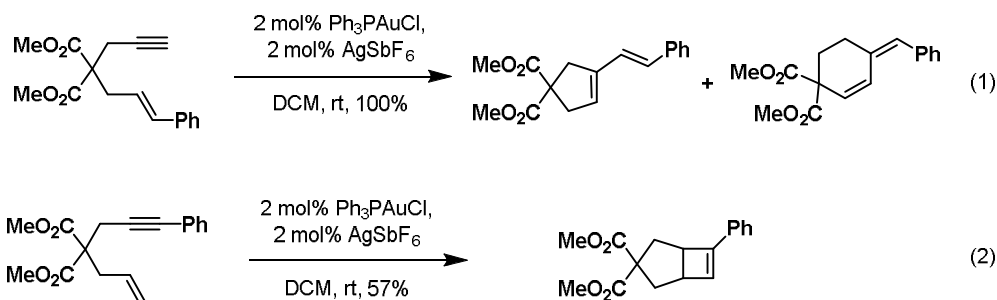
1.3.3 Enyne Cycloisomerization

Enyne cycloisomerizations represent one of the most widely studied subfields of gold/ π -acid catalysis.⁴⁵ Cycloisomerisation of 1,*n*-enynes is a class of emblematic transformations in which an alkene acts as the nucleophile towards an alkyne, activated by gold catalysts. Enyne cycloisomerizations involve C-C σ -bond formation from π -systems as well as processes where the skeletal C-C connectivity is reconfigured through single (alkene) or double (alkene and alkyne) cleavages. A diverse array of reactions are possible with a significant increase in molecular complexity and in a fully atom economic manner.

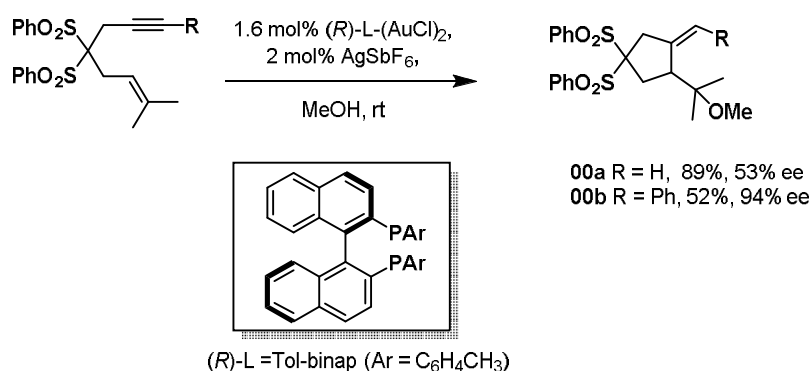
Echavarren *et al.* reported the first examples of skeletal rearrangement of enynes by alkynephilic gold(I) complexes that proceeded through the endocyclic cyclization pathway. A representative example is the single-cleavage rearrangement of 1,6-enynes to form conjugated dienes, which has been proposed to proceed through a cyclopropyl gold(I) carbene intermediate (Scheme 1.23). In the subsequent year, the same group developed the enantioselective version using chiral gold complexes bearing mono- and bidentate phosphine ligands for the enantioselective alkoxy cyclization of enynes (Scheme 1.24).⁴⁶ This procedure was one of the first examples of chiral bis-gold(I) complexes being applied for enantioselective gold catalysis.

Utilizing various enantiopure ferrocenylphosphine and binap derivatives, the authors synthesized and characterized a variety of chiral bis-gold(I) complexes.

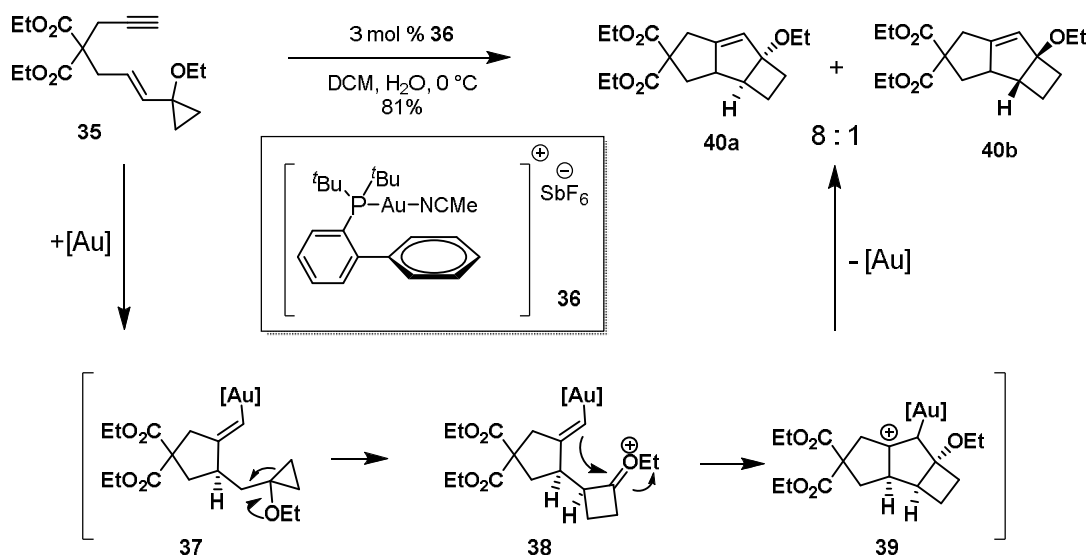
Scheme 1.23: Gold(I) catalyzed C-C bond formation via enyne cycloisomerization reaction



Scheme 1.24: Gold-catalyzed enantioselective enyne cycloisomerization reaction



Similarly, in 2007, Echavarren *et al.* developed enyne cycloisomerization-ring expansion-nucleophilic addition strategy that leads to the formation of a tricyclic carbon skeleton (Scheme 1.25).⁴⁷ For instance, enyne **35** underwent gold(I) (cf. **36**) catalyzed cascade reaction via cyclopropyl intermediate **37** followed by ring expansion to give cyclobutyl **38** that subsequently lead to the formation of final product **40** with high distereoselectivity from intermediate **39**.

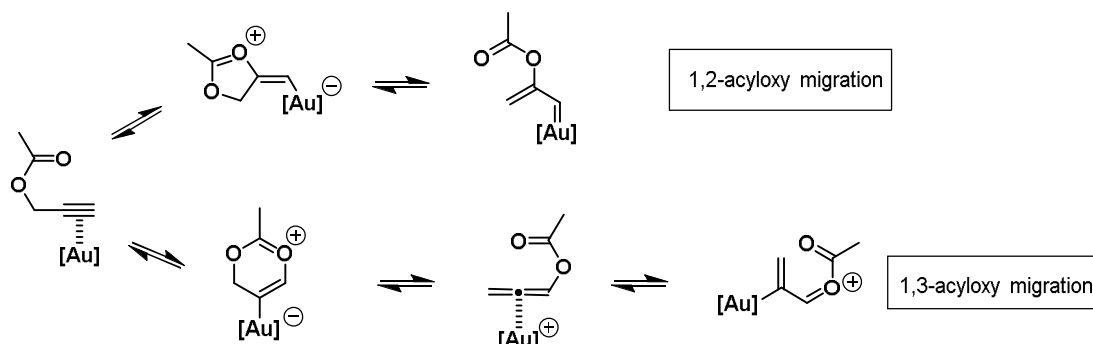
Scheme 1.25: Gold(I) catalyzed enyne cycloisomerization cascade

1.3.4 Rearrangement of Propargylic Carboxylates

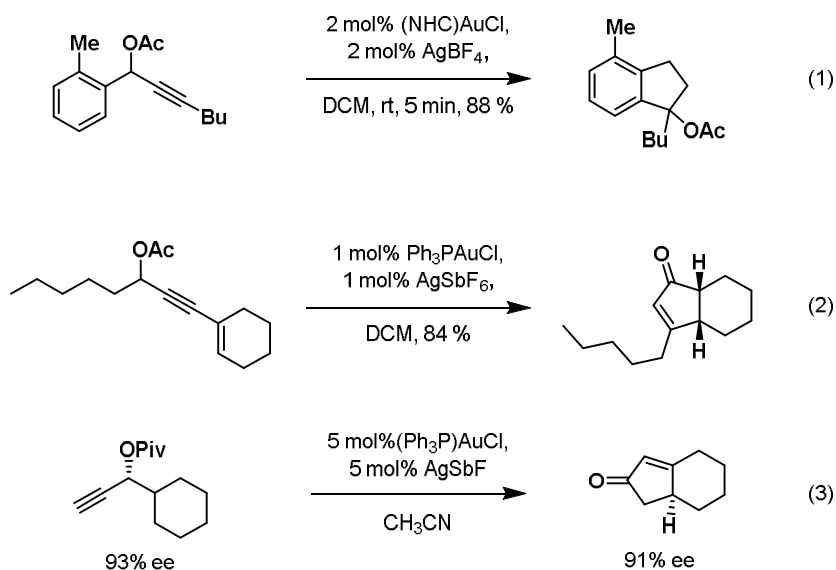
Activation of the triple bond in a propargylic carboxylates may provoke either anchimeric participation of the adjacent carboxylate as the primary step or attack by the double bond if enyne reactivity prevails similar to “Ohloff–Rautenstrauch rearrangement”. As a result, propargylic esters may be regarded as simple, safe and convenient alternatives to a-diazocarbonyl derivatives which are commonly used for the preparation of such products.

In the context of gold catalysis several groups have investigated the intriguing and highly valuable reactivity of these easily accessible compounds. Notably, their propensity to undergo 1,2- and 1,3-acyl migration (Scheme 1.26)⁴⁸ leading to the formation of a Au–carbene and to an allene, respectively, which are both poised for subsequent functionalization, allows for great structural diversity.⁴⁹ Computational and experimental studies show these complexes to be in rapid equilibrium with interconversion occurring in any direction. The activation mode ultimately depends on the subsequent irreversible formation of products after reaction with other functionality. The substituents on the propargylic carboxylate, the reaction conditions and the nature of the catalyst used all play a role in determining the final outcome of these reactions.

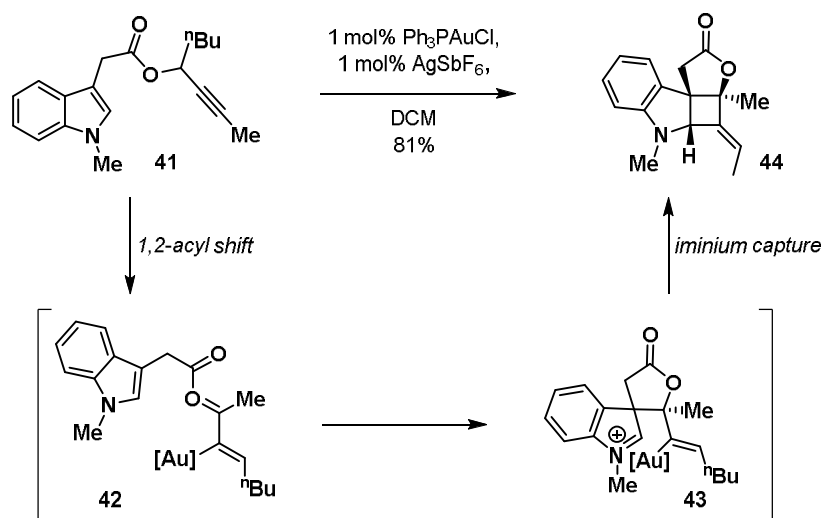
Scheme 1.26: General reactivity pattern and possible intermediates for rearrangement of propargylic carboxylates



In 2006, Toste and Zhang independently explored the rearrangement of propargylic carboxylates. The reactions of the incipient allenyl acetates with an adjacent benzene ring explain the gold-catalyzed formation of substituted indenenes (Scheme 1.27, Eq. 1)⁵⁰ and eq. 2 represents the Nazarov type cyclization (Scheme 1.27, Eq. 2)⁵¹. Later, Toste and co-workers reported another gold(I)-catalyzed diastereoselective rearrangement of propargyl esters to form cyclopentenones (Scheme 1.27, Eq. 3).⁵² Treatment of propargyl pivalates with cationic gold(I) catalyst triggered a Rautenstrauch rearrangement to afford cyclopenten-2-ones with good yields. Interestingly, when enantiomerically enriched propargyl esters were applied, excellent chirality transfer was observed and enantiomerically enriched cyclopentenones were prepared with excellent enantioselectivity. According to the authors, the reaction proceeds through an active vinyl gold species, where the C-C bond is formed prior to the cleavage of the stereogenic C-O bond.

Scheme 1.27: Au(I)-catalyzed propargylic carboxylate rearrangement reactions

In a similar context, Zhang *et al.* reported gold-catalyzed synthesis of highly functionalized 2,3-indoline-fused cyclobutanes **44** from propargylic esters **41** (Scheme 1.28).⁵³ This cascade reaction involves the 3,3-rearrangement of the indole-3-acetoxy group, which leads to the formation of allenylic esters **42** with 1,2 acyl shift followed by intramolecular trapping of the iminium ion **43**. The formation of the cyclobutane product can be explained through a [2 + 2] cycloaddition reaction via 1,4-zwitterionic intermediate. This example provides an excellent illustration of the structural complexity that can be garnered via easily performed gold catalysis.

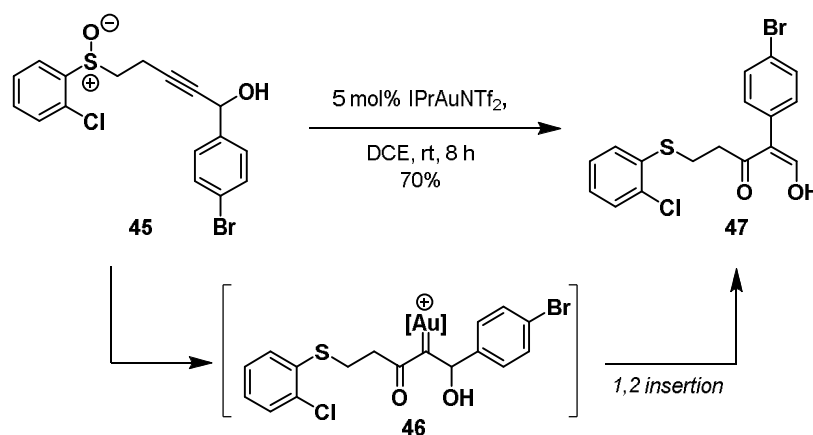
Scheme 1.28: Au(I)-catalyzed propargylic carboxylate rearrangement triggered cascade reaction

1.3.5 Reactivities of Gold Carbenoids

Metal carbenes, generated by the site-specific metal-promoted decomposition of a reactive functionality such as a diazo group, are employed extensively across an array of useful transformations. However, the need to introduce such potentially hazardous diazo functionality, often immediately prior to the carbene-based step, comes at the expense of synthetic efficiency and flexibility. Gold carbenoid strategy does not rely on the use of sacrificial functionality and can be employed as a direct equivalent to an α,α -disubstituted-diazo imide, or ester. A range of new reactions have evolved from the use of tethered sulfoxide, amine N-oxide or nitrene moieties to oxidise a gold-activated alkyne to an α -oxogold carbenoid intermediate.

The homopropargylic sulfoxides exhibit an interesting reactivity that has been investigated recently. As shown in scheme 1.29 the sulfoxide moiety **45** acts as a nucleophile through its oxygen atom and as a leaving group through its sulfur atom.⁵⁴ The net result is an intramolecular redox process where the sulfoxide function is converted into a sulfide function and the alkyne into α -carbonyl gold carbenoid **46**. Alternatively, alkyl or aryl 1,2-migration/1,2-insertion take place for substrates bearing a secondary or tertiary propargylic alcohol leading to β -hydroxy enone **47**. The use of *o*-chloroaryl reduces competing electrophilic aromatic substitution.

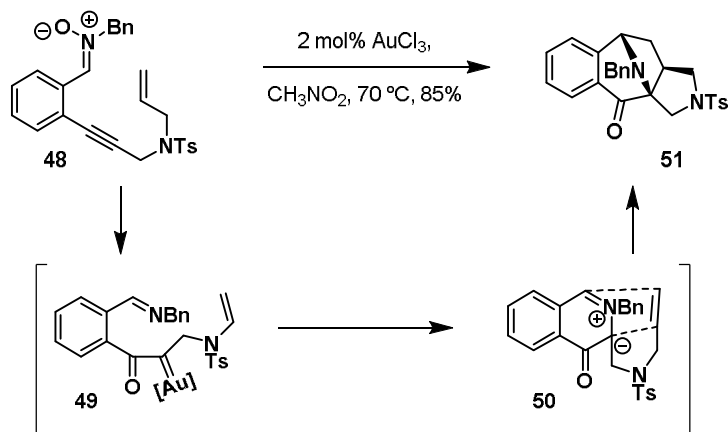
Scheme 1.29: Au(I)-catalyzed intramolecular redox reaction of sulfinyl propargylic alcohols



Similarly, Shin *et al.* described a gold-catalyzed generation of azomethine ylide, featuring an internal redox reaction between a tethered nitrene and an alkyne substrate **48** (Scheme 1.30).⁵⁵ In this case, the initial 7-*endo*-dig attack of the O-atom of the nitrene on the alkyne and subsequent N-O cleavage lead to α -oxo Au-carbenoid **49**. Subsequent addition of the imine to

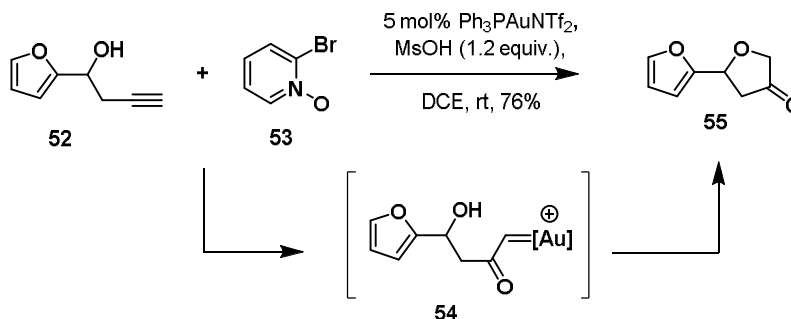
this carbenoid leads to **50** from which the catalyst is regenerated to provide **51**. The azomethine ylide undergoes an efficient intramolecular cycloaddition reaction cascade in highly diastereoselective manner.

Scheme 1.30: Gold-catalyzed azomethine ylide generation tandem cycloaddition reaction



Zhang and coworkers reported the first example of accessing α -oxo gold carbenes via intermolecular oxidation of terminal alkynes under mild reaction conditions. For instance reactive α -oxo gold carbenes **54** was accessed via gold-catalyzed intermolecular oxidation of terminal alkynes **52** under mild reaction conditions that lead to dihydrofuran-3-ones **55** (Scheme 1.31).⁵⁶ This intermolecular strategy provides much improved synthetic flexibility in comparison with the intramolecular version and offers a safe and economical alternative to those based on diazo substrates. In this reaction, pyridine *N*-oxides **53** have been used to effect intermolecular oxidation of alkynes, followed by O-H insertion of the incipient carbenoid in the presence of stoichiometric MsOH.

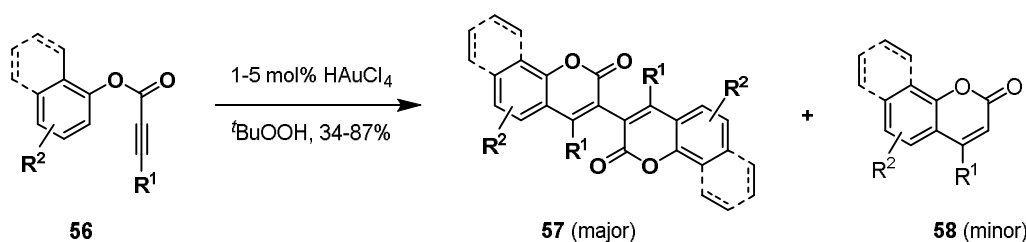
Scheme 1.31: Synthesis of dihydrofuran-3-ones by Au(I)-catalyzed intermolecular oxidation of terminal alkynes



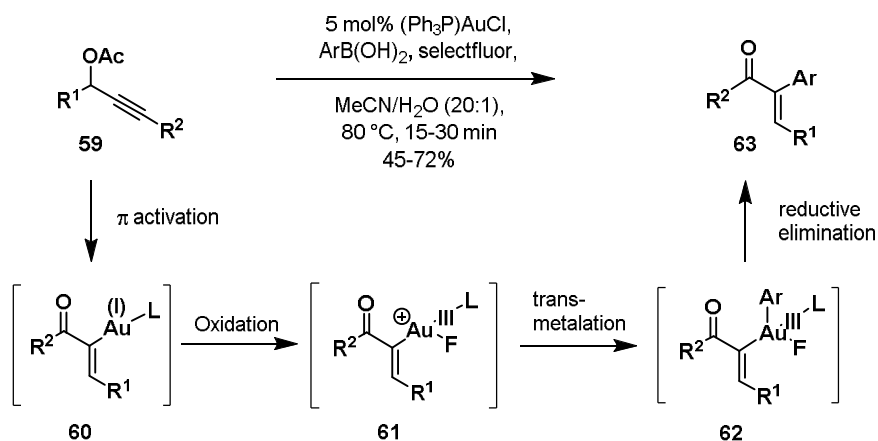
1.3.6 Oxidative Cross-coupling Reactions

Gold catalysts are also known to undergo oxidative addition to R-X bonds, although theoretical studies predict such a process to be highly unfavoured.⁵⁷ Also, insertion reactions into C-H bonds have been proposed. Thus the most powerful method is the in situ generation of the reactive species owing to the π -Lewis acid nature of the gold catalyst, which promotes the addition of a nucleophile to a C=C or C \equiv C bond with transfer of the gold catalyst to the second carbon atom. The studies clearly indicate that if an efficient oxidant could be identified for the regeneration of the Au(III) species required for the reductive elimination, the synthetic chemist would have a very efficient catalytic tool for the assembly of complex molecules. The second important aspect is the suppression of protodeauration. In practical terms, for the success of these type of reactions, the regeneration of the Au(III) species must be faster than the protodeauration step and the disproportionation of Au(I) to Au(0) and Au(III).⁵⁸

In 2008, Wegner research group developed a domino cyclization oxidative coupling reaction of alkynylarelesters **56** to dicoumarins **57** using catalytic amounts of Au-catalyst (Scheme 1.32).⁵⁹ Initially the authors isolated the dimer **57** only in trace amounts as a side product. Running the reaction with stoichiometric amounts of Au-catalyst gave the dimer **57** as the main product along with small amount of coumarin **58**. After screening a variety of conditions the use of HAuCl_4 in 1,2-dichloroethane (DCE) and $t\text{-BuOOH}$ as an oxidant the authors were able to regenerate the Au(III) species, necessary for the oxidative coupling to occur, and to obtain the dimer product as the main component, even with catalytic amounts of catalyst as low as 1 mol%.

Scheme 1.32: Gold catalyzed oxidative cross-coupling reaction of alkynylarylesters

In 2009, Zhang *et al.* for the first time reported the gold-catalyzed oxidative cross-coupling reaction, of propargylic acetates **59** and arylboronic acids, leading to a one-step synthesis of arylenones **63** via classical cross coupling intermediate (cf. **60**, **61** and **62**) (Scheme 1.33).⁶⁰ The authors suggested, the feasibility of Au(I) and Au(III) catalytic cycles, and indicates that oxidants such as selectfluor can readily oxidize Au(I) into Au(III). Moreover, this cross-coupling reaction reveals for the first time the synthetic potential of incorporating Au(I)/Au(III) catalytic cycles into gold chemistry and promises a new area of gold research by merging powerful contemporary gold catalysis, using alkyne/allene substrates, and oxidative metal-catalyzed cross-coupling reactions.

Scheme 1.33: Gold-catalyzed oxidative cross-coupling reaction of propargylic acetates and arylboronic acids

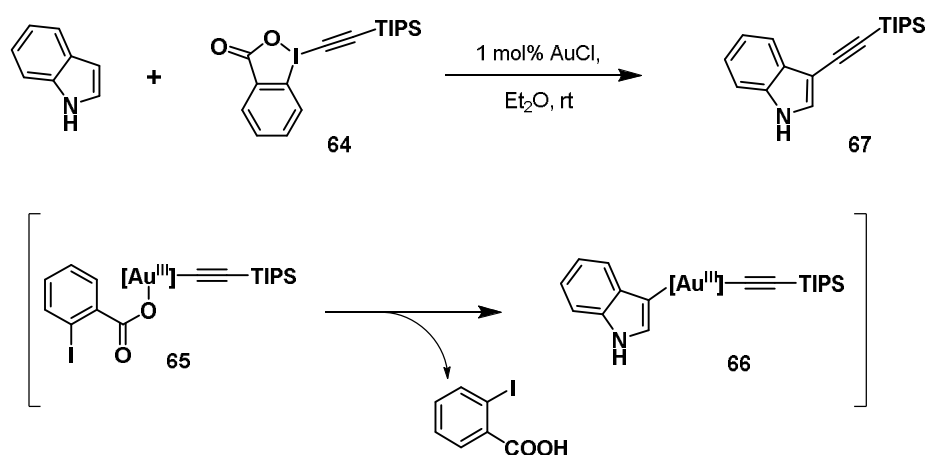
1.3.7 C-H Functionalization Reactions

C-H functionalization is clearly a powerful synthetic tool which provides a highly economic means to increase the complexity of unactivated molecules. The use of powerful and

environmentally benign gold(I) and gold(III) catalysts in such transformations has highlighted their remarkable reactivity and led to a significant increase in their utilisation.⁶¹ This mode of reactivity has allowed gold to participate in a range of bond-forming reactions, including cross-coupling reactions, a notable addition considering the reluctance of gold to cycle between oxidation states.

In this context, Waser *et al.* reported the use of highly reactive and oxidising hypervalent iodine reagents **64** in the gold-catalyzed direct alkylation of indoles (Scheme 1.34).⁶² Their method provided easily deprotected silylacetylene products in good to excellent yields. The authors proposed that this reaction proceeds via initial oxidation of the gold(I) chloride, by the alkynyliodonium species, to give a gold(III) acetylene complex **65**. The gold(III) centre then performs C–H activation of the indole, generating a organogold(III) intermediate **66**, which undergoes reductive elimination to furnish the alkynylated product **67** with the regeneration of gold(I) catalyst.

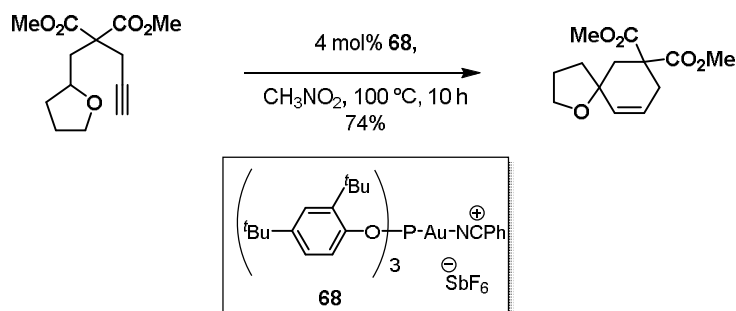
Scheme 1.34: Gold(I) catalyzed alkylation of indole



In 2010, Gagosz *et al.* reported the Au(I)-catalyzed hydroalkylation of alkynyl ethers, proceeding through a 1,5-hydride shift/cyclization sequence (Scheme 1.35).⁶³ The authors proposed that 6-exo activation of alkynyl ethers, by gold(I) catalyst **68**, promotes a 1,5-hydride shift, from the C_{sp³}–H α to the oxygen to the alkyne. Subsequent cyclization of the resulting vinylgold species generates the products in high yields, for a number of alkynyl ether substrates.

Thus, through activation of a terminal alkyne, with electrophilic gold(I) catalyst, a $C_{SP^3}-H$ bond is replaced with a new C–C bond.

Scheme 1.35: Gold catalyzed $C_{SP^3}-H$ bond functionalization of alkynyl ethers

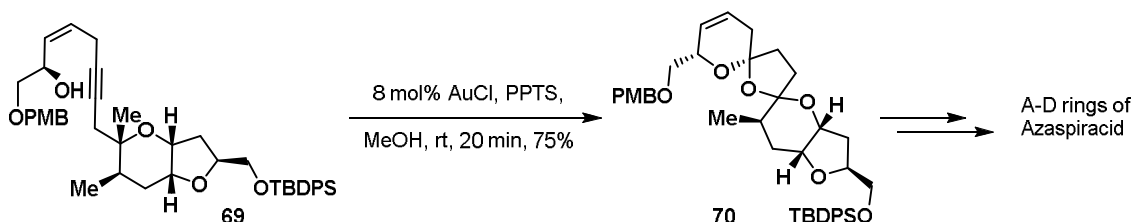


1.3.8 Application in Total Synthesis

The field of gold catalysis has evolved to be a true hot spot in catalysis research, and after an initial focus on methodical investigation, now a number of applications in the total synthesis of natural products have been published. The high gain in molecular complexity in many of these reactions, combined with exceptionally mild reaction conditions and high atom economy, led synthetic chemists to use the unique catalytic ability of gold catalysts for key steps in total synthesis.⁶⁴

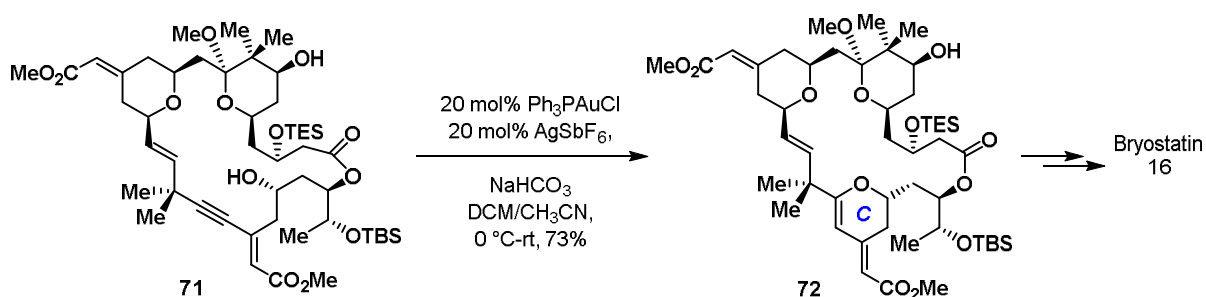
In 2007, Frost *et al.* reported an efficient synthesis of the A–D rings of toxin azaspiracid. The key step of synthesis was gold(I)-catalyzed bis-spiroketal formation using a bridging alkyne **69** as a precursor for the ketal **70** (Scheme 1.36).⁶⁵ The diastereoselectivity in the ketal formation is based on thermodynamic control.

Scheme 1.36: Synthesis of the A–D rings of the toxin Azaspiracid



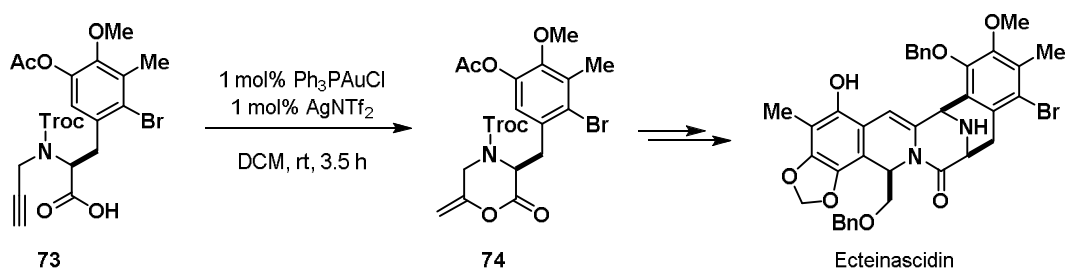
Trost and Dong has achieved concise synthesis of Bryostatin 16 utilizing gold(I)-catalyzed *endo-dig* cyclization of substrate of type **71** for the construction of ring C of Bryostatin 16 (intermediate **72**) (Scheme 1.37).⁶⁶ One of the key steps of the synthesis, the gold-catalyzed transformation, represents an impressive example of the high chemoselectivity which can be achieved via gold catalysis. Since the gold-catalyzed step is late in the synthesis, a plethora of functional groups are tolerated and it is remarkable that only the alkyne is addressed even if several unsaturated moieties are present.

Scheme 1.37: Gold catalyzed hydroalkoxylation as a key step in synthesis of Bryostatin 16



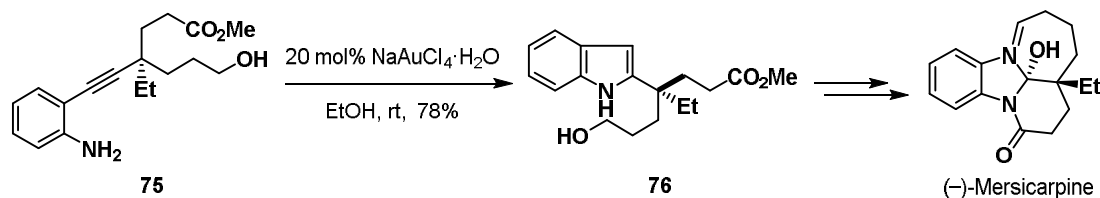
Takemoto and coworkers have reported a synthesis of the pentacyclic core of ecteinascidin from the key intermediate **74**, which was obtained via 6-*exo-dig* intramolecular hydrocarboxylation of alkyne **73** catalyzed by 1 mol% of $\text{Ph}_3\text{PAuCl}/\text{AgNTf}_2$ in DCM at rt (Scheme 1.38).⁶⁷

Scheme 1.38: Synthesis of the pentacyclic core of Ecteinascidin



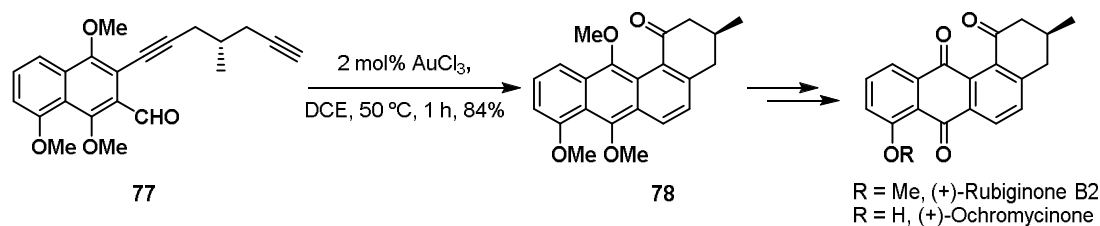
The gold-catalyzed regioselective 5-*endo-dig* hydroamination of *o*-alkynylanilines such as **75** enables them to be used as indole synthons **76**. This method was applied during the first enantioselective synthesis of indole alkaloid (–)-Mersicarpine (Scheme 1.39).⁶⁸ It is noteworthy that a competing attack of the unprotected hydroxyl group in the side chain was not observed.

Scheme 1.39: Total synthesis of (-)-Mersicarpine using gold catalyzed hydroamination as a key step

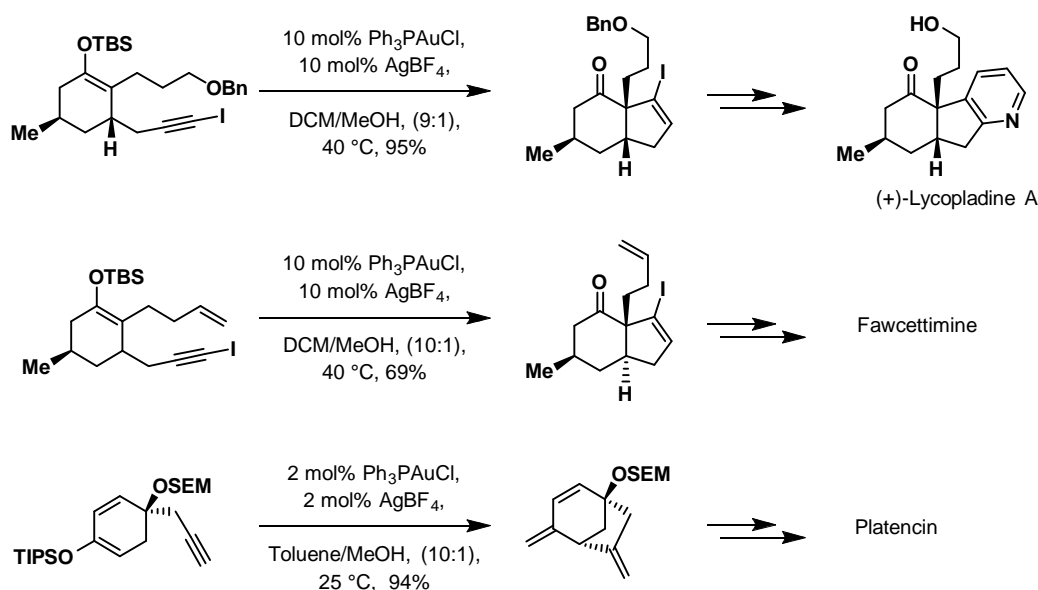


The total synthesis of (+)-Ochromycinone and (+)-Rubiginone B2 were accomplished via the AuCl_3 -catalyzed intramolecular [4+2] cycloaddition reaction as the key step from substrate type **77** (Scheme 1.40).⁶⁹ This result indicates that the intramolecular [4+2] benzannulation is useful for construction of 2,3-dihydrophenanthren-4(1H)-one skeleton **78**, an important structural framework in a wide range of bioactive compounds, such as tanshinone family containing the activity to ischemia disease.

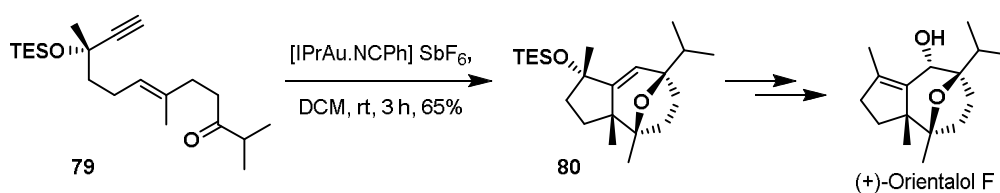
Scheme 1.40: Total synthesis of (+)-Ochromycinone and (+)-Rubiginone B2



The gold catalyzed cyclization of silyl enol ethers bearing alkynes is a powerful methodology for the formation of C-C bonds with O-Si cleavage in the presence of alcohol/water additives. An elegant applications of this reaction principle is resulted in the total synthesis of many natural product such as (+)-Lycopladine,⁷⁰ (+)-Fawcettimine⁷¹ and Platencin⁷² (Scheme 1.41).

Scheme 1.41: Application of the gold catalyzed enyne cycloisomerization in total synthesis

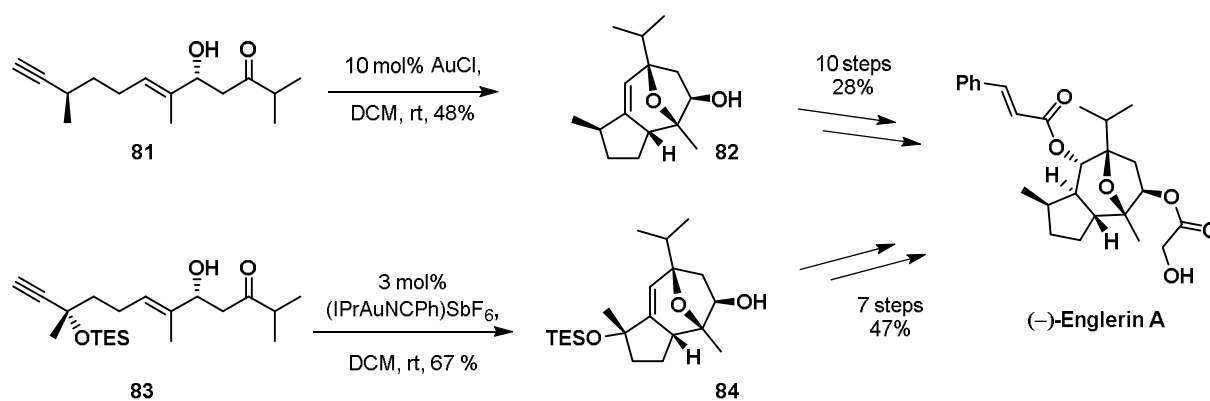
A special type of 1,6-enyne cyclization with a carbonyl group at the alkenyl side chain was established by the Echavarren group. The complex oxatricyclic skeleton **80**, which is obtained via formal [2+2+2] alkyne/alkene/carbonyl-cycloaddition from enyne substrate **79**, builds the foundation for several total syntheses. The same group reported the first example by the enantioselective synthesis of sesquiterpene (+)-Orientalol F (Scheme 1.42).⁷³

Scheme 1.42: Total synthesis of (+)-Orientalol F using gold catalyzed 1,6-enyne cyclization

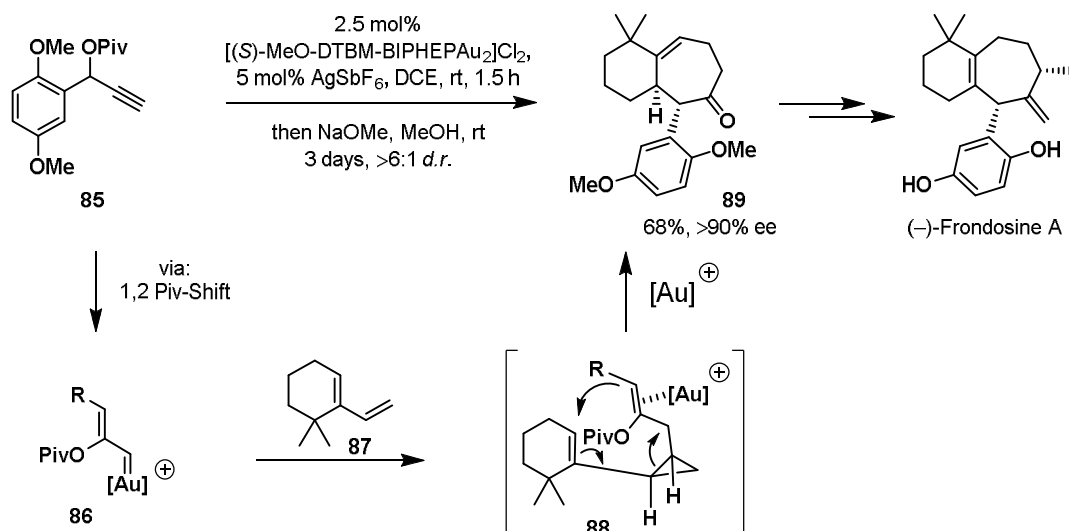
The structurally related Englerin A is an even more attractive target due to its ability to act as a selective inhibitor of renal cancer cell growth. Its synthesis was published side-by-side by the groups of Ma⁷⁴ and Echavarren⁷⁵ group (Scheme 1.43). Apart from the gold-catalyzed step, the synthetic approaches of the two groups were quite different. In the Ma's strategy, the precursor **81** of the enyne cyclization was available within only 4 steps from commercially

available citronellal. For the gold-catalyzed transformation simple gold(I) chloride was used, leading to **82** only moderate yields for this key reaction step. After the gold-catalysed step, ten further transformations were necessary to obtain the target compound. On the other hand Echavarren's approach started from commercially available geraniol. In their case a longer sequence towards the enyne precursor **83** was necessary, but this was more than out-weighted by the more efficient second part of their strategy. Not only the gold-catalyzed step was more efficient but the additional hydroxyl group at the five membered ring of intermediate **84** allowed efficient transfer of its stereochemistry to that required in the final product.

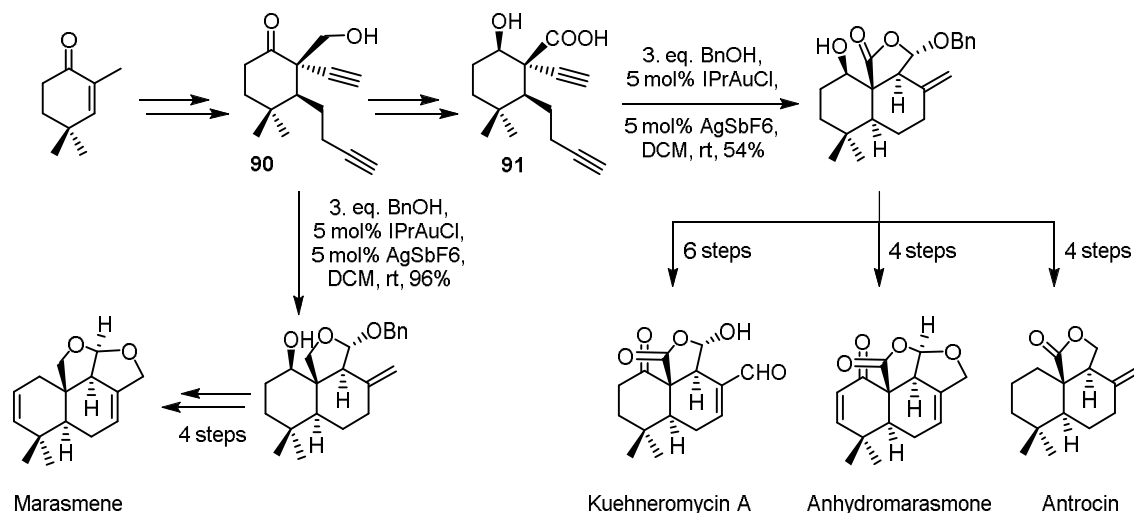
Scheme 1.43: Different approaches towards total synthesis of (-)-Englerin A



A formal enantioselective synthesis of frondosin A, a marine norsesquiterpenoid with promising biological activities has been achieved by Nevado's research group (Scheme 1.44).⁷⁶ Treatment of acetate **85** and 6,6-dimethyl-1-vinyl cyclohexene **87** with (*S*)-MeO-DTBM-BIPHEP-gold-(I) complex afforded, quantitatively, the corresponding bicyclic cycloheptenyl pivaloate. In this case, the initially generated vinyl gold carbenoid **86** triggers a cascade of intermolecular cyclopropanation followed by a formal homo-Cope rearrangement of the resulting functionalized intermediate **88**. In situ hydrolysis and subsequent equilibration with NaOMe/MeOH yielded thermodynamically favoured ketone **89** in 68% yield and >90% ee. Since this bicyclic enone has been already elaborated to frondosins A and B, this approach represents a streamlined formal enantioselective synthesis of both molecules.

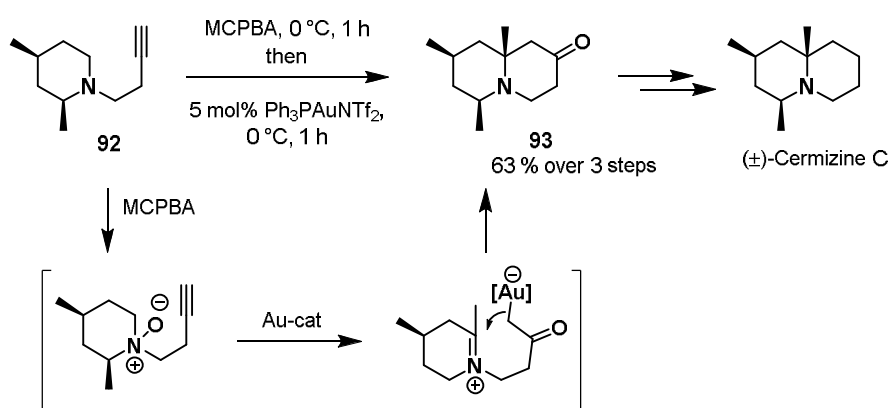
Scheme 1.44: Enantioselective formal total synthesis of (–)-FronDOSin A

Dienes **90** and **91** were used as key intermediates for the syntheses of various Drimane type sesquiterpenes, a group of natural products possessing a variety of interesting biological activities (Scheme 1.45).⁷⁷ The gold-catalyzed key step creates a remarkable increase of molecular complexity. From the products of the gold catalysis, four types of sesquiterpenes were available within only a few further modifications.

Scheme 1.45: Syntheses of Drimane type sesquiterpenes

The lycopodium alkaloid (\pm)-Cermizine C synthesis utilizes the use of tethered N-oxides as internal oxidizing reagents for the transformation of alkynes into α -oxo-gold carbenes. In an efficient one-pot protocol 3-butynylamines **92** was converted to piperidin-4-ones **93** (Scheme 1.46).⁷⁸ The key step of the racemic synthesis of lycopodium alkaloid Cermizine C consists of an efficient protocol which uses homopropargylation, oxidation and subsequent gold-catalysed skeletal rearrangement without purification of the intermediates. The authors suggested that resulting quinolizidinone core is formed by a hydride-shift of the α -amino hydrogen onto the intermediate gold carbenoid. The resulted iminium species then reacts with the nucleophilic gold enolate in a diastereoselective fashion and the catalyst is regenerated.

Scheme 1.46: Synthesis of (\pm)-Cermizine C



1.4 Conclusion

From this overview it is clear that the chemistry of gold catalysis is diverse, powerful and has advanced rapidly within a short period of time. There is great potential for application of gold catalysis in advanced organic synthesis: both in extending known reactivities and in developing novel transformations (including asymmetric variations). The reactions developed all fit within the known activation modes of gold catalysis starting with electrophilic activation and the ability of gold to stabilize positive charge. There is potential for further use of gold-species generated in situ by coupling or cyclization reactions. The high gain in molecular complexity in many of these reactions, combined with exceptionally mild reaction conditions and high atom economy led synthetic chemists to use the unique catalytic ability of gold catalysts for key steps in total synthesis.

1.5 References

- [1] Source: <http://en.wikipedia.org/wiki/Gold>
- [2] Reviews on heterogeneous gold catalysis: (a) Hutchings, G. J. *Chem. Commun.* **2008**, 1148–1164; (b) Thompson, D. *Gold Bull.* **1998**, *31*, 111–118; (c) Thompson, D. *Gold Bull.* **1999**, *32*, 12–19; (d) Bond, G. C. *Catal. Today* **2002**, *72*, 5–9; (e) Schwank, J., *Gold Bull.* **1985**, *18*, 2–10.
- [3] Hutchings, G. J. *J. Catal.* **1985**, *96*, 292–295.
- [4] Haruta, M.; Kobayashi, T.; Sano, H.; Yamada, N. *Chem. Lett.* **1987**, *16*, 405–408.
- [5] Reviews on gold nanocatalysis: (a) Zhang, Y.; Cui, X.; Shi, F.; Deng, Y. *Chem Rev.* **2011**, *112*, 2467–2505; (b) Corma, A.; Garcia, H., *Chem. Soc. Rev.* **2008**, *37*, 2096–2126; (c) Chen, M. S.; Goodman, D. W. *Catal. Today* **2006**, *111*, 22–33; (d) Burda, C.; Chen, X.; Narayanan, R.; El-Sayed, M. A. *Chem. Rev.* **2005**, *105*, 1025–1102; (e) Grzelczak, M.; Perez-Juste, J.; Mulvaney, P.; Liz-Marzan, L. M. *Chem. Soc. Rev.* **2008**, *37*, 1783–1791; (f) Chen, M. S.; Goodman, D. W. *Chem. Soc. Rev.* **2008**, *37*, 1860–1870.
- [6] Selected Reviews: (a) Patil, N. T.; Kavthe, R. D.; Yamamoto Y. *Advances in Heterocyclic Chemistry*, **2010**, *101*, 75–95; (b) Patil, N. T.; Yamamoto, Y. *Chem. Rev.* **2008**, *108*, 3395–3442; (c) Fürstner, A.; Davies, P. W. *Angew. Chem. Int. Ed.* **2007**, *46*, 3410–3449.
- [7] (a) Sawamura, M.; Ito, Y.; Hayashi, T. *Tetrahedron Lett.* **1990**, *31*, 2723–2726; (b) Sawamura, M.; Nakayama, Y.; Kato, T.; Ito, Y. *J. Org. Chem.* **1995**, *60*, 1727–1732.
- [8] (a) Corma, A.; Leyva-Pérez, A.; Sabater, M. J.; *Chem. Rev.* **2011**, *111*, 1657–1712; (b) Wegner, H. A.; Auzias, M. *Angew. Chem. Int. Ed.* **2011**, *50*, 8236–8247; (c) Bandini, M. *Chem. Soc. Rev.* **2011**, *40*, 1358–1367; (d) Patil, N. T.; Kavthe, R. D.; Yamamoto, Y. *Advances in Heterocyclic Chemistry*, **2010**, *101*, 75–95; (e) Ma, S. *Handbook of Cyclization Reactions*, Wiley-VCH Verlag GmbH & Co. KGaA, **2010**, Chapter 10; (f) Dudnik, A. S.; Chernyak, N.; Gevorgyan, V. *Aldrichimica Acta* **2010**, *43*, 37–46; (g) Garcia, P.; Malacria, M.; Aubert, C.; Gandon, V.; Fensterbank, L.; *ChemCatChem*, **2010**, *2*, 493–497; (h) Md. Abu Sohel, S.; Liu, R.-S. *Chem. Soc. Rev.* **2009**, *38*, 2269–2281; (i) Patil, N. T.; Yamamoto, Y. *Chem. Rev.* **2008**, *108*, 3395–3442; (j) Fürstner, A. *Chem. Soc. Rev.* **2009**, *38*, 3208–3221; (k) Gorin, D. J.; Sherry, B. D.; Toste, F. D. *Chem. Rev.* **2008**, *108*, 3351–3378; (l) Li, Z.; Brouwer, C.; He, C. *Chem. Rev.* **2008**, *108*, 3239–3265; (m)

- Arcadi, A. *Chem. Rev.* **2008**, *108*, 3266–3325; (n) Jiménez-Núñez, E.; Echavarren, A. M. *Chem. Rev.* **2008**, *108*, 3326–3350; (o) Hashmi, A. S. K.; Rudolph, M.; *Chem. Soc. Rev.* **2008**, *37*, 1766–1775; (p) Fürstner, A.; Davies, P. W. *Angew. Chem. Int. Ed.* **2007**, *46*, 3410–3449; (q) Hashmi, A. S. K. *Chem. Rev.* **2007**, *107*, 3180–3211; (r) Jiménez-Núñez, E.; Echavarren, A. M. *Chem. Commun.* **2007**, 333–346; (s) Zhang, L.; Sun, J.; Kozmin, S. A. *Adv. Synth. Catal.* **2006**, *348*, 2271–2296; (t) Hashmi, A. S. K.; Hutchings, G. J. *Angew. Chem. Int. Ed.* **2006**, *45*, 7896–7936; (u) Widenhofer, R. A.; Han, X. *Eur. J. Org. Chem.* **2006**, 4555–4563.
- [9] Gorin, D. J.; Toste, F. D. *Nature* **2007**, *446*, 395–403.
- [10] (a) Pyykkö, P. *Chem. Soc. Rev.* **2008**, *37*, 19677–1997; (b) Pyykkö, P. *Angew. Chem. Int. Ed.* **2004**, *43*, 4412–4456; (c) Schwartz, H. *Angew. Chem. Int. Ed.* **2003**, *42*, 4442–4454; (c) Pyykkö, P. *Angew. Chem. Int. Ed.* **2002**, *41*, 3573–3578; (d) Bond, G. C. *J. Mol. Catal. A: Chem.* **2000**, *156*, 17–20; (e) Pyykkö, P. *Chem. Rev.* **1988**, *88*, 5637–594.
- [11] (a) Patil N. T.; Kavthe, R. D.; Shinde V. S. *Tetrahedron* **2012**, *68*, 8079–8146; (b) Huang, H.; Zhou Y.; Liu H. *Beilstein J. Org. Chem.* **2011**, *7*, 897–936; (c) Hashmi, A. S. K.; Bührle, M. *Aldrichim. Acta* **2010**, *43*, 27–33.
- [12] Reppe, W. and co-workers *Liebigs Ann. Chem.* **1956**, *601*, 81.
- [13] Fukuda, Y.; Utimoto, K. *J. Org. Chem.* **1991**, *56*, 3729–3731.
- [14] Santos, L. L.; Ruiz, V. R.; Sabater, M. J.; Corma, A. *Tetrahedron* **2008**, *64*, 7902–7909.
- [15] (a) Hashmi, A. S. K.; Schwarz, L.; Choi, J.-H.; Frost, T. M. *Angew. Chem. Int. Ed.* **2000**, *39*, 2285–2288; (b) Liu, Y.; Song, F.; Song, Z.; Liu, M.; Yan, B. *Org. Lett.* **2005**, *7*, 5409–5412; (c) Du, X.; Song, F.; Lu, Y.; Chen, H.; Liu, Y. *Tetrahedron* **2009**, *65*, 1839–1845; (d) Antoniotti, S.; Genin, E.; Michelet, V.; Genêt, J.-P. *J. Am. Chem. Soc.* **2005**, *127*, 9976–9977; (e) Zhang, Y.; Xue, J.; Xin, Z.; Xie, Z.; Li, Y. *Synlett* **2008**, 940–944; (f) Liu, L.-P.; Hammond, G. B. *Org. Lett.* **2009**, *11*, 5090–5092; (g) Wilckens, K.; Uhlemann, M.; Czekelius, C. *Chem. Eur. J.* **2009**, *15*, 13323–13326.
- [16] (a) Genin, E.; Toullec, P. Y.; Antoniotti, S.; Brancour, C.; Genêt, J.-P.; Michelet, V. *J. Am. Chem. Soc.* **2006**, *128*, 3112–3113; (b) Genin, E.; Toullec, P. Y.; Marie, P.; Antoniotti, S.; Brancour, C.; Genêt, J.-P.; Michelet, V. *ARKIVOC* **2007**, (v) 67–78.

-
- [17] Harkat, H.; Dembelé, A. Y.; Weibel, J.-M, Blanc, A.; Pale, P. *Tetrahedron*, **2009**, *65*, 1871–1879.
- [18] Chary, B. C.; Kim, S. *J. Org. Chem.* **2010**, *75*, 7928–7931.
- [19] (a) Fukuda, Y.; Utimoto, K. *Synthesis* **1991**, 975–978; (b) Fukuda, Y.; Nozaki, H.; Utimoto K. *Heterocycles* **1987**, *25*, 297–300.
- [20] (a) Kang, J. E.; Kim, H. B.; Lee, J.-W.; Shin, S. *Org. Lett.* **2006**, *8*, 3537–3540; (b) Ritter, S.; Horino, Y.; Lex, J.; Schmalz, H.-G. *Synlett* **2006**, 3309–3313; (c) Enomoto, T.; Obika, S.; Yasui, Y.; Takemoto, Y. *Synlett* **2008**, 1647–1650; (d) Arcadi, A.; Bianchi, G.; Marinelli, F. *Synthesis* **2004**, 610–618.
- [21] (a) Wilckens, K.; Lentz, D.; Czekelius, C.; *Organometallics*, **2011**, *30*, 1287–1290; (b) Wilckens, K.; Uhlemann, M.; Czekelius, C. *Chem. Eur. J.* **2009**, *15*, 13323–13326.
- [22] Mourad, A. K.; Leutzow, J.; Czekelius, C. *Angew. Chem. Int. Ed.* **2012**, *51*, 11149–11152.
- [23] Lavallo, V.; Frey, G. D.; Donnadieu, B.; Soleihavoup, M.; Bertrand, G. *Angew. Chem. Int. Ed.* **2008**, *47*, 5224–5228.
- [24] Zeng, X.; Frey, G. D.; Kousar, S.; Bertrand, G. *Chem. Eur. J.* **2009**, *15*, 3056–3060.
- [25] (a) Mizushima, E.; Hayashi, T.; Tanaka, M. *Org. Lett.* **2003**, *5*, 3349–3352; (b) Leyva, A.; Corma, A. *Adv. Synth. Catal.* **2009**, *351*, 2876–2886; (c) Patil, N. T.; Kavthe, R. D.; Raut V. S.; Shinde, V. S.; Sridhar, B. *J. Org. Chem.* **2010**, *75*, 1277–1280.
- [26] (a) Monteiro, N.; Balme, J.; Gore, J. *Tetrahedron Lett.* **1991**, *32*, 1645–1648; (b) Monteiro, N.; Gore, J.; Balme, J. *Tetrahedron* **1992**, *48*, 10103–10114.
- [27] Kennedy-Smith, J. J.; Staben, S. T.; Toste, F. D. *J. Am. Chem. Soc.* **2004**, *126*, 4526–4527.
- [28] Mézailles, N.; Ricard, L.; Gagosz, F. *Org. Lett.* **2005**, *7*, 4133–4136.
- [29] Staben, S. T.; Kennedy-Smith, J. J.; Toste, F. D. *Angew. Chem. Int. Ed.* **2004**, *43*, 5350–5352.
- [30] Davies, P. W.; Detty-Mambo, C. *Org. Biomol. Chem.* **2010**, *8*, 2918–2922.
- [31] Binder, J. T.; Crone, B.; Haug, T. T.; Menz H.; Kirsch, S. F. *Org. Lett.* **2008**, *10*, 1025–1028.
- [32] (a) Martin-Matute, B.; Nevado, C.; Cárdenas, D. J.; Echavarren, A. M. *J. Am. Chem. Soc.* **2003**, *125*, 5757–5766. (b) Nevado, C.; Echavarren, A. M. *Chem. Eur. J.* **2005**, *11*, 3155–3164.

-
- [33] (a) Ferrer, C.; Echavarren, A. M. *Angew. Chem., Int. Ed.* **2006**, *45*, 1105–1109.
- [34] Ferrer, C.; Amijs, C. H. M.; Echavarren, A. M. *Chem. Eur. J.* **2007**, *13*, 1358–1373.
- [35] Reetz, M.; Sommer, K. *Eur. J. Org. Chem.* **2003**, 3485–3496.
- [36] Hashmi, A. S. K.; Blanco, M. C.; Kurpejović, E.; Frey, W.; Bats, J. W. *Adv. Synth. Catal.* **2006**, *348*, 709–713.
- [37] Nakamura, I.; Yamagishi, U.; Song, D.; Konta, S.; Yamamoto, Y. *Angew. Chem. Int. Ed.* **2007**, *46*, 2284–2287.
- [38] Nakamura, I.; Sato, T.; Terada, M.; Yamamoto, Y. *Org. Lett.* **2007**, *9*, 4081–4083.
- [39] Nakamura, I.; Sato, T.; Terada, M.; Yamamoto, Y. *Org. Lett.* **2008**, *10*, 2649–2652.
- [40] Istrate, F. M.; Gagosz, F. *Org. Lett.* **2007**, *9*, 3181–3184.
- [41] Asao, N.; Aikawa, H.; Yamamoto, Y.; *J. Am. Chem. Soc.* **2004**, *126*, 7458–7459.
- [42] Straub, F. *Chem. Commun.* **2004**, 1726–1728.
- [43] Asao, N.; Sato, K.; Menggenbateer; Yamamoto, Y. *J. Org. Chem.* **2005**, *70*, 3682–3685.
- [44] Asao, N.; Sato, K. *Org. Lett.* **2006**, *8*, 5361–5363.
- [45] (a) Jiménez-Núñez, E.; Echavarren, A. M. *Chem. Rev.* **2008**, *108*, 3326–3350; (b) Zhang, L.; Sun, J.; Kozmin, S. A. *Adv. Synth. Catal.* **2006**, *348*, 2271–2296.
- [46] MuCoz, M. P.; Adrio, J.; Carretero, J. C.; Echavarren, A. M. *Organometallics* **2005**, *24*, 1293–1300.
- [47] Jiménez-Núñez, E.; Claverie, C. K.; Nieto-Oberhuber, C.; Echavarren, A. M. *Angew. Chem. Int. Ed.* **2006**, *45*, 5452–5455.
- [48] Correa, A.; Marion, N.; Fensterbank, L.; Malacria, M.; Nolan, S. P.; Cavallo, L. *Angew. Chem. Int. Ed.* **2007**, *46*, 718–721.
- [49] Marion, N.; Nolan, S. P. *Angew. Chem. Int. Ed.* **2007**, *46*, 2750–2752.
- [50] Zhao, J.; Hughes, C. O.; Toste, F. D. *J. Am. Chem. Soc.* **2006**, *128*, 7436–7437.
- [51] Wang, S.; Zhang, L.; *J. Am. Chem. Soc.* **2006**, *128*, 8414–8415.
- [52] Shi, X.; Gorin, D. J.; Toste, F. D. *J. Am. Chem. Soc.* **2005**, *127*, 5802–5803.
- [53] Zhang, L. *J. Am. Chem. Soc.* **2005**, *127*, 16804–16805.
- [54] Li, G.; Zhang, L. *Angew. Chem. Int. Ed.* **2007**, *46*, 5156–5159.
- [55] Yeon, H.-S.; Lee, J.-E.; Shin, S. *Angew. Chem. Int. Ed.* **2008**, *47*, 7040–7043.
- [56] Ye, L.; Cui, L.; Zhang, G.; Zhang, L. *J. Am. Chem. Soc.* **2010**, *132*, 3258–3259.

-
- [57] Tamaki, A.; Kochi, J. K.; *J. Organomet. Chem.* **1973**, *64*, 411–425.
- [58] (a) Wegner, H. A.; Auzias M. *Angew. Chem. Int. Ed.* **2011**, *50*, 8236–8247; (b) Wegner, H. A. *Chimia* 2009, 44–48.
- [59] Wegner, H. A.; Ahles, S.; Neuenburg, M. *Chem. Eur. J.* **2008**, *14*, 11310–11313.
- [60] Zhang, G.; Peng, Y.; Cui, L.; Zhang, L. *Angew. Chem. Int. Ed.* **2009**, *48*, 3112–3115.
- [61] Boorman T.C.; Larrosa, I. *Chem. Soc. Rev.* 2011, **40**, 1910–1925. (b) Haro, T. de; Nevado, C. *Synthesis* **2011**, 2530–2539.
- [62] Brand, J. P.; Charpentier J.; Waser, J. *Angew. Chem. Int. Ed.* **2009**, *48*, 9346–9349.
- [63] Jurberg, I. D.; Odabachian Y.; Gagosz, F. *J. Am. Chem. Soc.* **2010**, *132*, 3543–3552.
- [64] (a) Hashmi A. S. K.; Rudolph M.; *Chem. Soc. Rev.* **2008**, *37*, 1766–1775; (b) Rudolph M.; Hashmi A. S. K. *Chem. Soc. Rev.* **2012**, *41*, 2448–2462.
- [65] Li, Y.; Zhou F.; Forsyth, C. J. *Angew. Chem. Int. Ed.* **2007**, *46*, 279–282.
- [66] (a) Trost, B. M.; Dong, G. *Nature chemistry*, **2008**, 485–488; (b) Trost, B. M.; Dong, G. *J. Am. Chem. Soc.* **2010**, *132*, 16403–16416.
- [67] Enomoto, T.; Yasui, Y.; Takemoto, Y. *J. Org. Chem.* **2010**, *75*, 4876–4879.
- [68] Nakajima, R.; Ogino, T.; Yokoshima, S.; Fukuyama, T. *J. Am. Chem. Soc.* **2010**, *132*, 1236–1237.
- [69] Sato, K.; Asao, N.; Yamamoto Y. *J. Org. Chem.* **2005**, *70*, 8977–8981.
- [70] Staben, S. T.; Kennedy-Smith, J. J.; Huang, D.; Corkey, B. K.; Lalonde, R. L.; Toste, F. D. *Angew. Chem. Int. Ed.* **2006**, *45*, 5991–5994.
- [71] Linghu, X.; Kennedy-Smith J. J.; Toste, F. D. *Angew. Chem. Int. Ed.* **2007**, *46*, 7671–7673.
- [72] K. C. Nicolaou *et al.* *Angew. Chem. Int. Ed.* **2008**, *47*, 1780–1783.
- [73] Jimenez-Nuñez, E.; Molawi, K.; Echavarren, A. M. *Chem. Commun.* **2009**, 7327–7329.
- [74] Zhou, Q.-F.; Chen X.-F.; Ma, D.-W. *Angew. Chem. Int. Ed.* **2010**, *49*, 3513–3516.
- [75] Molawi, K.; Delpont N.; Echavarren, A. M. *Angew. Chem. Int. Ed.* **2010**, *49*, 3517–3519.
- [76] Garayalde, D.; Kru"ger K.; Nevado, C. *Angew. Chem. Int. Ed.* **2011**, *50*, 911–915.
- [77] Shi, H.; Fang, L.; Tan, C.; Shi, L.; Zhang, W.; Li, C.-C.; Luo T.; Yang, Z. *J. Am. Chem. Soc.* **2011**, *133*, 14944–14947.
- [78] Cui, L.; Peng Y.; Zhang, L. *J. Am. Chem. Soc.* **2009**, *131*, 8394–8395.

Relay Catalytic Branching Cascade: A Technique to Access Diverse Molecular Scaffolds

Table of Contents

2.1 Introduction:	42
2.2 Hypothesis	46
One Pot Catalysis: A Strategic Classification	47
2.3 Results and Discussion	49
2.3.1 Substrate Scope	49
2.3.2 Mechanistic Studies:	53
2.4 Polyheterocyclic Scaffolds Accessed Through RCBC–Literature Known Synthesis and Their Applications.....	54
2.5 Conclusion	62
2.6 Experimental Procedures and Characterization Data	63
2.7 Spectra	95
2.8 References	1198

2.1 Introduction

Small organic molecules are useful probes for studying cellular pathways. Small molecules are capable of interacting with biomacromolecules such as proteins generally in a reversible manner, thereby modulating their function.¹ In order to find a selective small molecule modulator of any protein function a structurally diverse compound collection is required.² Natural products are one of the greatest sources of diverse small molecules with a broad bioactivity profile.³ However, there are some difficulties associated with natural products in screening experiments; for instance, their isolation, purification, identification of biologically active components, and more importantly, nature fails to provide several analogues which are necessary for structure activity relationship (SAR) studies. These problems have led to a complementary approach of synthesizing structurally diverse small molecules directly and efficiently, an approach known as diversity oriented synthesis (DOS).⁴

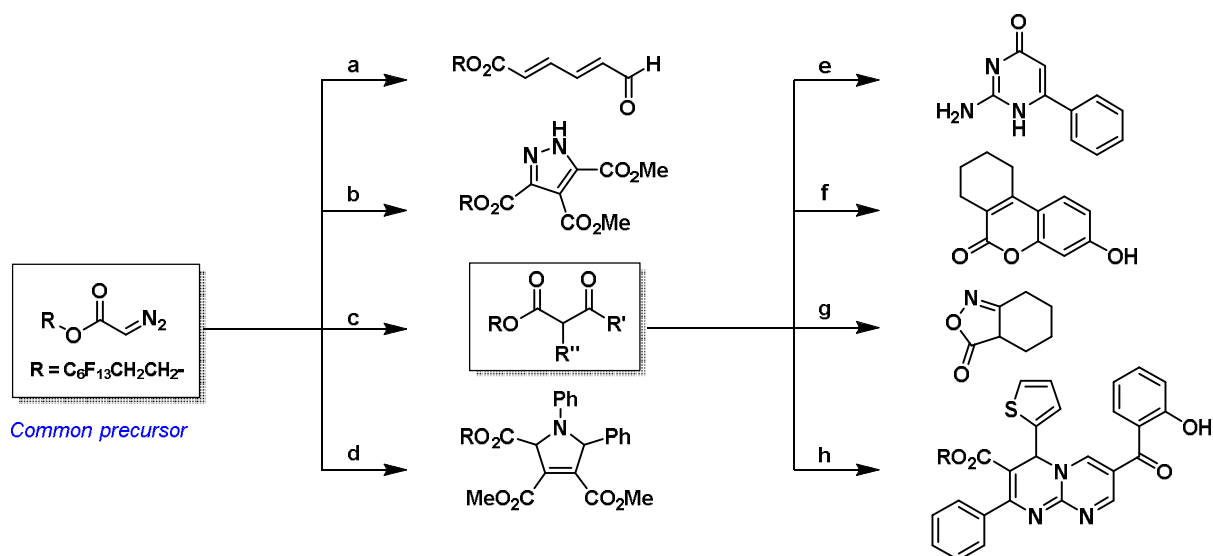
Diversity Oriented synthesis (DOS), a terminology initially coined by Prof. Schreiber⁵ considered as one of the techniques for identifying the biologically relevant chemical space.⁶ Several DOS strategies such as build-couple-pair strategy,⁷ click-click-cyclize strategy,⁸ fragment based approach⁹...etc¹⁰ have been introduced in the literature. In recent years, branching cascade technique has been gained much interest because of its potential to transform a common type of starting material into diverse and distinct molecular frameworks under the influence of either reagents or conditions.¹¹ The branching cascade approach is particularly appealing because it is possible to access a library of thousands of compounds in an efficient manner through a philosophy of permutation and combination.

To address this challenge of incorporating skeletal diversity in a compound collection, the “branching pathway” strategy has been proposed as a form of diversity oriented synthesis (DOS).¹² In this strategy, a common substrate is transformed into diverse and distinct molecular scaffolds under the influence of different reagents or reaction conditions.¹³ However, this approach exploits only intermolecular transformations and as a consequence yields only limited skeletal diversity, often following a multistep synthesis. For the enrichment of a compound library with molecular complexity and scaffold diversity the common precursor should facilitate a wide range of complexity-generating transformations in a rapid and concise manner.

In this context Spring and coworkers¹⁴ have reported branching strategy for the generation of structurally diverse scaffolds (Scheme 2.1). The authors used fluororous-tagged diazoacetate as a

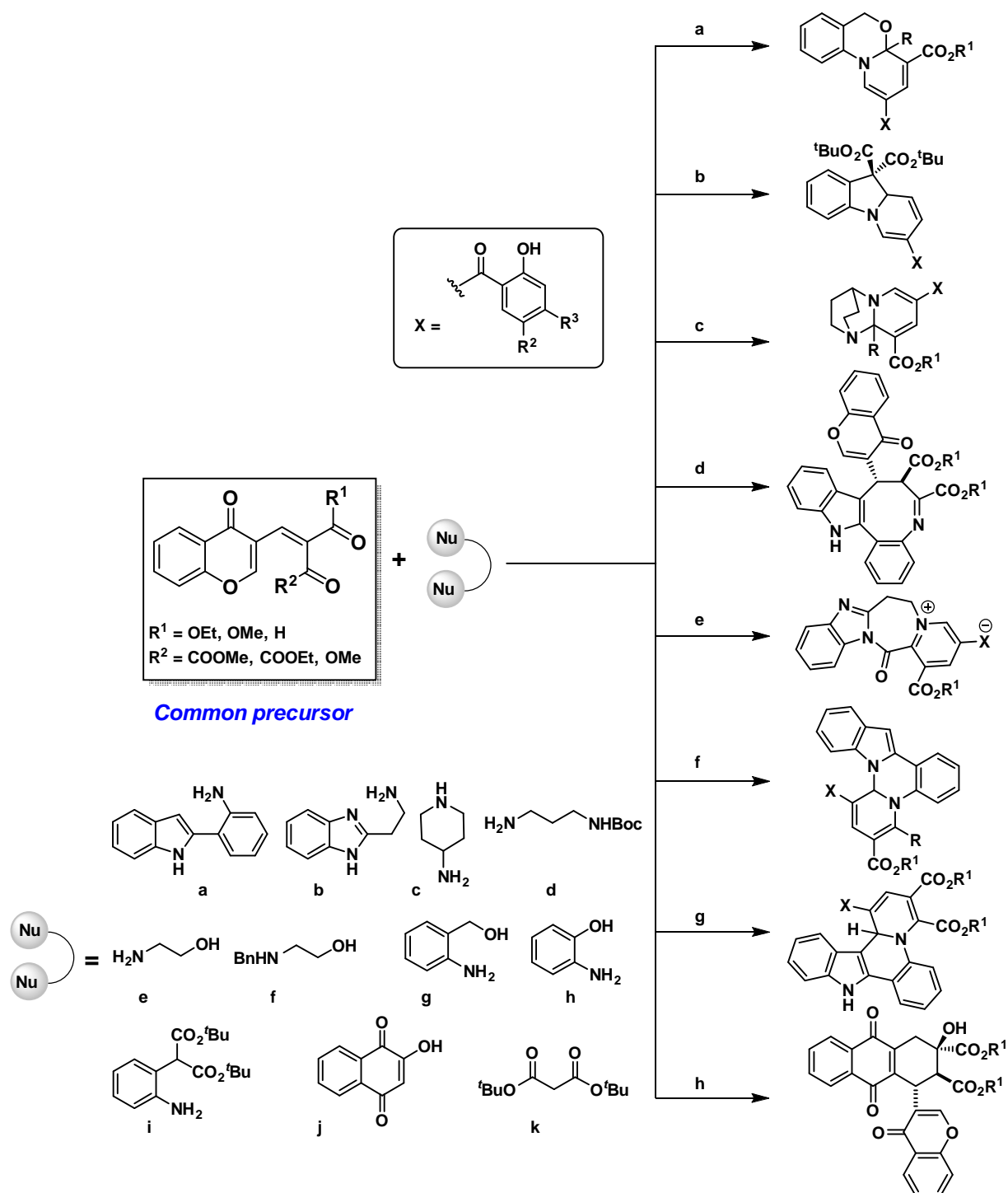
common substrate to access a broad range of skeletally distinct scaffolds by utilizing different reaction conditions (a-d). Since the key diazoacetate intermediate is relatively unfunctionalized, the diversity in the product results from the nature of the another starting material used in the reaction. In addition they also showed the scope and synthetic utility of this newly developed branching synthetic strategy by diversifying the one of product by using different reaction conditions (e-h).

Scheme 2.1: Branching strategy for the generation of structurally diverse scaffolds from fluororous-tagged diazoacetate as a common precursor



Reaction Conditions: (a) $Rh_2(OAc)_4$, furan, then I_2 , 60%. (b) DMAD, 84%. (c) LDA, $RCOR_9$, then $Rh_2(OAc)_4$, 68% (97%). (d) PhCHO, $PhNH_2$, then DMAD, $Rh_2(OAc)_4$, d.r. = 20 : 1, 51%. (e) Guanidine carbonate 62%. (f) Resorcinol, H_2SO_4 , 74%. (g) NH_2OH , 77%. (h) Thiophene-2-carboxaldehyde, guanidine carbonate, then 3-formylchromone, 43%.

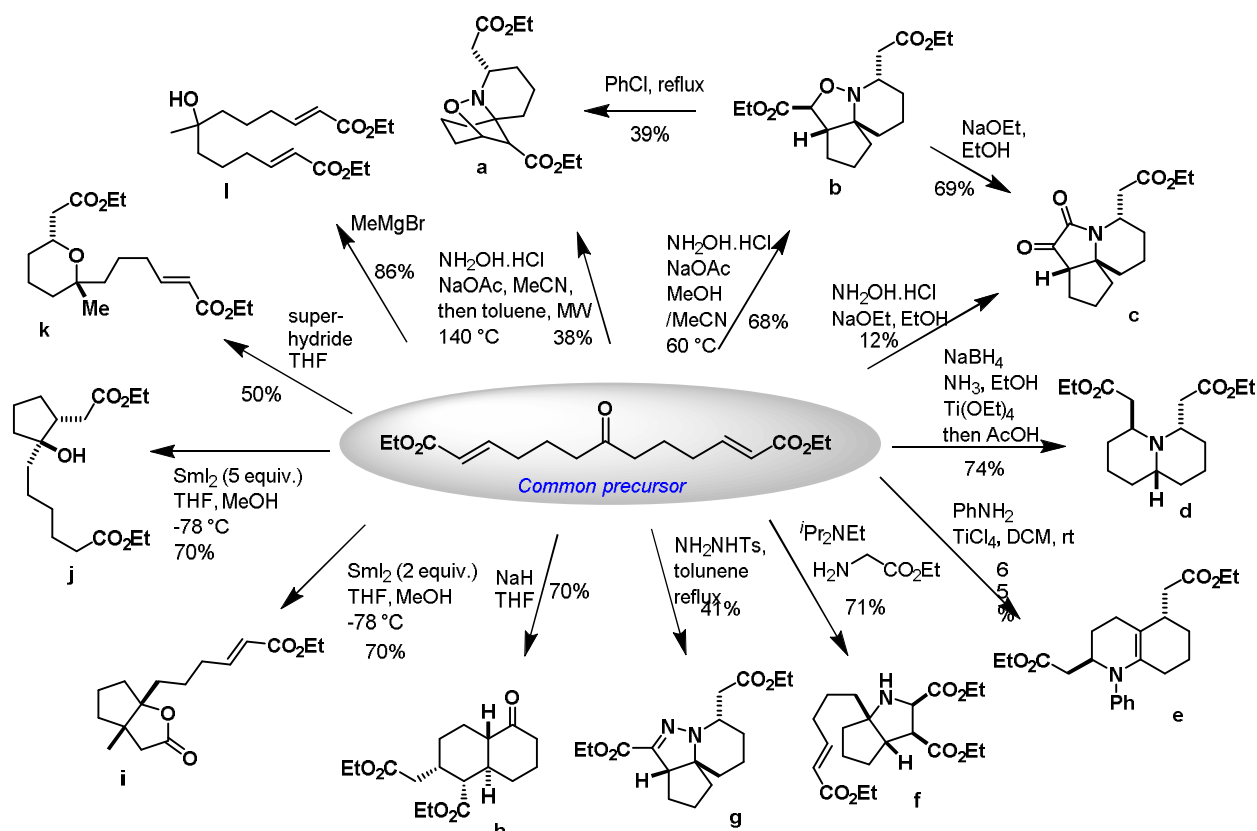
In 2011, Kumar and coworkers¹⁵ reported 12-fold branching cascade targeting diverse and complex molecular framework from chromone-based starting material. A chromone-based common precursor **2** had chosen since it contains multiple electrophilic as well as pronucleophilic sites and vinylogous ester (a leaving group) to trigger the cascade reaction with various bis-nucleophiles (Scheme 2.2).

Scheme 2.2: Branching cascade strategy from chromone-based compound as a common precursor

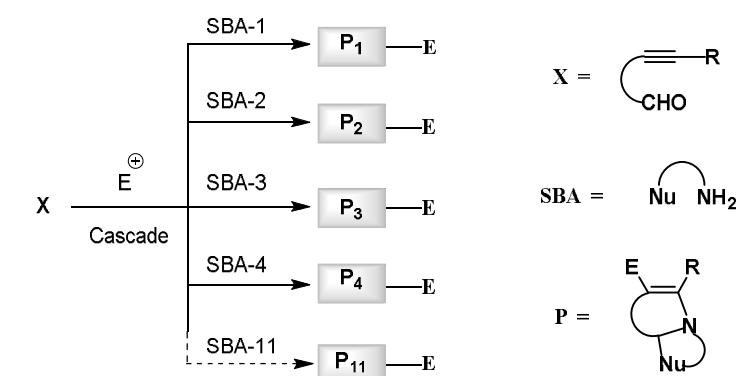
Almost at the same time, a 12-fold branching cascade was reported by O'Connell and Stockman¹⁶ to access a range of carbo-, aza- and oxo-cycles, with fused, spiro and bridged

polycyclic structures from a keto-diester as a common starting material (Scheme 2.3). The author selected keto-diester **5** as a substrate for investigation of a diversity-approach based on tandem reactions due to its very simple three-step synthesis from readily accessible starting materials and its functionality: a central ketone is able to be transformed into a range of nucleophilic functionalities, which can then react with the tethered α , β -unsaturated esters at the termini of the chain.

Scheme 2.3: 12-Fold branching cascade from a keto-diester compound as a common precursor

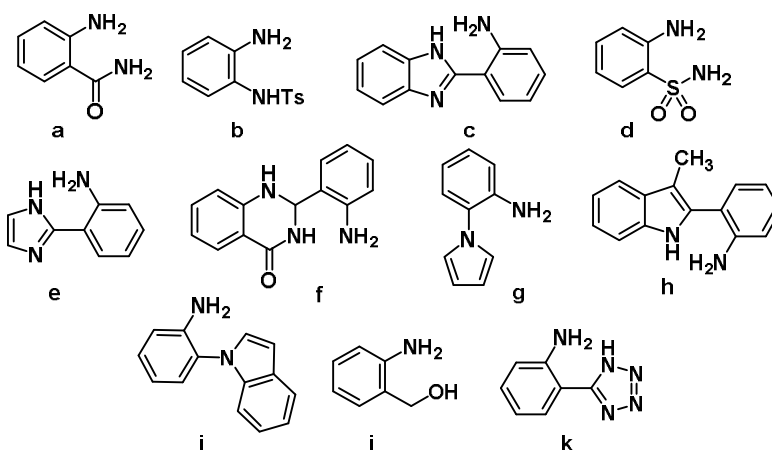


Very recently, our research group¹⁷ also devised electrophile induced branching cascade (EIBC) as an interesting and direct approach for the efficient generation of a library of drug like compounds. As shown in scheme 2.4, a wide array of scaffold building agents (termed as SBA hereafter) and bisnucleophiles **a-k** (amino-aromatics, amino-alcohols, diamines, etc.) participated smoothly with 2-alkynyl benzaldehyde **X** (common precursor) in the reaction leading to a powerful approach to polyheterocyclic scaffolds in moderate to good yields.

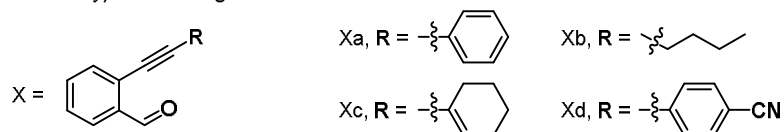
Scheme 2.4: 11-Fold branching cascade from 2-alkynyl benzaldehyde as a common precursor

X = common type of starting material; SBA = scaffold building agent; P = product;
E⁺ = electrophile

Scaffold Building Agents (SBAs):



Common Type of Starting Materials:

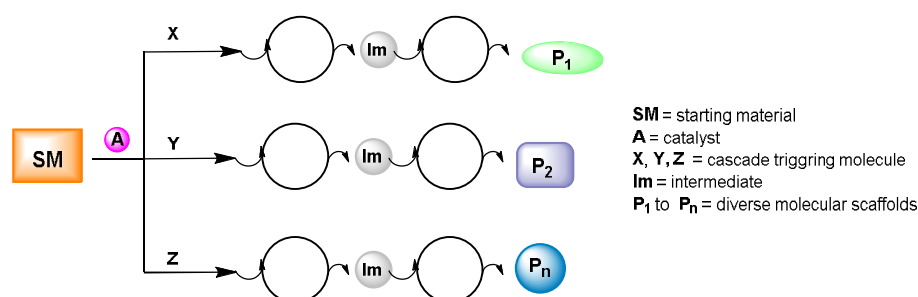


2.2 Hypothesis

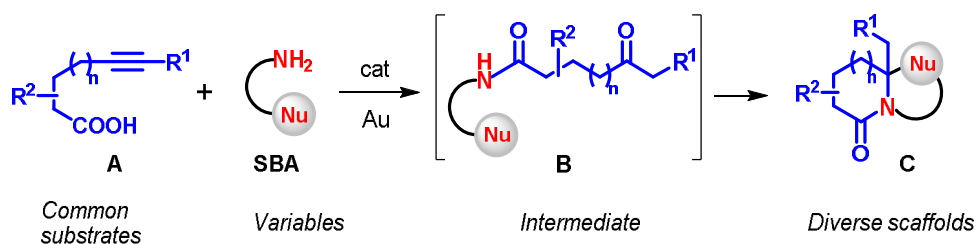
Although, there are quite a few reports on branching cascades, to the best of our knowledge, there was no precedence for analogues catalytic branching cascade of very high magnitude. Therefore, it was thought that whether it would be possible to develop catalytic branching cascade technique-a process which would allow the synthesis of several multifunctional polyheterocyclic scaffolds (Scheme 2.5).¹⁸ More specifically, it was envisaged that the alkyonic acid (a common type

of substrate) **A** would react with several SBA (variables) in the presence of suitable metal catalysts leading to the formation of **C**. The keto-amides **B** would then undergo metal catalyzed cyclization cascade to produce various heterocyclic scaffolds.¹⁹ Overall, the process can be termed as relay catalytic branching cascade (termed as RCBC hereafter) with view of classification of one-pot catalysis proposed by us (Fig 2.1).²⁰ A main challenge and beauty of the methodology would be the widely accessible scaffold diversity, due to the design of a large number of SBAs (Fig 2.5) in an apparently simple manner.

Figure 2.1: Concept of Relay Catalytic Branching Cascades



Scheme 2.5 Concept of relay catalytic branching cascades employing alkynoic acids (common type of substrate) and SBA (variables)



One Pot Catalysis: A Strategic Classification

The development of one-pot processes that allows many reactions to occur in a single flask has a significant impact in the synthesis of fine chemicals and drugs. One-pot catalysis avoids the time, labour and yield losses associated with the isolation and purification of intermediates in multistep sequences. Increased focus has recently been placed on the development of multiple

catalyst system for organic transformations that allow rapid construction of highly functionalized molecules from simple and readily available starting materials. The reaction catalyzed by two different catalysts (metal-metal, metal-organocatalyst and organo-organocatalyst) at the same time can provide an access to reactivity and selectivity of the reaction otherwise not possible by a single catalyst alone. Clearly, such a reaction can provide a powerful tool to synthesise highly complex molecules preserving energy and resources. The classification of one-pot catalysis has been reported by Fogg and Santos in 2004.²¹ However, the classification is very broad and is not well suited to describe the examples of recent literature in a precise manner. We recently have proposed the strategic classification of one-pot catalysis into three categories such as cooperative, relay and sequential catalysis (Figure 2.3, 2.4 and 2.5). The new classification encompasses the recent examples and we believe that this classification may find extensive application for understanding the type of catalysis precisely. In order to illustrate this classification, a series of recent examples which utilizes either metal-metal, metal-organo and organo-organo catalysts have been taken into consideration.²⁰

Figure 2.2 Cooperative catalysis

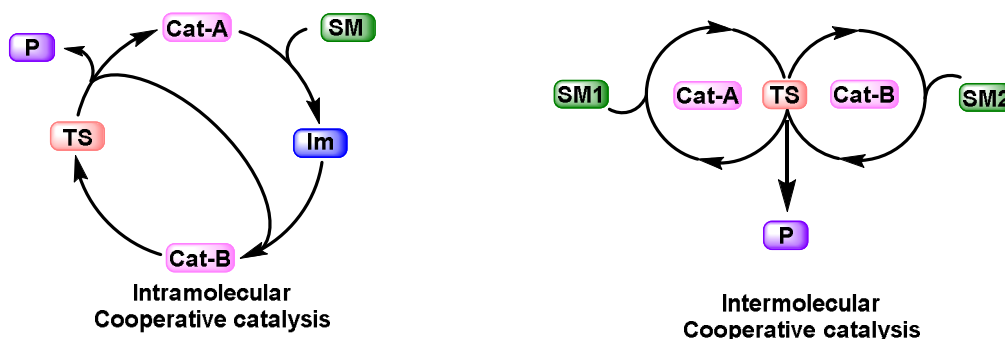


Figure 2.3 Relay catalysis

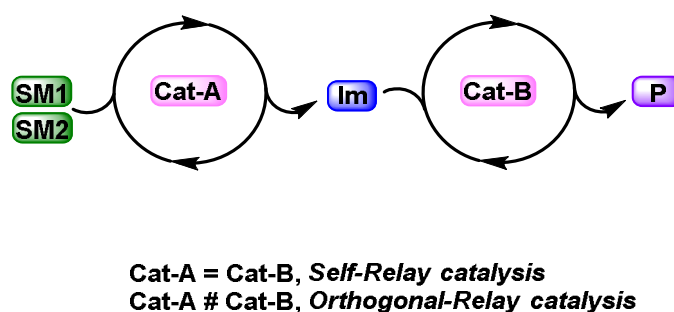
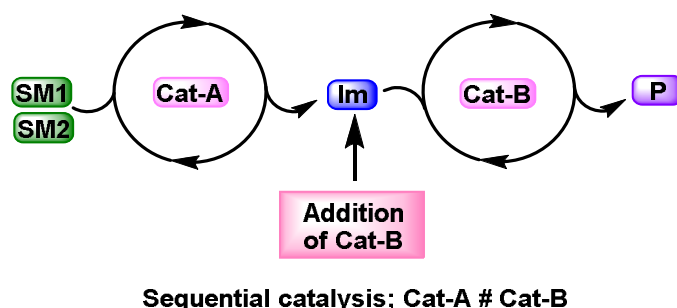


Figure 2.4 Sequential catalysis



2.3 Results and Discussion

At the outset of this study, efforts were directed to find an appropriate reaction conditions which would work well for a broad range of SBA's. Since it is known that the judicious choice of a π -acid²² influence the outcome of the reaction, it has been decided to study these reactions in greater detail using a variety of catalysts, solvents and temperature. The catalyst Ph₃PAuOTf in DCE was found to be the best over a large number SBAs. An equimolar mixture of scaffold building agents **1-30** and alkynoic acids **I-VIII** in the presence of Ph₃PAuOTf (5 mol %) was heated in DCE at 100 °C for 24-36 h (Fig 2.6). In almost all cases, the starting materials were completely consumed and afforded the products in good to high yields.

2.3.1 Substrate Scope

To begin with, first we focused the attention on indole based SBA as this heterocycle finds widespread occurrence in nature and have remarkable biological activities. Interestingly, the reaction was proved to be very general over 10 SBAs giving various indole fused heterocyclic scaffolds in good to high yields. For instance, 2-aminophenylindole **1** afforded dihydro-indolo[3,2-*c*]pyrrolo[1,2-*a*] quinolinone **1a** and **1b** in 79 and 69% yields [br(branch)-A] (Figure 2.6). Likewise, SBA **2**, and indol-4-yl methanamine **3** reacted well with terminal as well as internal alkyne to afford corresponding pyrroloquinolinones **2a** (br-B) and pyrrolo isoquinolinones **3a** and **3b** (br-C) with moderate to high yields.

Figure 2.5 Structures of various scaffold building agents (SBAs)

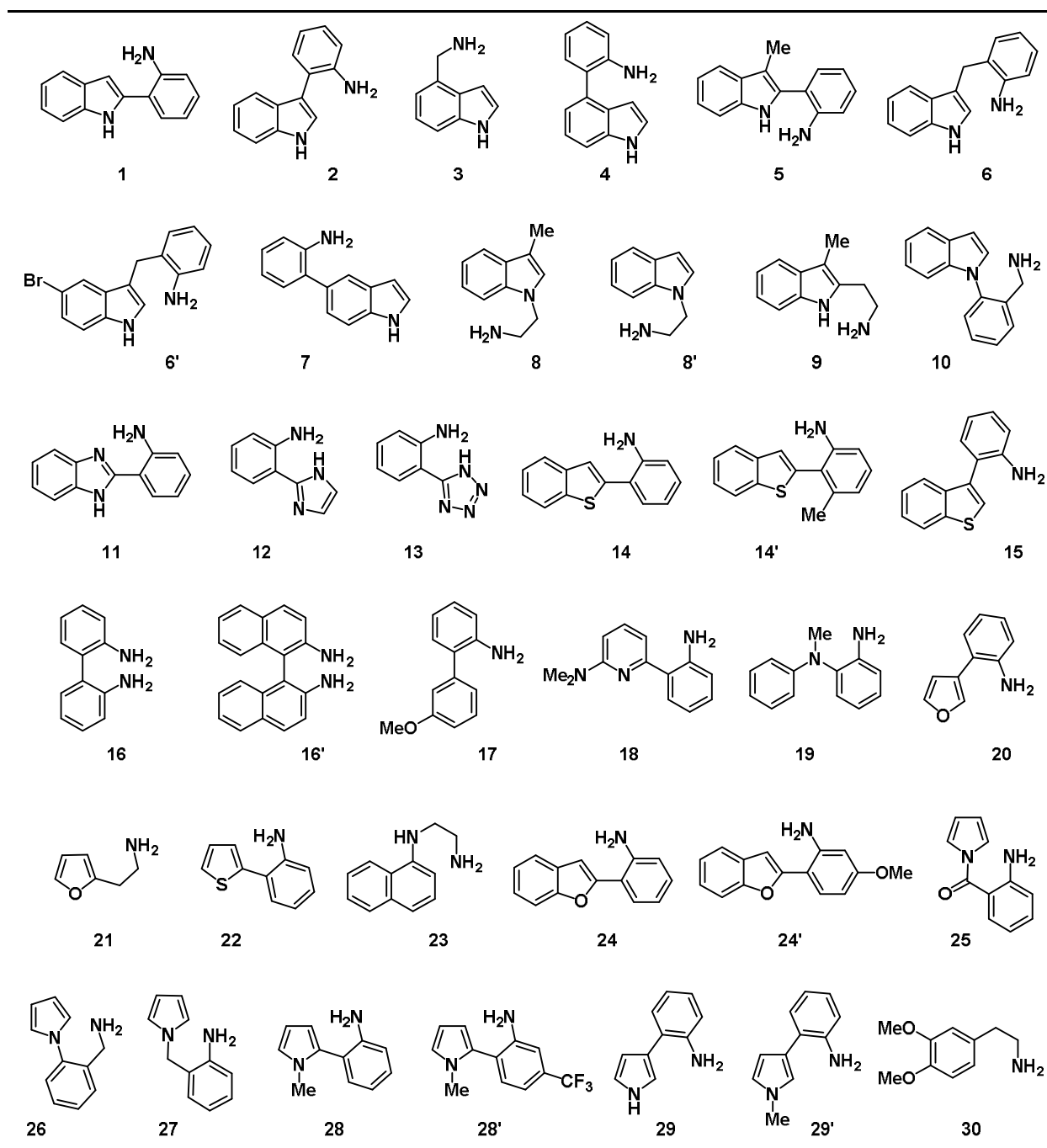
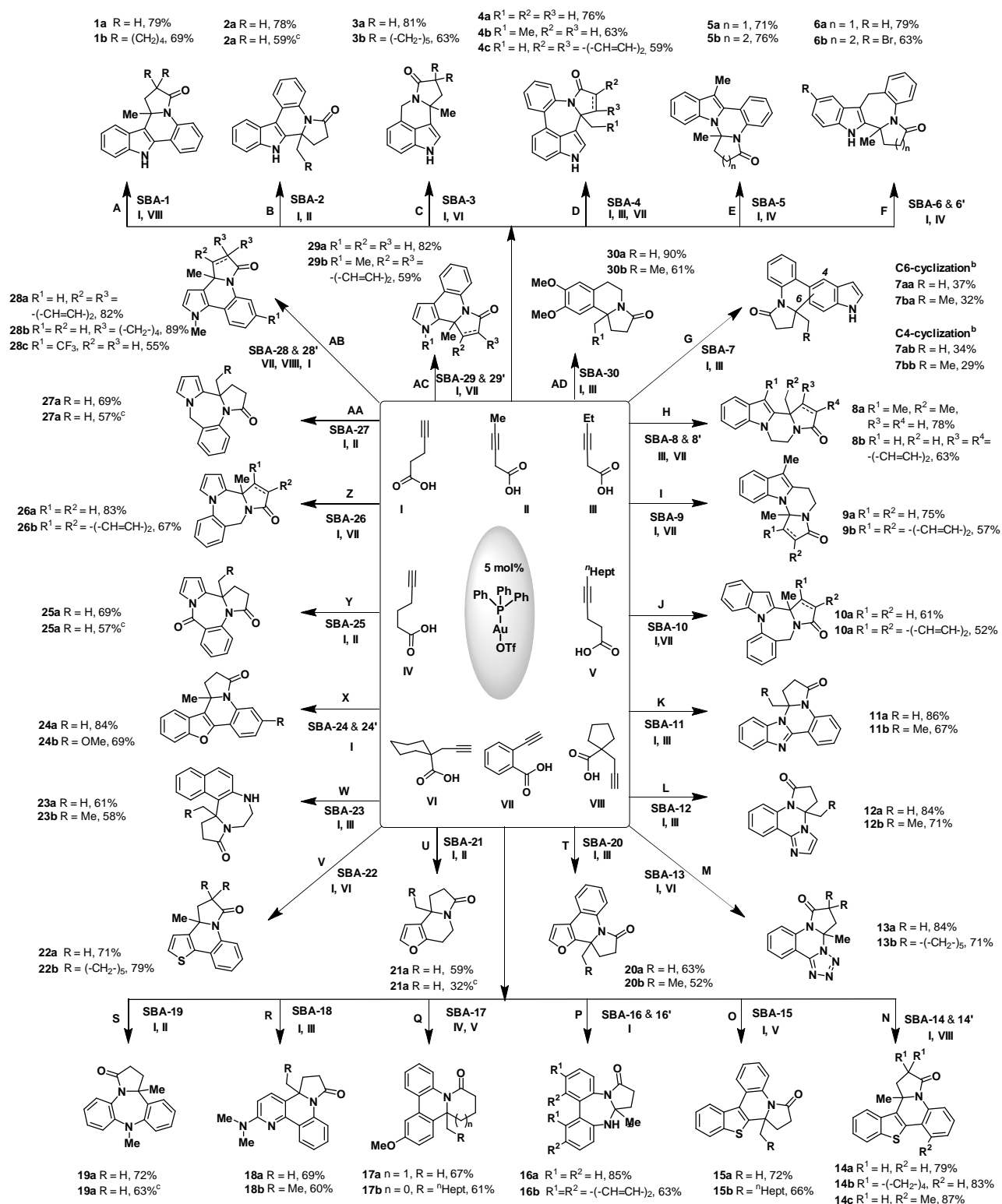


Figure 2.6 Generation of scaffold diversity through RCBC



[a] Reactions conditions: SBAs (0.5 mmol), alkyne acids (0.5 mmol), Ph₃PAuOTf catalyst (5 mol %) in DCE (1 M) at 100 °C for 24 h; [b] mixture of (1:1) regioisomer

[c] The alkyne acid I and II produced same cascade products.

NOTE: (1) Reaction time was prolonged upto 36 h for **4c**, **7**, **10a**, **10b**, **16b**, **8a**, **18b**, **23a**, **23b**, **25a**, **25b**, **26a**, **26a**, **27a**, **27b**; (2) SBA - Scaffold building agents; I-VIII represent alkyne acids and A, B, C.....AD -represents branches

Similarly, SBA **4** underwent cascade cyclization under the developed protocol to afford indolo-benzazepinones **4a** and **4b** in 76 and 63% yields, respectively (br-D). Interestingly, the 2-ethynyl benzoic acid also reacted well, giving **4c** in 59% yield. This experiment confirms that additional aromatic rings can be introduced in SBA to obtain functionalized polycyclic heteroaromatics. To further expand the scope, indolamine **5** and **9** were reacted with corresponding alkynoic acids to give indolo[1,2-*c*]pyrido[1,2-*a*]quinazolinones **5a/5b** (br-E) and **9a/9b** (br-I) which could have formed via intramolecular attack of indole N-H to the incipient iminium ions. The polycyclic benzazepinoneindolones **6a** and **6b** were also obtained in 79% and 63% yields from the SBA **6** and **6'** (br-F). The halo-substituted compound such as **6b** can serve as versatile synthons enabling the introduction of various functional groups and expanding the availability of the target diverse libraries of products. When indole based amino aromatic **10** were employed as a substrate various seven membered ring products were formed with moderate yields although relatively longer reaction time was needed for the full substrate conversion (br-J).

Interestingly; when SBA **7** was used, almost 1:1 mixture of two regioisomers (resulted through C4 and C6 cyclization) were obtained. The regioisomers found to be easily separable by column chromatography. It should be noted that each of the regioisomer obtained represents the skeletally distinct pyrrolo-phenanthridinone scaffolds (br-G). Both terminal as well as internal alkynoic acid shown similar reaction profile towards **7**, though reaction was somewhat sluggish and took 36 h for completion. The SBA **8** and **8'** also reacted well affording C2 cyclized polyheteroaromatic scaffolds in 78 and 63% yield (br-H).

To further explore the generality and scope of this approach, different benzimidazole **11**, 2-(2-aminophenyl imidazole) **12** as well as 2-(2-aminophenyl tetrazole) **13** were used and expected cascade products were isolated in very high yields. The SBA **12** and **13** reacted with terminal as well as internal alkynoic acids **I** and **II** that led to the formation various scaffolds such as imidazolo-quinazolinones (br-L) and tetrazolo-quinazolinones (br-M). The excellent reaction profiles observed with amino benzothiophenes SBA **14** and **15** affording C2 and C3 cyclization products respectively with good yields (br-N and O). The SBA, 2-(2-amino-thiophene), **22** also reacted well under the established conditions affording dihydropyrrolo[1,2-*f*]thieno[3,2-*c*]quinolinone **22a** and **22b** with 71% and 79% yields (br-V).

Interestingly, biaryl 1,4-diamines **16** and **16'** reacted with alkynoic acid **I** giving products with strained seven membered pyrrolo-diazepinones in good yields (br-P). Moreover, pyrido-phenanthridinone scaffolds were also obtained from 3'-methoxybiphenyl-2-amine (SBA **17**) (br-

Q). Gratifyingly, the pyridine based SBA **18** worked well for this transformation that produced fused ring products with moderate yields (br-R). Notably, donating effect of N, N-dimethylamine at 6 position has key role for the success of this reaction; the absence of which does not lead the formation of product. Considering the prevalence and importance of seven membered benzodiazepine scaffolds, the reactivity of SBA **19** has been explored and fortunately the reaction worked very well in this case (br-S). The SBA **23** having naphthalene core with aliphatic side chain connecting NH₂ and aryl system also produced 7-membered ring product with cyclization at β -position of naphthalene (br-W). The protocol was equally successful for 2-(furan-3-yl) aniline **20** and 2-furanyl ethanamine **21** as substrates that led to the formation of dihydrofuro[2,3-*c*]pyrrolo[1,2-*a*]quinolinone and tetrahydrofuro[2,3-*g*]indolizinone, respectively (br-T and U). The SBA **24** (2-aminophenylbenzofuran) also reacted well under the optimized conditions affording dihydrobenzofuro[3,2-*c*]pyrrolo[1,2-*a*]quinolinones in good yields (br-X).

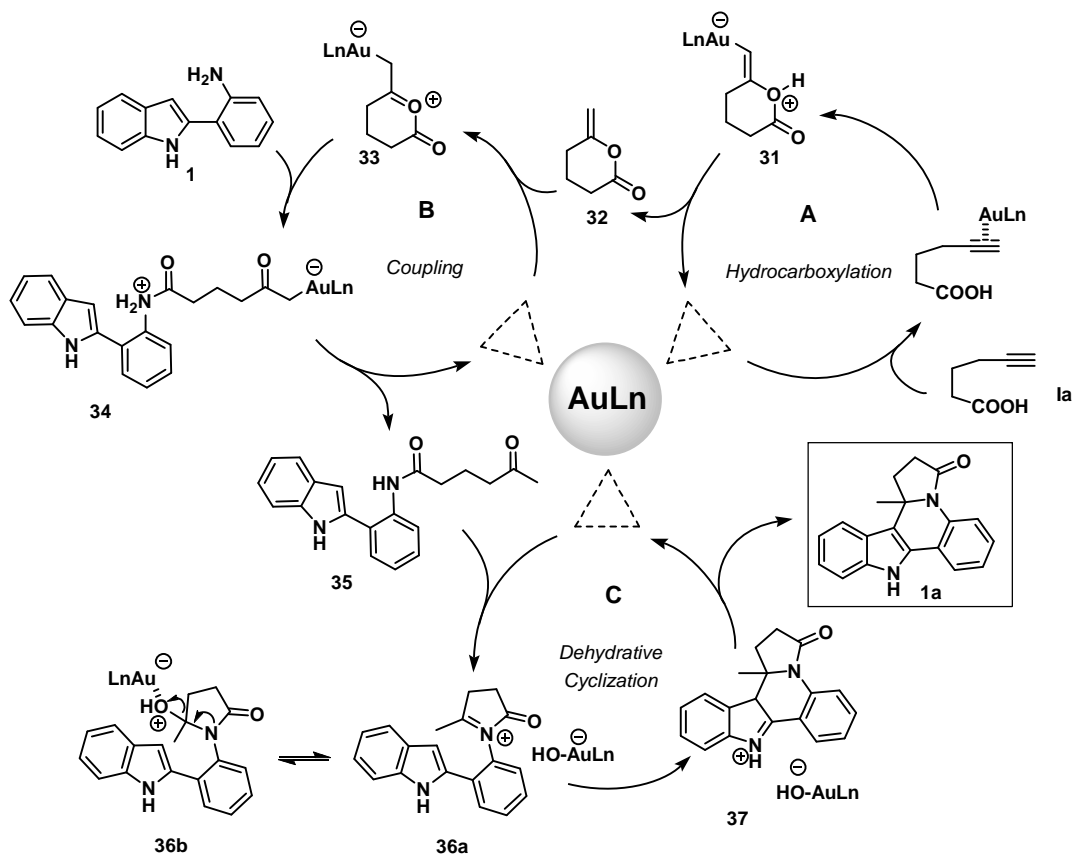
Next, the pyrrole based SBAs were used for extending the scope of protocol. As a general trend and as anticipated all reactions with pyrrole based SBAs such as **25**, **26**, **27**, **28**, **29** worked well affording fused heterocyclic products with five, six and seven membered rings. The SBA **25**, **26** and **27** produced seven membered benzo-dipyrrolo diazepinone scaffolds (br-Y/Z/AA). The SBA **28** and **28'** resulted in six membered C3 cyclized isoindolo[2,1-*a*]pyrrolo[3,2-*c*]quinolinone whereas SBA **29** and **29'** produced C2 cyclized dipyrrolo-quinolinone (br-AB/AC) with high to moderate yields. The SBA **30**, dimethoxy phenyl ethanamine, found to be reacted well under the established conditions with alkynoic acid **I** and **III** to produce tetrahydropyrrolo[2,1-*a*]isoquinolinones **30a** and **30b** in 90% and 61% yields respectively (Figure 2.6, br-AD).

2.3.2 Mechanistic Studies

A mechanism involving multiple catalytic cycles for the gold-catalyzed formal carboamination of alkynoic acid is outlined in Figure 2.7. The first step would be the complexation of Au(I) catalyst to the alkyne function undergoes intramolecular cyclization directly by the attack of proximal hydroxyl group to form the vinylgold intermediate **31**(cycle **A**). The next step would be the proto-demetalation to generate exocyclic enol lactone **32** with the release of catalyst. Once **32** is formed, it enter to another catalytic cycle **B** where Ph₃PAuOTf supposed to act as a Lewis acid. Thus, the Lewis acidic Au(I) complex catalyzes the formation of oxonium ion **33** from **32**. Intermolecular nucleophilic addition of the 2-(1*H*-indol-2-yl)aniline (**1**) to **34**) followed by proto-

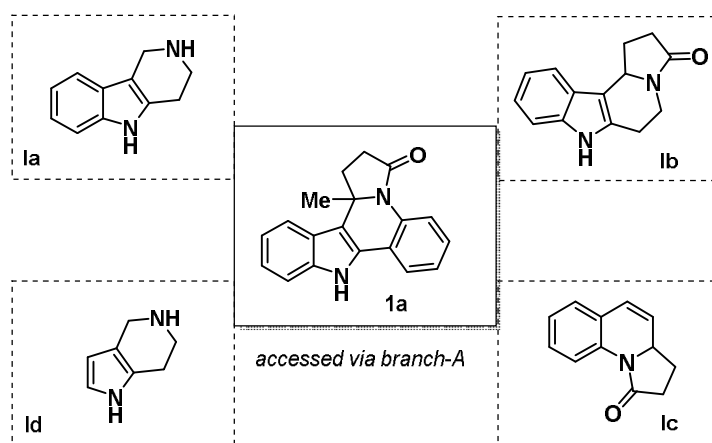
demetalation would lead to the keto amide **35** with the liberation of the catalyst. The keto amide **35** would then be poised to undergo *N*-acyl iminium ion^[29] formation **36a/36b** in the presence of Au(I) catalyst which after intramolecular trapping by tethered amine would produce final product **1a** (cf. **37**) with the regeneration of catalyst.

Figure 2.7 Proposed reaction mechanism



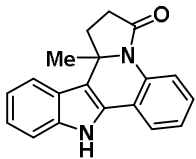
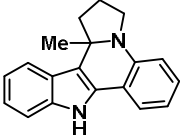
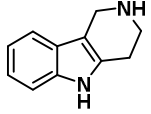
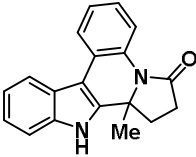
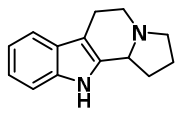
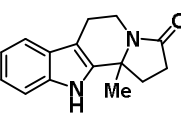
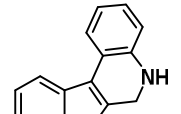
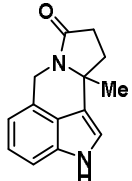
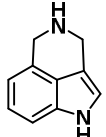
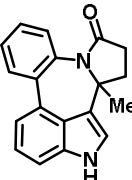
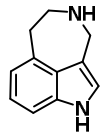
2.4 Polyheterocyclic Scaffolds Accessed Through RCBC–Literature Known Synthesis and Their Applications

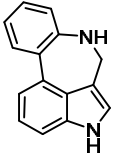
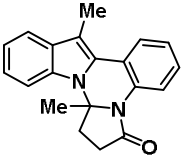
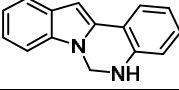
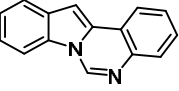
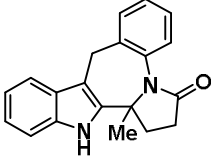
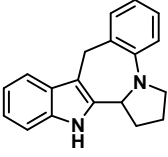
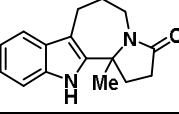
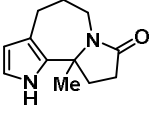
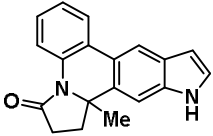
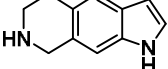
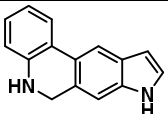
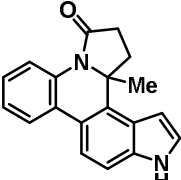
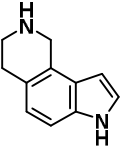
Nitrogen heterocycles are widespread in various natural products and biologically active molecules. They have been assigned as privileged structures in drug development because of their rigid conformation which in turn results in their ability to bind to a multitude of receptors through a variety of favourable interactions. Therefore the synthesis of nitrogen containing polycyclic heteroaromatics is an important goal in organic synthesis. In this regards, the library approach reported herein is appealing because there exists a possibility to generate a library of thousand of nitrogen containing compounds in an efficient manner.

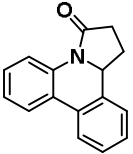
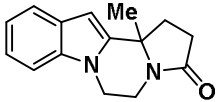
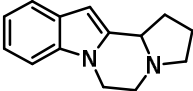
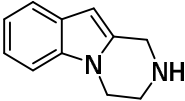
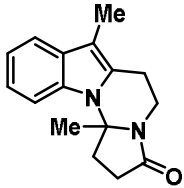
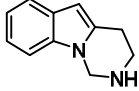
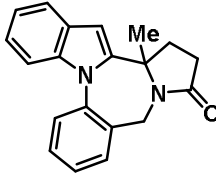
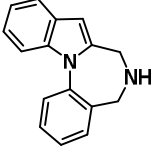
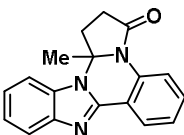
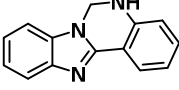
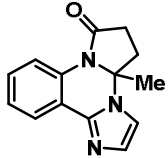
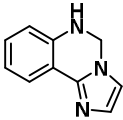
Figure 2.8 End product as a hybrid scaffold: branch A as an example

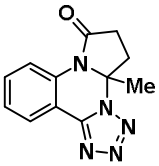
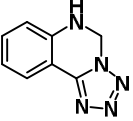
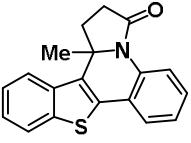
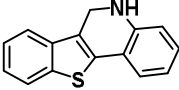
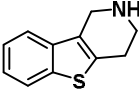
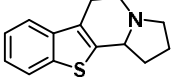
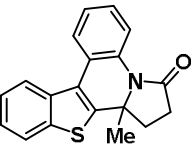
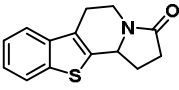
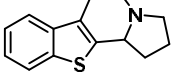
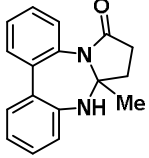
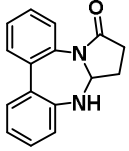
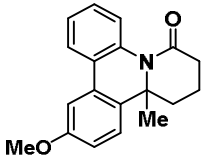
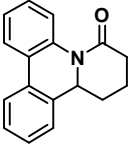
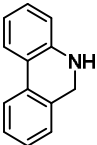
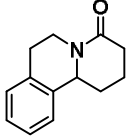
Very interestingly, each and every scaffold is unique and has embedded several privileged scaffold within its structure. For instance, consider branch A of the RCBC (refer Figure 2.6) which produced dihydro-indolo[3,2-*c*]pyrrolo[1,2-*a*]quinolinone **1a**. As shown in Figure 6, the importance pharmacophors such as tetrahydro-pyrroindole **Ia**,²³ tetrahydro-indolizinoindolone **Ib**,²⁴ dihydro-pyrroloquinolinone **Ic**²⁵ and tetrahydro-pyrrolopyridine **Id**²⁶...etc are embedded into a single structure. Since various privileged structures are present into a single scaffold, it can easily be envisioned that such hybrid structures could find potential application in modern drug discovery programmes. With the view that these scaffolds are expected to cover a significant chemical space⁶ one can anticipate their great potential in understanding biology as well. Following table gives overview of application of scaffolds accessed via RCBC in synthesis and biological activities.

Figure 2.9 Polyheterocyclic Scaffolds Accessed Through RCBC– Literature Known Synthesis and Their Applications

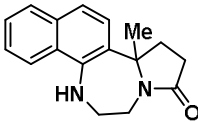
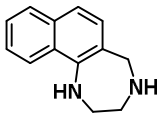
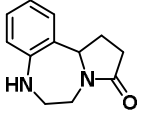
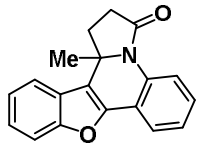
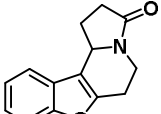
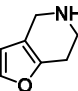
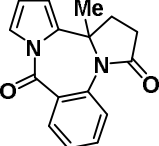
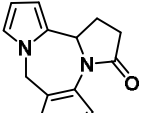
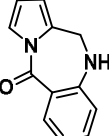
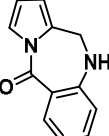
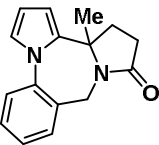
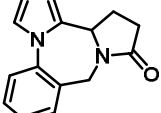
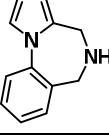
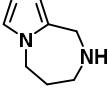
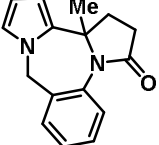
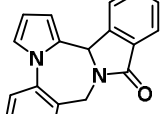
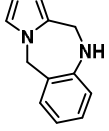
Sr. No	Scaffold	Sub-structures	Synthesis /Biological activity	References
1			Synthesis	<i>J. Org. Chem.</i> 2010 , 75, 3371-3380
			Immuno-suppressive effects	<i>J. Med. Chem.</i> 2012 , 55, 639-651
			cysLT1 Antagonists	<i>Bioorg. Med. Chem. Lett.</i> 2009 , 19, 4299-4302
			5-HT _{5A} serotonin receptors	<i>Bioorg. Med. Chem.</i> 2003 , 11, 717-722
2			Synthesis	<i>Chem.–Eur. J.</i> 2009 , 15, 12963-12967
			Isolation and their Anti-leishmanial Activity	<i>Phytochemistry</i> 1998 , 47, 145-147
			Alpha-2 adrenoceptor	WO2003/82866 A1, 2003
			Synthesis	<i>J. Am. Chem. Soc.</i> 2007 , 129, 13404-13405 <i>J. Am. Chem. Soc.</i> 2009 , 131, 1076-10797
				Synthesis
3			Synthesis/Antiobesity	WO 2008/110598 A1, 2008
			Synthesis/CNS and Antihypertensive Activity	<i>J. Med. Chem.</i> 1974 , 17, 1140-1145
			Synthesis/Antihypertensive and Antidepressant	US3950343, 1976
4			Alpha-2 adrenoceptor and 5-HT _{1A} receptor	<i>J. Med. Chem.</i> 1990 , 33, 633-641
			Synthesis/Brain dopamine and serotonin receptor	<i>Bioorg. Med. Chem. Lett.</i> 1998 , 8, 983-988

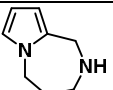
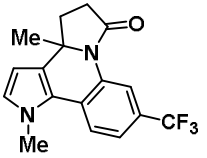
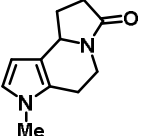
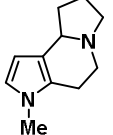
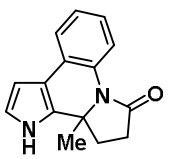
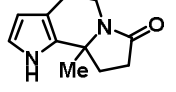
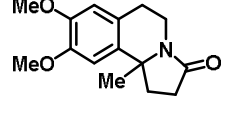
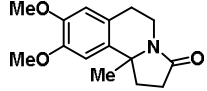
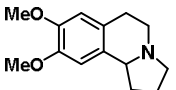
			Synthesis	<i>Eur. J. Org. Chem.</i> 2010 , 5108-5117
5			Synthesis	<i>Tetrahedron Lett.</i> 2002 , 43, 3347-3350
			Presence in Marine alkaloid Hinckdentine A: Synthesis and Cataleptogenic Activity	<i>J. Org. Chem.</i> 1994 , 59, 6777-6782 <i>Ger. Offen. 2051</i> , 961 (April 29, 1971) <i>Khim.-Farm. Zh.</i> 1978 , 12, 97 (Russ)
6			Synthesis	<i>Eur. J. Org. Chem.</i> 2009 , 1309-1312 <i>J. Am. Chem. Soc.</i> 2011 , 133, 2100-2103
			Synthesis	<i>J. Org. Chem.</i> 1967 , 32, 3618-3621
			Synthesis	<i>Synlett</i> 2008 , 1852-1856
7aa			Synthesis	<i>J. Chem. Soc., Perkin Trans.</i> <i>1</i> , 1991 , 8, 1997-2002
			Synthesis/ Potential DNA Binder	<i>Tetrahedron Lett.</i> 1993 , 34, 1347-1350
7ab			Muscarinic receptor antagonists	<i>Med. Chem. Res.</i> , 2002 , 11, 423-433 US2002/068752 A1 2002

			Synthesis	<i>J. Chem. Soc., Perkin Trans.</i> 1, 1992 , 7, 895-898
8			Synthesis	<i>Synlett</i> 2006 , 73-76
			Synthesis/5-HT ₂ Serotonin Receptors	<i>Bioorg. Med. Chem. Lett.</i> 2002 , 12, 155-158
			Synthesis/Melatoninergic Ligands	<i>Bioorg. Med. Chem. Lett.</i> 2009 , 17, 4583-4594
			Synthesis	<i>J. Org. Chem.</i> 2003 , 68, 4938-4940
9			Synthesis	<i>Synthesis</i> 1971 , 327
			Synthesis/ Melatonin Receptor Ligands	<i>Org. Biomol. Chem.</i> 2007 , 5, 2129-2137
10			Synthesis	<i>Org. Lett.</i> 2008 , 10, 3535-3538
			5-HT _{2C} Agonist	<i>Bioorg. Med. Chem. Lett.</i> 2003 , 13, 2369-2372
			Inhibitors of Human Palmitoyl Acyltransferases	<i>Mol. Cancer Ther.</i> 2006 , 5, 1647-1659
11			Synthesis/Lipid Peroxidation Inhibitory Activity	<i>Eur. J. Med. Chem.</i> 1998 , 33, 181-187
			Synthesis	<i>Ind. J. Chem.</i> 1970 , 8, 126-129
12			Synthesis	<i>J. Heterocyclic. Chem.</i> 1970 , 7, 1295-1297
			Synthesis/Lipid Peroxidation Inhibitory Activity	<i>Eur. J. Med. Chem.</i> 1998 , 33, 181-188

13			Synthesis/Bronchodilator Agents	US3835138, 1974
14			Synthesis	<i>Tetrahedron Lett.</i> 2003 , <i>44</i> , 4355-4359 <i>Tetrahedron</i> 2007 , <i>63</i> , 8999-9006
			Synthesis/Alpha-2-Antagonistic and Antidepressant Activity	<i>Bioorg. Med. Chem. Lett.</i> 2000 , <i>10</i> , 71-74 <i>J. Am. Chem. Soc.</i> 1953 , <i>75</i> , 697-699
			Synthesis	<i>Aust. J. Chem.</i> 1985 , <i>38</i> , 765-776
15			Synthesis	<i>Org. Lett.</i> 2008 , <i>10</i> , 1577-1580
			Synthesis	<i>Aust. J. Chem.</i> 1985 , <i>38</i> , 765-776
16			Synthesis	<i>J. Chem. Soc.</i> 1952 , 5024-5025
17			Synthesis	<i>J. Chem. Soc., Perkin Trans. 1</i> , 1992 , <i>7</i> , 895-898 <i>J. Heterocyclic Chem.</i> 1984 , <i>21</i> , 425-427 <i>Chem. Pharma. Bull.</i> 1966 , <i>14</i> , 752-755
			Synthesis	<i>Chem.-Eur. J.</i> 2002 , <i>8</i> , 2034-2046
			Synthesis	<i>J. Am. Chem. Soc.</i> 1989 , <i>111</i> , 2487-2496 <i>Heterocycles</i> ,

				1983, 20, 2397-2400
18			Synthesis	<i>Tetrahedron Lett.</i> 1997, 38, 6153-6156
			Synthesis/Histamine H3 Receptor Antagonist	WO2009/121812 A1, 2009
			Synthesis	<i>J. Org. Chem.</i> 1978, 43, 2125 -2127
			Synthesis/Non-Amidine Factor (fXa) Inhibitor	<i>J. Med. Chem.</i> 2004, 47, 5167-5182
19			Synthesis	<i>Tetrahedron</i> 2004, 60, 11029-11039
			Synthesis	<i>Chem.–Eur. J.</i> 2011, 17, 2981-2986
			Synthesis/Pesudocholinesterase Inhibitor	<i>J. Med. Chem.</i> 1963, 6, 767-770
			Synthesis/ Arginine Vasopressin Antagonists	<i>Bioorg. Med. Chem. Lett.</i> 2003, 13, 2195-2198
20			Synthesis	<i>J. Org. Chem.</i> 1998, 63, 6914-6928 <i>J. Org. Chem.</i> 2007, 72, 538- 549
			Synthesis/Non-amidine fXa Inhibitor with S4 Binding Element	<i>J. Med. Chem.</i> 2004, 47, 5167-5182
21			Synthesis	<i>J. Org. Chem.</i> 1998, 63, 6914-6928
			Blood Platelet Aggregation Activity	US5288726 1994
			Cholesterol Mobilization Activity	WO2012/54535 A2, 2012
22			Synthesis/Antiplatelet Activity (Present in Clopidogrel-Commercial Drug)	WO2009080469 A1 2009
			Synthesis/5-HT ₇ Receptor	<i>Bioorg. Med. Chem. Lett.</i> 2002, 12, 2549-2552

23			Synthesis/Blood Platelet Aggregation Inhibitor	<i>Helv. Chim. Acta.</i> 1986 , 69, 1671-1680
			Synthesis	<i>Tetrahedron</i> 2004 , 60, 11029-11039
24			Synthesis	<i>Tetrahedron</i> 2008 , 64, 8952-8962
			Synthesis/Cholesterol Mobilization	WO2012/54535 A2, 2012
25			Synthesis	<i>Heterocycles</i> 2000 , 52, 273-282
			Synthesis	<i>Synthesis</i> 2010 , 4087-4095
			Synthesis/Vasopressin and Oxytocin Antagonist Activity	US5733905 A1, 1998
26			Synthesis	<i>Heterocycles</i> 2000 , 52, 273-282
			Synthesis	<i>J. Heterocyclic Chem.</i> 1976 , 13, 711-716
			Synthesis/modulator of TGR5 (prevention of metabolic, cardiovascular and inflammatory diseases)	WO2008/67222 A1, 2008
27			Synthesis	<i>Tetrahedron Lett.</i> 2002 , 43, 2831-2833
			Arginine Vasopressin Antagonist with Selectivity for V2 Receptors	<i>J. Med. Chem.</i> 1998 , 41, 2442-2444

				<i>Bioorg. Med. Chem. Lett.</i> 2003 , <i>13</i> , 2195-2198
			Antidepressant	<i>J. Med. Chem.</i> 1992 , <i>35</i> , 4533
			Synthesis/modulator of TGR5	WO2008/67222 A1, 2008
28			Synthesis	<i>Tetrahedron</i> 2003 , <i>59</i> , 5265-5272 <i>J. Org. Chem.</i> 1983 , <i>48</i> , 5062-5074
			Serotonin 5-HT _{2A} , Dopamine and Histamine H ₁ Receptor Ligands	<i>Arch. Pharm. Chem. Life Sci.</i> 2010 , <i>343</i> , 73-80
29			Synthesis	<i>Org. Lett.</i> 2008 , <i>10</i> , 1577-1580
30			Synthesis	<i>Tetrahedron Lett.</i> 2012 , <i>53</i> , 2157-2159 <i>J. Org. Chem.</i> 2003 , <i>68</i> , 2609-2617 <i>J. Org. Chem.</i> 2001 , <i>66</i> , 148-152
			Present in Crispine and Harmicine: Synthesis and Cytotoxic Activities	<i>Tetrahedron</i> 2002 , <i>58</i> , 6795-6798
			Synthesis	<i>Org. Lett.</i> 2009 , <i>11</i> , 2659-2662

2.5 Conclusions

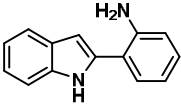
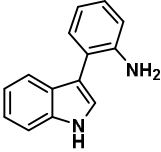
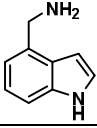
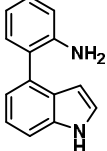
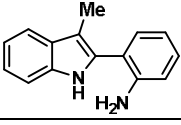
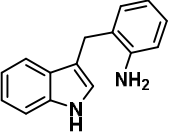
In summary, we have developed a relay catalytic branching cascade (RCBC) as a new technique for accessing a series of multifunctional poly-heterocyclic scaffolds in an efficient

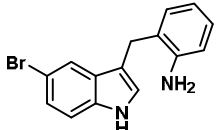
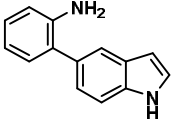
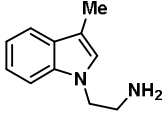
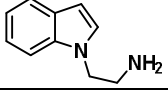
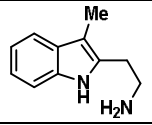
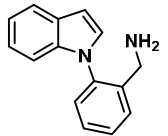
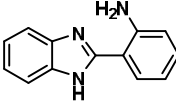
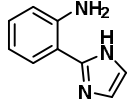
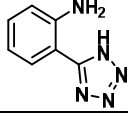
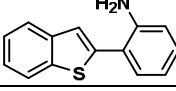
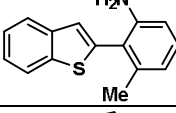
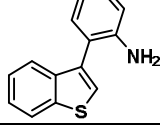
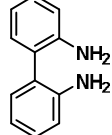
manner. The key feature of this approach is extraordinary scope which allows the preparation of a library with much higher skeletal diversity with broad scope for further diversification. Considering the multitude of reactions catalyzed by metal- and organo-catalysts at the same time and given the vast possibilities for common substrates and variables, we envision tremendous potential in the field of diversity oriented synthesis.

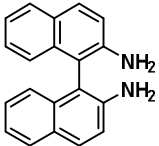
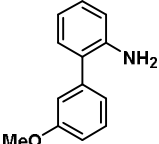
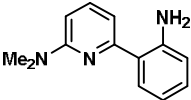
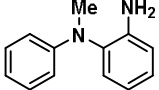
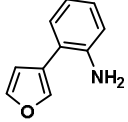
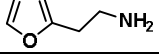
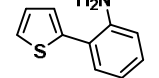
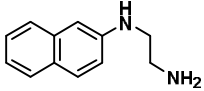
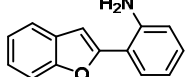
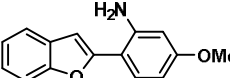
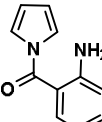
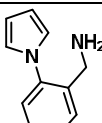
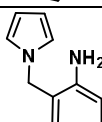
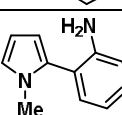
2.6 Experimental Procedures and Characterization Data

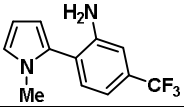
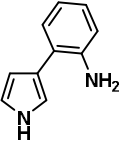
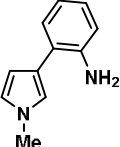
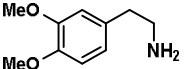
2.6.1 Synthesis of Scaffold Building Agents (SBAs)

The scaffold building agents **1**, **11**, **23** and **30** were commercially available while others prepared by literature known procedures. The details are given below in tabular form.

SBA No.	Structures	References
1		<i>Commercially available</i>
2		<i>Eur. J. Org. Chem.</i> 2009 , 2, 292–303
3		<i>J. Med. Chem.</i> 2010 , 53, 2646–2650
4		<i>Eur. J. Org. Chem.</i> 2010 , 26, 5108–5117
5		<i>Tetrahedron</i> , 1973 , 29, 1429–1432
6		<i>Tetrahedron</i> 2011 , 67, 4327–4332

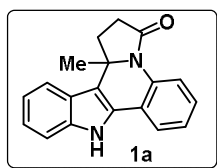
6'		<i>Tetrahedron</i> 2011 , 67, 4327–4332
7		<i>Tetrahedron</i> 2007 , 63, 10320–10329
8		<i>Tetrahedron</i> 2005 , 61, 9513–9518
8'		<i>Tetrahedron</i> 2005 , 61, 9513–9518
9		<i>Chem. Pharm. Bull.</i> 1994 , 42, 2556–2564 <i>J. Heterocyclic Chem.</i> 2000 , 37, 1281–1288
10		<i>Chem. Pharm. Bull.</i> 2008 , 56, 720–722
11		<i>Commercially available</i>
12		<i>Eur. J. Med. Chem.</i> 2009 , 44, 2347–2353
13		<i>Chem. Comm.</i> 2010 , 46, 448–450
14		<i>Tetrahedron</i> 2007 , 63, 8999–9006
14'		<i>Tetrahedron</i> 2007 , 63, 8999–9006
15		<i>Chem. Asian J.</i> 2011 , 6, 517–523
16		<i>Org. Biomol. Chem.</i> 2009 , 7, 4355–4357

16'		<i>Commercially available</i>
17		<i>J. Org. Chem.</i> 2009 , 74, 3225–3228
18		<i>Tetrahedron</i> , 2010 , 66, 862–870
19		<i>J. Med. Chem.</i> 1997 , 40, 4222–4234
20		US2005/113566 A1, 2005
21		<i>Org. Lett.</i> 2006 , 8, 2373–2376
22		<i>Chem. Asian J.</i> 2011 , 6, 1952–1957
23		<i>Commercially available</i>
24		<i>Org. Lett.</i> 2006 , 8, 1467–1470
24'		<i>Org. Lett.</i> 2006 , 8, 1467–1470
25		<i>Synthesis</i> 2010 , 23, 4087–4095
26		<i>Bioorg. Med. Chem. Lett.</i> 2005 , 15, 3453–3458
27		<i>Bioorg. Med. Chem. Lett.</i> 2007 , 17, 5796–5800
28		<i>J. Org. Chem.</i> 2009 , 74, 9517–9520 <i>Bioorg. Med. Chem. Lett.</i> 2003 , 13, 1183–1186

28'		<i>J. Org. Chem.</i> 2009 , <i>74</i> , 9517–9520 <i>Bioorg. Med. Chem. Lett.</i> 2003 , <i>13</i> , 1183–1186
29		<i>Org. Lett.</i> 2010 , <i>12</i> , 4224–4227
29'		<i>Org. Lett.</i> 2010 , <i>12</i> , 4224–4227
30		<i>Commercially available</i>

2.6.2 General Procedure and Characterization Data of Compounds:

To a screw-cap vial containing stir bar, were added scaffold building agents (SBA) 1-30 (1.0 equiv.), alkynoic acids I-VIII (1.0 equiv.) and catalyst $\text{Ph}_3\text{PAuCl/AgOTf}$ (5 mol%) in DCE (1 M). The reaction vial was fitted with a cap, evacuated and filled with nitrogen. The reaction vial was heated with stirring at 100 °C for 24-36 hours (as specified in Figure 2.6). The reaction mixture was cooled to ambient temperature, diluted with ethyl acetate and filtered through a plug of silica gel. The filtrate was concentrated and the residue thus obtained was purified by silica gel column chromatography using EtOAc/hexane or MeOH/DCM as an eluent to afford analytically pure compounds.



(**1a**): light yellow solid

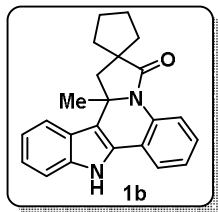
Yield: 79% yield; **mp** = 242-245 °C; **R_f** 0.55 (hexane/EtOAc = 60/40)

¹H NMR (500 MHz, CDCl₃): δ 8.48 (brs, D₂O exchangeable, 1H), 8.26-8.24 (d, J = 8.0 Hz, 1H), 7.54-7.52 (d, J = 8.0 Hz, 1H), 7.43-7.40 (t, J = 8.0 Hz, 2H), 7.24-7.21 (t, J = 7.0 Hz, 2H), 7.17-7.14 (t, J = 7.0 Hz, 2H), 2.91-2.86 (m, 1H), 2.75-2.70 (m, 2H), 2.61-2.56 (m, 1H), 1.46 (s, 3H).

¹³C NMR (75 MHz, CDCl₃): δ 173.8, 147.3, 134.3, 125.2, 123.9, 123.8, 123.4, 123.1, 122.0, 120.2, 118.4, 116.7, 111.6, 110.8, 107.9, 55.4, 32.0, 30.2, 25.4.

IR (KBr): ν_{max} 3445, 3293, 3146, 2926, 2853, 1634, 1494, 1442, 748 cm⁻¹.

MS (ESI): m/z 289 ($M^+ + H$); **HRMS** calcd for $C_{19}H_{16}N_2O$ ($M^+ + H$) 289.1335, found 289.1338.



(1b): pale yellow solid

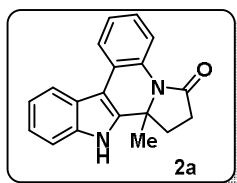
Yield = 69%; mp = 205-208 °C; R_f 0.45 (hexane/EtOAc = 60/40)

1H NMR (300 MHz, $CDCl_3$) δ : 8.72-8.69 (brs, D_2O exchangeable, 1H), 8.07-8.05 (dd, $J = 7.5$ & 1.5 Hz, 1H), 7.53-7.51 (d, $J = 8.3$ Hz, 1H), 7.46-7.44 (d, $J = 8.3$ Hz, 1H), 7.31-7.28 (dd, $J = 7.5$ & 1.5 Hz, 1H), 7.22-7.20 (d, $J = 7.5$ Hz, 1H), 7.16-7.11 (t, $J = 7.5$ Hz, 1H), 7.03-6.93 (m, 2H), 2.78-2.66 (q, $J = 23.4$ & 10.6 Hz, 2H), 2.37-2.18 (m, 2H), 2.04-1.78 (m, 4H), 1.69-1.52 (m, 2H), 1.46 (s, 3H).

^{13}C NMR (75 MHz, $CDCl_3$) δ : 179.9, 137.6, 132.2, 128.4, 126.8, 124.6, 124.1, 123.4, 122.5, 120.5, 120.0, 118.4, 111.9, 60.4, 50.9, 47.7, 40.2, 38.9, 27.8, 26.2, 25.7.

IR (KBr): ν_{max} cm^{-1} ; 3248, 2955, 1660, 1368, 749 cm^{-1} .

MS (ESI): m/z 343 ($M^+ + H$); **HRMS** calcd for $C_{23}H_{22}N_2O$ ($M^+ + H$) 343.4452, found 343.4457.



(2a): Violet colored solid

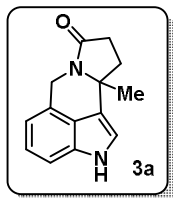
Yield = 78%; mp = 216-218 °C; R_f 0.40 (hexane/EtOAc = 75/25)

1H NMR (300 MHz, $CDCl_3$): δ 8.73-8.57 (brs, D_2O exchangeable, 1H), 8.17-8.14 (dd, $J = 8.6$ & 1.1 Hz, 1H), 8.06-8.03 (t, $J = 8.8$ Hz, 1H), 7.97-7.94 (dd, $J = 7.7$ & 1.5 Hz, 1H), 7.42-7.39 (dd, $J = 8.5$ & 1.1 Hz, 1H), 7.31-7.28 (dd, $J = 7.4$ & 1.1 Hz, 1H), 7.24-7.19 (m, 3H), 2.96-2.79 (m, 1H), 2.61-2.51 (m, 2H), 2.46-2.39 (m, 1H), 1.43 (s, 3H).

^{13}C NMR (75 MHz, $CDCl_3$): δ 173.5, 139.9, 136.6, 130.4, 126.1, 125.5, 124.9, 123.9, 122.8, 122.4, 121.0, 119.9, 111.7, 106.4, 61.2, 30.9, 30.4, 25.5.

IR (KBr): ν_{max} 3320, 3062, 2923, 2856, 1658, 1595, 1499, 1383, 1123, 745 cm^{-1} .

MS (ESI): m/z 288.34 ($M^+ + H$); **HRMS** calcd for $C_{19}H_{16}N_2O$ ($M^+ + H$) 289.1335, found 289.1338.



(3a): pale yellow solid

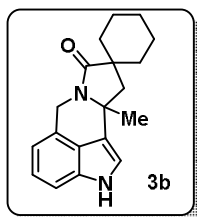
Yield: 81%; mp = 140-143 °C; R_f 0.35 (MeOH/DCM= 5/95)

1H NMR (300 MHz, $CDCl_3$): δ 8.14 (s, D_2O exchangeable, 1H), 7.24-7.15 (m, 2H), 6.95-6.93 (m, 2H), 5.42-5.36 (d, $J = 17.3$ Hz, 1H), 4.34-4.29 (d, $J = 16.6$ Hz, 1H), 2.76-2.36 (m, 4H), 1.57 (s, 3H).

^{13}C NMR (75 MHz, $CDCl_3$): δ 173.8, 133.6, 125.9, 123.7, 122.8, 119.2, 115.8, 114.2, 109.2, 61.4, 38.7, 33.0, 30.9, 28.1.

IR (KBr): ν_{max} 3244, 2928, 2853, 1655, 1607, 1440, 1329, 1237, 1153, 1068, 749 cm^{-1} .

MS (ESI): m/z 227 ($M^+ + H$); **HRMS** calcd for $C_{14}H_{14}N_2O$ ($M^+ + H$) 227.1184, found 227.1179.



(3b): yellowish white solid

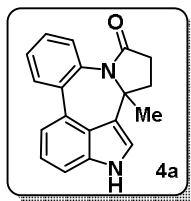
Yield: 63%; mp = 204-206 °C; R_f 0.27 (MeOH/DCM = 05/95)

1H NMR (300 MHz, $CDCl_3$): δ 8.47 (s, D_2O exchangeable, 1H), 7.19-7.11 (m, 2H), 6.92-6.89 (m, 2H), 5.45-5.39 (d, $J = 16.6$ Hz, 1H), 4.36-4.31 (d, $J = 16.6$ Hz, 1H), 2.51-2.47 (d, $J = 12.8$ Hz, 1H), 2.28-2.24 (d, $J = 12.8$ Hz, 1H), 1.84-1.61 (m, 4H), 1.40-1.08 (m, 6H), 1.57 (s, 3H).

^{13}C NMR (75 MHz, $CDCl_3$): δ 178.6, 133.9, 126.9, 123.9, 123.0, 120.8, 115.5, 114.5, 109.2, 58.8, 46.5, 44.0, 38.9, 34.7, 33.9, 30.9, 25.4, 22.4, 22.0.

IR (KBr): ν_{max} 3249, 2957, 2849, 1659, 1611, 1432, 1346, 1229, 1089, 771 cm^{-1} .

MS (ESI): m/z 295 ($M^+ + H$); **HRMS** calcd for $C_{19}H_{22}N_2O$ ($M^+ + H$) 295.1810, found 295.1811.



(**4a**): white solid

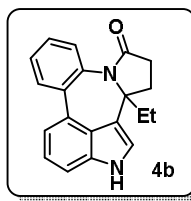
Yield: 76%; mp = 247-249 °C (decomposed); R_f 0.21 (hexane/EtOAc = 50/50)

^1H NMR (500 MHz, CDCl_3): δ 8.39 brs, D_2O exchangeable (1H), 7.98-7.96 (d, $J = 7.7$ Hz, 1H), 7.54-7.52 (d, $J = 7.7$ Hz, 1H), 7.44-7.38 (m, 3H), 7.32-7.25 (m, 2H), 7.06-7.05 (d, $J = 2.2$ Hz, 1H), 2.62-2.58 (m, 1H), 2.51-2.38 (m, 2H), 2.32-2.25 (m, 1H), 1.36 (s, 3H).

^{13}C NMR (75 MHz, CDCl_3): δ 173.6, 136.9, 135.6, 134.8, 130.7, 129.5, 129.0, 128.0, 127.8, 124.0, 122.8, 121.6, 119.4, 117.9, 111.0, 64.2, 35.6, 30.7, 30.4.

IR (KBr): ν_{max} 3206, 2925, 1665, 1485, 1413, 1338, 1112, 830, 750 cm^{-1} .

MS (ESI): m/z 289 ($\text{M}^+ + \text{H}$); **HRMS** calcd for $\text{C}_{19}\text{H}_{16}\text{N}_2\text{O}$ ($\text{M}^+ + \text{H}$) 289.1341, found 289.1342.



(**4b**): white solid

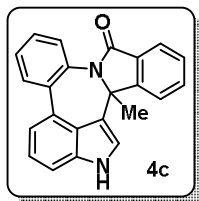
Yield 63%; mp = 243-247 °C decomposed; R_f 0.25 (hexane/EtOAc = 50/50)

^1H NMR (500 MHz, CDCl_3): δ 8.73 (brs, 1H, D_2O exchangable), 8.00- 7.95 (d, $J = 7.6$ Hz, 1H), 7.50-7.49 (d, $J = 6.7$ Hz, 1H), 7.42-7.35 (m, 3H), 7.30-7.28 (d, $J = 8.6$ Hz, 1H), 7.25-7.24 (d, $J = 7.6$ Hz, 1H), 7.00 (brs, 1H), 2.49-2.33 (m, 3H), 2.24-2.19 (m, 1H), 1.59-1.49 (m, 2H) 0.81-0.78 (t, $J = 7.7$ Hz, 3H).

^{13}C NMR (75 MHz, CDCl_3): δ 174.2, 137.0, 135.7, 134.9, 132.2, 130.8, 129.3, 128.8, 127.9, 127.6, 122.5, 119.7, 119.3, 118.8, 111.2, 68.2, 34.2, 32.6, 30.4, 7.8.

IR (KBr): ν_{max} 3223, 2895, 1667, 1473, 1429, 1333, 1121, 827, 764 cm^{-1} .

MS (ESI): m/z 303 ($\text{M}^+ + \text{H}$); **HRMS** calcd for $\text{C}_{20}\text{H}_{18}\text{N}_2\text{O}$ ($\text{M}^+ + \text{H}$) 303.1489, found 303.1491.



(4c): white solid

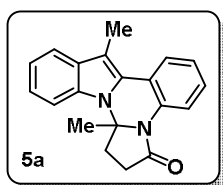
Yield: 59%; mp = 185-187 °C; R_f 0.35 (hexane/EtOAc = 50/50)

$^1\text{H NMR}$ (500 MHz, CDCl_3): δ 8.27 (brs, D_2O exchangeable, 1H), 8.04-8.03 (d, $J = 8.0$ Hz, 1H), 7.96-7.94 (d, $J = 8.0$ Hz, 1H), 7.86-7.85 (d, $J = 8.0$ Hz, 1H), 7.73-7.70 (t, $J = 6.9$ Hz, 1H), 7.59-7.57 (m, 2H), 7.56-7.53 (t, $J = 6.9$ Hz, 1H), 7.48-7.39 (m, 2H), 7.31-7.30 (m, 2H), 7.10-7.09 (d, $J = 3.4$ Hz, 1H), 1.63 (s, 3H).

$^{13}\text{C NMR}$ (75 MHz, CDCl_3): δ 167.4, 151.0, 141.0, 136.2, 132.8, 132.1, 131.5, 130.5, 129.8, 129.2, 128.3, 127.8, 127.6, 124.5, 122.7, 121.1, 120.6, 119.3, 111.1, 66.8, 27.9.

IR (KBr): ν_{max} 3211, 2925, 1671, 1485, 1413, 1338, 1112, 827 cm^{-1} .

MS (ESI): m/z 337 ($\text{M}^+ + \text{H}$); **HRMS** calcd for $\text{C}_{19}\text{H}_{16}\text{N}_2\text{O}$ ($\text{M}^+ + \text{H}$) 337.1341, found 337.1341.



(5a): yellowish thick liquid

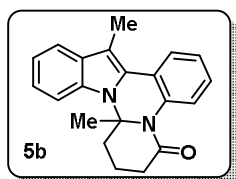
Yield: 71% ; R_f 0.27 (hexane/EtOAc = 70/30).

$^1\text{H NMR}$ (300 MHz, CDCl_3): δ 8.27-8.23 (dd, $J = 7.5$ & 1.5 Hz, 1H), 7.95-7.91 (dd, $J = 7.5$ & 2.3 Hz, 1H), 7.67-7.64 (dd, $J = 2.3$ & 1.5 Hz, 1H), 7.43-7.40 (d, $J = 7.5$ Hz, 1H), 7.39-7.28 (m, 2H), 7.24-7.14 (m, 2H), 3.05-3.00 (m, 2H), 2.94-2.78 (m, 2H), 2.63 (s, 3H), 1.59 (s, 3H).

$^{13}\text{C NMR}$ (75 MHz, CDCl_3): δ 171.1, 132.9, 130.2, 127.6, 127.3, 125.4, 125.0, 122.5, 122.1, 122.0, 119.6, 119.3, 110.2, 108.4, 77.4, 33.5, 30.4, 24.3, 10.7.

IR (film): ν_{max} 3439, 2937, 1667, 1457, 1349, 1311, 1119, 779 cm^{-1} .

MS (ESI): m/z 303 ($\text{M}^+ + \text{H}$); **HRMS** calcd for $\text{C}_{20}\text{H}_{18}\text{N}_2\text{O}$ ($\text{M}^+ + \text{H}$) 303.1497, found 303.1498.



(5b): yellowish white solid

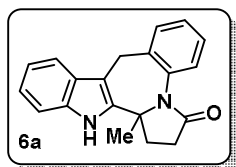
Yield: 76%; mp = 185-188 °C; R_f 0.25 (hexane/EtOAc = 70/30)

^1H NMR (300 MHz, CDCl_3): δ 7.86-7.83 (m, 1H), 7.66-7.63 (dd, J = 6.8 & 2.2 Hz, 1H), 7.59-7.53 (m, 2H), 7.35-7.32 (m, 2H), 7.22-7.12 (m, 2H), 3.25-3.17 (m, 1H), 2.87-2.72 (m, 2H), 2.58-2.48 (m, 1H), 2.61 (s, 3H), 2.13-2.01 (m, 2H), 1.52 (s, 3H).

^{13}C NMR (75 MHz, CDCl_3): δ 169.7, 132.7, 130.2, 127.5, 126.6, 126.3, 125.2, 122.6, 119.4, 119.2, 111.1, 75.6, 35.2, 33.6, 27.8.

IR (KBr): ν_{max} 3444, 2919, 1663, 1452, 1340, 1305, 1125, 1100, 774 cm^{-1} .

MS (ESI): m/z 317 ($\text{M}^+ + \text{H}$); **HRMS** calcd for $\text{C}_{21}\text{H}_{20}\text{N}_2\text{O}$ ($\text{M}^+ + \text{H}$) 317.16484, found 317.16444.



(6a): yellowish white solid

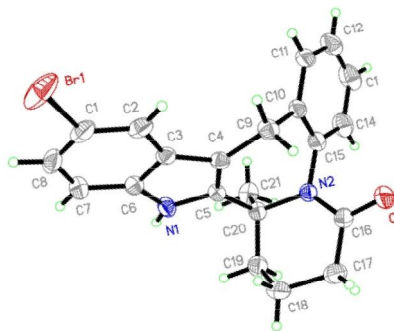
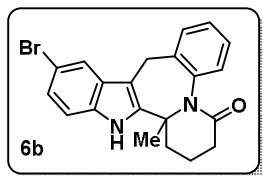
Yield: 79%; mp = 242-245 °C (decomposed); R_f 0.15 (hexane/EtOAc = 40/60)

^1H NMR (300 MHz, CDCl_3): δ 7.91 (brs, D_2O exchangeable 1H), 7.64-7.61 (m, 1H), 7.38-7.35 (m, 1H), 7.30-7.26 (m, 4H), 7.18-7.15 (m, 2H), 4.17-4.12 (d, J = 15.8 Hz, 1H), 3.87-3.82 (d, J = 15.8 Hz, 1H), 2.78-2.67 (m, 1H), 2.64-2.52 (m, 2H), 2.40-2.32 (m, 1H), 1.53 (s, 3H).

^{13}C NMR (75 MHz, CDCl_3): δ 175.2, 141.1, 137.1, 135.3, 130.0, 129.0, 128.5, 127.2, 122.1, 119.6, 118.0, 110.6, 108.9, 63.5, 34.9, 30.1, 27.8, 27.5.

IR (KBr): ν_{max} 3249, 2935, 1671, 1385, 1229, 1148, 1031, 753 cm^{-1} .

MS (ESI): m/z 303 ($\text{M}^+ + \text{H}$); **HRMS** calcd for $\text{C}_{20}\text{H}_{18}\text{N}_2\text{O}$ ($\text{M}^+ + \text{H}$) 303.1492, found 303.1495.



(6b): brownish solid

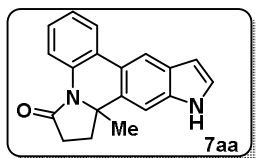
Yield: 63%; mp = 242 - 245 °C (decomposed); R_f 0.15 (MeOH/DCM = 02/98)

^1H NMR (300 MHz, DMSO): δ 10.85 (brs, D_2O exchangeable, 1H), 7.70 (s, 1H), 7.38-7.37 (d, J = 7.4 Hz, 1H), 7.29-7.23 (m, 2H), 7.21-7.13 (m, 3H), 3.96-3.93 (d, J = 15.8 Hz, 1H) 3.78-3.75 (d, J = 15.8 Hz, 1H), 2.77-2.74 (d, J = 14.8 Hz, 1H), 2.55-2.46 (m, 2H), 2.16-2.11 (t, J = 15.8 Hz, 1H), 1.84-1.82 (m, 1H) (1.57-1.50, m, 1H), 1.41 (s, 3H).

^{13}C NMR (300 MHz, DMSO): δ 169.7, 141.1, 140.1, 139.3, 133.6, 130.8, 128.8, 128.1, 127.5, 126.5, 123.4, 120.1, 112.7, 111.1, 60.5, 36.1, 32.3, 29.9, 26.7, 17.7.

IR (KBr): ν_{max} 3439, 3277, 3123, 2937, 2834, 1637, 1471, 748 cm^{-1} .

MS (ESI): m/z 396 ($\text{M}^+ + \text{H}$); **HRMS** calcd for $\text{C}_{21}\text{H}_{19}\text{BrN}_2\text{O}$ ($\text{M}^+ + \text{H}$) 396.0759, found 396.0759.



(7aa): pale yellow colored semisolid

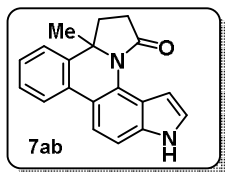
Yield: 37%; R_f 0.40 (hexane/EtOAc = 60/40)

^1H NMR (300 MHz, CDCl_3): δ 8.41 (brs, D_2O exchangeable, 1H), 8.31-8.30 (dd, J = 7.9 & 1.3 Hz, 1H), 8.08 (s, 1H), 7.95-7.92 (dd, J = 7.9 & 1.3 Hz 1H), 7.36-7.29 (m, 1H), 7.25-7.22 (m, 3H), 6.6 (s, 1H), 2.88-2.76 (m, 1H), 2.63-2.54 (m, 3H), 1.4 (s, 3H).

^{13}C NMR (75 MHz, CDCl_3 + DMSO): δ 172.2, 136.4, 134.0, 131.9, 127.1, 126.2, 125.7, 124.4, 123.3, 122.5, 121.2, 119.4, 116.6, 111.4, 100.9, 62.9, 33.1, 29.9, 24.1.

IR (KBr): ν_{max} 3293, 3146, 2916, 2853, 1641, 1487, 1432, 756 cm^{-1} .

MS (ESI): m/z 289 ($\text{M}^+ + \text{H}$); **HRMS** calcd for $\text{C}_{18}\text{H}_{15}\text{N}_3\text{O}$ ($\text{M}^+ + \text{H}$) 289.1341, found 289.1347.



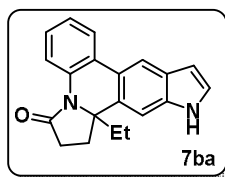
(**7ab**): pale yellow colored semisolid

Yield: 34%; R_f 0.25 (hexane/EtOAc = 60/40)

^1H NMR (300 MHz, DMSO): δ 11.05 (brs, D_2O exchangeable, 1H), 8.20-8.17 (dd, $J = 7.4$ & 1.7 Hz, 1H), 7.83-7.80 (dd, $J = 7.8$ & 1.5 Hz, 1H), 7.64-7.61 (d, $J = 8.7$ Hz, 1H), 7.47-7.44 (d, $J = 8.7$ Hz, 1H), 7.30-7.19 (m, 3H), 6.55 (s, 1H), 2.91-2.66 (m, 3H), 2.55-2.47 (m, 1H), 1.46 (s, 3H); **^{13}C NMR (75 MHz, CDCl_3):** δ 172.0, 136.5, 135.8, 132.2, 127.2, 126.9, 126.4, 126.2, 124.3, 123.0, 120.8, 120.4, 114.6, 105.8, 101.3, 62.5, 32.2, 30.3, 26.9.

IR (film): ν_{max} 3406, 2972, 1712, 1609, 1583, 1476, 1381, 1289.16, 1192, 1055.39, 746 cm^{-1} .

MS (ESI): m/z 289 ($\text{M}^+ + \text{H}$); **HRMS** calcd for $\text{C}_{18}\text{H}_{16}\text{N}_2\text{O}$ ($\text{M}^+ + \text{H}$) 289.1288, found 289.1288.



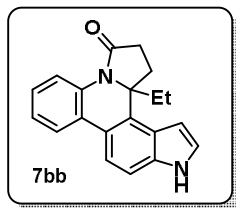
(**7bb**): pale yellow colored semisolid

Yield: 36%; R_f 0.45 (hexane/EtOAc = 60/40)

^1H NMR (500 MHz, CDCl_3): δ 8.38 (brs, D_2O exchangeable, 1H), 8.23-8.22 (d, $J = 8.0$ Hz, 1H), 8.1 (s, 1H), 7.92-7.91 (d, $J = 7.0$ Hz, 1H), 7.33-7.30 (t, $J = 7.0$ Hz, 1H), 7.26 (s, 1H), 7.24-7.19 (m, 2H), 6.59 (s, 1H), 2.84-2.74 (m, 1H), 2.58-2.48 (m, 3H), 1.72-1.60 (m, 2H), 0.80-0.77 (t, $J = 7.0$ Hz, 3H).

^{13}C NMR (75 MHz, CDCl_3): δ 173.2, 136.7, 135.5, 132.1, 132.0, 128.5, 127.3, 125.4, 125.1, 123.3, 122.2, 115.7, 106.6, 102.9, 66.5, 33.3, 31.4, 29.7, 29.4, 8.7; **IR (KBr):** ν_{max} 3297, 3139, 2921, 1649, 1481, 1439, 763 cm^{-1} .

MS (ESI): m/z 303 ($\text{M}^+ + \text{H}$); **HRMS** calcd for $\text{C}_{20}\text{H}_{18}\text{N}_2\text{O}$ ($\text{M}^+ + \text{H}$) 303.1496, found 303.1489.



(**7ba**): pale yellow colored semisolid

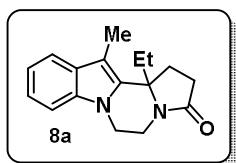
Yield: 33%; R_f 0.25 (hexane/EtOAc = 60/40)

^1H NMR (500 MHz, DMSO): δ 10.6 (brs, D_2O exchangeable, 1H), 8.16-8.14 (dd, $J = 7.0$ & 1.2 Hz, 1H), 7.81-7.80 (d, $J = 8.1$ Hz, 1H), 7.64-7.63 (d, $J = 8.1$ Hz, 1H), 7.46-7.44 (d, $J = 8.1$ Hz, 1H), 7.29-7.21 (m, 3H), 6.52 (s, 1H), 2.88-2.78 (m, 3H), 2.54-2.45 (m, 1H), 1.91-1.74 (m, 2H), 0.87-0.84 (t, $J = 7.0$ Hz, 3H).

^{13}C NMR (75 MHz, CDCl_3): δ 172.7, 136.2, 133.8, 131.9, 127.7, 126.0, 125.0, 124.4, 123.0, 122.9, 121.5, 120.0, 116.6, 111.1, 66.0, 31.6, 30.7, 30.3, 8.0.

IR (KBr): ν_{max} 3417, 2969, 1709, 1617, 1476, 1192, 757 cm^{-1} .

MS (ESI): m/z 303 ($\text{M}^+ + \text{H}$); **HRMS** calcd for $\text{C}_{20}\text{H}_{18}\text{N}_2\text{O}$ ($\text{M}^+ + \text{H}$) 303.1483, found 303.1489.



(**8a**): pale yellow thick liquid

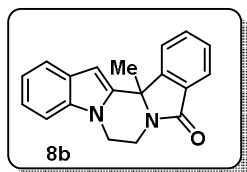
Yield: 74%; R_f 0.55 (MeOH/DCM = 01/99)

^1H NMR (300 MHz, CDCl_3): δ 7.55-7.52 (d, $J = 7.6$ Hz, 1H), 7.23-7.21 (m, 3H), 4.58-4.52 (dd, $J = 13.6$ & 4.5 Hz, 1H), 4.23-4.17 (dd, $J = 12.1$ & 3.8 Hz, 1H), 3.89-3.78 (m, 1H), 3.39-3.29 (dt, $J = 12.9$ & 4.5 Hz, 1H), 2.66-2.44 (m, 4H), 2.31 (s, 3H), 2.05-1.93 (m, 2H), 0.99-0.94 (t, $J = 7.5$ Hz, 3H).

^{13}C NMR (75 MHz, CDCl_3): δ 173.2, 136.6, 135.3, 128.7, 121.5, 119.6, 118.2, 108.7, 104.4, 62.7, 40.9, 34.0, 31.9, 30.7, 30.3, 9.2, 8.2.

IR (film): ν_{max} 3426, 2923, 1691, 1463, 1318, 1285, 1155, 1074, 944, 799, 745 cm^{-1} .

MS (ESI): m/z 269 ($\text{M}^+ + \text{H}$); **HRMS** calcd for $\text{C}_{20}\text{H}_{18}\text{N}_2\text{O}$ ($\text{M}^+ + \text{H}$) 269.3614, found 269.3615.



(8b): pale yellow solid

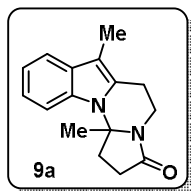
Yield: 49%; mp = 124-126 °C; R_f 0.65 (MeOH/DCM = 01/99).

^1H NMR (300 MHz, CDCl_3): δ 7.89-7.85 (t, $J = 7.5$ Hz, 1H), 7.69-7.64 (t, $J = 7.55$ Hz, 1H), 7.58-7.55 (d, $J = 8.3$ Hz, 1H), 7.51-7.47 (t, $J = 7.5$ Hz, 1H), 7.27-7.26 (m, 1H), 7.22-7.16 (t, $J = 6.8$ Hz, 1H), 7.13-7.09 (t, $J = 7.5$ Hz, 1H), 6.63 (s, 1H), 4.90-4.84 (dd, $J = 13.6$ & 4.5 Hz, 1H), 4.30-4.24 (dd, $J = 11.3$ & 4.5 Hz, 1H), 4.02-3.92 (dt, $J = 12.1$ & 6.8 Hz, 1H), 3.75-3.65 (dt, $J = 12.1$ & 5.2 Hz, 1H), 1.91 (s, 3H).

^{13}C NMR (75 MHz, CDCl_3): δ 168.3, 150.1, 137.7, 135.7, 132.5, 130.4, 128.6, 127.7, 124.0, 122.1, 121.8, 120.5, 120.4, 109.2, 97.9, 61.7, 41.3, 34.6, 28.7.

IR (KBr): ν_{\max} 2924, 2854, 1695, 1462, 1385, 1319, 1169, 1082, 750 cm^{-1} .

MS (ESI): m/z 289 ($\text{M}^+ + \text{H}$); **HRMS** calcd for $\text{C}_{19}\text{H}_{16}\text{N}_2\text{O}$ ($\text{M}^+ + \text{H}$) 289.1341, found 289.1341.



(9a): pale yellow thick liquid

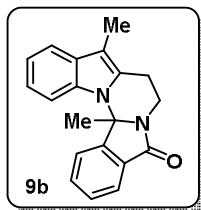
Yield: 75%; R_f 0.65 (MeOH/DCM = 2/98)

^1H NMR (300 MHz, CDCl_3): δ 7.55-7.53 (d, $J = 7.9$ Hz, 1H), 7.24-7.21 (dd, $J = 7.9$ & 2.6 Hz, 2H), 7.18-7.16 (dd, $J = 7.9$ & 1.1 Hz, 1H), 7.14-7.11 (dd, $J = 6.2$ & 1.7 Hz, 1H), 4.56-4.50 (dd, $J = 13.6$ & 4.3 Hz, 1H), 4.25-4.20 (dd, $J = 11.5$ & 4.7 Hz, 1H), 2.67-2.39 (m, 4H), 2.32 (s, 3H), 1.62 (s, 3H)

^{13}C NMR (75 MHz, CDCl_3): δ 172.5, 135.6, 132.1, 131.9, 128.6, 121.5, 119.6, 118.2, 108.7, 59.5, 41.0, 33.9, 33.5, 29.6, 24.7, 8.9

IR (film): ν_{\max} 3293, 2926, 1687, 1494, 1442, 1178, 1071, 748 cm^{-1} .

MS (ESI): m/z 255 ($\text{M}^+ + \text{H}$); **HRMS** calcd for $\text{C}_{16}\text{H}_{18}\text{N}_2\text{O}$ ($\text{M}^+ + \text{H}$) 255.1492, found 255.1493.



(9b): pale yellow thick liquid

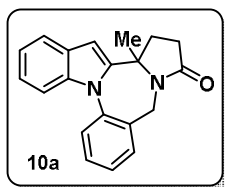
Yield: 59%; mp = 195-197 °C; R_f 0.50 (MeOH/DCM = 02/98)

^1H NMR (300 MHz, CDCl_3): δ 8.05-8.02 (d, J = 8.3 Hz, 1H) 7.89-7.87 (d, J = 7.6 Hz, 1H), 7.66-7.61 (t, J = 7.6 Hz, 1H), 7.56-7.51 (t, J = 7.5 Hz, 1H) 7.50-7.46 (d, J = 6.0 Hz, 1H), 7.22-7.20 (m, 2H), 7.16-7.09 (m, 1H), 4.87-4.81 (dd, J = 13.6 & 3.8 Hz, 1H), 4.23-4.18 (dd, J = 11.3 & 4.5 Hz, 1H) 4.10-4.00 (dt, J = 12.0 & 5.2 Hz, 1H), 3.61-3.51 (dt, J = 13.6 & 4.5 Hz, 1H) 2.66 (s, 3H), 1.96 (s, 3H).

^{13}C NMR (75 MHz, CDCl_3): δ 167.8, 149.7, 135.0, 132.1, 131.8, 130.8, 128.6, 128.5, 124.0, 123.2, 122.0, 119.6, 118.3, 108.8, 106.3, 63.5, 41.5, 35.0, 25.4, 11.2.

IR (film): ν_{max} 3426, 2923, 1691, 1463, 1318, 1285, 1155, 1074, 944, 799, 745 cm^{-1} .

MS (ESI): m/z 303 ($\text{M}^+ + \text{H}$); **HRMS** calcd for $\text{C}_{20}\text{H}_{18}\text{N}_2\text{O}$ ($\text{M}^+ + \text{H}$) 303.1497, found 303.1498.



(10a): yellowish thick liquid

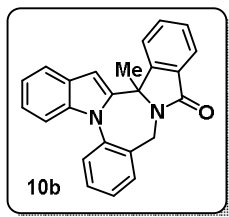
Yield: 61%; R_f 0.50 (hexane/EtOAc = 60/40)

^1H NMR (500 MHz, CDCl_3): δ 7.72-7.69 (d, J = 7.5 Hz, 2H), 7.55-7.50 (t, J = 7.5 Hz, 2H), 7.37-7.35 (m, 1H), 7.24-7.15 (m, 3H), 6.56 (s, 1H), 5.03-4.99 (d, J = 13.6 Hz, 1H), 3.95-3.91 (d, J = 13.6 Hz, 1H), 2.81-2.59 (m, 2H), 2.50-2.41 (m, 1H), 2.29-2.23 (m, 1H), 1.08 (s, 3H).

^{13}C NMR (75 MHz, CDCl_3): δ 172.8, 141.3, 139.3, 130.9, 130.1, 129.4, 128.8, 128.6, 128.5, 127.0, 123.9, 123.0, 121.2, 110.8, 100.1, 61.0, 43.4, 33.8, 29.3, 26.2.

IR (film): ν_{max} 3445, 3293, 2926, 1647, 1494, 748 cm^{-1} .

MS (ESI): m/z 303 ($\text{M}^+ + \text{H}$); **HRMS** calcd for $\text{C}_{20}\text{H}_{18}\text{N}_2\text{O}$ ($\text{M}^+ + \text{H}$) 303.1497, found 303.1496.



(10b): yellowish thick liquid

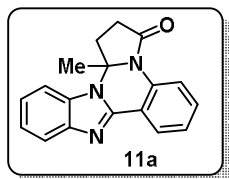
Yield: 52%; R_f 0.55 (hexane/EtOAc = 60/40).

$^1\text{H NMR}$ (300 MHz, CDCl_3): δ 7.95-7.93 (d, $J = 7.5$ Hz, 1H), 7.80-7.78 (d, $J = 7.2$ Hz, 1H), 7.71-7.44 (m, 9H), 7.21-7.17 (m, 1H), 6.23 (s, 1H), 5.14-5.10 (d, $J = 14.2$ Hz, 1H), 4.27-4.22 (d, $J = 14.2$ Hz, 1H), 1.35 (s, 3H).

$^{13}\text{C NMR}$ (75 MHz, CDCl_3): δ 168.9, 149.3, 145.0, 141.6, 137.0, 134.2, 132.9, 132.1, 131.4, 130.8, 129.7, 129.1, 128.8, 127.2, 124.3, 124.1, 122.9, 121.2, 110.5, 101.7, 64.5, 45.4, 27.4.

IR (film): ν_{max} 3447, 3287, 2931, 1653, 1487, 753 cm^{-1} .

MS (ESI): m/z 351 ($\text{M}^+ + \text{H}$); **HRMS** calcd for $\text{C}_{24}\text{H}_{18}\text{N}_2\text{O}$ ($\text{M}^+ + \text{H}$) 351.1397, found 351.1399.



(11a): white fluppy solid

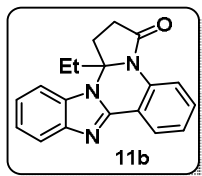
Yield 86%; mp = 157-160 $^\circ\text{C}$; R_f 0.31 (MeOH/DCM = 02/98).

$^1\text{H NMR}$ (300 MHz, CDCl_3): δ 8.35-8.32 (dd, $J = 7.7$ & 1.5 Hz, 1H), 8.27-8.25 (d, $J = 8.3$ Hz, 1H), 7.87-7.84 (dd, $J = 8.6$ & 1.5 Hz, 1H), 7.57-7.51 (dd, $J = 8.3$ & 1.5 Hz, 1H), 7.47-7.45 (dd, $J = 8.1$ & 1.6 Hz, 1H), 7.40-7.36 (dd, $J = 7.74$ & 1.3 Hz, 1H), 7.35-7.29 (m, 2H), 3.08-2.74 (m, 4H), 1.67 (s, 3H).

$^{13}\text{C NMR}$ (75 MHz, CDCl_3): δ 171.2, 145.8, 144.2, 132.3, 131.9, 131.2, 125.9, 125.6, 123.2, 123.0, 121.6, 120.4, 117.9, 110.1, 78.3, 32.7, 25.0, 24.8.

IR (KBr): ν_{max} 3406, 2972, 1712, 1609, 1583, 1476, 1381, 1289, 1192, 1144, 1056, 837, 746 cm^{-1} .

MS (ESI): m/z 290 ($\text{M}^+ + \text{H}$); **HRMS** calcd for $\text{C}_{18}\text{H}_{15}\text{N}_3\text{O}$ ($\text{M}^+ + \text{H}$) 290.12879, found 290.12880.



(11b): white fluppy solid

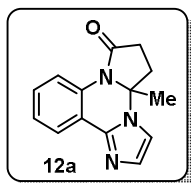
Yield: 67%; mp = 181-183 °C; R_f 0.35 (MeOH/DCM = 02/98).

$^1\text{H NMR}$ (500 MHz, CDCl_3): δ 8.33-8.31 (d, $J = 7.9$ Hz, 1H), 8.21-8.19 (d, $J = 7.9$ Hz, 1H), 7.86-7.84 (d, $J = 7.1$ Hz, 1H), 7.55-7.52 (t, $J = 6.9$ Hz, 1H), 7.45-7.43 (d, $J = 7.9$ Hz, 1H), 7.38-7.35 (t, $J = 7.9$ Hz, 1H), 7.32-7.28 (m, 2H), 3.11-3.01 (m, 2H), 2.92-2.85 (m, 1H), 2.78-2.72 (m, 1H), 2.09-1.96 (m, 2H), 0.89-0.86 (t, $J = 8.0$ Hz, 3H).

$^{13}\text{C NMR}$ (300 MHz, CDCl_3): δ 172.0, 146.0, 143.9, 132.6, 132.3, 131.2, 126.0, 125.6, 123.2, 121.9, 120.3, 118.4, 110.5, 81.2, 32.6, 30.4, 30.0, 8.3.

IR (KBr): ν_{max} 3411, 2979, 1719, 1613, 1387, 1293, 1059, 835, 741 cm^{-1} .

MS (ESI): m/z 304 ($\text{M}^+ + \text{H}$); HRMS calcd for $\text{C}_{19}\text{H}_{17}\text{N}_3\text{O}$ ($\text{M}^+ + \text{H}$) 304.1444, found 304.1443.



(12a): white solid

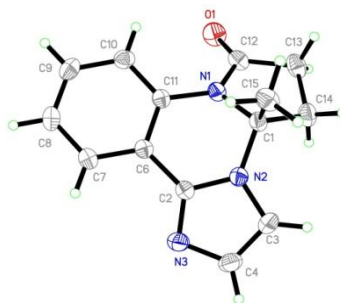
Yield: 84%; mp = 162-164 °C; R_f 0.20 (hexane/EtOAc = 50/50).

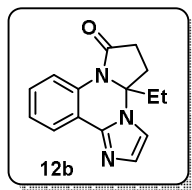
$^1\text{H NMR}$ (300 MHz, CDCl_3): δ 8.13-8.07 (m, 2H), 7.46-7.41 (dt, $J = 7.6$ & 1.5 Hz, 1H), 7.35-7.29 (dt, $J = 7.6$ & 1.5 Hz, 1H), 7.25-7.24 (d, $J = 1.5$ Hz, 1H), 7.03-7.02 (d, $J = 1.5$ Hz, 1H), 2.86-2.66 (m, 4H), 1.57 (s, 3H).

$^{13}\text{C NMR}$ (75 MHz, CDCl_3): δ 171.3, 140.7, 130.6, 130.5, 129.2, 125.8, 123.5, 121.7, 113.6, 77.0, 31.9, 29.7, 26.6.

IR (KBr): ν_{max} 2925, 1707, 1485, 1363, 1220, 1132, 740 cm^{-1} .

MS (ESI): m/z 240 ($\text{M}^+ + \text{H}$); HRMS calcd for $\text{C}_{14}\text{H}_{13}\text{N}_3\text{O}$ ($\text{M}^+ + \text{H}$) 240.1131, found 240.1129.





(12b): Yellowish thick liquid

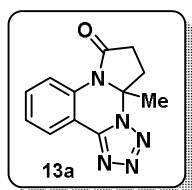
Yield: 71%; R_f 0.25 (hexane/EtOAc = 50/50)

^1H NMR (500 MHz, CDCl_3): δ 8.09-8.05 (t, $J = 8.5$ Hz, 2H), 7.44-7.41 (t, $J = 7.3$ Hz, 1H), 7.33-7.30 (t, $J = 7.3$ Hz, 1H), 7.24 (s, 1H), 7.01 (s, 1H), 2.84-2.57 (m, 4H), 1.89-1.78 (m, 2H), 0.86-0.83 (t, $J = 6.7$ Hz, 3H).

^{13}C NMR (75 MHz, CDCl_3): δ 172.1, 141.0, 131.1, 129.7, 129.5, 126.1, 123.8, 122.1, 118.9, 114.8, 80.1, 33.1, 30.1, 29.2, 8.2.

IR (KBr): ν_{max} 2925, 1711, 1491, 1357, 1205, 1132, 747 cm^{-1} .

MS (ESI): m/z 254 ($\text{M}^+ + \text{H}$); **HRMS** calcd for $\text{C}_{15}\text{H}_{15}\text{N}_3\text{O}$ ($\text{M}^+ + \text{H}$) 254.1288, found 254.1285.



(13a): white solid

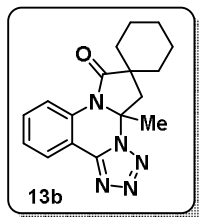
Yield: 85%; mp = 202-204 $^{\circ}\text{C}$; R_f 0.55 (hexane/EtOAc = 60/40)

^1H NMR (500 MHz, CDCl_3): δ 8.23-8.21 (d, $J = 8.0$ Hz, 1H), 8.14-8.12 (d, $J = 8.9$ Hz, 1H), 7.67-7.64 (d, $J = 8.0$ Hz, 1H), 7.47-7.44 (t, $J = 8.0$ Hz, 1H), 3.20-3.11 (m, 1H), 2.94-2.86 (m, 2H), 2.80-2.73 (m, 1H), 1.68 (s, 3H).

^{13}C NMR (75 MHz, CDCl_3): δ 172.0, 147.8, 132.9, 132.1, 126.7, 125.9, 123.2, 113.5, 79.8, 30.8, 29.5, 26.6.

IR (KBr): ν_{max} 3032, 2925, 1713, 1540, 1485, 1440, 1256, 1132, 740 cm^{-1} .

MS (ESI): m/z 242 ($\text{M}^+ + \text{H}$); **HRMS** calcd for $\text{C}_{12}\text{H}_{11}\text{N}_5\text{O}$ ($\text{M}^+ + \text{H}$) 242.1042, found 242.1043.



(**13b**): white solid

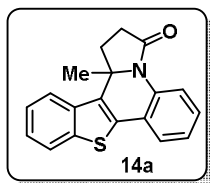
Yield: 79%; mp = 132-134 °C; R_f 0.60 (hexane/EtOAc = 60/40)

^1H NMR (500 MHz, CDCl_3): δ 8.22-8.21 (d, $J = 7.8$ Hz, 1H), 8.03-8.01 (d, $J = 8.7$ Hz, 1H), 7.69-7.66 (d, $J = 7.8$ Hz, 1H), 7.49-7.46 (t, $J = 7.8$ Hz, 1H), 3.28-3.25 (d, $J = 13.6$ Hz, 1H), 2.78-2.75 (d, $J = 13.6$ Hz, 1H), 1.95-1.86 (m, 2H), 1.75-1.70 (m, 4H), 1.68 (s, 3H), 1.54-1.34 (m, 3H), 1.26-1.24 (m, 1H).

^{13}C NMR (75 MHz, CDCl_3): δ 177.7, 147.9, 132.7, 132.2, 126.9, 125.8, 124.2, 114.3, 77.8, 45.2, 41.2, 34.3, 34.2, 28.5, 24.8, 22.1, 21.6.

IR (KBr): ν_{max} 3065, 2925, 1707, 1485, 1391, 1162, 1117, 767 cm^{-1} .

MS (ESI): m/z 310 ($\text{M}^+ + \text{H}$); **HRMS** calcd for $\text{C}_{12}\text{H}_{11}\text{N}_5\text{O}$ ($\text{M}^+ + \text{H}$) 310.1668, found 310.1669.



(**14a**): pale yellow solid

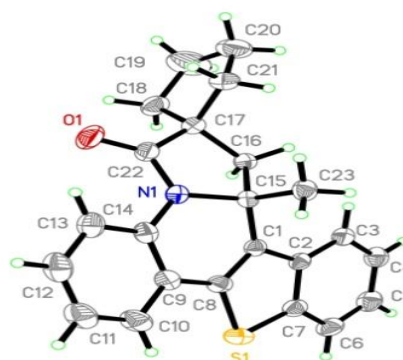
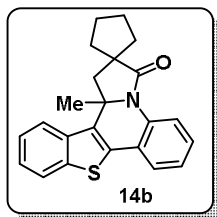
Yield: 79%; mp = 142-145 °C; R_f 0.37 (hexane/EtOAc = 60/40)

^1H NMR (300 MHz, CDCl_3): δ 8.27-8.24 (d, $J = 8.3$ Hz, 1H), 7.75-7.72 (dd, $J = 7.5$ & 1.5 Hz, 1H), 7.57-7.55 (d, $J = 7.5$ Hz, 1H), 7.51-7.48 (d, $J = 8.3$ Hz, 1H), 7.38-7.36 (m, 3H), 7.28-7.25 (m, 1H), 2.95-2.82 (m, 1H), 2.73-2.51 (m, 3H), 1.50 (s, 3H).

^{13}C NMR (75 MHz, CDCl_3): δ 173.4, 131.6, 128.9, 125.6, 125.4, 124.5, 123.3, 123.1, 122.2, 120.4, 101.5, 61.8, 32.4, 30.5, 26.6.

IR (KBr): ν_{max} 2939, 1677, 1477, 1330, 1140, 1055, 733.

MS (ESI): m/z 306 ($\text{M}^+ + \text{H}$); **HRMS** calcd for $\text{C}_{19}\text{H}_{15}\text{NOS}$ ($\text{M}^+ + \text{H}$) 306.0947, found 306.0949.



(**14b**): white fluppy solid

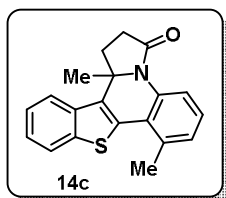
Yield: 83%; mp = 201-203 °C; R_f 0.45 (hexane/EtOAc = 75/25)

$^1\text{H NMR}$ (300 MHz, CDCl_3): δ 8.26-8.24 (d, J = 8.1 Hz, 1H), 7.88-7.86 (d, J = 7.55 Hz, 1H), 7.76-7.74 (d, J = 7.93 Hz, 1H), 7.50-7.47 (d, J = 7.55 Hz, 1H), 7.42-7.32 (m, 3H), 7.23-7.18 (t, J = 7.5, 1H), 2.83-2.71 (q, J = 12.46 & 22.2 Hz, 2H), 2.30-2.19 (m, 2H), 2.02 -1.87 (m, 4H), 1.77-1.48 (m, 2H), 1.55 (s, 3H).

$^{13}\text{C NMR}$ (75 MHz, CDCl_3): δ 178.9, 139.6, 136.6, 136.5, 132.6, 132.2, 128.6, 125.0, 124.6, 124.5, 124.2, 123.4, 123.2, 122.6, 122.0, 61.5, 50.4, 47.9, 40.2, 39.1, 26.9, 26.3, 25.5.

IR (KBr): ν_{max} 3443, 2925, 2859, 1683, 1452, 1357, 1160, 1067, 748.

MS (ESI): m/z 360 ($\text{M}^+ + \text{H}$); HRMS calcd for $\text{C}_{23}\text{H}_{21}\text{NOS}$ ($\text{M}^+ + \text{H}$) 360.1417, found 360.1413.



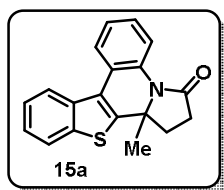
(**14c**): pale yellow solid

Yield: 87%; mp = 179-181 °C; R_f 0.37 (hexane/EtOAc = 60/40)

$^1\text{H NMR}$ (300 MHz, CDCl_3): δ 8.16-8.14 (d, J = 8.1 Hz, 1H), 7.91-7.89 (dd, J = 8.5 & 1.3 Hz, 1H), 7.83-7.80 (dd, J = 7.2 Hz & 1.3 Hz, 1H), 7.43-7.33 (m, 2H), 7.31-7.28 (d, J = 7.7 Hz, 1H), 7.10-7.07 (d, J = 7.6 Hz, 1H), 2.93-2.80 (m, 3H), 2.63-2.54 (m, 1H), 2.77 (s, 3H), 1.50 (s, 3H). $^{13}\text{C NMR}$ (75 MHz, CDCl_3): δ 173.2, 140.0, 136.6, 134.9, 128.3, 128.0, 124.4, 124.2, 122.4, 122.0, 120.6, 63.1, 33.0, 30.4, 24.4, 22.9.

IR (KBr): ν_{max} 3387, 2924, 1704, 1486, 1452, 1345, 1205, 1157, 942, 751 cm^{-1} .

MS (ESI): m/z 320 ($\text{M}^+ + \text{H}$); HRMS calcd for $\text{C}_{20}\text{H}_{17}\text{NOS}$ ($\text{M}^+ + \text{H}$) 320.1103 found 320.1104.



(15a): brownish thick liquid

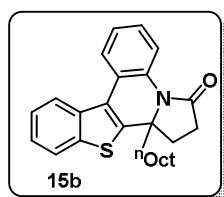
Yield: 72%; R_f 0.25 (hexane/EtOAc = 75/25)

^1H NMR (500 MHz, CDCl_3): δ 8.30-8.27 (d, $J = 8.3$ Hz, 1H), 7.89-7.86 (dd, $J = 7.5$ & 1.5 Hz, 1H), 7.76-7.73 (dd, $J = 7.5$ & 1.5 Hz, 1H), 7.50-7.47 (dd, $J = 7.5$ & 1.5 Hz, 1H), 7.42-7.32 (m, 3H), 7.24-7.19 (t, $J = 7.5$ Hz, 1H), 2.97-2.70 (m, 3H), 2.65-2.57 (m, 1H), 1.51 (s, 3H).

^{13}C NMR (75 MHz, CDCl_3): δ 173.6, 136.5, 135.6, 132.8, 132.1, 128.8, 125.1, 124.8, 124.7, 124.3, 123.2, 123.1, 122.1, 121.9, 64.3, 32.9, 30.3, 24.9.

IR (film): ν_{max} 3372, 3051, 2949, 1694, 1460, 1349, 1145, 1025, 943, 782 cm^{-1} .

MS (ESI): m/z 306 ($\text{M}^+ + \text{H}$); **HRMS** calcd for $\text{C}_{19}\text{H}_{15}\text{NOS}$ ($\text{M}^+ + \text{H}$) 306.0952, found 306.0953.



(15b): yellowish thick liquid

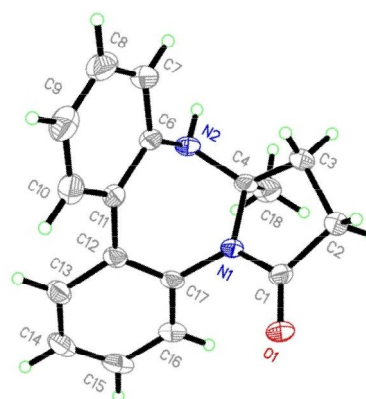
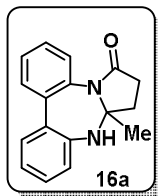
Yield: 66%; R_f 0.40 (hexane/EtOAc = 75/25)

^1H NMR (300 MHz, CDCl_3): δ 8.24-8.21 (d, $J = 8.3$ Hz, 1H), 7.88-7.85 (d, $J = 7.6$ Hz, 1H), 7.75-7.72 (dd, $J = 6.0$ & 2.3 Hz, 1H), 7.50-7.47 (dd, $J = 7.6$ & 1.5 Hz, 1H), 7.40-7.34 (m, 3H), 7.23-7.18 (t, $J = 7.6$ Hz, 1H), 2.95-2.75 (m, 3H), 2.63-2.53 (m, 1H), 1.93-1.73 (s, 2H), 1.18-1.10 (m, 12H), 0.84-0.70 (t, $J = 6.8$ Hz, 3H).

^{13}C NMR (75 MHz, CDCl_3): δ 173.6, 139.6, 136.4, 135.5, 132.7, 132.1, 128.8, 125.0, 124.7, 124.6, 124.2, 123.2, 122.4, 122.0, 121.9, 64.2, 40.2, 36.6, 32.9, 31.6, 30.3, 29.6, 29.2, 24.9, 22.5, 14.0.

IR (film): ν_{max} 3334, 3041, 2943, 1689, 1444, 1337, 1129, 786 cm^{-1} .

MS (ESI): m/z 404 ($\text{M}^+ + \text{H}$); **HRMS** calcd for $\text{C}_{26}\text{H}_{29}\text{NOS}$ ($\text{M}^+ + \text{H}$) 404.2048, found 404.2047.



(16a): yellowish white solid

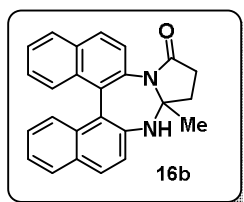
Yield: 85%; mp = 179-181 °C; R_f 0.22 (hexane/EtOAc = 50/50)

^1H NMR (300 MHz, CDCl_3): δ 7.56-7.52 (m, 1H), 7.49-7.42 (m, 3H), 7.35-7.24 (m, 3H), 7.07-7.04 (dd, J = 6.8 & 2.3 Hz, 1H), 3.38 (s, D_2O exchangeable, 1H), 2.63-2.49 (m, 1H), 2.43-2.31 (m, 2H), 2.09-2.02 (m, 1H), 1.54 (s, 3H).

^{13}C NMR (75 MHz, CDCl_3): δ 172.1, 140.9, 138.1, 136.3, 133.6, 129.7, 129.1, 128.8, 128.6, 128.4, 126.2, 125.6, 88.1, 31.1, 31.0, 25.6.

IR (KBr): ν_{max} 3312, 1679, 1489, 1381, 1202, 900, 762 cm^{-1} .

MS (ESI): m/z 265 ($\text{M}^+ + \text{H}$); **HRMS** calcd for $\text{C}_{17}\text{H}_{16}\text{N}_2\text{O}$ ($\text{M}^+ + \text{H}$) 265.1335, found 265.1334.



(16b): yellowish white solid

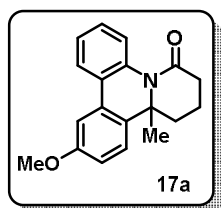
Yield: 63%; mp = 179-181 °C; R_f 0.20 (hexane/EtOAc = 50/50)

^1H NMR (300 MHz, CDCl_3): δ 8.07-8.04 (d, J = 8.3 Hz, 1H), 7.98-7.96 (d, J = 8.3 Hz, 1H), 7.92-7.87 (t, J = 8.3 Hz, 2H), 7.59-7.57 (d, J = 8.3 Hz, 1H), 7.52-7.47 (dt, J = 8.3 & 1.5 Hz, 1H), 7.43-7.40 (dt, J = 8.3 & 1.5 Hz, 1H), 7.37-7.33 (m, 2H), 7.29-7.26 (m, 2H), 7.24-7.17 (m, 1H), 2.60-2.48 (m, 1H), 2.32-2.18 (m, 2H), 2.11-2.03 (m, 1H), 1.49 (s, 3H).

^{13}C NMR (75 MHz, CDCl_3): δ 172.1, 139.7, 133.2, 132.9, 132.8, 132.5, 132.2, 131.8, 130.2, 129.6, 129.3, 128.3, 127.9, 127.5, 127.2, 126.3, 126.2, 126.1, 126.0, 89.1, 31.2, 30.6, 25.6.

IR (KBr): ν_{max} 3319, 1683, 1481, 1377, 1214, 912, 767 cm^{-1} .

MS (ESI): m/z 365 ($\text{M}^+ + \text{H}$); **HRMS** calcd for $\text{C}_{17}\text{H}_{16}\text{N}_2\text{O}$ ($\text{M}^+ + \text{H}$) 365.1653, found 365.1654.



(17a): white solid

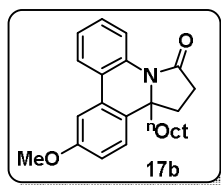
Yield: 67%; mp = 152-154 °C; R_f 0.40 (hexane/EtOAc = 60/40)

$^1\text{H NMR}$ (300 MHz, CDCl_3): δ 7.75-7.72 (dd, $J = 7.5$ & 1.3 Hz, 1H) 7.68-7.65 (dd, $J = 7.5$ & 1.0 Hz, 1H), 7.38-7.28 (m, 3H) 7.23-7.20 (d, $J = 8.7$ Hz, 1H), 6.90-6.86 (dd, $J = 8.7$ & 2.64 Hz, 1H), 3.88 (s, 3H), 2.72-2.55 (m, 2H), 2.50-2.40 (m, 1H), 2.31-2.23 (m, 1H), 1.99-1.87 (m, 2H), 1.24 (s, 3H).

$^{13}\text{C NMR}$ (75 MHz, CDCl_3): δ 169.6, 159.0, 135.3, 132.6, 128.9, 127.8, 127.7, 125.9, 123.6, 123.4, 113.4, 109.5, 59.4, 55.4, 33.7, 33.6, 28.8, 17.5.

IR (KBr): ν_{max} 2629, 1649, 1493, 1344, 1302, 1212, 1024, 752 cm^{-1} .

MS (ESI): m/z 294 ($\text{M}^+ + \text{H}$); **HRMS** calcd for $\text{C}_{19}\text{H}_{19}\text{NO}_2$ ($\text{M}^+ + \text{H}$) 294.1494, found 294.1495.



(17b): pale yellow thick liquid

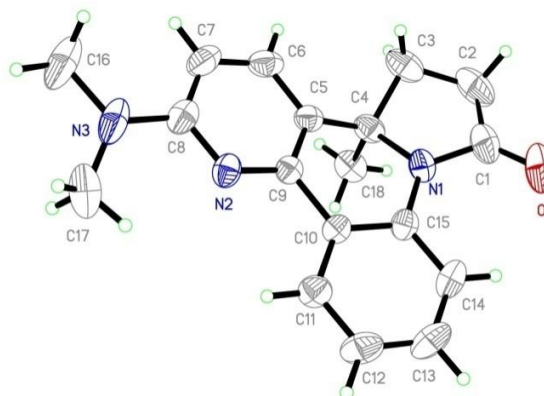
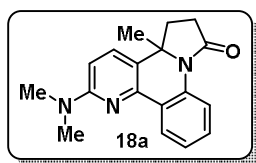
Yield: 65%; R_f 0.50 (hexane/EtOAc = 70/30)

$^1\text{H NMR}$ (300 MHz, CDCl_3): δ 8.24-8.21 (dd, $J = 8.3$ & 1.5 Hz, 1H), 7.81-7.77 (dd, $J = 8.3$ & 1.5 Hz, 1H), 7.41-7.35 (t, $J = 7.5$ Hz, 1H), 7.30-7.29 (d, $J = 3.0$ Hz, 1H), 7.24-7.21 (d, $J = 7.5$ Hz, 1H), 7.13-7.10 (d, $J = 8.3$ Hz, 1H), 6.91-6.87 (dd, $J = 8.3$ & 3.0 Hz, 1H), 3.88 (s, 3H), 2.85-2.71 (m, 1H), 2.56-2.48 (m, 3H), 1.59-1.53 (t, $J = 7.5$ Hz, 2H), 1.25-1.10 (m, 12H), 0.85-0.80 (t, $J = 6.8$ Hz, 3H).

$^{13}\text{C NMR}$ (75 MHz, CDCl_3): δ 173.2, 159.0, 134.1, 133.6, 130.9, 128.8, 126.0, 125.4, 124.9, 123.5, 122.2, 113.6, 108.4, 65.3, 55.4, 40.2, 31.7, 31.2, 29.8, 29.3, 29.0, 24.0, 22.5, 14.0.

IR (film): ν_{max} 2629, 1661, 1478, 1353, 1223, 1027, 759 cm^{-1} .

MS (ESI): m/z 378 ($\text{M}^+ + \text{H}$); **HRMS** calcd for $\text{C}_{25}\text{H}_{31}\text{NO}_2$ ($\text{M}^+ + \text{H}$) 378.2433, found 378.2434.



(**18a**): brownish solid

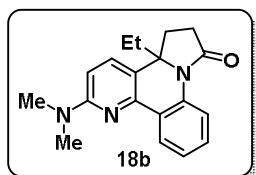
Yield: 69%; mp = 132-134 °C; R_f 0.22 (hexane/EtOAc = 60/40)

^1H NMR (300 MHz, CDCl_3): δ 8.33-8.29 (dd, $J = 8.3$ & 1.5 Hz, 1H), 8.27-8.24 (dd, $J = 8.3$ & 1.5 Hz, 1H), 7.39-7.33 (dt, $J = 7.5$ & 1.5 Hz, 1H), 7.22-7.17 (m, 2H), 6.48-6.45 (d, $J = 9.1$ Hz, 1H), 3.17 (s, 6H), 2.86-2.68 (m, 1H), 2.58-2.41 (m, 3H), 1.36 (s, 3H).

^{13}C NMR (75 MHz, CDCl_3): δ 172.9, 158.2, 148.8, 132.4, 129.5, 129.0, 124.9, 124.6, 122.5, 121.0, 105.5, 62.8, 59.0, 37.9, 32.3, 30.8, 27.3.

IR (KBr): ν_{max} 2963, 2923, 1697, 1609, 1486, 1429, 1353, 1180, 759 cm^{-1} .

MS (ESI): m/z 294 ($\text{M}^+ + \text{H}$); **HRMS** calcd for $\text{C}_{18}\text{H}_{19}\text{N}_3\text{O}$ ($\text{M}^+ + \text{H}$) 294.1600, found 294.1598.



(**18b**): brown solid

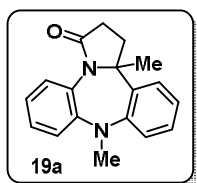
Yield: 59%; mp = 120-123 °C; R_f 0.35 (hexane/EtOAc = 60/40)

^1H NMR (500 MHz, CDCl_3): δ 8.36-8.35 (d, $J = 7.1$ Hz, 1H), 8.23-8.21 (d, $J = 8.1$ Hz, 1H), 7.52-7.45 (m, 1H), 7.40-7.37 (t, $J = 8.1$ Hz, 1H), 7.24-7.23 (m, 1H), 6.52-6.50 (d, $J = 9.1$ Hz, 1H), 3.2 (s, 6H), 2.80-2.73 (m, 1H), 2.56-2.46 (m, 2H), 2.41-2.34 (m, 1H), 1.68-1.64 (q, $J = 7.1$ Hz, 2H), 0.77-0.74 (t, $J = 7.1$ Hz, 3H).

^{13}C NMR (75 MHz, CDCl_3): δ 173.2, 158.2, 133.4, 131.9, 129.4, 128.8, 124.9, 124.6, 121.2, 119.7, 105.1, 65.8, 37.9, 33.2, 31.0, 29.2, 8.5.

IR (KBr): ν_{max} 2958, 2931, 1689, 1600, 1471, 1178, 771 cm^{-1} .

MS (ESI): m/z 308 ($\text{M}^+ + \text{H}$); **HRMS** calcd for $\text{C}_{19}\text{H}_{21}\text{N}_3\text{O}$ ($\text{M}^+ + \text{H}$) 308.1763, found 308.1761.



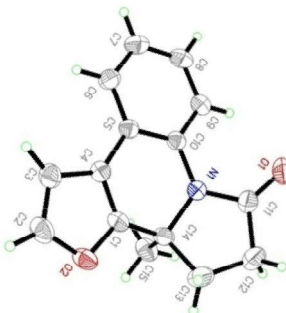
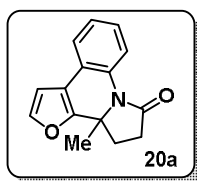
(**19a**): white solid

Yield: 72%; mp = 168-172 °C; R_f 0.15 (hexane/EtOAc = 60/40)

$^1\text{H NMR}$ (300 MHz, CDCl_3): δ 7.31-7.29 (d, $J = 7.6$ Hz, 1H), 7.21-7.19 (m, 2H), 7.16-7.06 (m, 4H), 6.96-6.91 (dt, $J = 7.6$ & 1.5 Hz, 1H), 3.36 (s, 3H), 2.64-2.57 (m, 2H), 2.45-2.39 (m, 2H), 1.58 (s, 3H); $^{13}\text{C NMR}$ (75 MHz, CDCl_3): δ 174.0, 147.3, 143.9, 134.3, 130.6, 128.8, 128.4, 127.4, 123.4, 121.0, 117.6, 66.0, 40.3, 37.5, 30.1, 30.0.

IR (KBr): ν_{max} 3422, 2955, 1689, 1592, 1485, 1330, 1233, 1132, 1053, 876, 772 cm^{-1} .

MS (ESI): m/z 279 ($\text{M}^+ + \text{H}$); **HRMS** calcd for $\text{C}_{18}\text{H}_{18}\text{N}_2\text{O}$ ($\text{M}^+ + \text{H}$) 279.1565, found 279.1566.



(**20a**): white solid

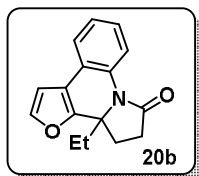
Yield: 57%; mp = 132-134 °C; R_f 0.70 (hexane/EtOAc = 80/20)

$^1\text{H NMR}$ (500 MHz, CDCl_3): δ 8.13-8.11 (d, $J = 8.0$ Hz, 1H) 7.39-7.37 (m, 2H), 7.27-7.24 (t, $J = 8.0$ Hz, 1H), 7.19-7.17 (t, $J = 7.0$ Hz, 1H), 6.66-6.56 (d, $J = 2.0$ Hz, 1H), 2.84-2.77 (m, 1H), 2.62-2.50 (m, 2H), 2.39-2.35 (m, 1H), 1.37 (s, 3H).

$^{13}\text{C NMR}$ (75 MHz, CDCl_3): δ 173.9, 153.4, 142.7, 131.3, 126.6, 125.1, 122.8, 114.4, 105.9, 61.6, 30.1, 29.9, 24.8.

IR (KBr): ν_{max} 2923, 1700, 1498, 1349, 1174, 758 cm^{-1} .

MS (ESI): m/z 240 ($\text{M}^+ + \text{H}$); **HRMS** calcd for $\text{C}_{15}\text{H}_{13}\text{NO}_2$ ($\text{M}^+ + \text{H}$) 240.1019, found 240.1021.



(20b): yellowish thick liquid

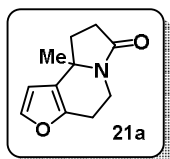
Yield: 52% R_f 0.75 (hexane/EtOAc = 80/20)

$^1\text{H NMR}$ (300 MHz, CDCl_3): δ 8.09-8.06 (dd, $J = 6.8$ & 1.5 Hz, 1H), 7.41-7.37 (m, 2H), 7.29-7.23 (m, 1H), 7.21-7.15 (dt, $J = 7.5$ & 1.5 Hz, 1H), 6.69-6.67 (d, $J = 2.3$ Hz, 1H), 2.86-2.73 (m, 1H), 2.58-2.41 (m, 3H), 1.83-1.59 (m, 2H), 0.83-0.78 (t, $J = 7.6$ Hz, 3H).

$^{13}\text{C NMR}$ (75 MHz, CDCl_3): δ 174.5, 152.7, 142.8, 132.2, 126.6, 125.1, 122.8, 115.1, 105.8, 65.0, 32.1, 30.3, 27.2, 8.0.

IR (film): ν_{max} 2921, 1697, 1503, 1371, 1179, 764 cm^{-1} .

MS (ESI): m/z 254 ($\text{M}^+ + \text{H}$); **HRMS** calcd for $\text{C}_{16}\text{H}_{15}\text{NO}_2$ ($\text{M}^+ + \text{H}$) 254.1176, found 254.1174.



(21a): pale yellow thick liquid

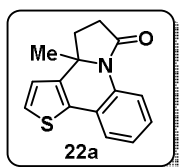
Yield: 49%; R_f 0.45 MeOH/DCM = 05/95

$^1\text{H NMR}$ (300 MHz, CDCl_3): δ 7.29-7.28 (d, $J = 3.0$ Hz, 1H), 6.23-6.22 (d, $J = 3.0$ Hz, 1H), 4.44-4.40 (dd, $J = 13.9$ & 6.0 Hz, 1H), 3.06-3.00 (dt, $J = 13.9$ & 6.0 Hz, 1H), 2.76-2.74 (t, $J = 6.0$ Hz, 2H), 2.65-2.57 (m, 3H), 2.46-2.40 (m, 1H), 1.44 (s, 3H).

$^{13}\text{C NMR}$ (75 MHz, CDCl_3): δ 175.8, 146.4, 141.7, 124.0, 106.4, 59.8, 37.8, 33.8, 33.2, 25.6, 23.2.

IR (film): ν_{max} 2932, 1715, 1668, 1414, 1215, 1165, 1075, 742 cm^{-1} .

MS (ESI): m/z 192 ($\text{M}^+ + \text{H}$); **HRMS** calcd for $\text{C}_{11}\text{H}_{13}\text{NO}_2$ ($\text{M}^+ + \text{H}$) 192.1019, found 192.1020.



(22a): thick yellow liquid

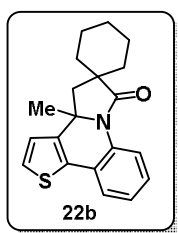
Yield: 71%; R_f 0.35 (hexane/EtOAc = 80/20)

^1H NMR (300 MHz, CDCl_3): δ 8.24-8.21 (dd, $J = 8.1$ & 1.0 Hz, 1H), 7.47-7.44 (dd, $J = 7.7$ & 1.3 Hz, 1H), 7.32-7.27 (m, 2H), 7.19-7.13 (dt, $J = 7.7$ & 1.3 Hz, 1H), 6.93-6.91 (d, $J = 5.1$ Hz, 1H), 2.88-2.75 (m, 1H), 2.60-2.44 (m, 3H), 1.36 (s, 3H).

^{13}C NMR (75 MHz, CDCl_3): δ 173.5, 142.4, 132.0, 131.5, 127.8, 125.3, 124.9, 123.3, 123.2, 123.1, 122.1, 63.1, 32.4, 30.4, 26.5.

IR (film): ν_{max} 2937, 2851, 1689, 1477, 1353, 1212, 761 cm^{-1} .

MS (ESI): m/z 256 ($\text{M}^+ + \text{H}$); **HRMS** calcd for $\text{C}_{15}\text{H}_{13}\text{NOS}$ ($\text{M}^+ + \text{H}$) 256.0796, found 256.0795.



(22b): yellowish thick liquid

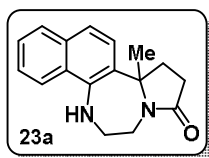
Yield: 79%; R_f 0.42 (hexane/EtOAc = 95/05)

^1H NMR (300 MHz, CDCl_3): δ 8.10-8.08 (d, $J = 8.3$ Hz, 1H), 7.47-7.44 (dd, $J = 7.5$ & 1.5 Hz, 1H), 7.34-7.28 (dt, $J = 7.5$ & 1.5 Hz, 1H), 7.27-7.26 (d, $J = 5.3$ Hz, 1H), 7.20-7.15 (dt, $J = 7.5$ & 1.5 Hz, 1H), 6.96-6.95 (d, $J = 5.3$ Hz, 1H), 2.45 (s, 2H), 1.93-1.64 (m, 7H), 1.37 (s, 3H), 1.35-1.26 (m, 3H).

^{13}C NMR (75 MHz, CDCl_3): δ 178.2, 143.7, 131.4, 127.5, 125.0, 123.3, 123.2, 123.0, 120.4, 60.0, 45.2, 42.7, 35.3, 34.3, 29.7, 25.2, 22.4, 21.9.

IR (film): ν_{max} 2929, 2855, 1692, 1487, 1352, 1211, 754 cm^{-1} .

MS (ESI): m/z 324 ($\text{M}^+ + \text{H}$); **HRMS** calcd for $\text{C}_{20}\text{H}_{21}\text{NOS}$ ($\text{M}^+ + \text{H}$) 324.1417, found 324.1416.



(23a): yellowish white solid

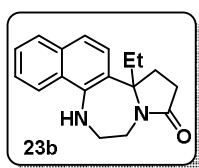
Yield: 61%; mp = 104-106 $^{\circ}\text{C}$; R_f 0.30 (MeOH/DCM = 05/95)

^1H NMR (300 MHz, CDCl_3): δ 7.85-7.33 (m, 2H), 7.49-7.42 (m, 2H), 7.37-7.35 (d, $J = 8.3$ Hz, 1H), 7.32-7.30 (d, $J = 8.3$ Hz, 1H), 4.50-4.41 (m, 1H), 3.59-3.51 (m, 1H), 3.43-3.33 (m, 1H), 3.20-3.10 (m, 1H), 2.77-2.56 (m, 4H), 1.85 (s, 3H).

^{13}C NMR (75 MHz, CDCl_3): δ 176.5, 144.1, 132.7, 128.2, 126.0, 125.8, 125.7, 125.3, 120.1, 120.0, 65.6, 46.4, 37.8, 29.4, 29.1, 27.7.

IR (KBr): ν_{max} 3407, 2923, 1665, 1409, 1356, 1112, 814, 751 cm^{-1} .

MS (ESI): m/z 267 ($\text{M}^+ + \text{H}$); **HRMS** calcd for $\text{C}_{17}\text{H}_{18}\text{N}_2\text{O}$ ($\text{M}^+ + \text{H}$) 267.1492, found 267.1490.



(23b): white solid

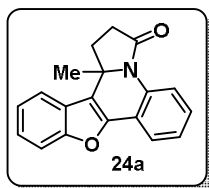
Yield: 58%; mp = 166-168 $^{\circ}\text{C}$; R_f 0.30 (MeOH/DCM = 05/95)

^1H NMR (300 MHz, CDCl_3): δ 7.83-7.75 (m, 2H), 7.50-7.42 (m, 2H), 7.38-7.29 (q, $J = 7.5$ Hz, 2H), 4.49-4.40 (m, 1H), 3.45-3.39 (m, 2H), 3.15-3.07 (m, 1H), 2.55-2.19 (m, 5H), 2.11-1.99 (m, 1H), 0.94-0.89 (t, $J = 7.5$ Hz, 3H).

^{13}C NMR (75 MHz, CDCl_3): δ 175.8, 144.0, 132.9, 128.3, 126.6, 126.3, 125.9, 125.8, 120.2, 120.0, 70.1, 46.9, 40.6, 32.1, 29.7, 8.3.

IR (KBr): ν_{max} 3398, 2927, 1669, 1398, 1347, 1109, 819, 759 cm^{-1} .

MS (ESI): m/z 281 ($\text{M}^+ + \text{H}$); **HRMS** calcd for $\text{C}_{18}\text{H}_{20}\text{N}_2\text{O}$ ($\text{M}^+ + \text{H}$) 281.1654, found 281.1656.



(24a): pale yellow solid

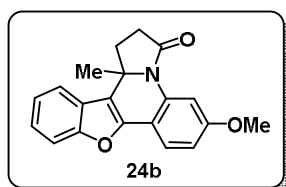
Yield: 84%; mp = 142-145 $^{\circ}\text{C}$; R_f 0.50 (hexane/EtOAc = 60/40)

^1H NMR (300 MHz, CDCl_3): δ 8.30-8.27 (dd, $J = 8.3$ & 1.5 Hz, 1H), 7.88-7.85 (dd, $J = 9.0$ & 1.5 Hz, 1H), 7.76-7.73 (dd, $J = 7.5$ & 2.2 Hz, 1H), 7.50-7.47 (dd, $J = 7.55$ & 1.5 Hz, 1H), 7.41-7.32 (m, 3H), 7.23-7.18 (m, 1H), 2.96-2.68 (m, 3H), 2.64-2.56 (m, 1H), 1.5 (s, 3H).

^{13}C NMR (75 MHz, CDCl_3): δ 173.4, 139.5, 136.4, 135.5, 132.8, 132.1, 128.7, 125.0, 124.7, 124.6, 124.2, 123.2, 123.0, 122.0, 121.9, 64.2, 32.9, 30.3, 24.9.

IR (KBr): ν_{max} 3387, 2921, 1703, 1592, 1486, 1451, 1346, 1205, 1156, 1089, 941, 752 cm^{-1} .

MS (ESI): m/z 290 ($\text{M}^+ + \text{H}$); HRMS calcd for $\text{C}_{19}\text{H}_{15}\text{NO}_2$ ($\text{M}^+ + \text{H}$) 290.1176, found 290.1175.



(24b): pale yellow solid

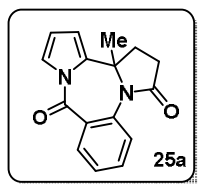
Yield: 69%; mp = 142-144 $^{\circ}\text{C}$; R_f 0.52 (hexane/EtOAc = 60/40)

^1H NMR (300 MHz, CDCl_3): δ 7.95-7.94 (d, $J = 2.3$ Hz, 1H), 7.66-7.63 (d, $J = 9.0$ Hz, 1H), 7.55-7.52 (dd, $J = 9.0$ & 1.5 Hz, 1H), 7.48-7.45 (dd, $J = 7.6$ & 2.3 Hz, 1H), 7.37-7.27 (m, 2H), 6.82-6.78 (dd, $J = 8.31$ & 6.04 Hz, 1H), 3.88 (s, 3H), 2.94-2.55 (m, 4H), 1.49 (s, 3H).

^{13}C NMR (75 MHz, CDCl_3): δ 173.8, 160.1, 150.03, 147.2, 123.9, 123.1, 122.0, 118.4, 111.6, 110.8, 107.9, 125.1, 120.2, 116.7, 123.4, 63.2, 55.4, 32.1, 30.2, 22.4.

IR (KBr): ν_{max} 2924, 2855, 1707, 1602, 1503, 1451, 1347, 1290, 1167, 760 cm^{-1} .

MS (ESI): m/z 320 ($\text{M}^+ + \text{H}$); HRMS calcd for $\text{C}_{20}\text{H}_{16}\text{NO}_3$ ($\text{M}^+ + \text{H}$) 320.1281, found 320.1280.



(25a): pale yellow thick liquid

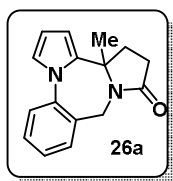
Yield: 69%; R_f 0.45 (hexane/EtOAc = 60/40)

^1H NMR (300 MHz, CDCl_3): δ 8.49-8.46 (dd, $J = 8.3$ & 1.5 Hz, 1H), 7.78-7.62 (dd, $J = 7.8$ & 1.5 Hz,), 7.71-7.66 (dt, $J = 6.8$ & 2.2 Hz, 1H), 7.59-7.55 (dd, $J = 8.3$ & 1.5 Hz, 1H), 7.47-7.41 (dt, $J = 8.3$ & 1.5 Hz, 1H), 6.27-6.24 (t, $J = 3.8$ Hz, 1H), 6.22-6.20 (dd, $J = 3.8$ & 2.3 Hz, 1H), 2.77-2.73 (m, 1H), 2.67-2.59 (m, 3H), 1.40 (s, 3H).

^{13}C NMR (75 MHz, CDCl_3): δ 177.7, 173.1, 135.1, 134.9, 134.4, 133.8, 128.0, 126.9, 125.8, 123.5, 111.5, 109.0, 62.3, 37.6, 29.7, 27.7.

IR (film): ν_{max} 3429, 1704, 1655, 1485, 1449, 1366, 756 cm^{-1} .

MS (ESI): m/z 267 ($\text{M}^+ + \text{H}$); HRMS calcd for $\text{C}_{16}\text{H}_{14}\text{N}_2\text{O}_2$ ($\text{M}^+ + \text{H}$) 267.1128, found 267.1129.



(26a): yellowish solid

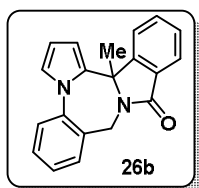
Yield: 83%; mp = 195-197 °C; R_f 0.65 (MeOH/DCM = 02/98)

^1H NMR (300 MHz, CDCl_3): δ 7.48-7.37 (m, 3H), 7.31-7.29 (d, $J = 7.2$ Hz, 1H) 7.04-7.03 (m, 1H), 6.31-6.29 (t, $J = 3.2$ Hz, 1H), 6.21-6.19 (m, 1H), 4.97-4.93 (d, $J = 14.0$ Hz, 1H), 3.99-3.95 (d, $J = 14.0$ Hz, 1H), 2.78-2.41 (m, 4H), 1.06 (s, 3H).

^{13}C NMR (75 MHz, CDCl_3): δ 173.0, 134.7, 130.4, 129.6, 127.5, 126.7, 122.3, 122.2, 108.9, 106.5, 60.8, 43.4, 33.6, 29.6, 29.4.

IR (KBr): ν_{max} 3101, 2961, 1723, 1677, 1458, 1251, 1074, 749 cm^{-1} .

MS (ESI): m/z 253 ($\text{M}^+ + \text{H}$); **HRMS** calcd for $\text{C}_{16}\text{H}_{16}\text{N}_2\text{O}$ ($\text{M}^+ + \text{H}$) 253.1335, found 253.1335.



(26b): yellow thick liquid

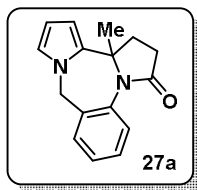
Yield: 67%; R_f 0.15 (MeOH/DCM= 02/98)

^1H NMR (500 MHz, CDCl_3): δ 7.94-7.92 (d, $J = 8.1$ Hz, 1H), 7.68-7.62 (m, 2H), 7.57-7.47 (m, 5H), 7.38-7.36 (t, $J = 7.1$ Hz, 1H), 7.09 (brs, 1H), 6.22 (brs, 1H), 5.93 (brs, 1H), 5.12-5.09 (d, $J = 14.2$ Hz, 1H), 4.32-4.29 (d, $J = 14.2$ Hz, 1H), 1.35 (s, 3H).

^{13}C NMR (75 MHz, CDCl_3): δ 168.7, 149.5, 141.4, 141.2, 131.9, 130.9, 130.8, 129.8, 128.6, 127.9, 126.9, 124.0, 122.8, 122.6, 108.7, 108.1, 64.2, 45.4, 28.2.

IR (film): ν_{max} 3101, 2952, 1718, 1653, 1458, 1252, 1079, 753 cm^{-1} .

MS (ESI): m/z 301 ($\text{M}^+ + \text{H}$); **HRMS** calcd for $\text{C}_{20}\text{H}_{16}\text{N}_2\text{O}$ ($\text{M}^+ + \text{H}$) 301.1341, found 301.1338.



(27a): yellow orange solid

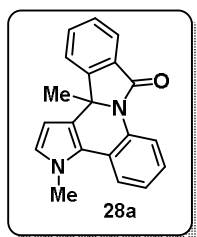
Yield: 69%; mp = 125-127 °C; R_f 0.3 (hexane/EtOAc = 60/40)

^1H NMR (300 MHz, CDCl_3): δ 7.43-7.25 (m, 4H), 6.57-6.56 (t, $J = 2.3$ Hz, 1H), 6.06-6.04 (t, $J = 3.02$ Hz, 1H), 6.00-5.98 (dd, $J = 3.0$ & 1.51 Hz, 1H), 5.31-5.26 (d, $J = 14.3$ Hz, 1H), 4.65-4.60 (d, $J = 14.3$ Hz, 1H), 2.77-2.28 (m, 4H), 1.51 (s, 3H).

^{13}C NMR (75 MHz, CDCl_3): δ 174.4, 136.1, 135.6, 134.7, 129.2, 128.2, 128.0, 121.3, 107.1, 106.9, 64.5, 50.9, 37.1, 30.1, 27.7.

IR (KBr): ν_{max} 2958, 2917, 1688, 1495, 1370, 1152, 756 cm^{-1} .

MS (ESI): m/z 253 ($\text{M}^+ + \text{H}$); **HRMS** calcd for $\text{C}_{16}\text{H}_{16}\text{N}_2\text{O}$ ($\text{M}^+ + \text{H}$) 253.1335, found 253.1334.



(28a): white solid

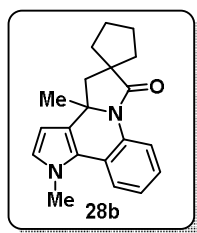
Yield: 82%; mp = 149-151 °C; R_f 0.22 (hexane/EtOAc = 75/25)

^1H NMR (300 MHz, CDCl_3): δ 8.04-8.01 (dd, $J = 6.8$ Hz & 1.5 Hz, 1H), 7.91-7.89 (d, $J = 7.5$ Hz, 1H), 7.76-7.74 (d, $J = 7.5$ Hz, 1H), 7.66-7.60 (d, $J = 7.5$ Hz, 1H), 7.59-7.56 (dd, $J = 7.5$ & 1.5 Hz, 1H), 7.51-7.46 (t, $J = 7.5$ Hz, 1H), 7.32-7.27 (dt, $J = 7.5$ & 1.5 Hz, 1H), 7.22-7.16 (dt, $J = 6.8$ & 1.5 Hz, 1H), 6.51-6.50 (d, $J = 2.3$ Hz, 1H), 6.08-6.07 (d, $J = 3.0$ Hz, 1H), 3.89 (s, 3H), 1.58 (s, 3H).

^{13}C NMR (75 MHz, CDCl_3): δ 166.2, 144.3, 134.0, 131.7, 129.9, 129.5, 128.8, 126.9, 125.8, 125.2, 124.8, 124.7, 124.6, 124.3, 121.9, 117.9, 102.3, 65.7, 37.4, 26.6.

IR (KBr): ν_{max} 3438, 2921, 1690, 1452, 1352, 749.2 cm^{-1} .

MS (ESI): m/z 301 ($\text{M}^+ + \text{H}$); **HRMS** calcd for $\text{C}_{20}\text{H}_{16}\text{N}_2\text{O}$ ($\text{M}^+ + \text{H}$) 301.1345, found 301.1348.



(**28b**): white solid

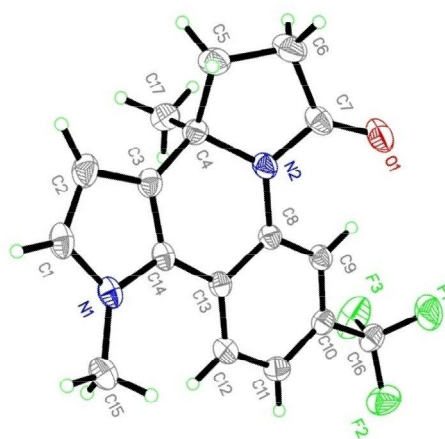
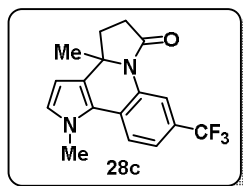
Yield: 89%; mp = 164-166 °C; R_f 0.25 (hexane/EtOAc = 75/25)

^1H NMR (300 MHz, CDCl_3): δ 8.06-8.03 (dd, $J = 7.5$ & 1.5 Hz, 1H), 7.52-7.49 (dd, $J = 7.5$ & 1.5 Hz, 1H), 7.22-7.17 (dt, $J = 7.5$ & 1.5 Hz, 1H), 7.15-7.09 (dt, $J = 7.5$ & 1.5 Hz, 1H), 5.90-5.88 (d, $J = 3.0$ Hz, 1H), 6.54-6.53 (d, $J = 3.0$ Hz, 1H), 3.90 (s, 3H), 2.48-2.43 (d, $J = 12.8$ Hz, 1H), 2.31-2.27 (d, $J = 12.8$ Hz, 1H), 2.21-2.06 (m, 2H), 1.95-1.56 (m, 5H), 1.50-1.41 (m, 1H) 1.32 (s, 3H);

^{13}C NMR (75 MHz, CDCl_3): δ 178.6, 132.0, 129.9, 125.5, 124.6, 124.1, 123.4, 122.6, 120.4, 101.7, 59.1, 50.9, 47.6, 39.6, 30.1, 36.8, 28.8, 25.9, 25.4.

IR (KBr): ν_{max} 3447, 2948, 1677, 1513, 1354, 1229, 753.4 cm^{-1} .

MS (ESI): m/z 307 ($\text{M}^+ + \text{H}$); **HRMS** calcd for $\text{C}_{20}\text{H}_{22}\text{N}_2\text{O}$ ($\text{M}^+ + \text{H}$) 307.1810, found 307.1811.



(**28c**): white coloured solid

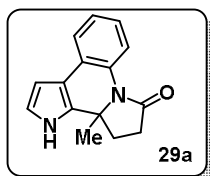
Yield: 55% mp = 149-151 °C; R_f 0.40 (hexane/ EtOAc = 70/30)

^1H NMR (300 MHz, CDCl_3): δ 8.47 (s, 1H), 7.65-7.62 (d, $J = 8.3$ Hz, 1H), 7.42-7.38 (d, $J = 8.3$ Hz, 1H), 6.69-6.68 (d, $J = 2.3$ Hz, 1H), 6.03-6.02 (d, $J = 3.0$ Hz, 1H), 3.92 (s, 3H), 2.85-2.72 (m, 1H) 2.59-2.39 (m, 3H), 1.31 (s, 3H).

^{13}C NMR (75 MHz, CDCl_3): δ 173.6, 131.8, 130.6, 127.2, 125.1, 122.2, 121.4, 121.3, 120.3, 120.2, 120.1, 102.0, 62.0, 37.0, 32.6, 30.5, 26.9.

IR (KBr): ν_{max} 3441, 2957, 1689, 1541, 1354, 1229, 753.4 cm^{-1} .

MS (ESI): m/z 321 ($\text{M}^+ + \text{H}$); HRMS calcd for $\text{C}_{17}\text{H}_{15}\text{F}_3\text{N}_2\text{O}$ ($\text{M}^+ + \text{H}$) 321.1209, found 321.1206.



(29a): white solid

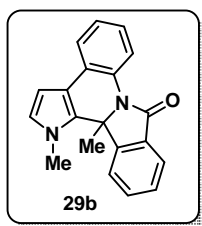
Yield: 82%; mp = 164-166 °C; R_f 0.25 (hexane/EtOAc = 75/25)

^1H NMR (500 MHz, CDCl_3): δ 8.44 (brs, D_2O exchangeable, 1H), 8.11-8.10 (m, 1H), 7.47-7.45 (m, 1H), 7.19-7.14 (m, 2H), 6.73-6.72 (m, 1H), 6.44-6.43 (m, 1H), 2.82-2.76 (m, 1H), 2.55-2.46 (m, 2H), 2.37-2.33 (m, 1H), 1.35 (s, 3H).

^{13}C NMR (75 MHz, CDCl_3): δ 173.9, 132.8, 132.2, 128.7, 128.5, 125.2, 124.9, 122.5, 122.2, 118.6, 102.8, 61.6, 31.1, 30.4, 26.0.

IR (KBr): ν_{max} 3245, 2925, 1713, 1371, 1164, 757 cm^{-1} .

MS (ESI): m/z 239 ($\text{M}^+ + \text{H}$); HRMS calcd for $\text{C}_{15}\text{H}_{14}\text{N}_2\text{O}$ ($\text{M}^+ + \text{H}$) 239.1859, found 239.1861.



(29b): yellowish solid

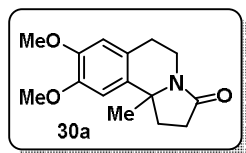
Yield: 59%; mp = 154-156 °C; R_f 0.35 (hexane/EtOAc = 75/25)

^1H NMR (300 MHz, CDCl_3): δ 8.00-7.97 (d, $J = 7.5$ Hz, 1H), 7.86-7.84 (d, $J = 7.5$ Hz, 1H), 7.80-7.77 (m, 1H), 7.66-7.61 (t, $J = 7.5$ Hz, 2H), 7.55-7.46 (m, 2H), 7.24-7.21 (m, 1H), 6.42-6.41 (d, $J = 2.3$ Hz, 1H), 6.34-6.32 (d, $J = 2.3$ Hz, 1H), 3.82 (s, 3H), 1.64 (s, 3H).

^{13}C NMR (75 MHz, CDCl_3): δ 166.0, 149.1, 132.3, 131.2, 128.1, 126.0, 125.2, 124.8, 124.2, 124.0, 122.6, 121.3, 118.9, 118.7, 116.9, 63.1, 17.8, 11.7.

IR (KBr): ν_{max} 3245, 2925, 1713, 1371, 1164, 757 cm^{-1} .

MS (ESI): m/z 301 ($M^+ + H$); **HRMS** calcd for $C_{20}H_{22}N_2O$ ($M^+ + H$) 301.1341, found 301.1339.



(30a): yellowish thick liquid

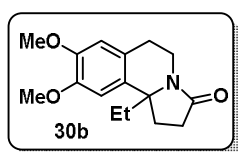
Yield: 90%; R_f 0.15 (MeOH/DCM = 05/95)

1H NMR (300 MHz, $CDCl_3$): δ 6.56 (s, 2H), 4.33-4.27 (m, 1H) 3.88 (s, 3H), 3.86 (s, 3H), 3.12-3.02 (m, 1H), 2.94-2.83 (m, 1H), 2.70-2.57 (m, 2H), 2.48-2.33 (m, 2H), 2.13-2.03 (m, 1H), 1.51 (s, 3H).

^{13}C NMR (75 MHz, $CDCl_3$): δ 172.1, 147.8, 147.6, 134.4, 124.2, 111.3, 107.7, 60.8, 55.9, 55.6, 34.5, 33.8, 30.6, 27.9, 27.1.

IR (film): ν_{max} 3449, 2930, 1678, 1514, 1421, 1260, 1212, 1062, 853, 765 cm^{-1} .

MS (ESI): m/z 262 ($M^+ + H$); **HRMS** calcd for $C_{15}H_{19}NO_3$ ($M^+ + H$) 262.1437, found 262.1438.



(30b): pale yellow thick liquid

Yield: 61%; R_f 0.20 (MeOH/DCM = 05/95)

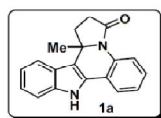
1H NMR (300 MHz, $CDCl_3$): δ 6.56 (s, 1H), 6.55 (s, 1H), 4.36-4.29 (m, 1H), 3.87 (s, 3H), 3.86 (s, 3H), 3.13-3.03 (m, 1H), 2.97-2.85 (m, 1H), 2.70-2.58 (m, 2H), 2.47-2.38 (m, 2H), 2.20-2.12 (m, 1H), 1.95-1.80 (m, 2H), 0.94-0.89 (t, $J = 7.5$ Hz, 3H).

^{13}C NMR (75 MHz, $CDCl_3$): δ 173.4, 147.8, 134.9, 128.5, 124.6, 111.5, 108.1, 64.1, 56.1, 55.8, 34.4, 31.4, 31.2, 27.7, 8.5.

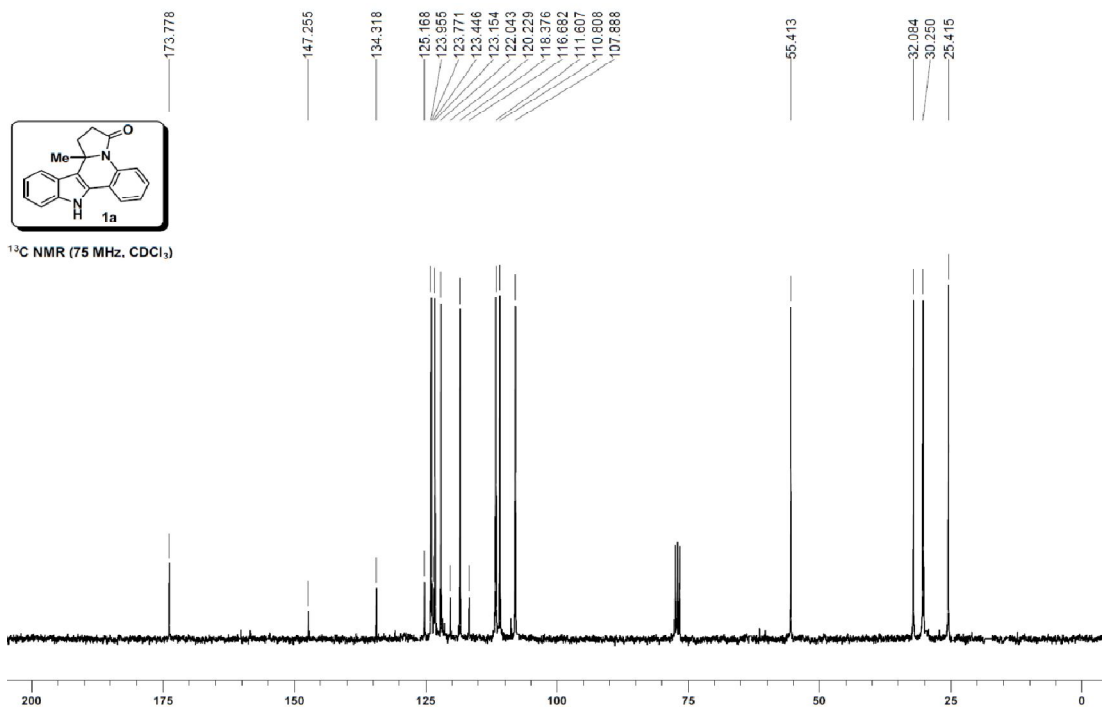
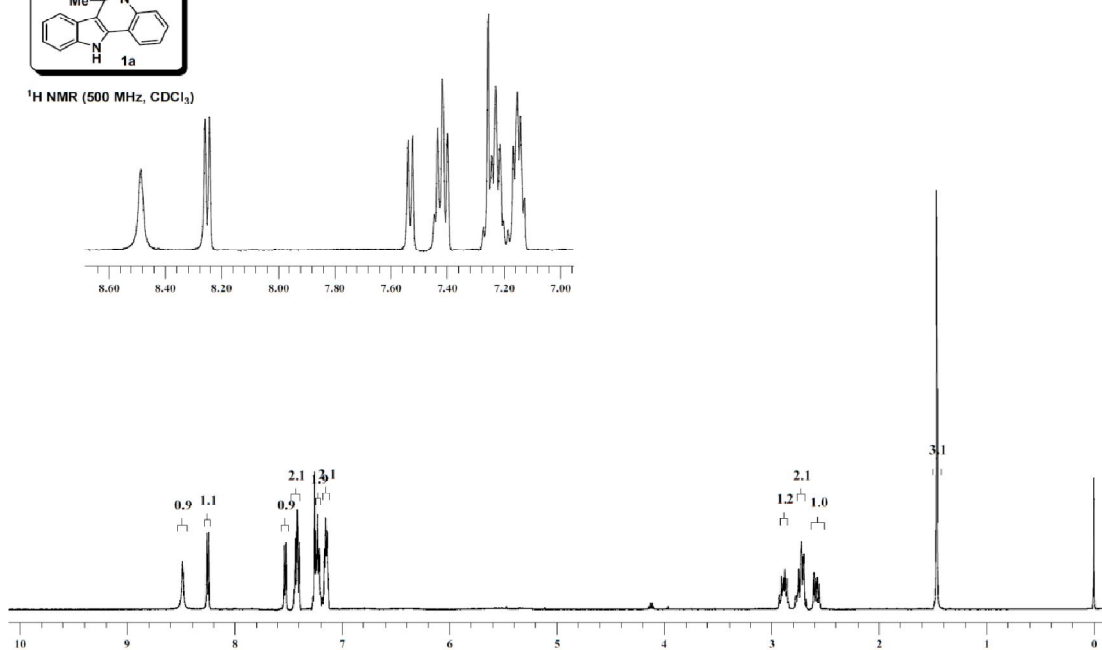
IR (film): ν_{max} 3444, 2930, 1684, 1507, 1413, 1271, 1062, 857, 756 cm^{-1} .

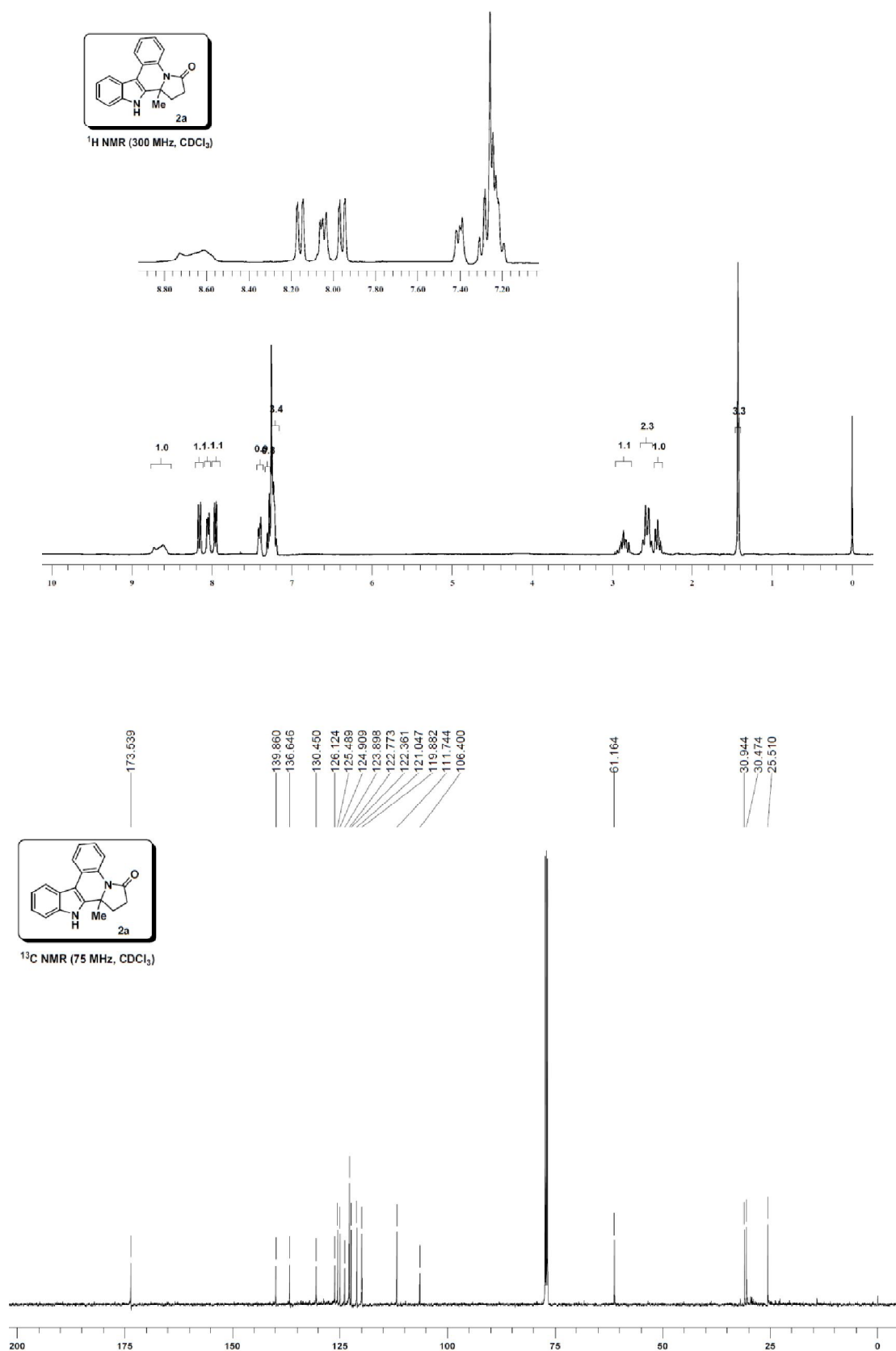
MS (ESI): m/z 276 ($M^+ + H$); **HRMS** calcd for $C_{16}H_{21}NO_3$ ($M^+ + H$) 276.1597, found 262.1598.

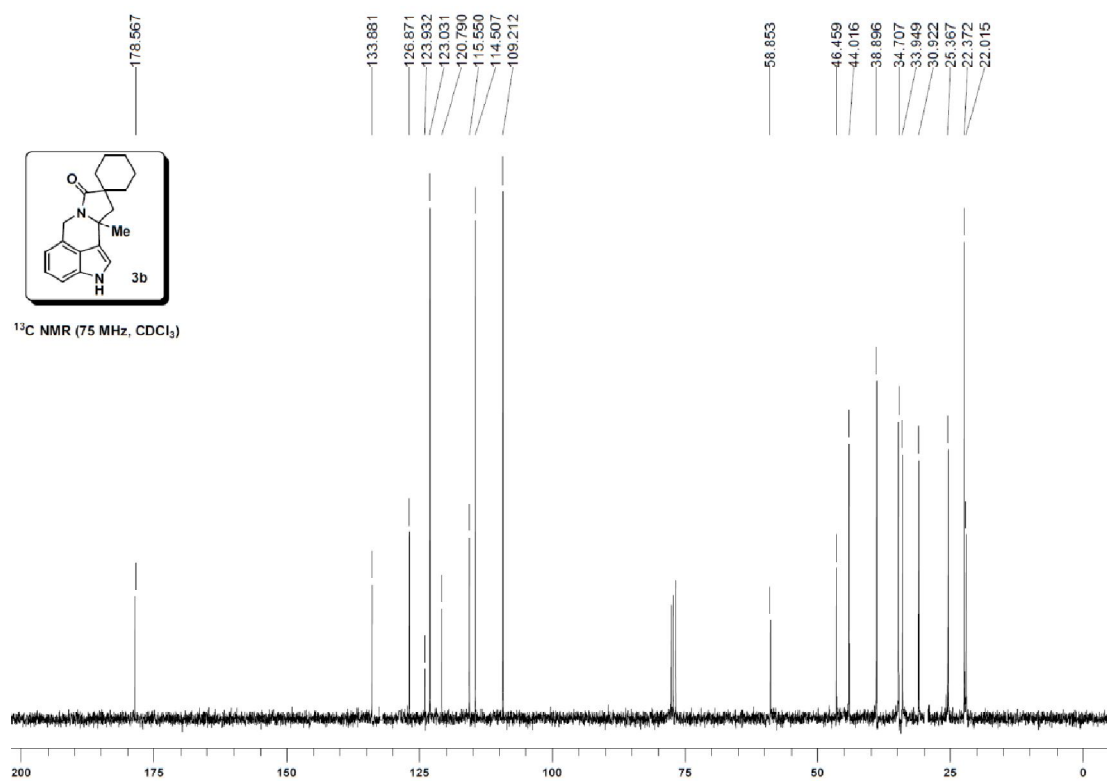
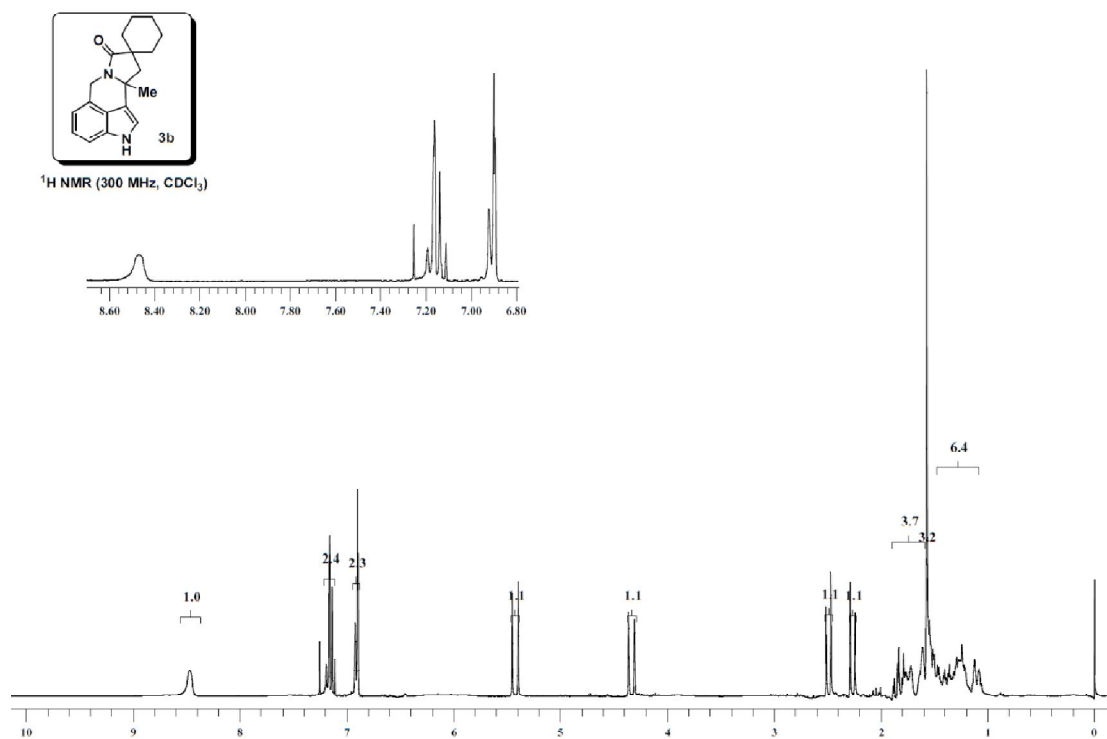
2.7 Spectra

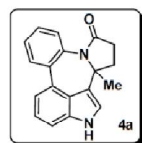


$^1\text{H NMR}$ (500 MHz, CDCl_3)

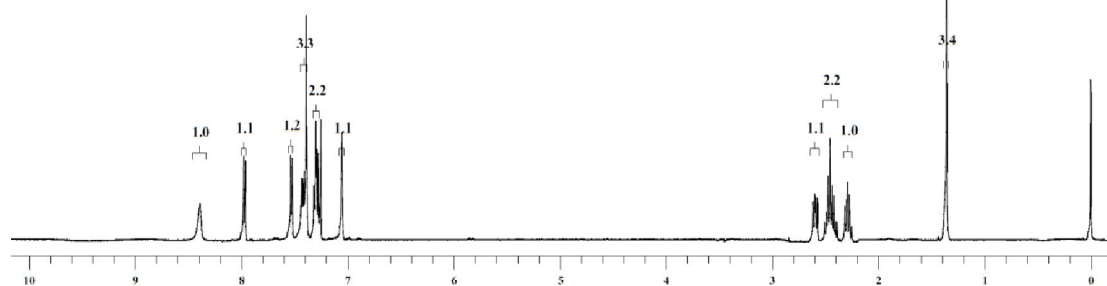
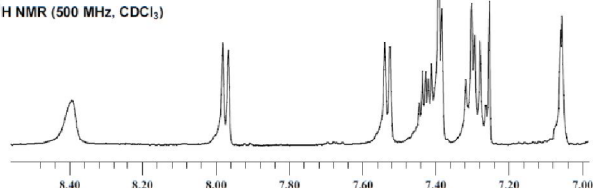








¹H NMR (500 MHz, CDCl₃)

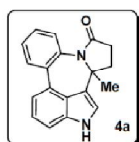


173.655

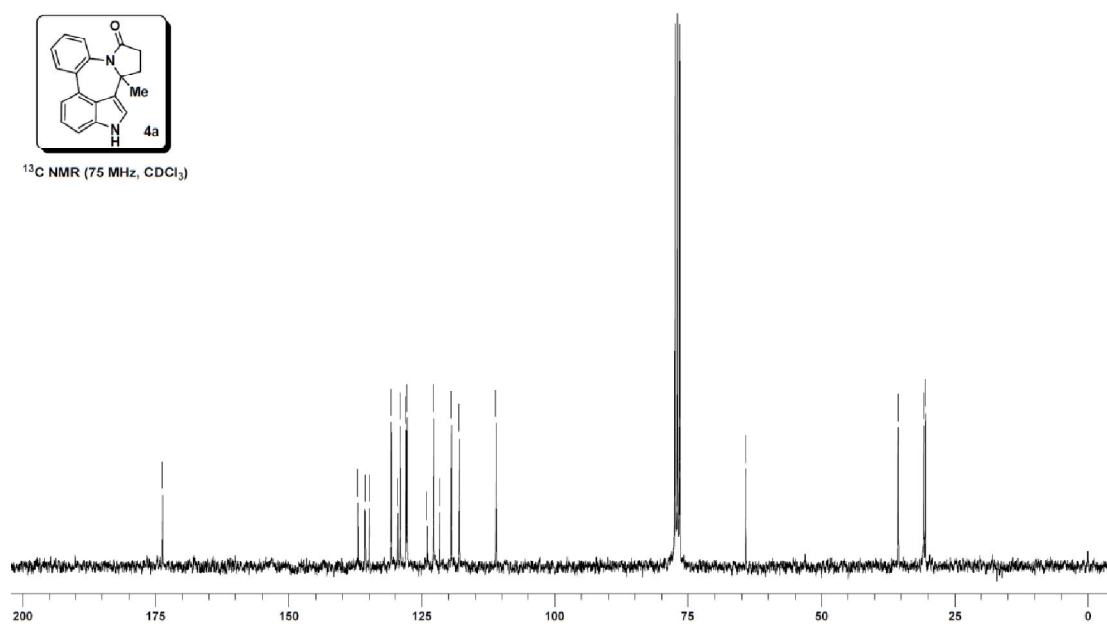
136.906
135.655
134.828
130.749
129.493
129.033
127.976
127.781
123.975
122.794
121.658
119.434
117.931
111.021

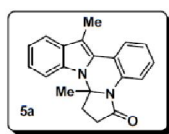
64.177

35.673
30.716
30.434

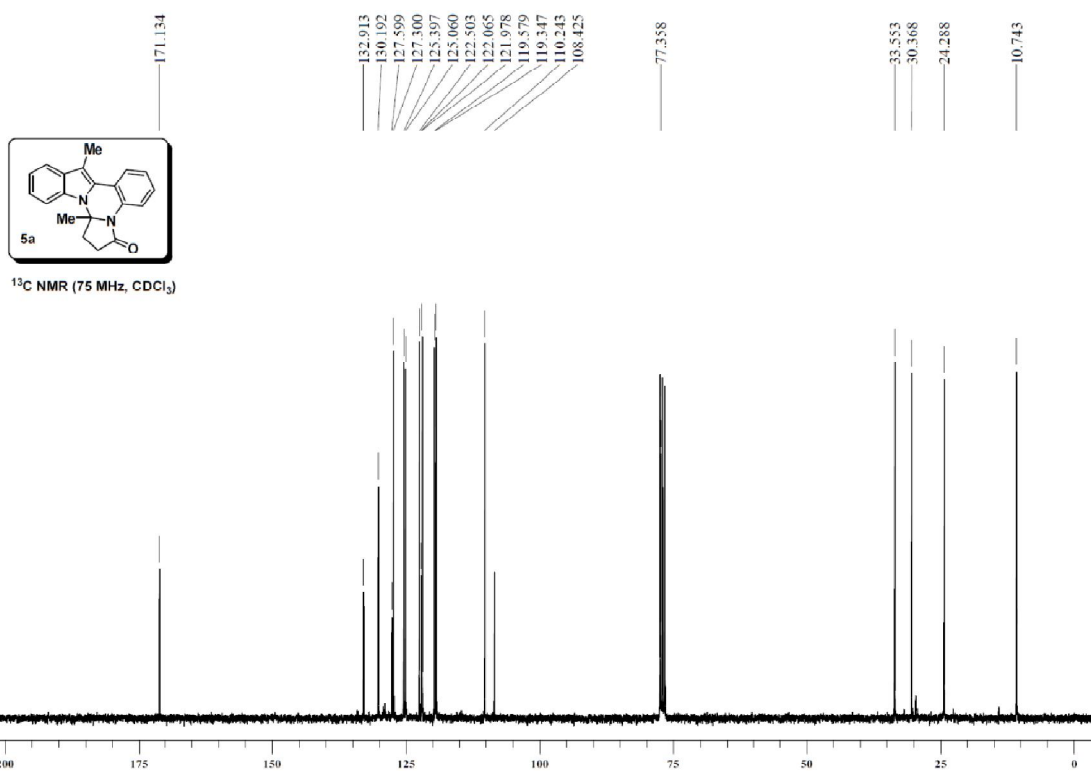
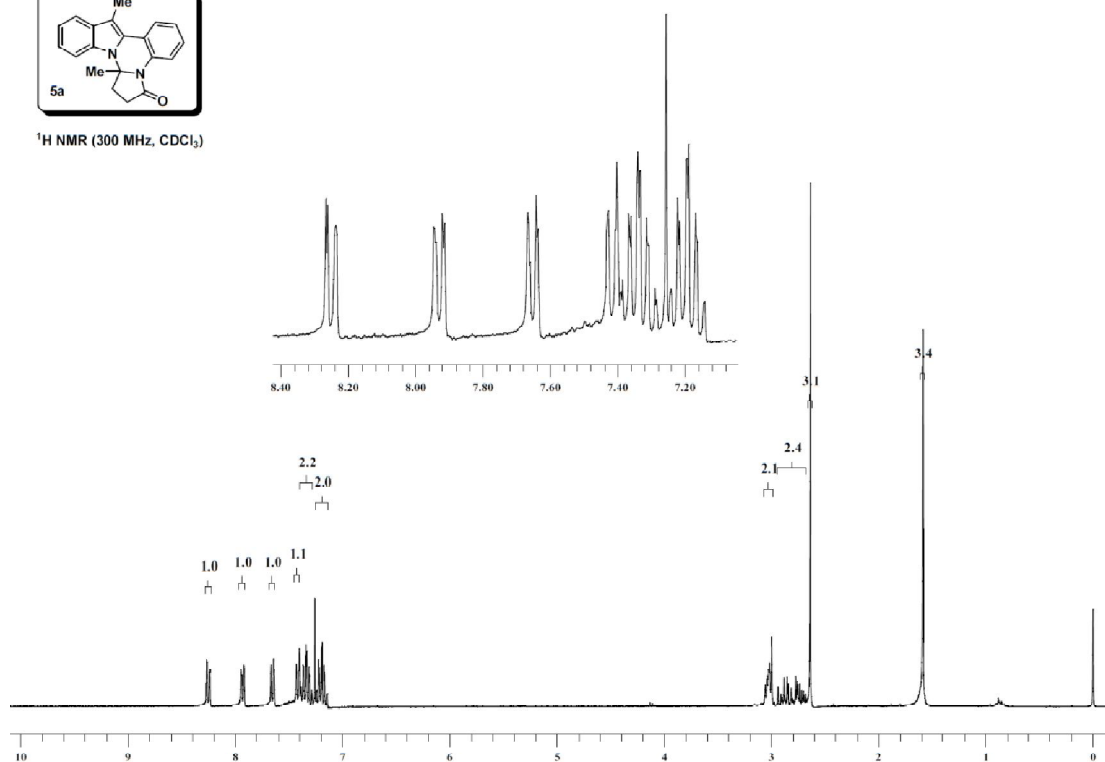


¹³C NMR (75 MHz, CDCl₃)

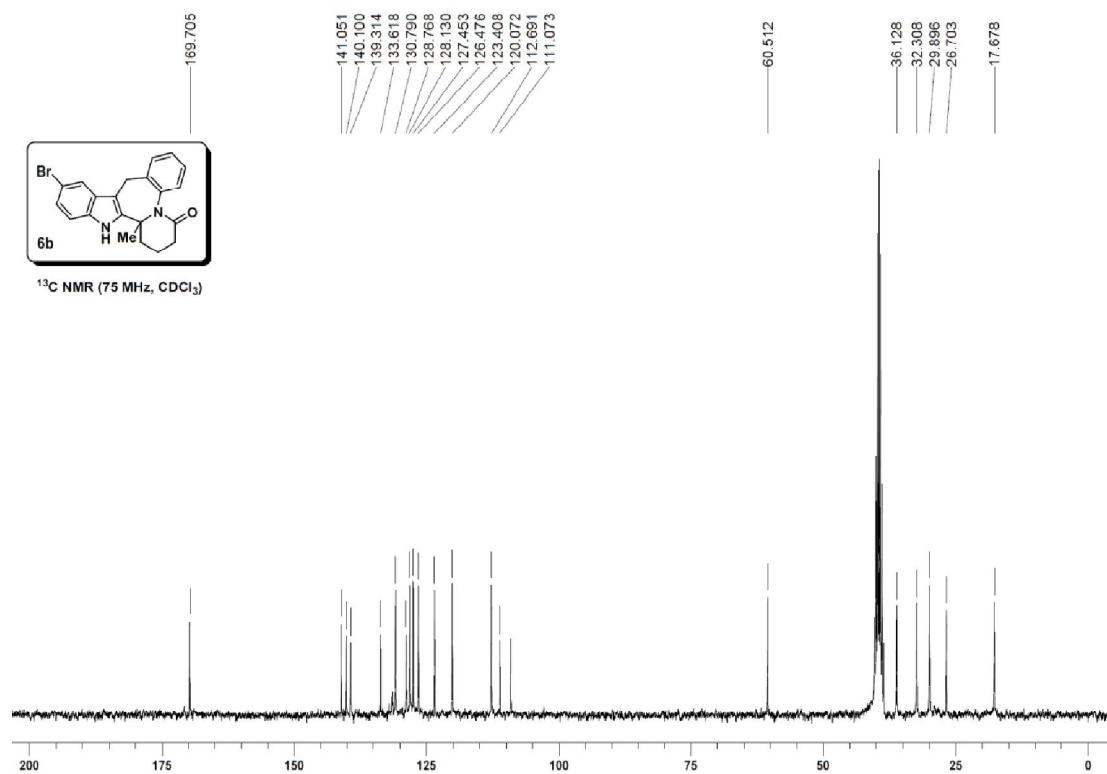
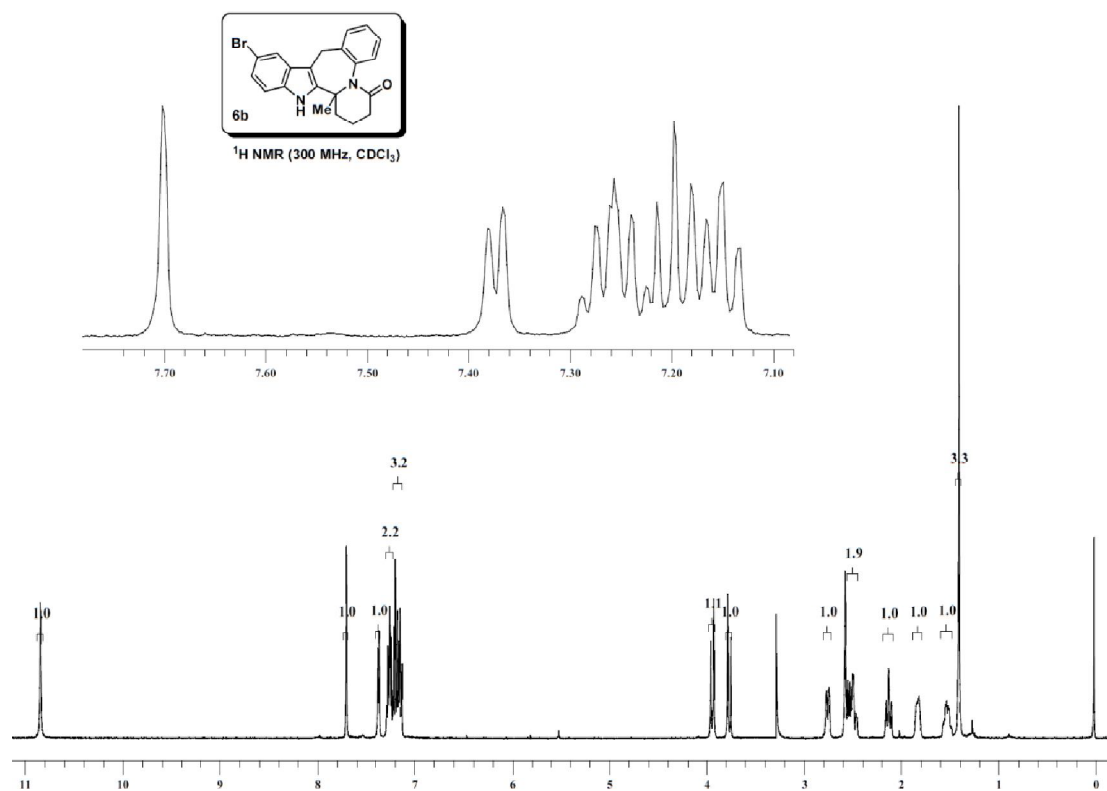


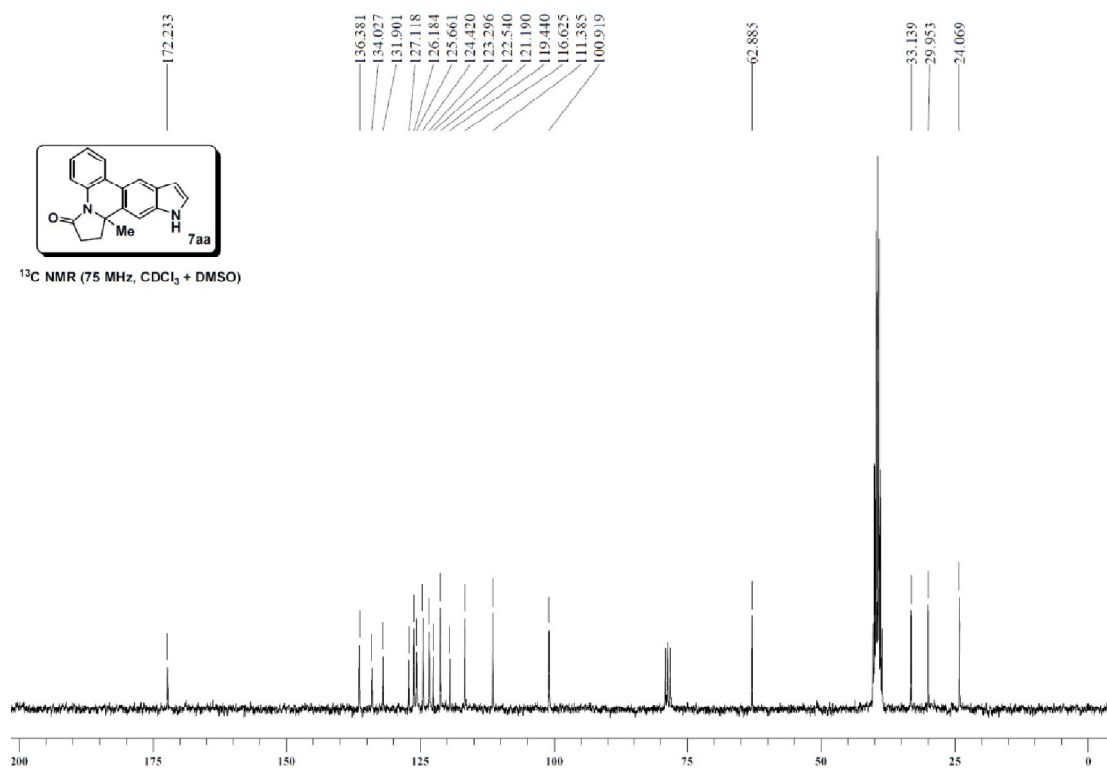
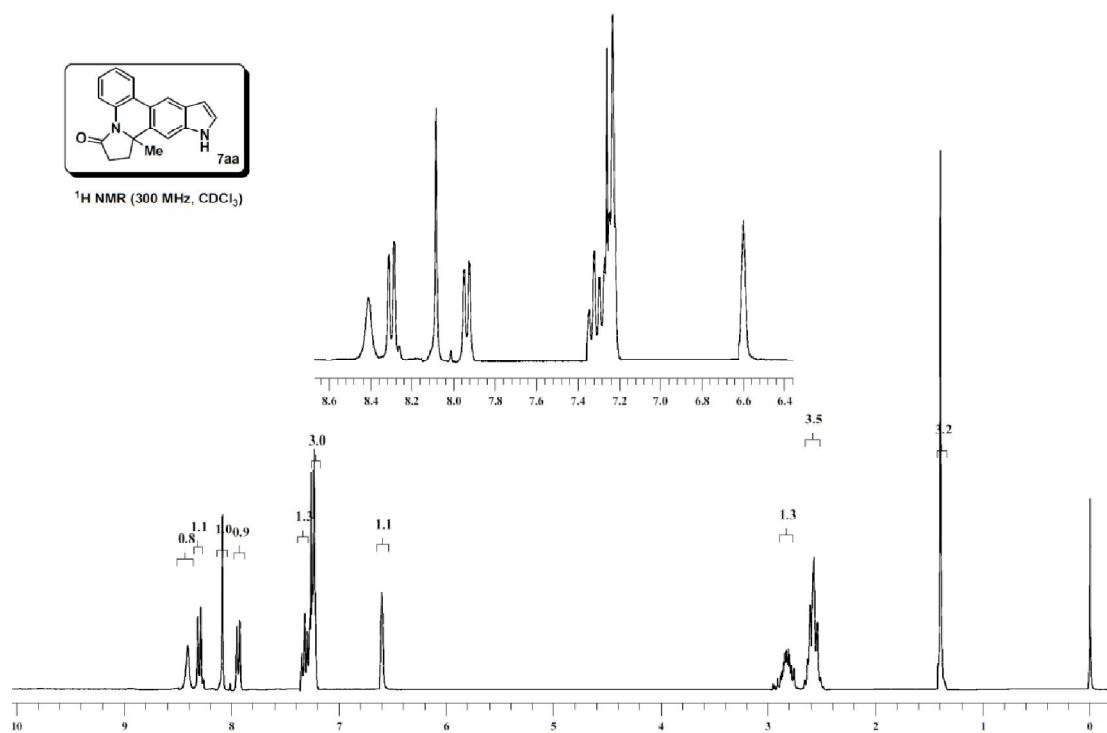


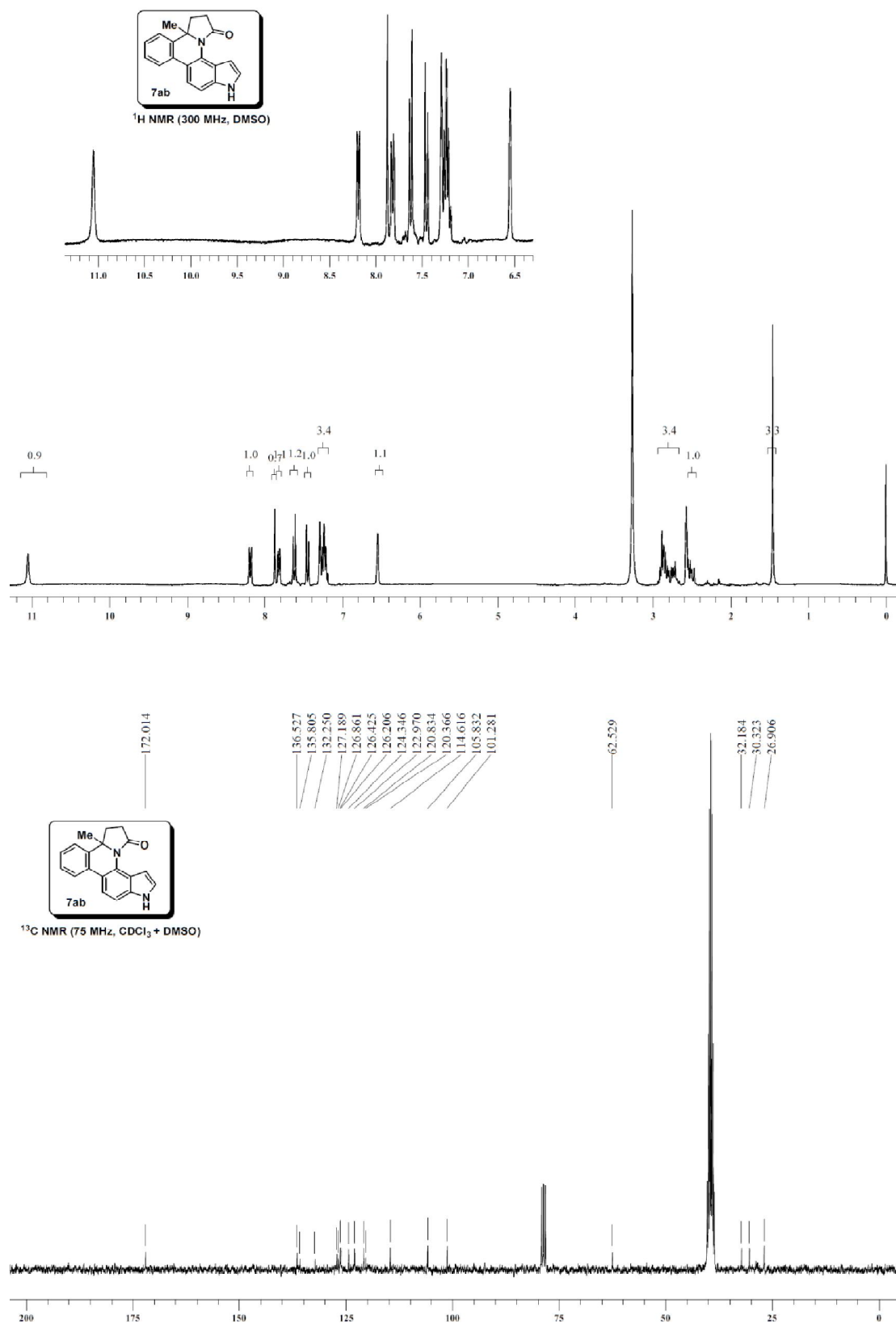
$^1\text{H NMR}$ (300 MHz, CDCl_3)

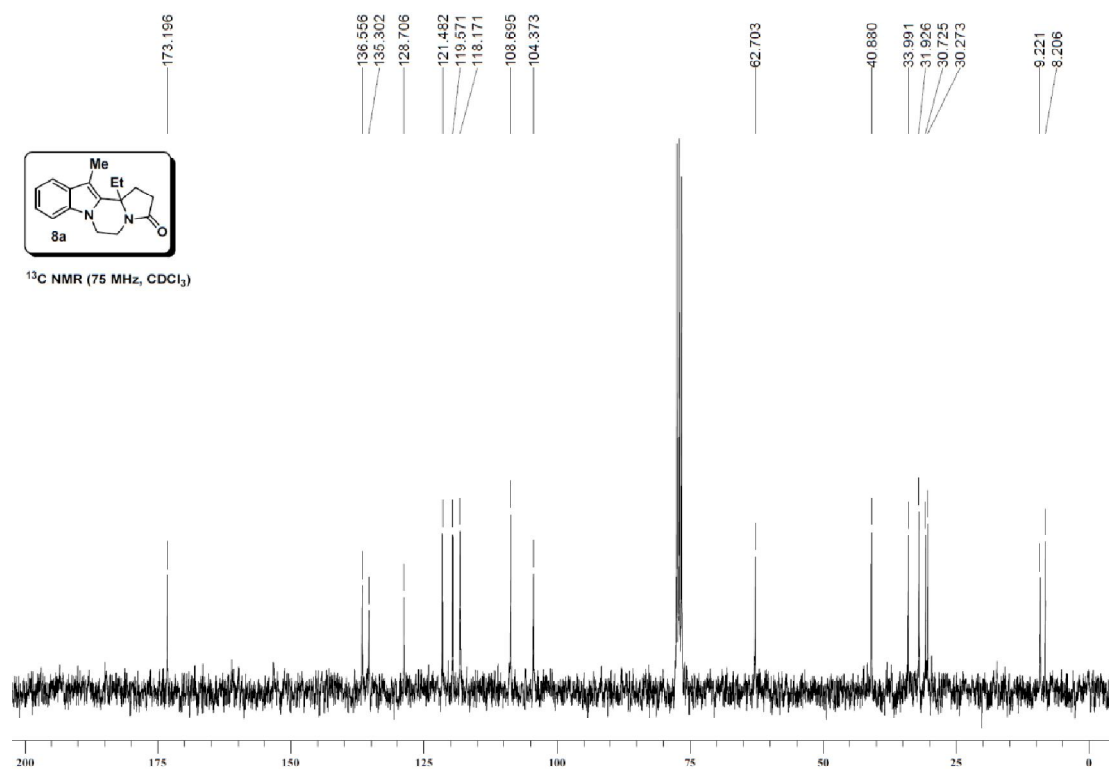
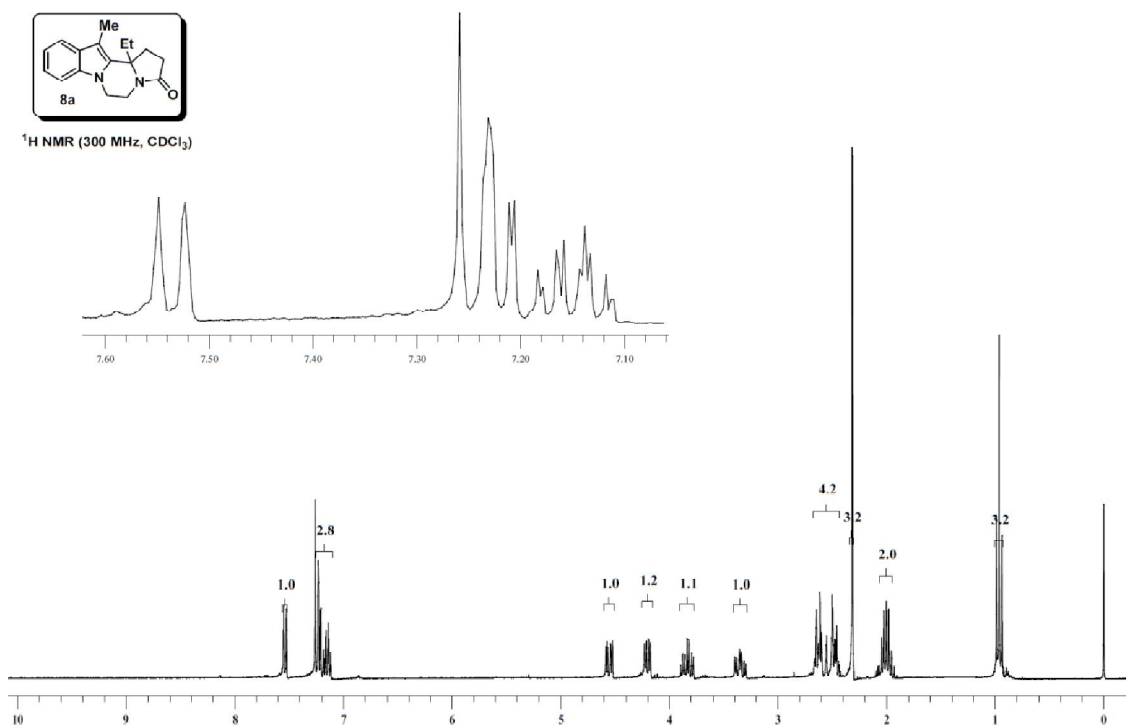


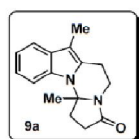
$^{13}\text{C NMR}$ (75 MHz, CDCl_3)



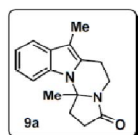
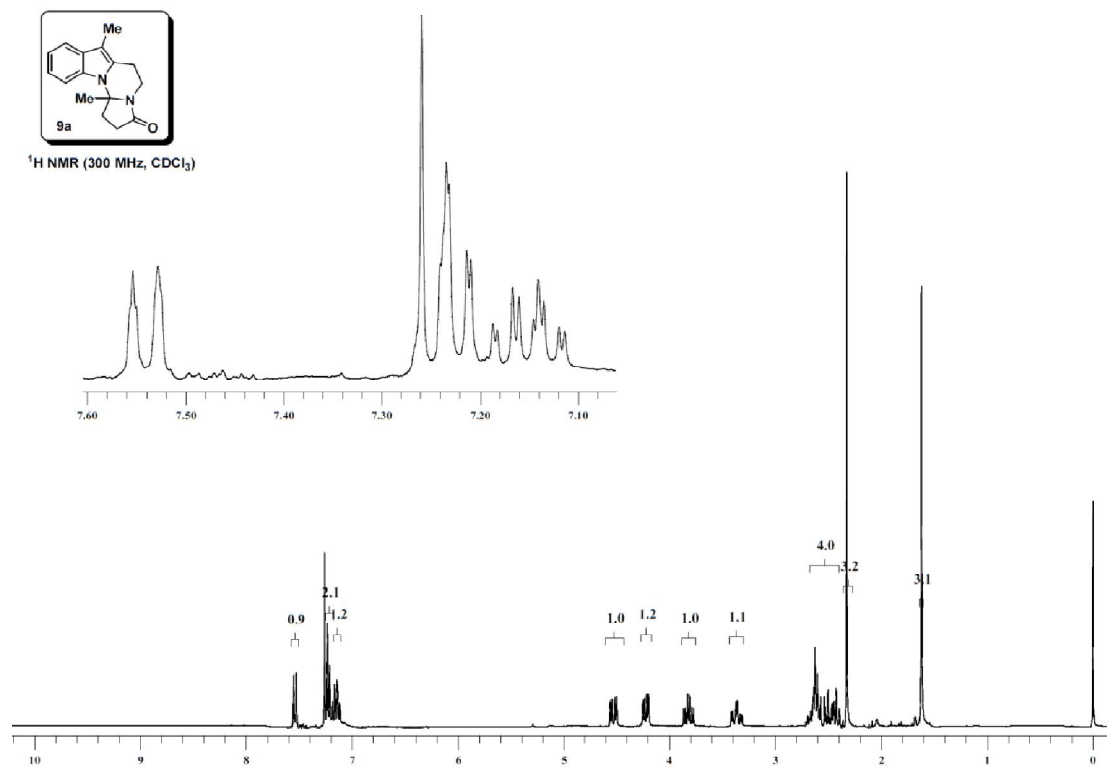




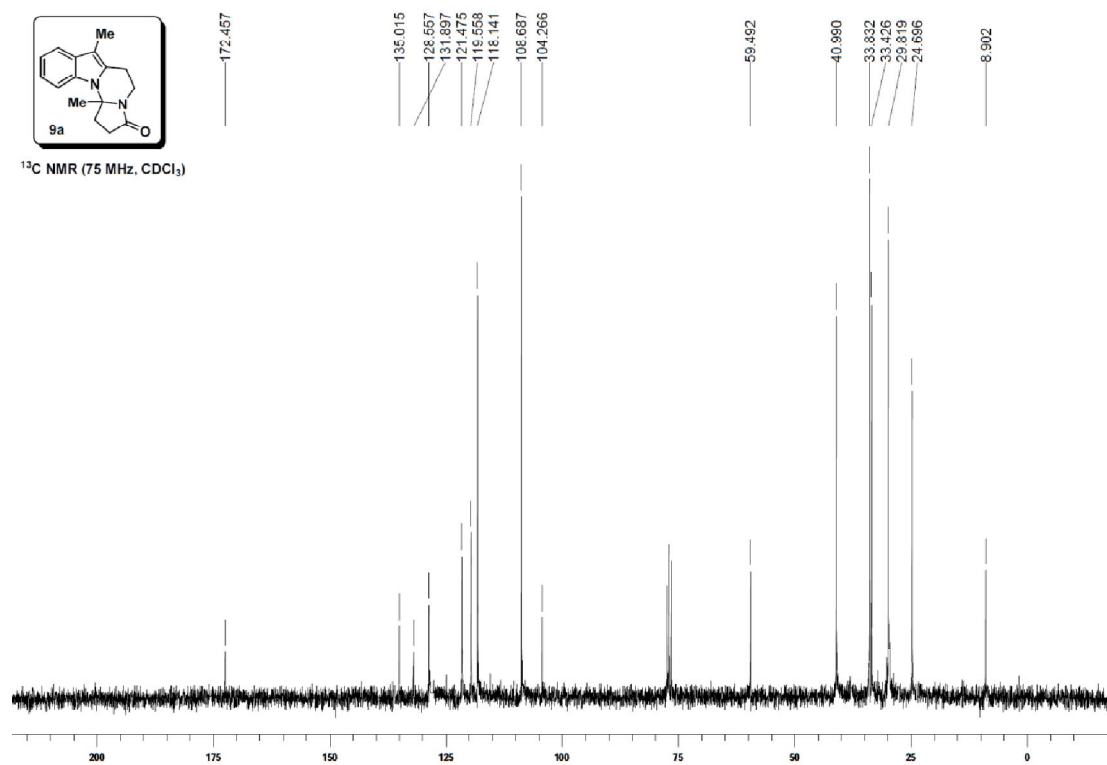


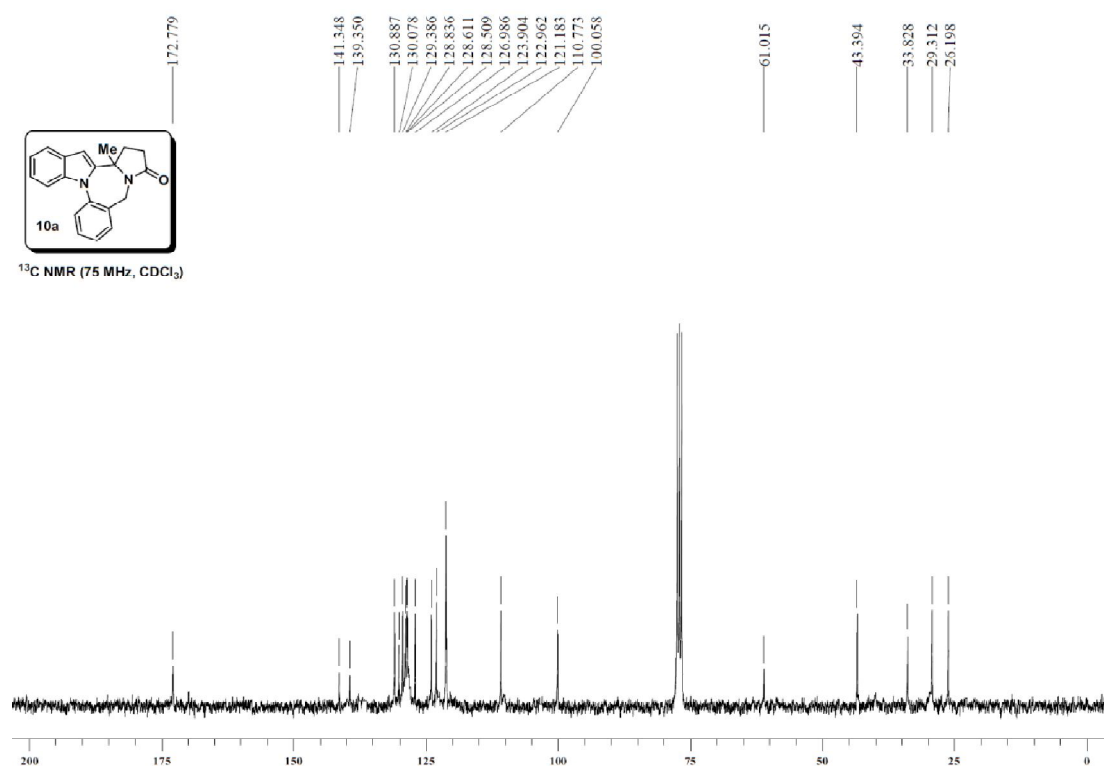
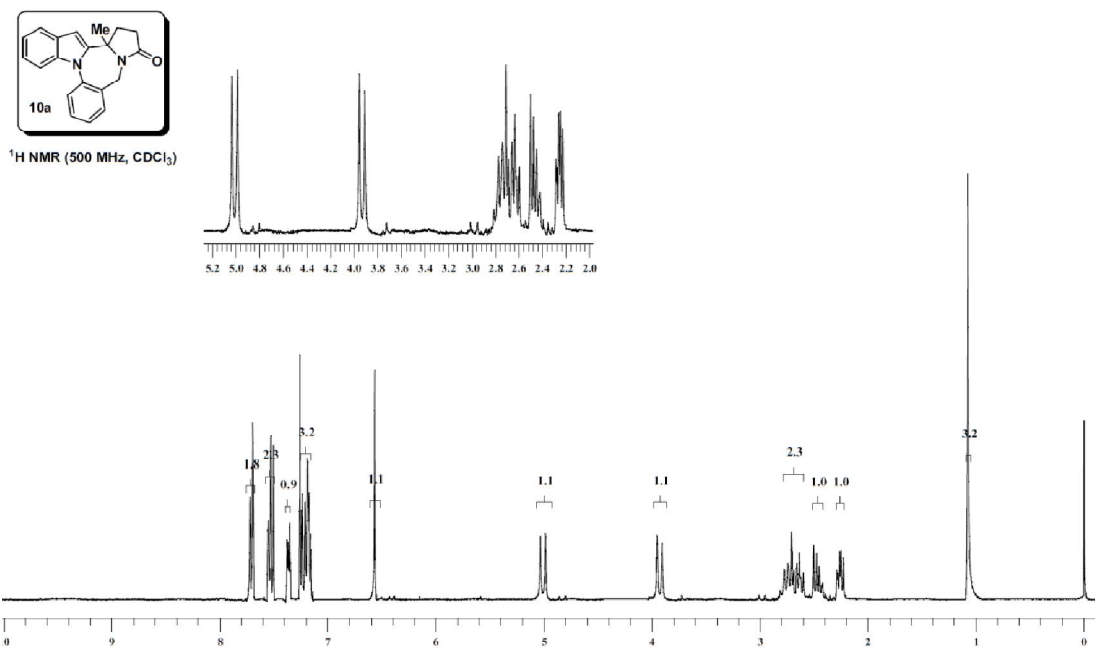


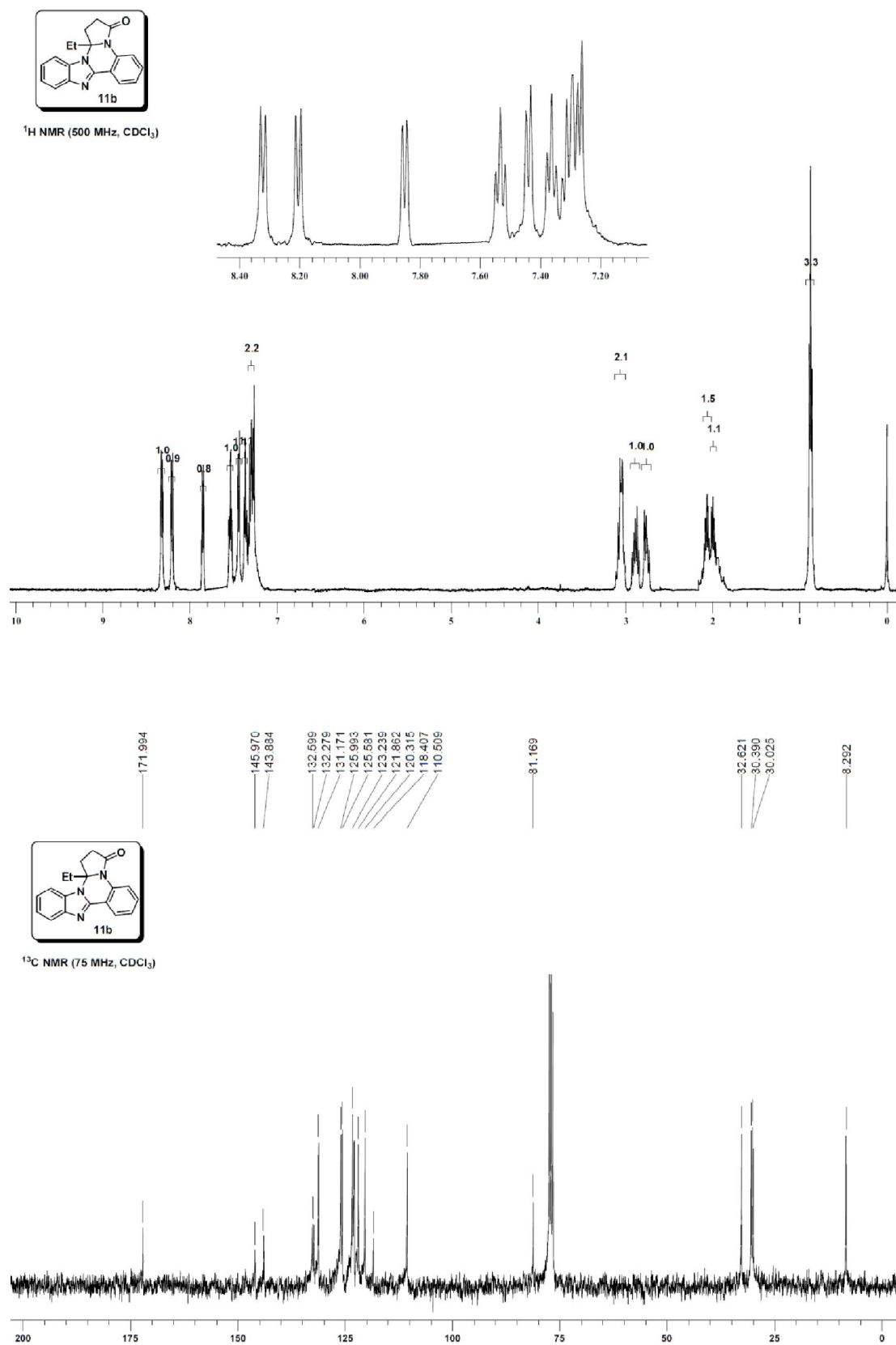
$^1\text{H NMR}$ (300 MHz, CDCl_3)

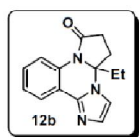


$^{13}\text{C NMR}$ (75 MHz, CDCl_3)

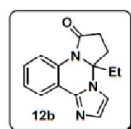
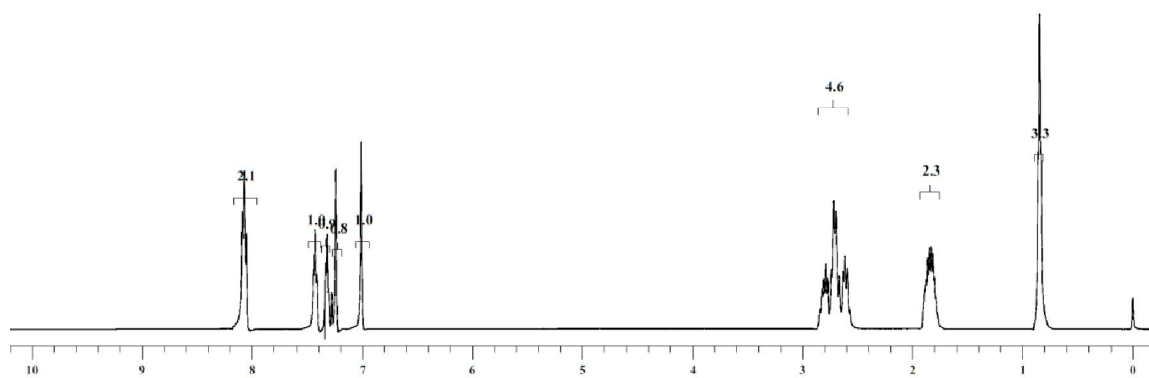
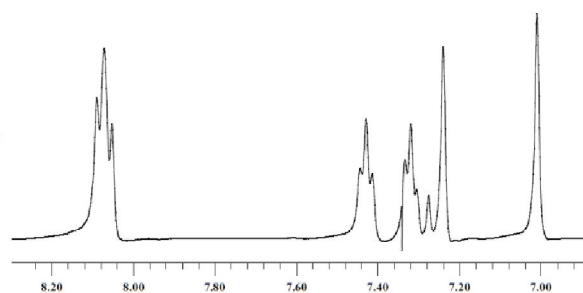




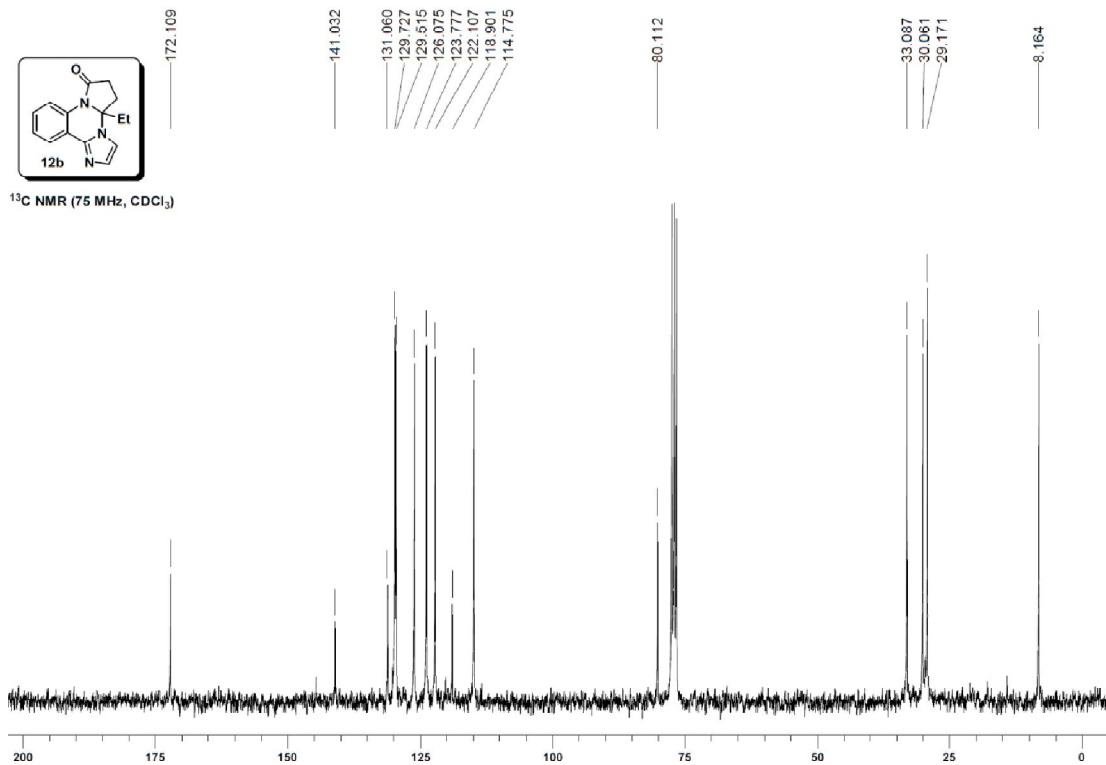


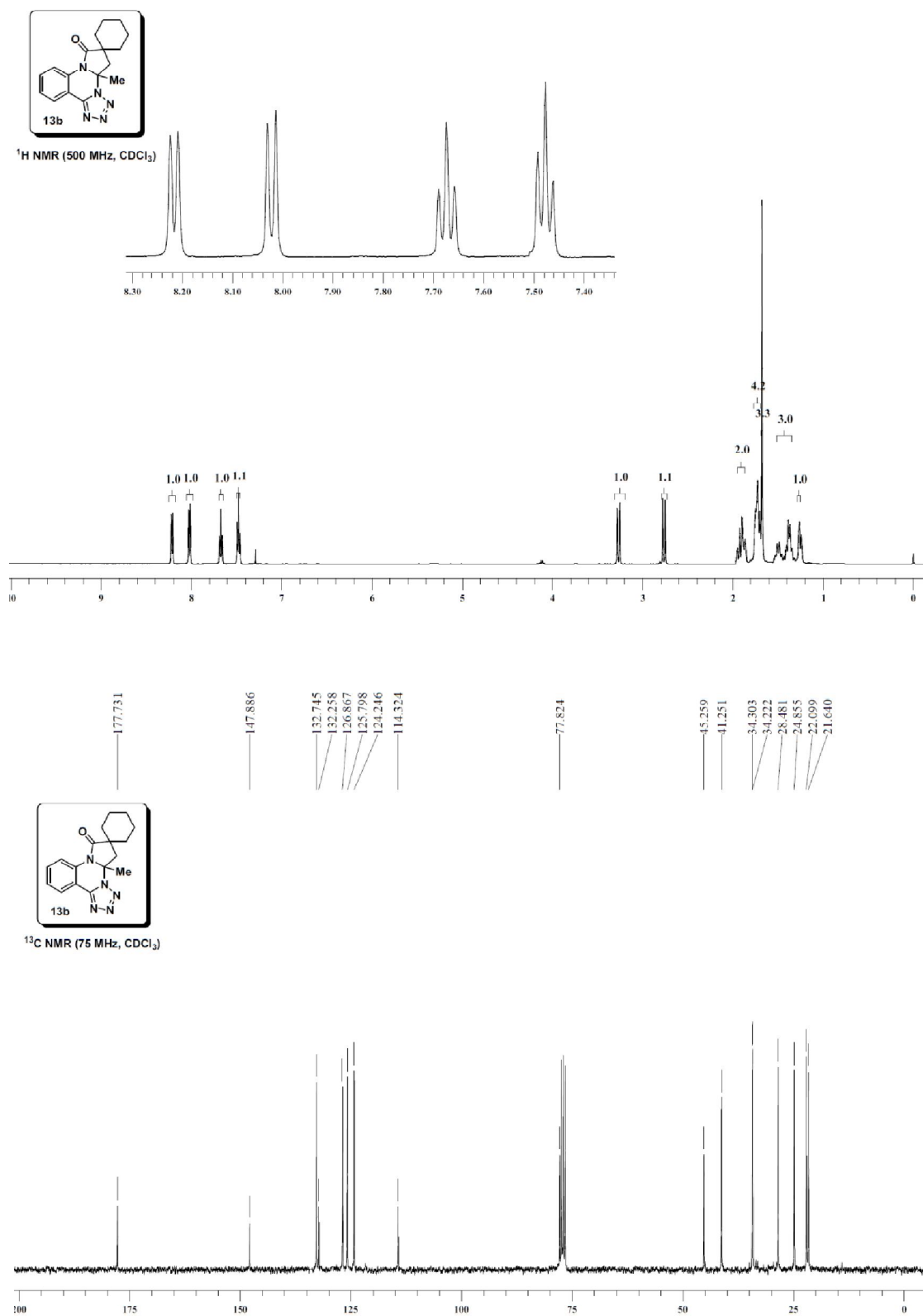


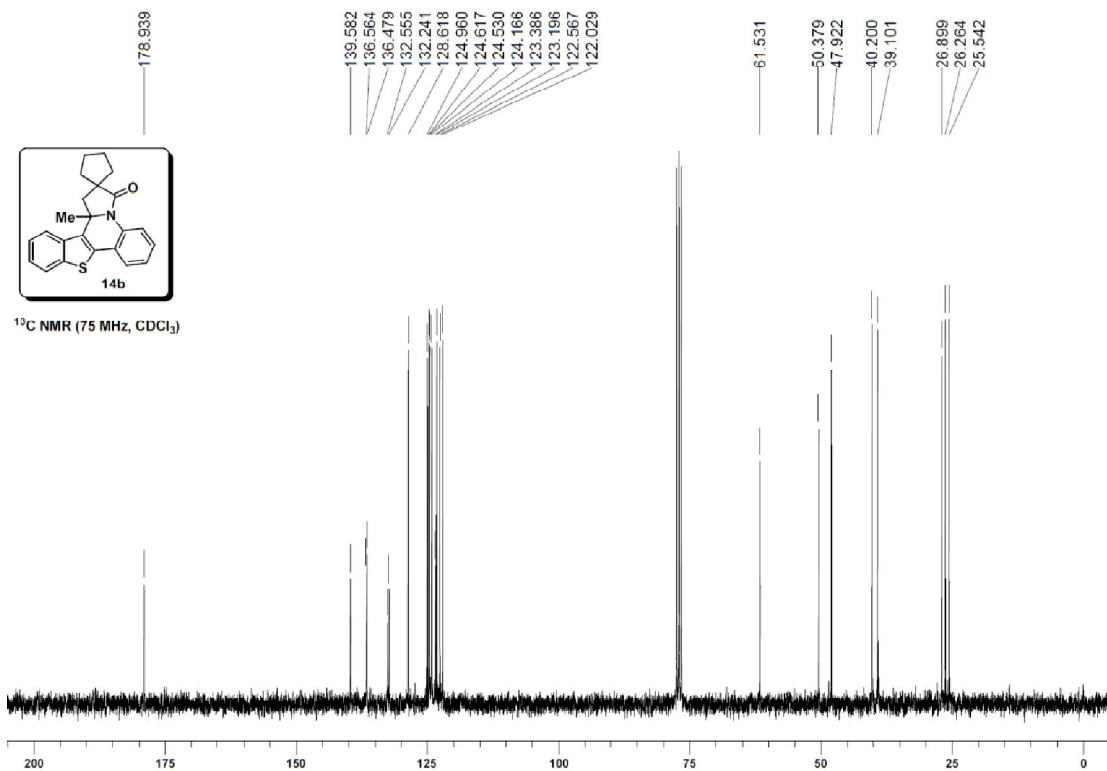
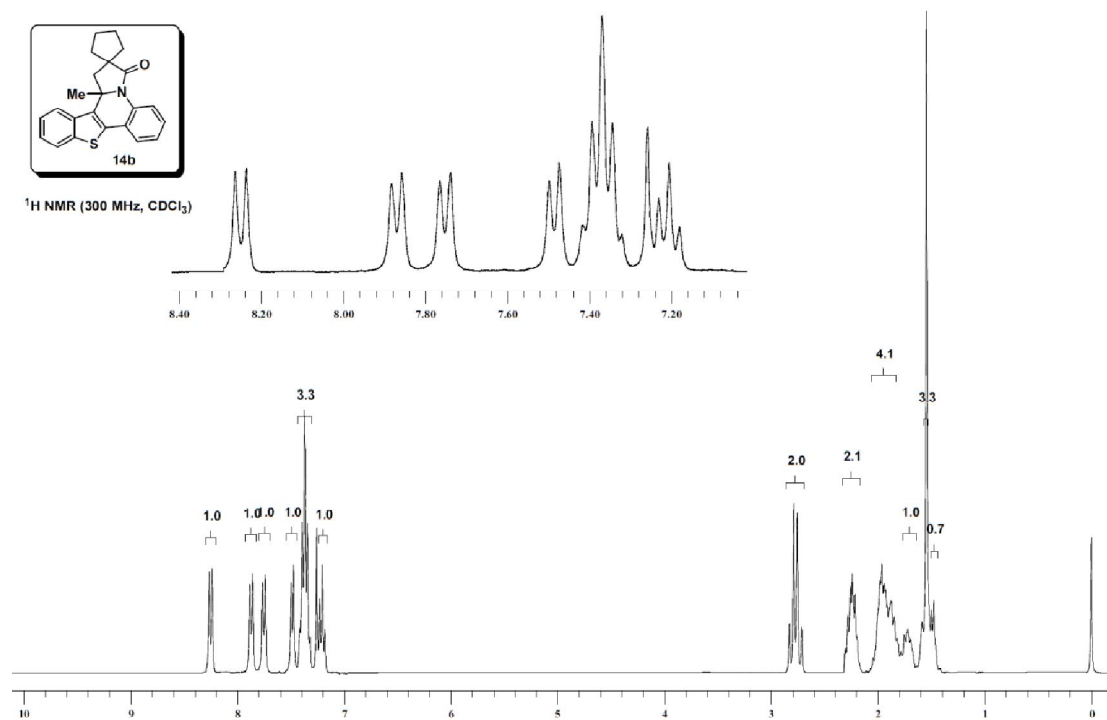
$^1\text{H NMR}$ (500 MHz, CDCl_3)

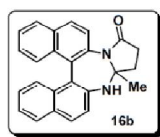


$^{13}\text{C NMR}$ (75 MHz, CDCl_3)

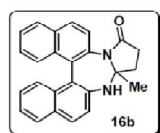
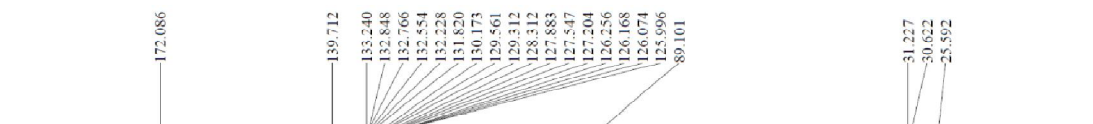
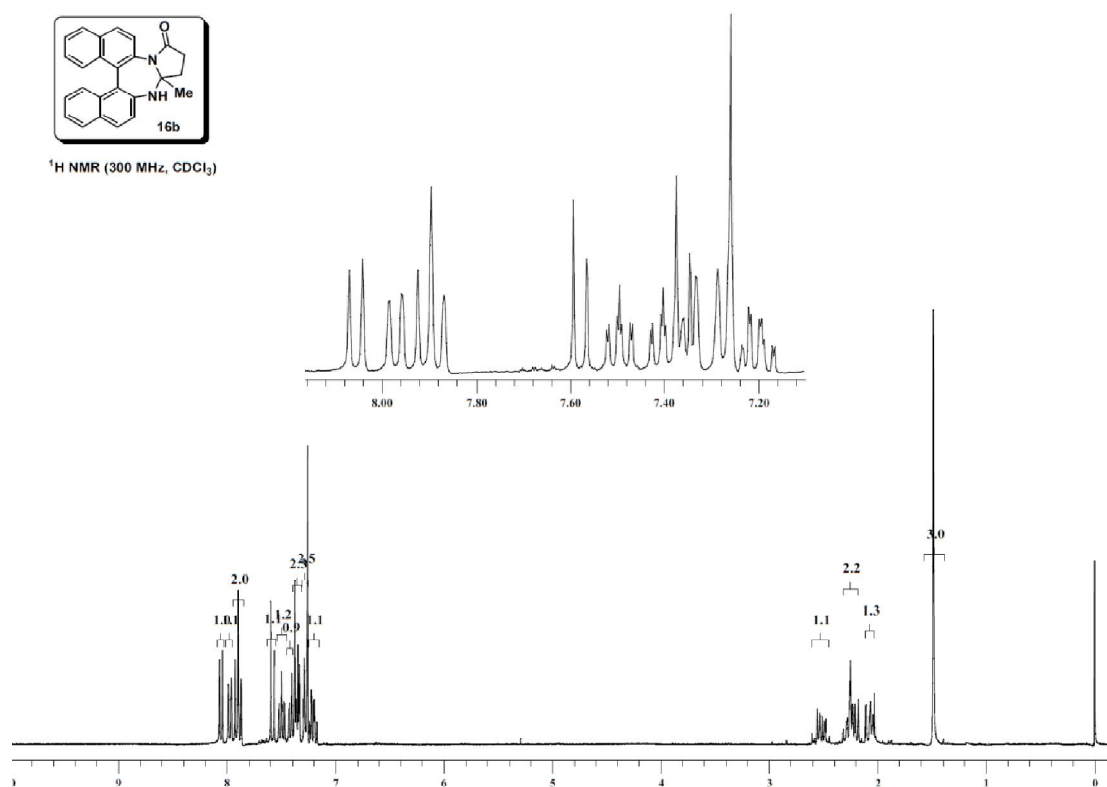




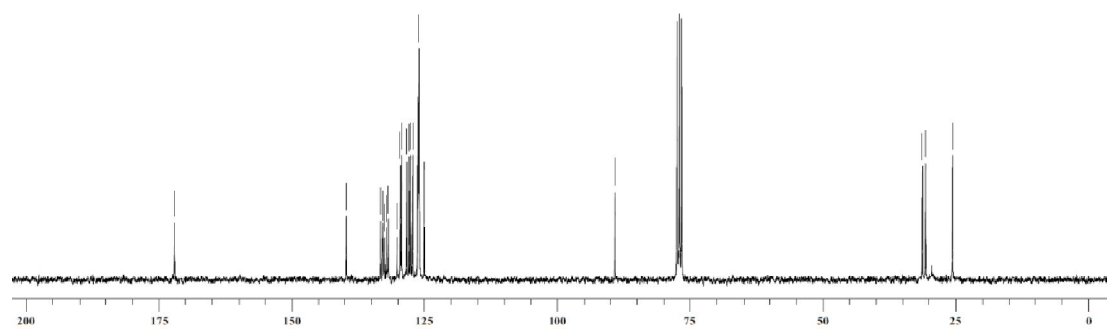


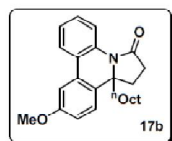


$^1\text{H NMR}$ (300 MHz, CDCl_3)

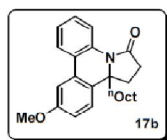
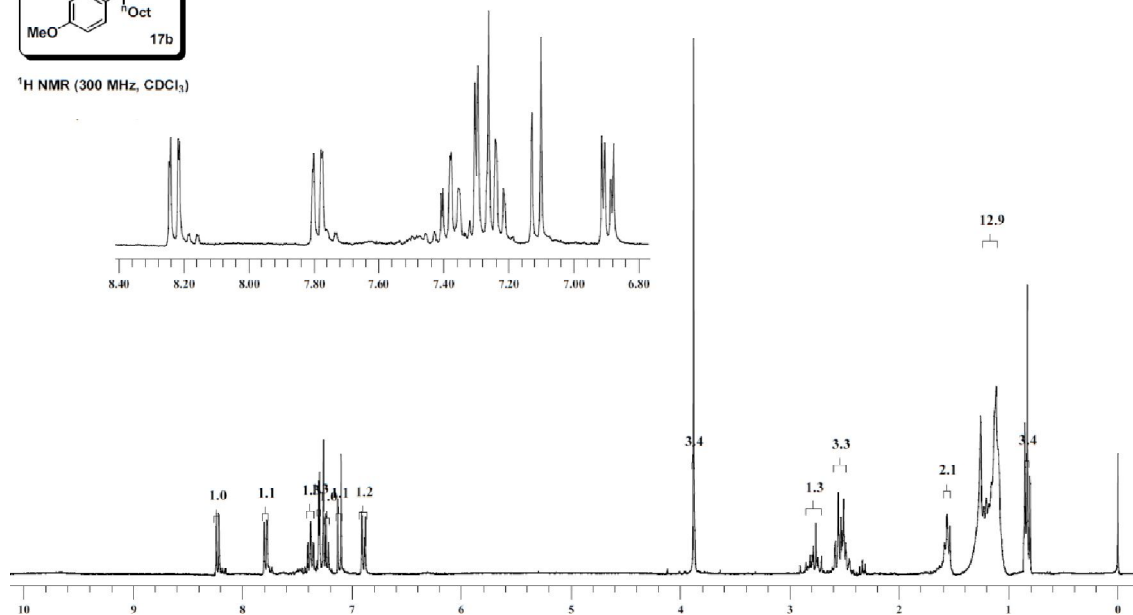


$^{13}\text{C NMR}$ (75 MHz, CDCl_3)

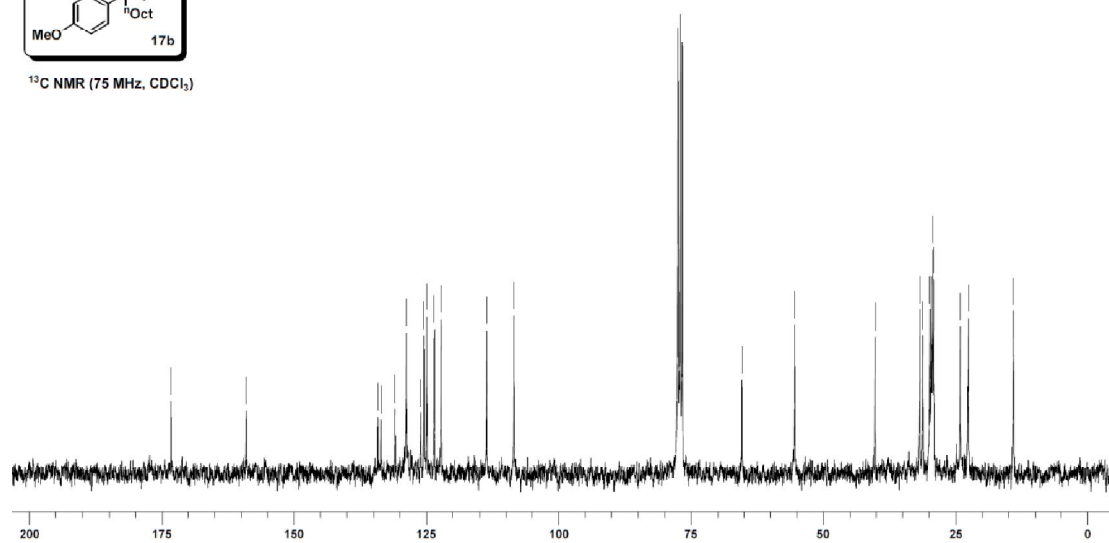


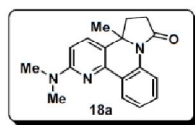


$^1\text{H NMR}$ (300 MHz, CDCl_3)

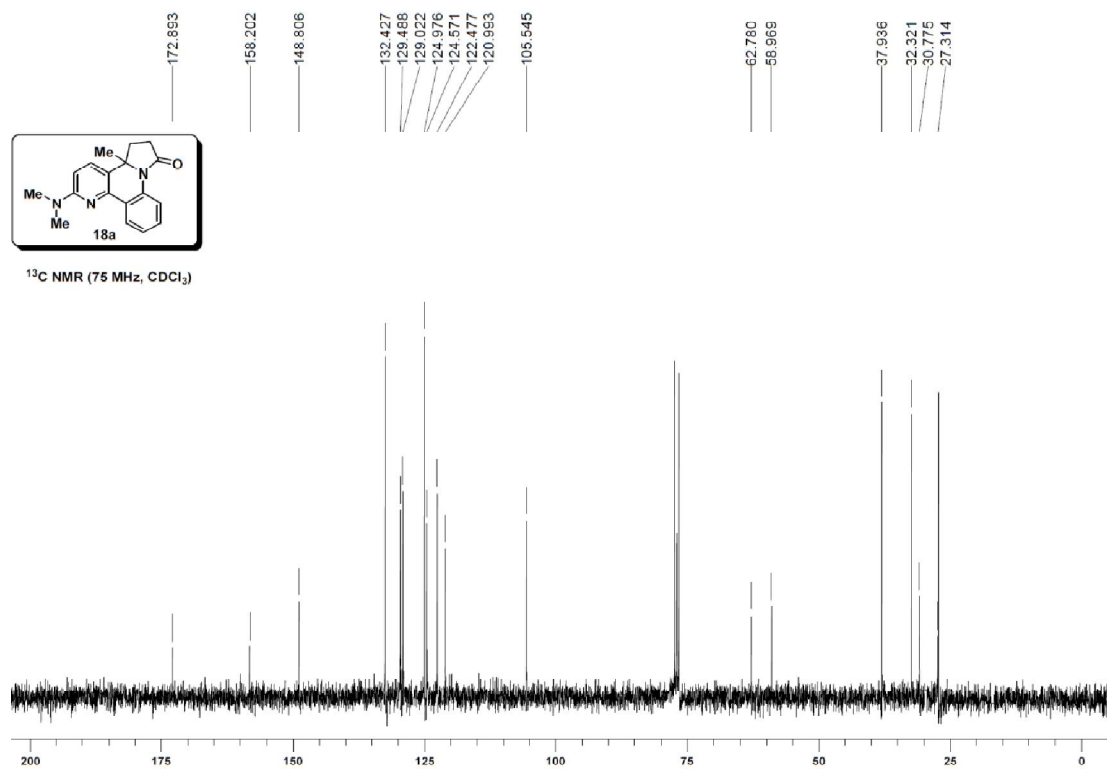
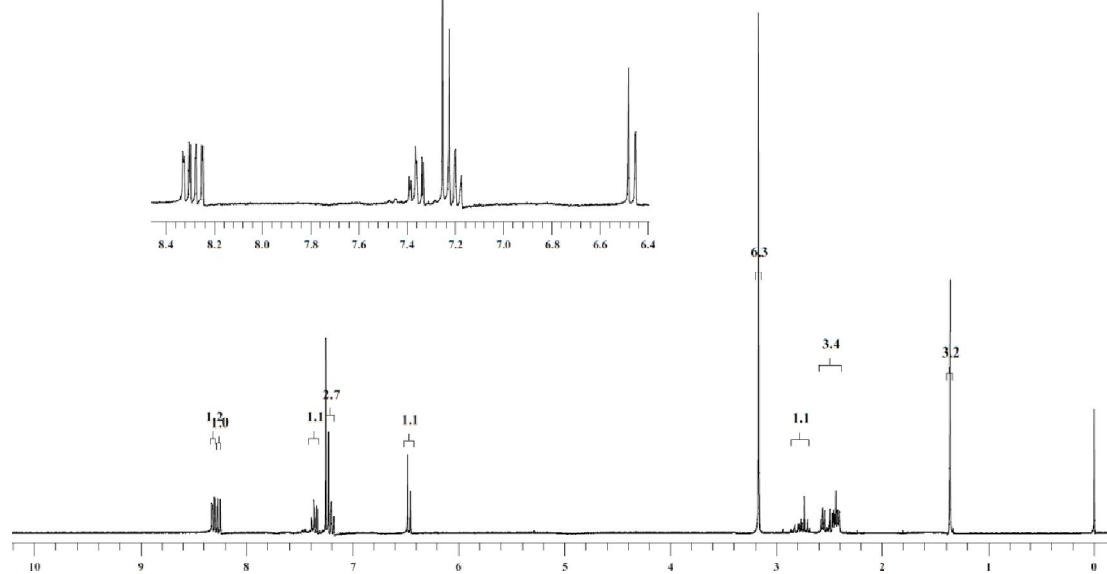


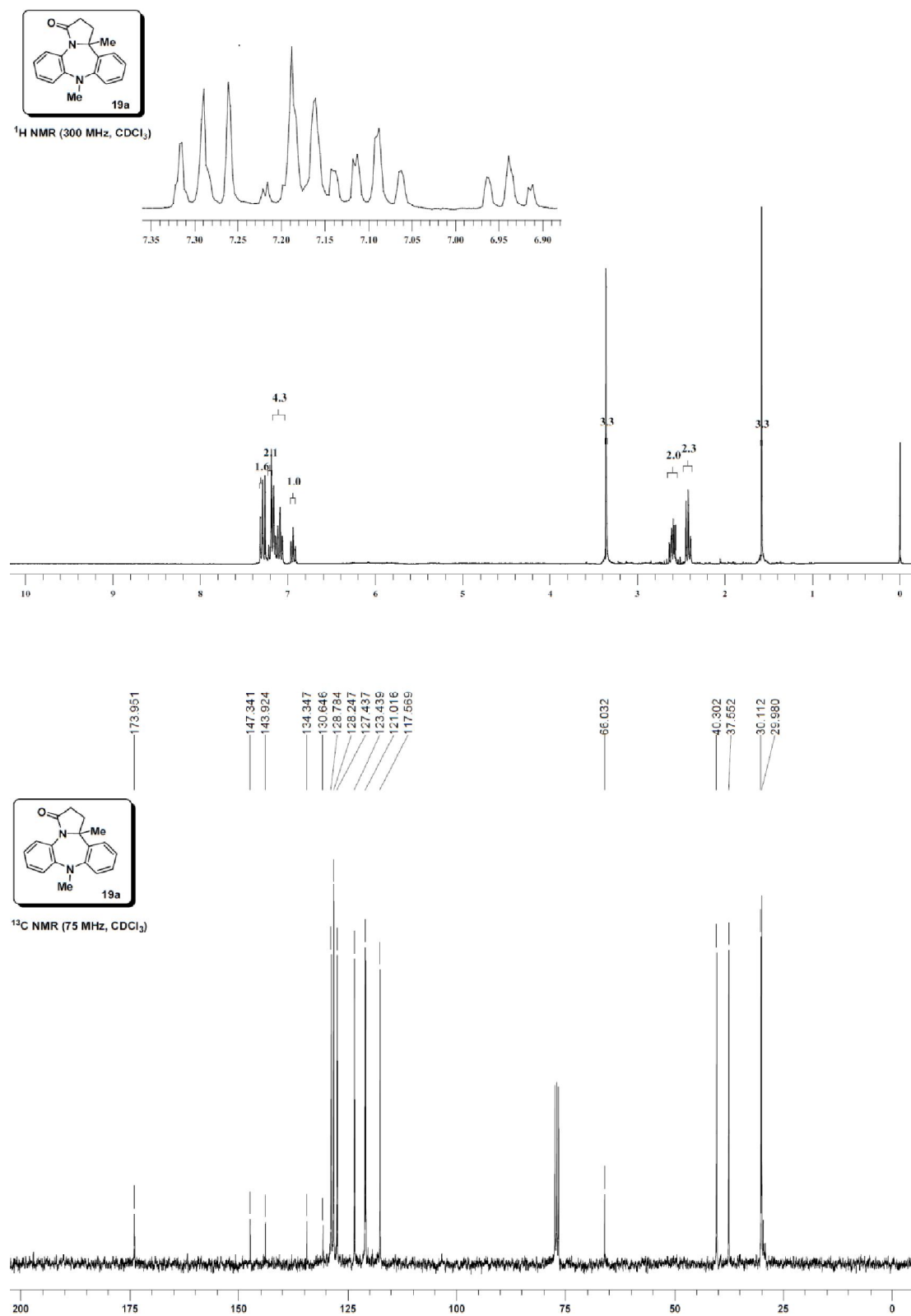
$^{13}\text{C NMR}$ (75 MHz, CDCl_3)

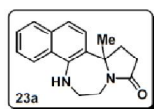




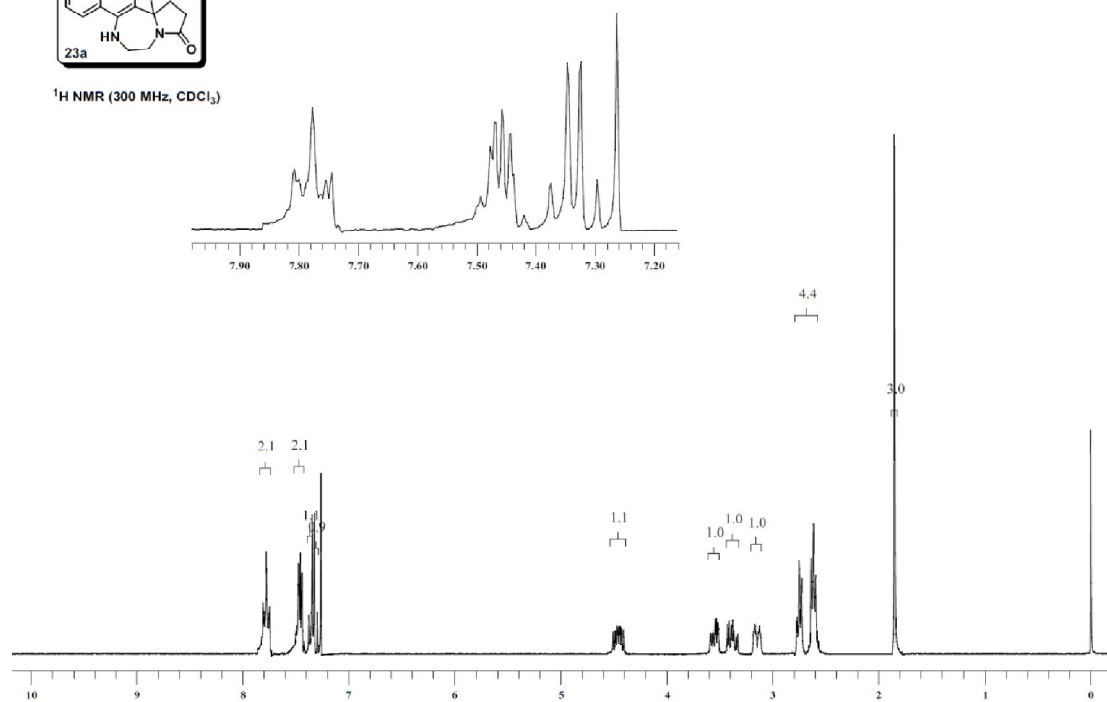
$^1\text{H NMR}$ (300 MHz, CDCl_3)







^1H NMR (300 MHz, CDCl_3)



176.482

144.109

132.701

128.190

125.965

125.777

125.695

125.230

120.103

119.880

66.581

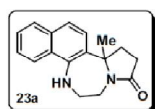
46.390

37.781

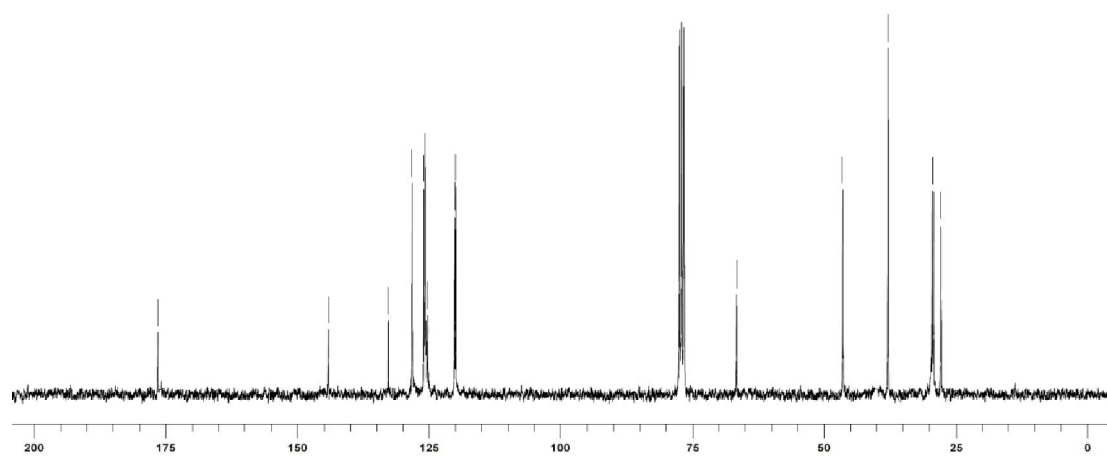
29.386

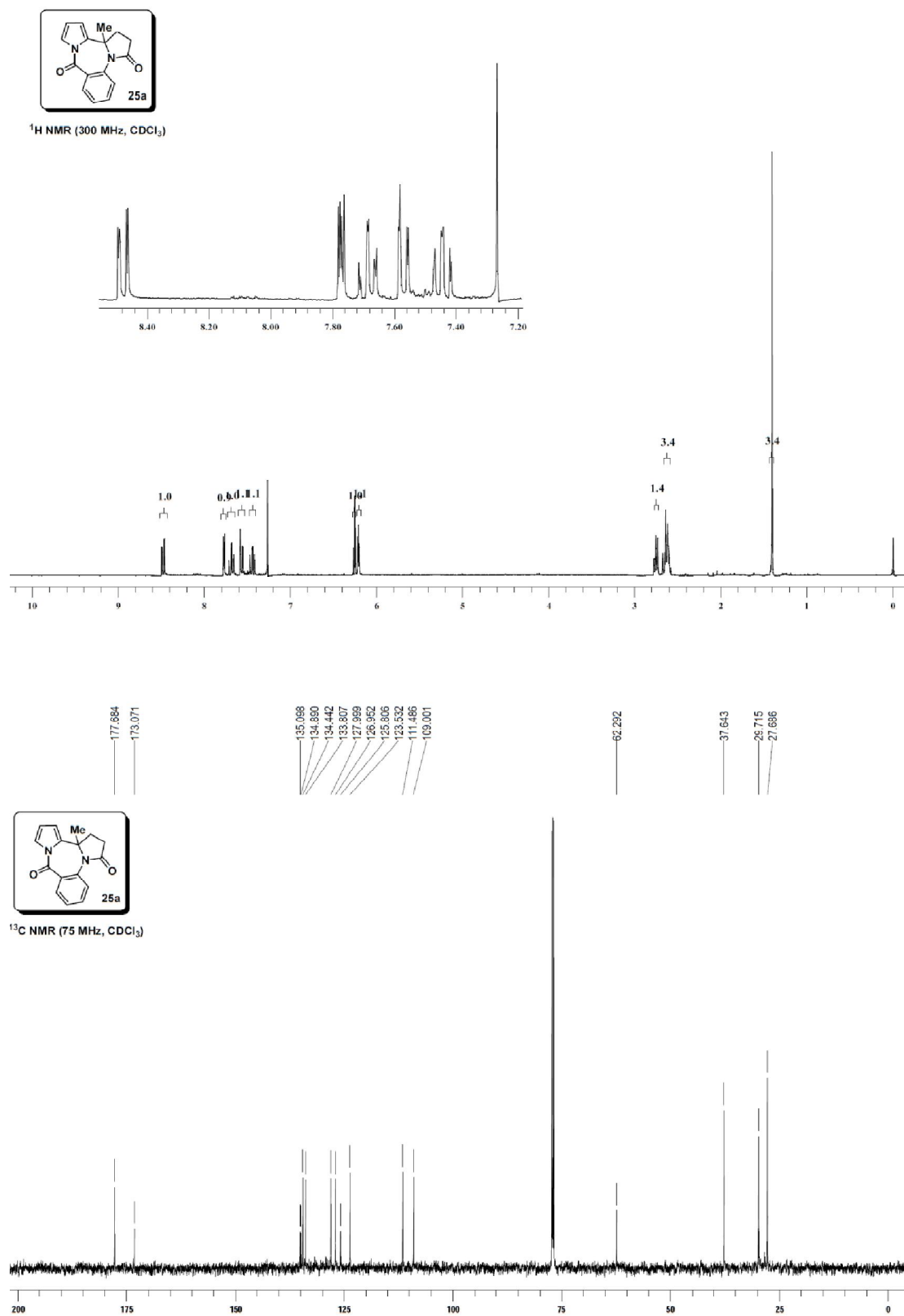
29.127

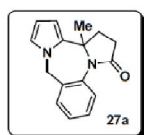
27.735



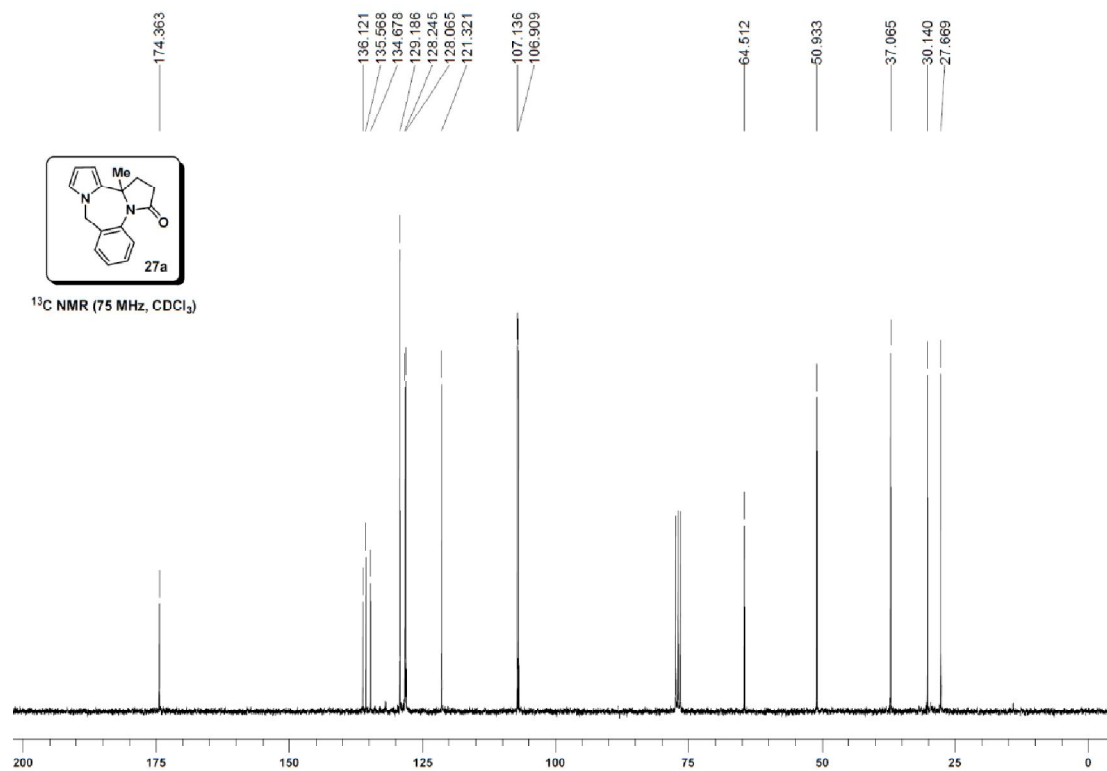
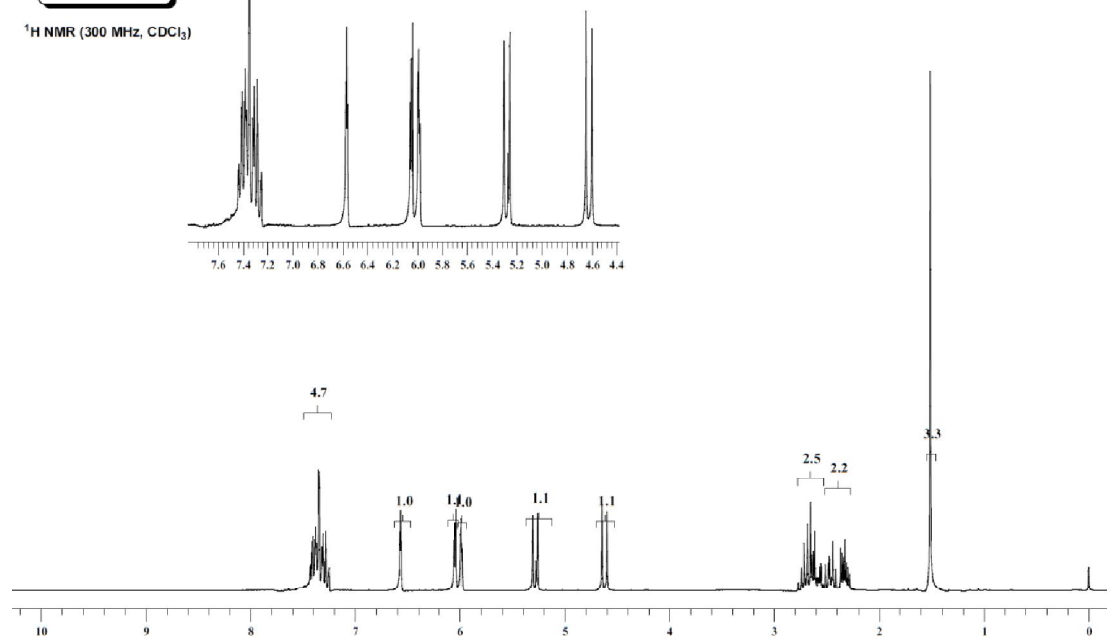
^{13}C NMR (75 MHz, CDCl_3)

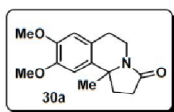




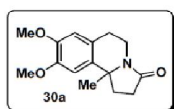
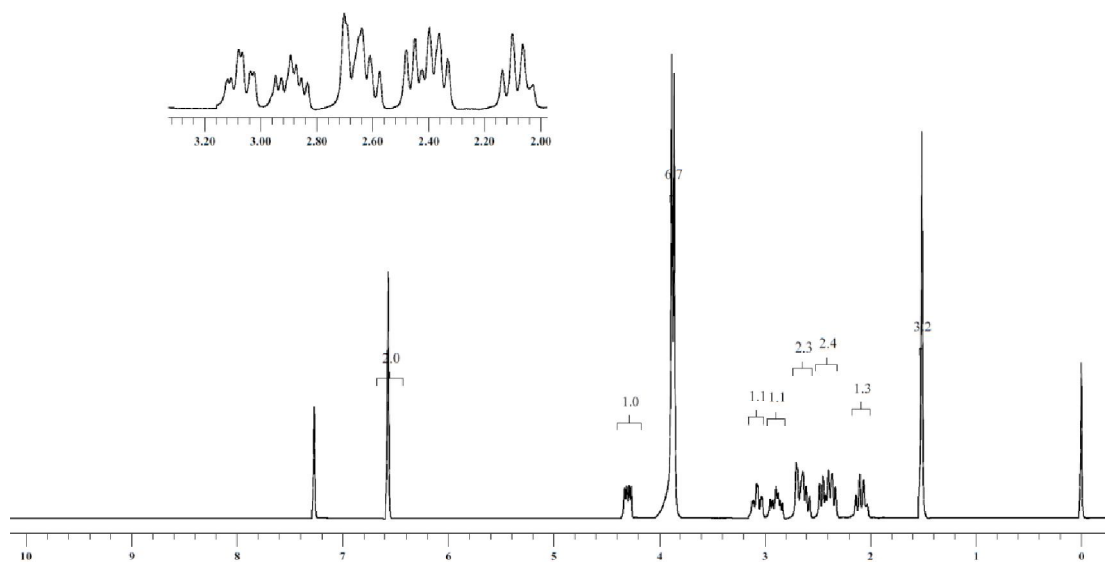


$^1\text{H NMR}$ (300 MHz, CDCl_3)

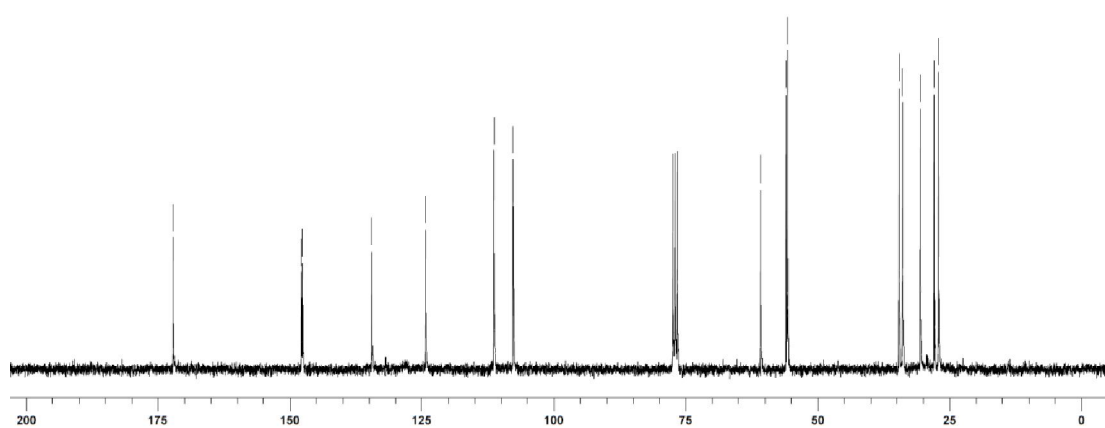




$^1\text{H NMR}$ (300 MHz, CDCl_3)



$^{13}\text{C NMR}$ (75 MHz, CDCl_3)



2.8 References

- [1] (a) Haggarty, S. J. *Curr. Opin. Chem. Biol.* **2005**, *9*, 296–303; (b) Burke, M. D.; Berger, E. M.; Schreiber, S. L. *Science*, **2003**, *302*, 613–618; (c) Shelat, A. A.; Guy, R. K. *Nat. Chem. Biol.* **2007**, *3*, 442–446; (d) Isidro-Llobet, A.; Murillo, T.; Bello, P. Cilibrizzi, A. Hodgkinson, J. T. Galloway, W. R. J. D. Bender, A. Welch, M. Spring, D. R. *Proc. Natl. Acad. Sci. U. S. A.* **2011**, *108*, 6793–6798.
- [2] (a) Zamir, E.; Bastiaens, P. I. H. *Nat. Chem. Biol.* **2008**, *4*, 643–647; (b) Wetzel, S.; Schuffenhauer, A.; Roggo, S.; Ertl, P.; Waldmann, H. *Chimia* **2007**, *61*, 355–360; (c) Grabowski, K.; Baringhaus, K.-H.; Schneider, G. *Nat. Prod. Rep.* **2008**, *25*, 892–904; (d) Schreiber, S. L. *Nat. Chem. Biol.* **2005**, *1*, 64–66; (e) Spring, D. R. *Chem. Soc. Rev.* **2005**, *34*, 472–482; (f) Lipinski, C.; Hopkins, A. *Nature* **2004**, *432*, 855–861; (g) Frye, S. V. *Nat. Chem. Biol.* **2010**, *6*, 159–161.
- [3] (a) Breinbauer, R.; Vetter, I. R.; Waldmann, H. *Angew. Chem. Int. Ed.* **2002**, *41*, 2878–2890; (b) Clardy, J. Walsh, C. *Nature* **2004**, *432*, 829–837.
- [4] (a) Spring, D. R. *Org. Biomol. Chem.* **2003**, *1*, 3867–3870; (b) Burke, M. D.; Schreiber, S. L. *Angew. Chem., Int. Ed.* **2004**, *43*, 46–58; (c) Tan, D. S. *Nat. Chem. Biol.* **2005**, *1*, 74–84; (d) Arya, P.; Joseph, R.; Gan Z.; Rakic, B. *Chem. Biol.* **2005**, *12*, 163–180.
- [5] Schreiber S. L. *Science* **2000**, *287*, 1964–1969.
- [6] Reviews: (a) Tavassoli, A.; Hamilton, A. D.; Spring, D. R. *Chem. Soc. Rev.* **2011**, *40*, 4269–4270; (b) Cooper, T. W. J.; Campbell, I. B.; Macdonald, S. J. F. *Angew. Chem. Int. Ed.* **2010**, *49*, 8082–8091; (c) Galloway, W. R. J. D.; Isidro-Llobet, A.; Spring, D. R. *Nature Commun.* **2010**, *1*, 80; (d) Grabowski, K. Baringhaus, K.-H. Schneider, G. *Nat. Prod. Rep.* **2008**, *25*, 892–904; (e) Kaiser, M. Wetzel, S. Kumar, K. Waldmann, H. *Cell. Mol. Life. Sci.* **2008**, *65*, 1186–1201; (f) Spring, D. R. *Chem. Soc. Rev.* **2005**, *34*, 472–482; (g) Dobson, C. M. *Nature* **2004**, *432*, 824–828.; (h) Stockwell, B. R. *Nature* **2004**, *432*, 846–854.
- [7] (a) Ascic, E.; Le Qument, S.; Ishoey, T. M.; Daugaard, M.; Nielsen, T. E. *ACS Comb. Sci.* **2012**, *14*, 253–257; (b) Luo, T. Schreiber, S. L. *J. Am. Chem. Soc.* **2009**, *131*, 5667–5674; (c) Nielsen, T. E.; Schreiber, S. L. *Angew. Chem. Int. Ed.* **2008**, *47*, 48–56.

-
- [8] (a) Zang, Q.; Javed, S.; Ullah, F.; Zhou, A.; Knudtson, C. A.; Bi, D.; Basha, F. Z.; Organ, M. G.; Hanson, P. R. *Synthesis* **2011**, 2743–2750; (b) Rolfe, A.; Lushington, G. H.; Hanson, P. R. *Org. Biomol. Chem.* **2010**, *8*, 2198–2203.
- [9] (a) Hung, A. W.; Ramek, A.; Wang, Y.; Kaya, T.; Wilson, J. A.; Clemons, P. A.; Young, D. W. *Procs. Nat. Acad. Sci.* **2011**, *108*, 6799–6804; (b) Murray, C. W.; Rees, D. C. *Nat. Chem.* **2009**, *1*, 187–192; (c) Hajduk, P. J.; Greer, J. A. *Nat. Rev. Drug Discov.* **2007**, *6*, 211–219.
- [10] Dandapani, S.; Marcaurelle, L. A. *Curr. Opin. Chem. Biol.* **2010**, *14*, 362–370.
- [11] Kwon, O.; Park, S. B.; Schreiber, S. L. *J. Am. Chem. Soc.* **2002**, *124*, 13402–13404.
- [12] (a) Burke, M. D.; Schreiber, S. L. *Angew. Chem. Int. Ed.* **2004**, *43*, 46–58; (b) Tan, D. S. *Nat. Chem. Biol.* **2005**, *1*, 74–84; (c) Schreiber, S. L. *Nature* **2009**, *457*, 153–154; (d) Galloway, W. R. J. D.; Isidro-Llobet, A.; Spring, D. R. *Nat. Commun.* **2010**, *80* (e) Thomas, G. L.; Wyatt, E. E.; Spring, D. R. *Curr. Opin. Drug Discov. Devel.* **2006**, *9*, 700–712.
- [13] (a) Kwon, O.; Park, S. B.; Schreiber, S. L.; *J. Am. Chem. Soc.* **2002**, *124*, 13402–13404; (b) Ko, S. K.; Jang, H. J.; Kim, E.; Park, S. B. *Chem. Commun.* **2006**, 2962–2964; (c) Wyatt, E. E.; Fergus, S.; Galloway, W. R. J. D.; Bender, A.; Fox, D. J.; Plowright, A. T.; Jessiman, A. S.; Welch, M.; Spring, D. R. *Chem. Commun.* **2006**, 3296–3298; (d) Rolfe, A.; Lushington, G. H.; Hanson, P. R.; *Org. Biomol. Chem.* **2010**, *8*, 2198–2203.
- [14] Wyatt, E. E.; Fergus, S.; Galloway, W. R. J. D.; Bender, A.; Fox, D. J.; Plowright, A. T.; Jessiman A. S.; Spring, D. R. *Chem. Commun.*, **2006**, 3296–3298.
- [15] Liu, W.; Khedkar, V.; Baskar, B.; Schumann, M.; Kumar, K. *Angew. Chem., Int. Ed.* **2011**, *50*, 6900–6905.
- [16] Robbins, D.; Newton, A. F.; Gignoux, C.; Legeay, J.-C.; Sinclair, A.; Rejzek, M.; Laxon, C. A.; Yalamanchili, S. K.; Lewis, W.; O’Connell M. A.; Stockman, R. A. *Chem. Sci.* **2011**, *2*, 2232–2235.
- [17] Patil, N. T.; Konala, A.; Sravanti, S.; Singh, A.; Ummanni, R.; Sridhar, B. *Chem. Commun.* **2013**, *49*, 10109–10111.
- [18] Reports on the catalytic approaches to multifunctional polyheterocyclic from our laboratory, see: (a) Patil, N. T.; Raut, V. S.; Shinde, V. S.; Gayatri, G.; Sastry, G. N. *Chem.–Eur. J.* **2012**, *18*, 5530–5535; (b) Patil, N. T.; Mutyala, A. K.; Konala, A.; Tella, R. B.; *Chem. Commun.* **2012**, *48*, 3094–3096; (c) Patil, N. T.; Lakshmi, P. G. V. V.; Sridhar, B.; Patra, S.; Bhadra, M. P.; Patra, C. R. *Eur. J. Org. Chem.* **2012**, 1790–1799; (d) Patil, N. T.; Singh, V.

- Chem. Commun.* **2011**, *47*, 11116–11118; (e) Patil, N. T.; Raut, V. S. *J. Org. Chem.* **2010**, *75*, 6961–6964; (f) Patil, N. T.; Lakshmi, P. G. V. V.; Singh, V. *Eur. J. Org. Chem.* **2010**, 4719–4731; (g) Patil, N. T.; Kavthe, R. D.; Shinde, V. S.; Sridhar, B. *J. Org. Chem.* **2010**, *75*, 3371–3380; (h) Patil, N. T.; Mutyala, A. K.; Lakshmi, P. G. V. V.; Raju, P. V. K.; Sridhar, B. *Eur. J. Org. Chem.* **2010**, 1999–2007; (i) Patil, N. T.; Kavthe, R. D.; Raut, V. S.; Shinde, V. S. Sridhar, B. *J. Org. Chem.* **2010**, *75*, 1277–1280; (j) Patil, N. T.; Konala, A. *Eur. J. Org. Chem.* **2010**, 6831–6839; (k) Patil, N. T.; Kavthe, R. D.; Raut, V. S.; Reddy, V. V. N. *J. Org. Chem.* **2009**, *74*, 6315–6318.
- [19] Patil, N. T.; Mutyala, A. K.; Lakshmi, P. G. V. V.; Gajula, B.; Sridhar, B.; Pottireddygar, G. R.; Rao, T. P. *J. Org. Chem.* **2010**, *75*, 5963–5975.
- [20] Patil, N. T.; Shinde, V. S.; Gajula, B. *Org. Biomol. Chem.* **2012**, *10*, 211–224.
- [21] Fogg D. E.; Santos E. N. D. *Coord. Chem. Rev.*, **2004**, *248*, 2365–2379.
- [22] (a) Hashmi, A. S. K.; M. Rudolph *Chem. Soc. Rev.* **2008**, *37*, 1766–1775; (b) Jiménez-Núñez, E.; Echavarren, A. M. *Chem. Rev.* **2008**, *108*, 3326–3350; (c) Arcadi, A. *Chem. Rev.* **2008**, *108*, 3266–3325; (d) Li, Z.; Brouwer, C.; He, C. *Chem. Rev.* **2008**, *108*, 3239–3265; (e) Gorin, D. J.; Sherry, B. D.; Toste, F. D.; *Chem. Rev.* **2008**, *108*, 3351–3378; (f) Abu Sohel, S. Md.; Liu, R.-S. *Chem. Soc. Rev.* **2009**, *38*, 2269–2281; (g) Dudnik, A. S.; Chernyak, N.; Gevorgyan, V. *Aldrichimica Acta* **2010**, *43*, 37–46; (h) Bandini, M. *Chem. Soc. Rev.* **2011**, *40*, 1358–1367; (i) Patil, N. T.; Singh V. *J. Organomet. Chem.* **2011**, *696*, 419–432; (j) Patil N. T. *Chem. Asian J.* **2012**, *7*, 2186–2194.
- [23] (a) Kalin, J. H.; Butler, K. V.; Akimova, T.; Hancock, W. W.; Kozikowski, A. P. *J. Med. Chem.* **2012**, *55*, 639–651; (b) Bonjoch, J.; Diaba, F.; Pagès, L.; Pérez, D.; Soca, L.; Miralpeix, M.; Vilella, D.; Anton, P.; Puig, C. *Bioorg. Med. Chem. Lett.* **2009**, *19*, 4299–4302; (c) Khorana, N.; Purohit, A.; Herrick-Davis, K.; Teitler, M.; Glennon, R. A. *Bioorg. Med. Chem.* **2003**, *11*, 717–722.
- [24] Grigg, R.; Sridharan, V.; Sykes D. A.; *Tetrahedron* **2008**, *64*, 8952–8962.
- [25] Liu, X.-Y.; Che, C.-M.; *Angew. Chem. Int. Ed.* **2008**, *47*, 3805–3810.
- [26] (a) Oniciu, D. C.; Henri, J.-L.; Barbaras, R.; Kochubey, V.; Kovalsky, D.; Rodin, O. G.; Geoffroy, O.; Rzepiela, A. (Cerenis Therapeutics SA), WO 2012/054535 A2, **2012**; (b) Khorana, N.; Smith, C.; Herrick-Davis, K.; Purohit, A.; Teitler, M.; Grella, B.; Dukat, M.; Glennon R. A. *J. Med. Chem.* **2003**, *46*, 3930–3937; (c) Altomare, C.; Summo, L.; Cellamare,

S.; Varlamov, A. V.; Voskressensky, L. G.; Borisova, T. N.; Carotti A. *Bioorg. Med. Chem. Lett.* **2000**, *10*, 581–584.

Enantioselective Relay Catalytic Branching Cascade: The Importance of Merging Gold(I) with Chiral Brønsted Acid Catalysis

Table of Contents

3.1 Introduction	124
3.2 Hypothesis	133
3.3 Results and Discussion.....	134
3.3.1 Optimization of Reaction Conditions	134
3.3.2 Scope and Generality Studies	138
3.3.3 Control Experiments.....	143
3.4 Computational Studies:	144
3.5 Conclusion.....	146
3.6 Experimental Procedures.....	146
3.7 Characterization Data of Starting Materials and Products.....	150
3.8 ¹ H NMR and ¹³ C NMR Spectra.....	175
3.9 HPLC Chromatograms.....	191
3.10References	203

3.1 Introduction

Traditionally, it is assumed that catalysis has been the realm of metals. The transition metal mediated reactions for the formation of carbon-carbon (C-C) and carbon-heteroatom (C-X) bonds have revolutionized the field of organic synthesis. In the study of the evolution of metal catalysis, one can quickly judge that many C-C and C-X bond forming processes, have been developed and found extensive relevance in the synthesis of natural products and privileged structures.

Since 2000, organocatalysis has grown explosively to become one of the most exciting research areas in current organic chemistry. Organocatalysts can promote various organic transformations through distinct activation modes. The organocatalysts offer new reactivities and most importantly the properties of them can be tuned according to the need and design of molecular structure.

In recent years, the combination of transition metal catalysts and organocatalysts has emerged as a new and powerful strategy for developing new reactions, and has attracted increasing attention as it enables the development of unprecedented transformations that is not possible by use of either of the catalytic systems alone. Clearly, such reaction provides a powerful tool to synthesise highly complex molecules preserving energy and resources.

Advantages and challenges of combining organo- and transition metal catalysis

While transition metal and organocatalysis individually have their own place in modern organic chemistry, the combination of transition metal and organocatalysis is particularly attractive as this concept has the unique advantages:

- (1) It enables the development of new, previously unattainable transformations that can lead to new types of reactivities.
- (2) It can create or improve the enantioselectivity where stereochemical control was previously absent or challenging.
- (3) It provides more possibilities to make a reaction enantioselective using a single catalyst chiral or both catalysts chiral.
- (4) If a metal catalyst and an organocatalyst are able to initiate reactions individually, an asymmetric relay catalytic reaction may be realized with either or both chiral catalysts controlling the stereochemistry.

In addition to above remarkable features and advantages there are some perceived challenges facing this concept due to which the concept of combining transition metal

catalysis and organocatalysis is still limited. Unlike the biological processes, where nature takes advantage of enzyme architecture to facilitate a multiple reaction manifold, it is very difficult to exploit on such process in a flask. The main challenge in the development of combined transition metal and organocatalyzed transformations is to ensure compatibility of catalysts, substrates, intermediates and solvents throughout the whole reaction sequence. The key to overcome this challenge is the judicious selection of appropriate catalyst combinations which are compatible with each other and reaction conditions.

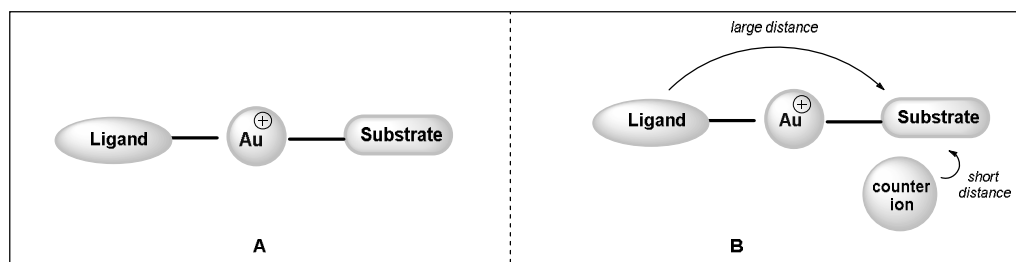
Merging Gold- and Brønsted acid Catalysis

The past decade has witnessed an impressive development of homogeneous gold catalysis, which exhibits incomparable efficiency for the activation of carbon-carbon multiple bonds, leading to numerous synthetically useful transformations. One of the key properties especially in Au(I) catalysis is the general tolerance of the catalytic system towards moisture and air, which makes a combination with an organocatalytic system highly feasible. Traditionally, transition-metal catalyzed enantioselective transformations rely on chiral ligands tightly bound to the metal in order to induce asymmetric product distributions.

The development of asymmetric gold(I)-catalyzed methods, however, is challenging because mononuclear gold(I) complexes adopt linear geometries, which places ligands 180° from substrate.¹ This combined with the average gold-carbon and gold-phosphorus bond lengths means that any chiral information stored in a chiral phosphine ligand is more than 4 Å away from the active site, rendering transfer of chiral information difficult.

One solution to this problem is the implementation of a dinuclear gold complex. In this case, a second gold(I) center or a second counter-ion can provide an additional point of interaction with the reactive site. Although the precise nature of this secondary interaction is not well-understood, dinuclear gold(I)-complexes have been applied to a variety of asymmetric transformations with good selectivity.² The majority of gold(I)-catalyzed enantioselective transformations described are relied on the application of chiral ligands bound to the gold center. However, as a result of the linear two coordinate geometry adopted by gold(I) complexes, the chiral ligand is often placed far from the substrate and enantioselectivities are usually low. The solution to this problem is use of chiral counter-ion which can reach to substrate molecule and impart chiral information to the reactive site.

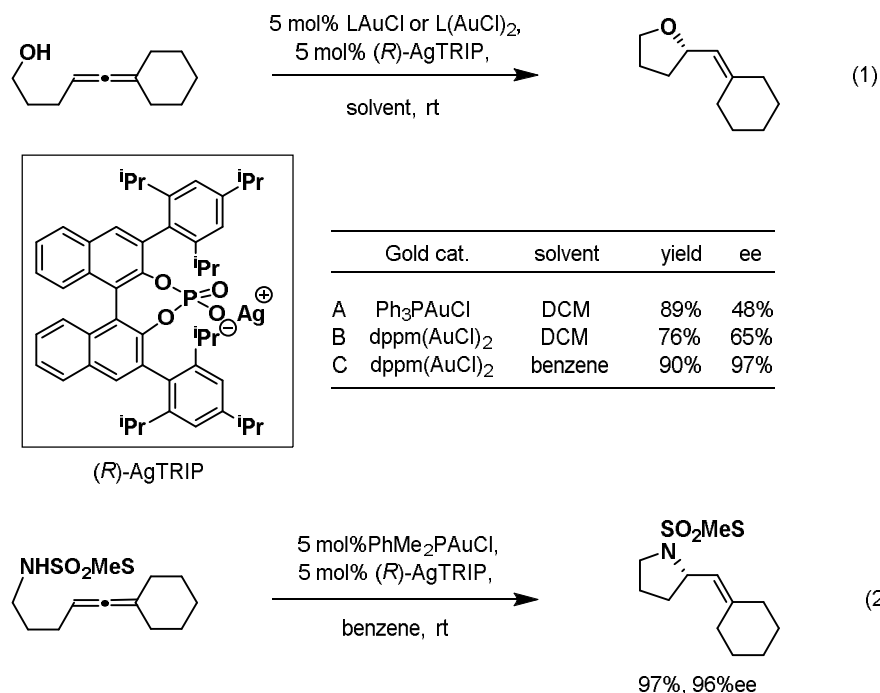
Figure 3.1: Unique geometry of Au(I)-complexes (A) and possible intervention of a chiral counter-ion (B).



The reaction catalyzed by gold- and organocatalysts, so-called “merged organo/gold catalysis” is especially interesting and the horizon for enantioselective gold catalysis expected to be expanded since there exists a possibility of using either of the catalyst chiral and/or both catalysts chiral in a synergistic fashion. While in literature many reports describe this chemistry which also has been documented in the form of reviews, the few distinct examples of an enantioselective processes that utilizes achiral Au-complexes and chiral binol phosphoric acids as catalysts are discussed below.

In 2007, Toste and coworkers reported the use of chiral gold phosphate (LnAuB), derived from LnAuCl and silver phosphate AgB for the intramolecular hydroalkoxylation of allenol (Scheme 1, Eq. 1).³ The silver phosphate was conveniently prepared in situ from chiral Brønsted acids (BH) by the reaction with Ag₂O. The phosphates were utilized as catalysts for the intramolecular hydroalkoxylation of allenol to produce tetrahydropyran derivative. In this case, the use of a chiral ligands and chiral counter-ion on Au-center provided desired product in good ee's (up to 97%). On the contrary, the use of a single chiral ligand on gold center is not satisfactory and poor ee was observed in such cases. The concept was further extended for the hydroamination of allene tethered sulfonamides to afford the cyclic-sulfonamides in good yields with high level of ee's (Scheme 1, Eq. 2)

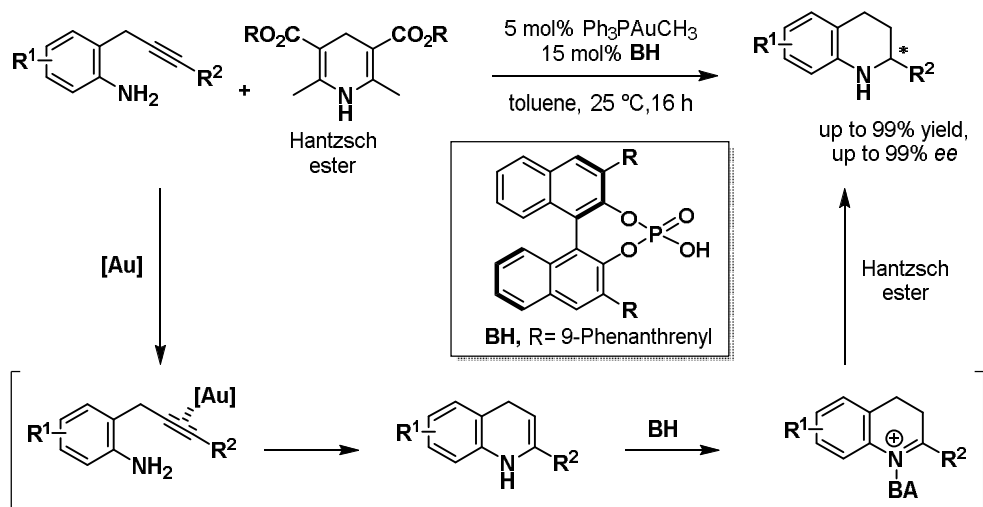
Scheme 3.1: Chiral Au-phosphate catalyzed enantioselective hydroalkoxylation, hydroamination and hydrocarboxylation reactions



The above mentioned discovery made by the Toste's research group is very promising. They have shown that the high ee was conferred by a chiral counterion. In addition, they have shown that the chiral counterion can be combined additively with chiral ligands to enable an asymmetric transformation that cannot be achieved by either method alone. Following this report by Toste *et al.* the field of combining Brønsted acid and Au(I) catalysis was spearheaded by three key publications by Gong, Che and Dixon respectively in 2009.

In early 2009, Gong and coworkers reported gold (I)/chiral Brønsted acid catalyzed synthesis of tetrahydroquinolines from *ortho*-aminoalkyne *via* intramolecular hydroamination followed by enantioselective transfer hydrogenation in good to excellent yields and ee's (Scheme 5).⁴ The reaction proceeded through gold phosphate catalyzed intramolecular hydroamination to form 1,4-dihydroquinoline that subsequently underwent isomerisation to form 3,4-dihydroquinoline. Under the catalysis of chiral Brønsted acid the enantioselective transfer hydrogenation using Hantzsch ester took place to form tetrahydroquinolines. Controlled studies revealed that gold phosphate had little effect on the enantioselective transfer hydrogenation, while chiral Brønsted acid solely controlled the enantioselectivity.

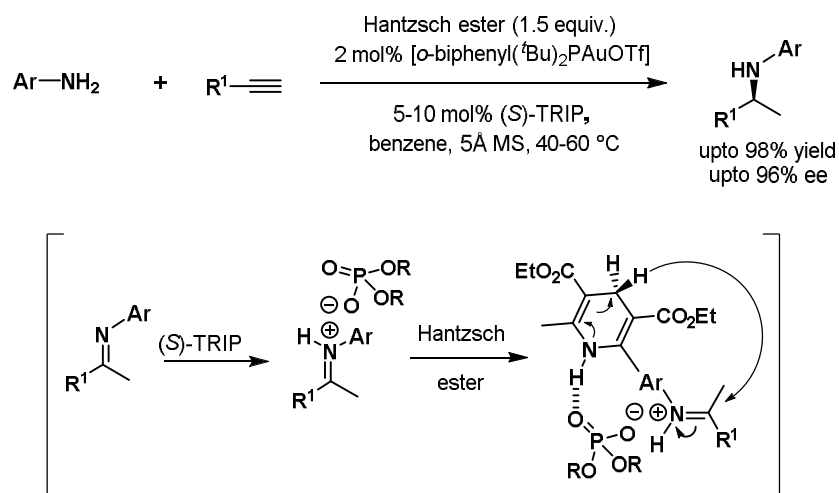
Scheme 3.2: Gold(I)/chiral Brønsted acid catalyzed intramolecular hydroamination-hydrogenation cascade



The important fact of the report by Gong *et al.* was that the catalyst LnAuMe reacts with chiral Brønsted acid to generate gold phosphates with the liberation of methane gas. Hence the reactive species in the reaction is chiral gold phosphate and chiral Brønsted acid (if used in excess). Hence, the possibility of formation of residual achiral Brønsted acid (such as TfOH in the case of LnAuOTf), which could be the culprit for background reactions, does not exist. It is surprising to note that the preparation of LnAuMe is known for last 20 years; however, the application in gold catalysis⁵ and especially in asymmetric gold catalysis⁶ is not known. The reports by Gong and Che has led good foundation for preparation of chiral gold phosphate in one-pot in contrary to Toste's procedure³ wherein two step process is required.

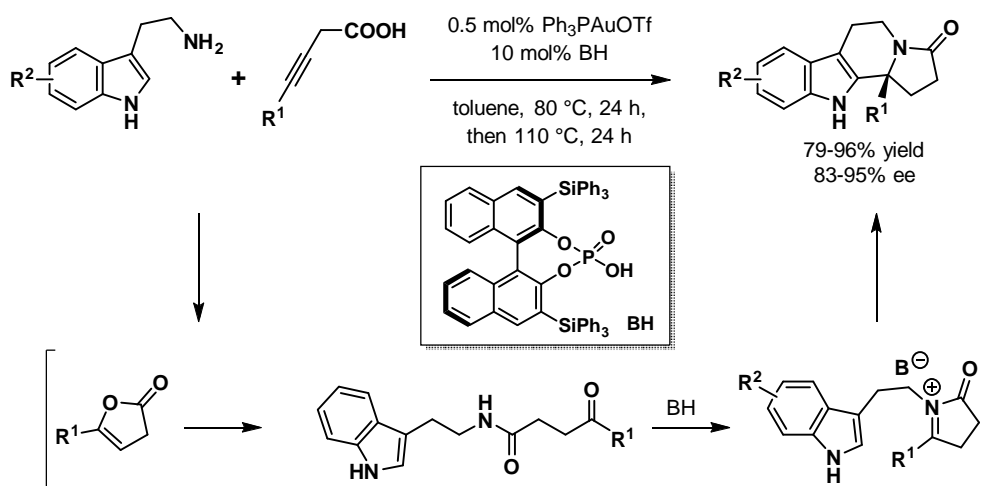
Independently, Che and coworkers reported analogues example based on consecutive hydroamination/transfer hydrogenation reaction between terminal alkynes and aromatic amines (Scheme 3).⁷ The proposed mechanism is similar to that reported by Gong and coworkers. Mechanistically, the formation of Au-phosphate took place which catalyzes intermolecular hydroamination of alkyne with amine to generate the imine intermediate. This imine is then activated by Brønsted acid catalysis to generate the iminium salt which subsequently undergoes enantioselective transfer hydrogenation in the presence of Hantzsch ester to afford secondary amines in good yields and ee's.

Scheme 3.3: Gold(I)/chiral Brønsted acid catalyzed intermolecular hydroamination-hydrogenation cascade



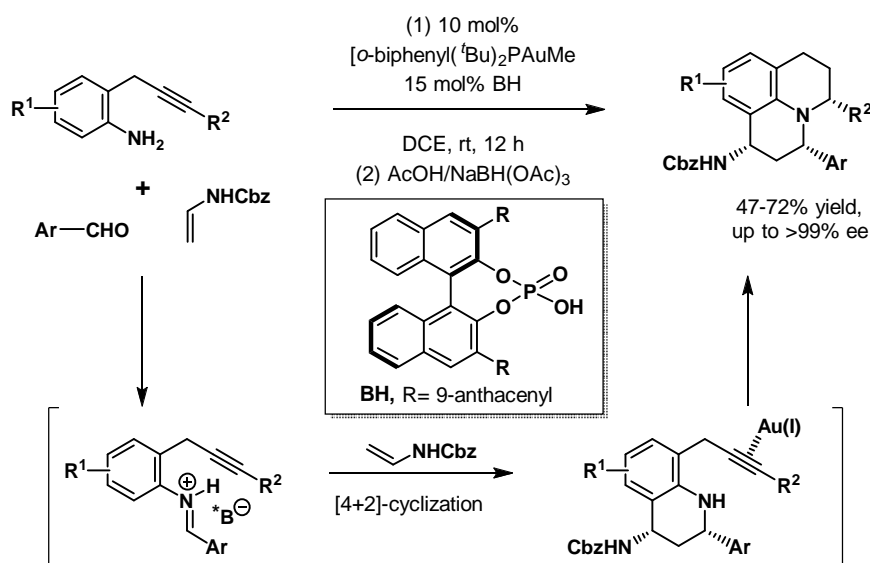
In the same year, Dixon *et al.* reported Au(I)/chiral Brønsted acid-catalyzed formal hydroamination/hydroarylation of alkynes tethered with carboxylic group (Scheme 4).⁸ They utilized alkynoic acids and tryptamine as starting materials and the process led to an efficient synthesis of enantiopure tetracyclic heterocyclic compounds. The reaction was initiated with Au(I)-catalyzed 5-*endo-dig* cyclization to form five membered enol lactones. In presence of chiral Brønsted acid, the enol lactone was attacked by the amine moiety of tryptamine to form isolable keto-amide which subsequently underwent a dehydrative cyclization through *N*-acyliminium intermediate. The presence of the chiral counteranion allowed stereocontrol in the nucleophilic attack (Pictet-Spengler type reaction) of the indole to provide the polycyclic indole derivatives in good yields and ee's.

Scheme 3.4: Au(I)/chiral Brønsted acid catalyzed iminium ion cascade



In 2010, Gong *et al.* described an interesting example of Au(I) and chiral Brønsted acid catalyzed enantioselective three component cascade reaction between 2-(2-propynyl) anilines, aldehydes and enamide for the preparation of optically pure julolidine derivatives (Scheme 5).⁹ Mechanistically, a Brønsted acid-catalyzed [4+2] cycloaddition reaction between the iminium species with enamide took place to generate enantiopure amino-alkyne which subsequently underwent intramolecular hydromination catalyzed by a gold phosphate. The stable julolidine derivatives were isolated after reduction with AcOH/NaBH(OAc)₃. Control experiments revealed that gold phosphate generated in situ was unable to catalyze the [4+2] cycloaddition reaction and only chiral Brønsted acid served as real catalyst for this step; while, intramolecular hydroamination of 2-(2-propynyl) anilines, was found to be solely catalyzed by gold phosphate.

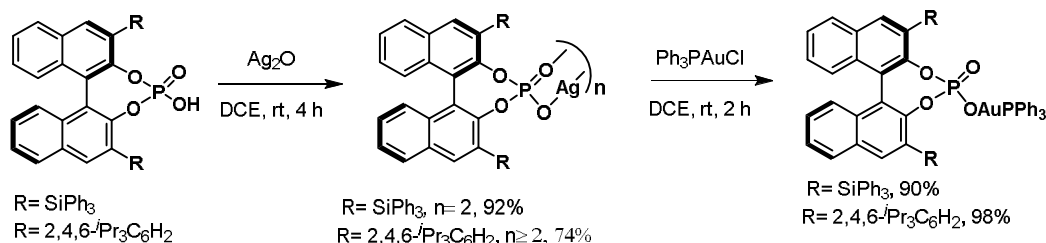
Scheme 3.5: Gold(I)/chiral Brønsted acid catalyzed cascade reaction for the synthesis of julolidine derivatives



It is evident that the gold phosphates are efficient catalysts which are generated in situ from the corresponding gold catalysts and chiral Brønsted acids. However, until recently, no reports exist on the isolation and characterization of gold phosphates. In 2012, Echavarren *et al.* reported the preparation, isolation and characterization of Au-phosphate complexes. These Au-phosphate complexes were prepared in two steps following the procedure reported by Toste and coworkers^[3] which involves the treatment of Brønsted acid with Ag₂O to afford silver phosphate complex followed by displacement of silver by gold catalysts (Scheme 6).¹⁰ The gold phosphates, thus obtained, are very robust and can be purified by flash

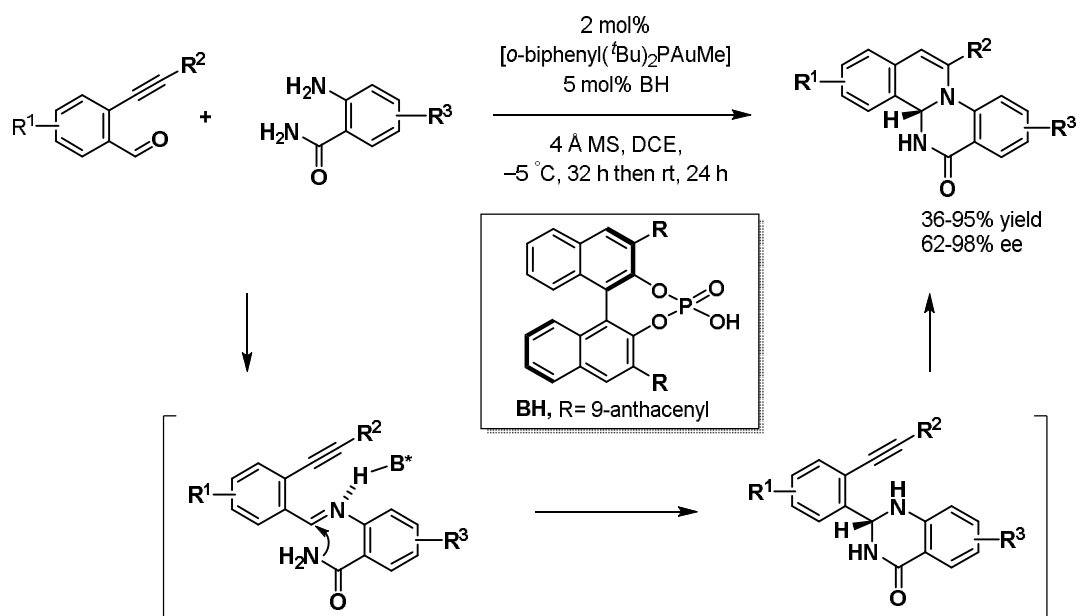
chromatography on SiO₂ and were well characterized by ³¹P NMR and X-ray diffraction techniques.

Scheme 3.6: Synthesis of chiral gold(I) phosphates



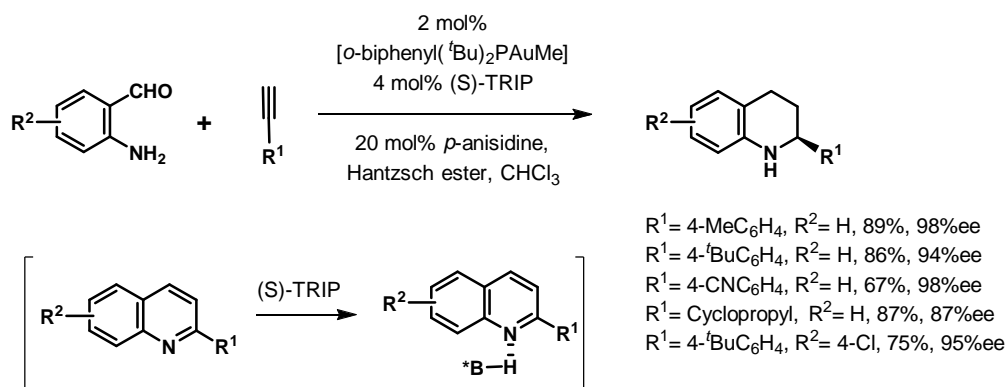
A central theme of the research in our laboratory is the development of π -acid catalyzed reactions and merging gold catalysis with organocatalysis for the synthesis of nitrogen containing heterocycles. In this context, our research group developed an enantioselective reaction utilizing achiral Au(I) complexes and chiral Brønsted acids for the synthesis of optically pure fused 1,2-dihydroisoquinolines (Scheme 7).¹¹ The treatment of 2-alkynyl benzaldehydes with 2-aminobenzamides in the presence of 5 mol% **BH-3** and 2 mol% **L-7**.AuMe and MS 4Å in DCE (−25 → +25 °C) afforded enantiopure 1,2-dihydroisoquinolines in high yield and up to 99% ee. Mechanistically, the reaction proceeded *via* the formation of chiral amins, by condensation between two starting material under the catalysis of chiral Brønsted acid,¹² which after intramolecular hydroamination catalyzed by in situ gold generated phosphate afforded fused optically pure 1,2-dihydroisoquinolines. The gold phosphate was characterized by ¹H NMR, ¹³C NMR, HRMS and ³¹P NMR spectroscopy.

Scheme 3.7: Gold(I)/chiral Brønsted acid catalyzed synthesis of optically pure fused 1,2-dihydroisoquinolines



In continuation, our research group reported an enantioselective cooperative triple catalysis system consisting of **LAuMe**/*p*-anisidine/chiral Brønsted acid catalysts for the synthesis of 2-substituted tetrahydroquinolines from the reaction of 2-aminobenzaldehydes, terminal alkynes and Hantzsch ester (Scheme 20).^[13] The reaction worked well with a wide range of substituent on both starting materials to afford the desired optically pure 2-substituted tetrahydroquinolines in good yield with excellent ee's (up to 99%). Several controlled experiments have been performed to understand the role of each catalyst. The study indicate that all three catalysts *p*-anisidine, **BH-1**, gold phosphate (generated in situ from Au-catalyst and **BH-1**) are necessary to obtain 2-substituted quinolines while enantioselective transfer hydrogenation was solely catalyzed by the chiral Brønsted acid to afford 2-substituted tetrahydroquinolines.

Scheme 3.8: Gold(I)/*p*-anisidine/chiral Brønsted acid ternary catalysts system for synthesis of 2-substituted tetrahydroquinolines

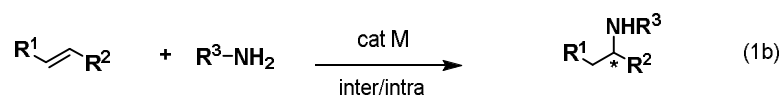
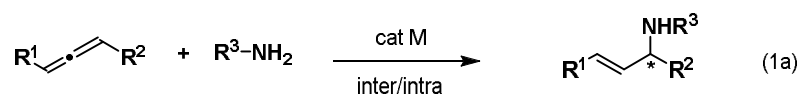


3.2 Hypothesis

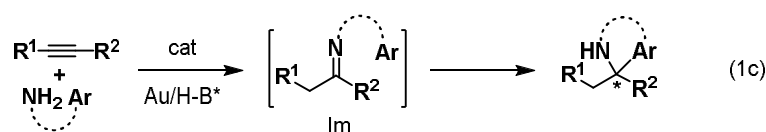
The hydroamination of allenes, olefins and alkynes catalyzed by transition metal complexes is fundamentally important reaction which has been widely used in organic synthesis.¹⁴ The addition of amines to allenes and or olefins generates chiral secondary amines and there exists quite a large number of reports on catalytic enantioselective variants (Scheme 1a and 1b).¹⁵ We envisioned an altogether different approach involving the addition of amines and electron rich aromatics to alkynes leading to chiral secondary amines (Scheme 9, Eq. 1c). The process can be termed as catalytic enantioselective hydroamination-hydroarylation which could be of great importance since one can generate chiral aza-heterocycles bearing quaternary carbon centers. Surprisingly, there have been no reports on the catalytic enantioselective versions of such processes.¹⁶

Scheme 3.9: Enantioselective addition of H-Nu on to C-C multiple bonds

Literature Known:



Our Hypothesis:



The reason for the hampered development of a catalytic enantioselective hydroamination-hydroarylation might be the requirement of catalysts which can perform hydroamination as well as enantioselective addition of H-Nu to transient imines. It is envisaged that the hydroamination of alkynes with amino-aromatics would occur by the chiral Au catalyst¹⁷ to form imines **Im** which would undergo intra-molecular attack by the tethered aromatics to produce an enantioenriched double addition product (Scheme 1c). A crucial aspect behind the success of the proposed reaction would be the formation of a tight ion pair between the imine nitrogen and the chiral Au-catalyst. Based on the available knowledge on the enantioselective gold catalysis,¹⁸ two strategies could be easily envisaged. The first strategy involves the use of L*AuX complexes. However, the enantioselective addition of nucleophiles on to imines under the catalysis of L*AuX complexes have rarely been reported.¹⁹ We opined that the paucity of such reports might be due to inability of Au-complexes to coordinate strongly with the imines - the phenomenon can be well understood in terms of relativistic effects.²⁰ The alternate strategy involves the use of LAuX* complexes, generated in situ from LAuMe and H-X* (X* = chiralphosphate anion).²¹ This strategy was supported by two facts: a) a chiral phosphate counter-ion act as ligand bonded to the gold species facilitating the hydroamination reactions²² and b) the residual X*H generated in situ can act as a catalyst for addition of H-Nu on to imines.²³ This hypothesis was supported by the pioneering work of Gong and coworkers who have reported consecutive Au(I)-catalyzed intramolecular hydroamination of alkyne and a chiral Brønsted acid catalyzed enantioselective transfer hydrogenation (see scheme 2).

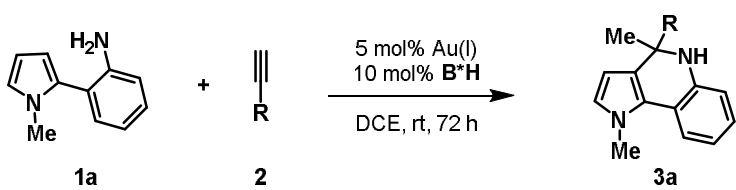
3.3 Results and Discussion

3.3.1 Optimization of Reaction Conditions

Since chiral pyrroles are prevalent building blocks in variety of natural products and pharmaceuticals, we started our investigation using 2-(2-aminophenyl)pyrroles (**1a**) as bis-nucleophiles (Table 1). At the outset, the reaction was performed using octyne **2a**, and 2-(1-methyl-1H-pyrrol-2-yl) aniline (**1a**) in the presence of 5 mol% PPh₃AuMe and 10 mol% **5a** (Fig 2). Pleasingly, the product **3a** was obtained in 22% yield; however, the ee was found to be only 4.7% (entry 1). In order to know the effect of the phosphine ligands, the Au-complexes **4a** and **4b** were tested for their catalytic efficiencies; however, none of them found to be beneficial (entries 2 and 3). When chiral Brønsted acids **5b**, **5c** and **5d** used, a slight increase in yields of reaction was observed; however ee remained still low (entries 4, 5

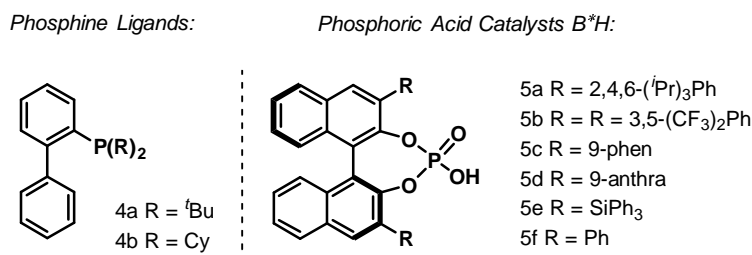
and 6). Later, based on our previous report we opted to use an alkyne which bears –OH group in the tether.²⁴ When 4-pentyn-1-ol **2b** was reacted with **1a** in the presence of 5 mol% PPh₃AuMe and 10 mol% **5a**, the reaction proceeded smoothly to afford **3a** in 76% yield with 91% ee (entry 7). The ee dropped down to 78% when **5b** was used instead of **5a** (entry 8). The use of bulky gold catalyst **4a**-AuMe and **4b**-AuMe in combination with **5a** gave **3a** in 80 and 81% yields with 98% and 95% ee's, respectively (entry 9 and 10).

Table 3.1: Optimization of the reaction conditions^a



Entry	2a	Au (I)	B*H (5)	Yield (%) ^b	ee(%) ^c
1	2a R ¹ = ⁿ Hex	Ph ₃ PAuMe	5a	22	4.7
2	2a	4a -AuMe	5a	27	5.3
3	2a	4b -AuMe	5a	31	4.4
4	2a	4a -AuMe	5b	48	3.2
5	2a	4a -AuMe	5c	56	3.0
6	2a	4a -AuMe	5d	57	6.2
7	2b R = (CH ₂) ₃ OH	Ph ₃ PAuMe	5a	76	91
8	2b	Ph ₃ PAuMe	5b	84	78
9	2b	4a -AuMe	5a	80	98
10	2b	4b -AuMe	5a	81	95
11	2b	4a -AuMe	5b	76	39
12	2b	4a -AuMe	5c	69	57
13	2b	4a -AuMe	5d	57	41
14	2b	4a -AuMe	5e	83	63
15	2b	4a -AuMe	5f	83	29

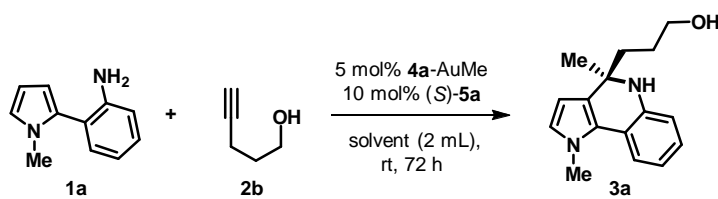
^aReaction conditions: 0.15 mmol **1a**, 0.15 mmol **2a**, 5 mol% Au(I), 10 mol% H-B*, DCE (2.0 mL), rt, 24 h; ^bIsolated yields; ^cee was determined by HPLC analysis on a chiral stationary phase.

Figure 3.2: Catalyst employed for optimization

Next, we screened chiral phosphoric acid catalysts **5** bearing various type of substituents at the 3, 3' position on the binaphthyl backbone (Figure 2). As shown in entries 11–15, all of the chiral catalysts **5** exhibited satisfactory performance in terms of yields (except entry 13); however, ee's were found to be strongly dependent on the C-3 substituents. We further extensively studied the effect of solvents, catalysts loading, and temperature on reaction outcome in terms of yields and ee's. The study revealed that the best condition is treating **1b** and **2a** in presence of 5 mol% **4a**-AuMe, 10 mol% **5a**, in DCE as solvent at room temperature (entry 9).

Optimization of Solvent

Next we studied effect of solvent on reaction outcome in terms of ee's and yields. It was known that non-coordinating solvents provided higher enantioselectivity in such reactions. Certainly, this is what one would expect if chiral ion pair was responsible for favouring one diastereomeric transition state over another. The non-polar solvents should promote a tighter association between the chiral anion and the cationic catalytic center. The study revealed DCE as the best solvent for this reaction (Table 2, entry 7).

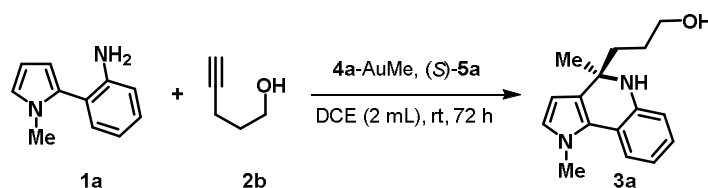
Table 3.2: Optimization of solvents^a


Entry	Solvent	Yield (%)	ee (%)
1	acetonitrile	83	67
2	THF	79	71
3	toluene	67	94
4	benzene	71	89
5	xylene	77	90
6	DCM	80	92
7	DCE	81	98
8	CHCl ₃	77	93
9	chlorobenzene	66	92
10	fluorobenzene	70	91
11	DCE + toluene	79	95

^a**Reaction conditions:** 0.15 mmol **1a**, 0.15 mmol **2b**, 5 mol% **4a-AuMe**, 10 mol%, (*S*)-**5a**, solvent (2 mL), rt, 72 h. All are isolated yields and ee's determined by HPLC analysis on a chiral stationary phase.

Optimization of Catalyst Loading

The catalyst loading study has also been performed to know the optimum loading of both the catalysts (Table 3). As can be seen from entry 6, when 1 mol% **4a-AuMe** and 3 mol% of **5a** catalysts were used the yield of reaction was dropped down significantly. The best results were achieved by using 5 mol% **4a-AuMe** and 10 mol% chiral Brønsted acid catalyst **5a** (Table 3, entry 4).

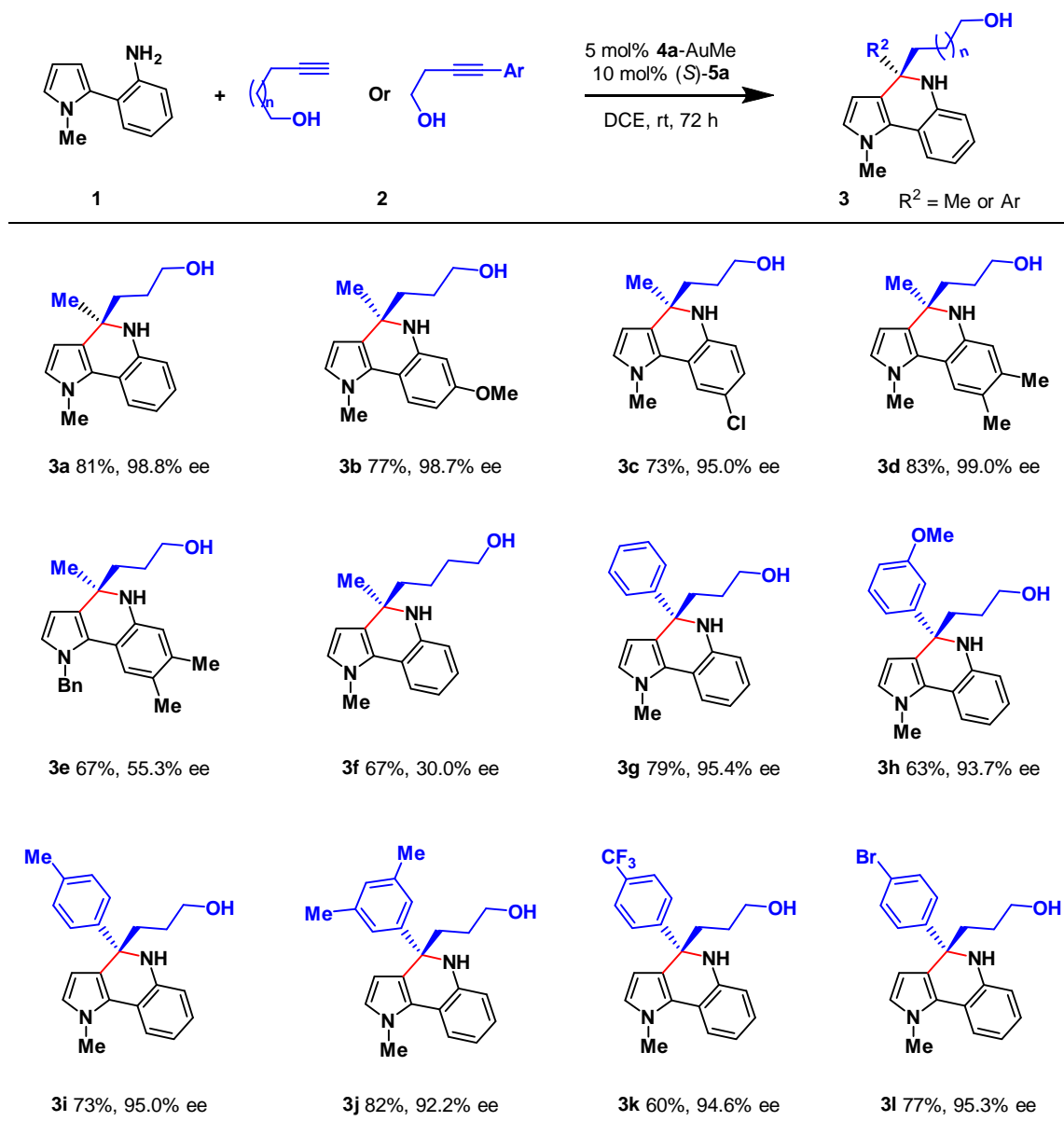
Table 3.3: Optimization of catalyst loadings^a

Entry	4a-AuMe	5d	Yield (%)	ee (%)
1	0 mol%	10 mol%	00	00
2	10 mol%	0 mol%	10	00
3	10 mol%	20 mol%	93	94
4	5 mol%	10 mol%	81	98
5	5 mol%	2.5 mol%	78	84
6	5 mol%	5 mol%	53	95

^aReaction conditions: 0.15 mmol **1a**, 0.15 mmol **2b**, **4a-AuMe**, (**S**)-**5a**, DCE (2 mL), rt, 72 h. All are isolated yields and ee's determined by HPLC analysis on a chiral stationary phase.

3.3.2 Scope and Generality Studies

With the optimized conditions in hand, we explored the generality of the catalytic enantioselective hydroamination-hydroarylation reaction using various 2-(2-aminoaryl)pyrroles and alkynes (Table 4). The 4-pentyn-1-ol reacted smoothly with various 2-(2-aminophenyl)pyrroles (bearing -OMe, -Cl and -Me substituents) under established condition to obtain the desired products **3a-d** in yields ranging from 73-83% and ee's ranging from 95-99% (C2-C3 cyclization). When methyl group on pyrrole nitrogen was replaced by benzyl group, the ee dropped down to 55% (**3d** vs **3e**). It should be noted that the carbon chain length between OH group and alkyne moiety has major effect as the use of 5-hexyn-1-ol provided **3f** with only 30% ee. The internal aromatic alkynol bearing halo, methoxy and methyl group at meta and para positions were well tolerated to afford corresponding dihydropyrrolo[3,2-*c*]quinolines in yields ranging from 60-82% and ee's more than 90% in all the cases.

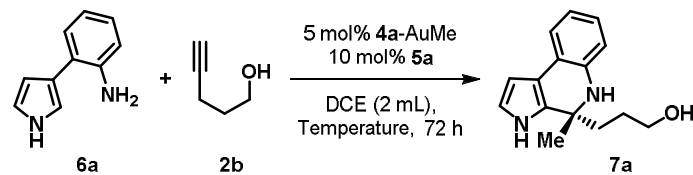
Table 3.4: Reaction of N-Methyl-(2-aminophenyl)pyrroles and alkynols (C2→C3 cyclization)^a

^aReaction conditions: 0.15 mmol **1**, 0.15 mmol **2**, 5 mol% **4a**-AuMe, 10 mol% (S)-**5a**, DCE (2 mL), rt, 72 h. All are isolated yield and ee's determined by HPLC analysis on a chiral stationary phase.

In order to further extend the scope of the reaction, we turned our attention to 3-(2-aminophenyl)pyrroles as a substrates (C3-C2 cyclization). As can be seen from table 5 the lowering of reaction temperature turned out to be beneficial to obtain dihydropyrrolo[2,3-c]quinolines in good yields and higher enantiomeric purities. A variety of substrates were tested to examine the scope and limitations of the protocol (Table 6). Notably, 4-pentyn-1-ol and internal alkynol bearing aromatic ring with various steric and electronic modification were well tolerated. As can be judged from **7a/7b** and **7c/7d** that the free N-H group of

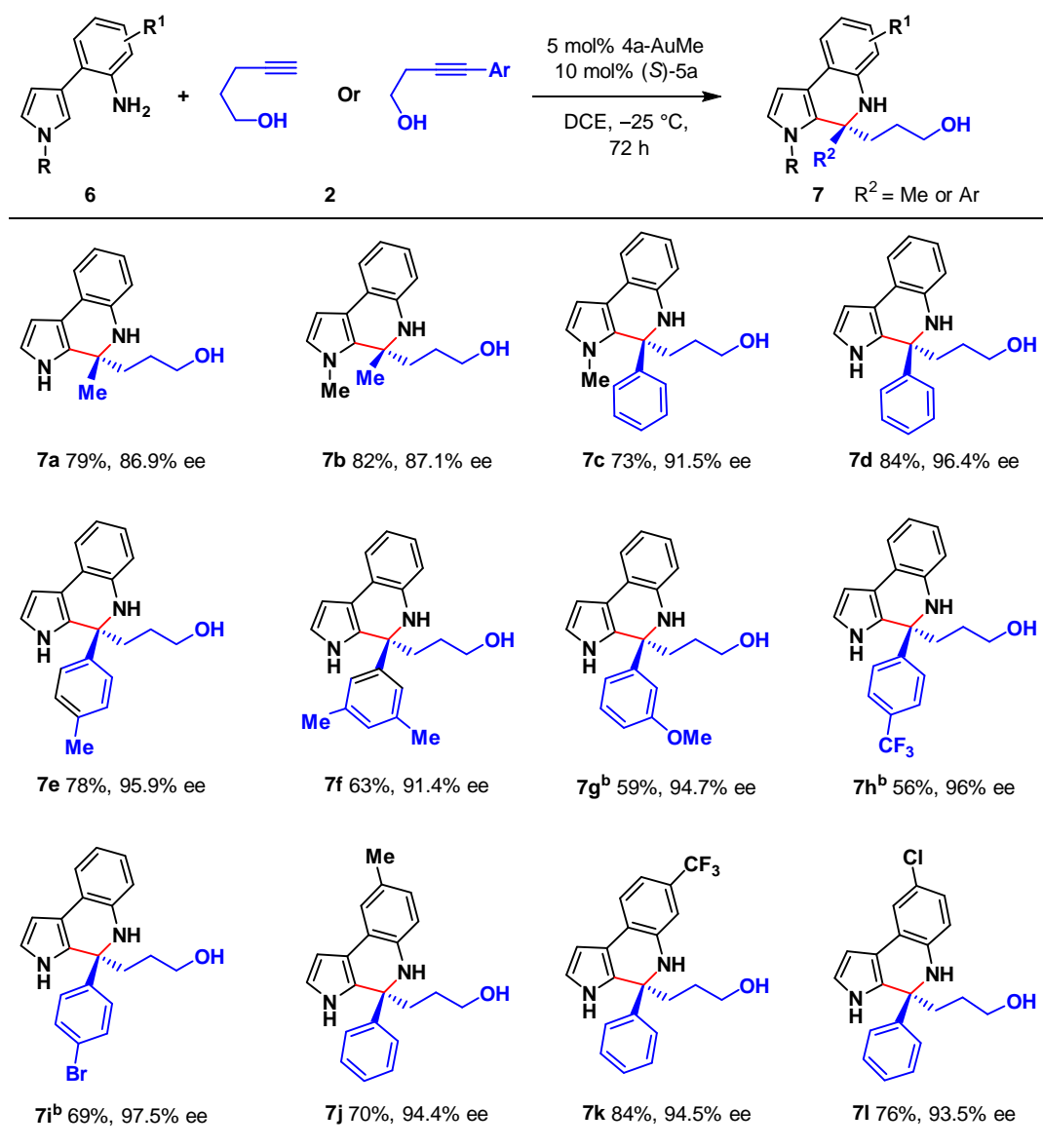
pyrrole is not necessary and even protected pyrrole derivatives equally works well to give the corresponding products in good yields and ee's.

Table 3.5: Optimization of the temperature (6a → 7a)



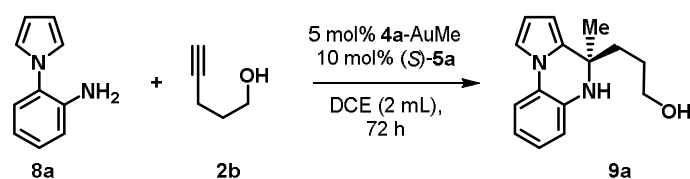
Entry	Temperature (°C)	Yield (%)	ee (%)
1	30	87	66
2	10	85	69
3	5	84	73
4	0	81	76
5	-10	80	80
6	-25	79	87

^aReaction conditions: 0.15 mmol 6a, 0.15 mmol 2b, 5 mol% 4a-AuMe, 10 mol% (S)-5a, DCE (2 mL), -30 °C, 72 h. All are isolated yields and ee's determined by HPLC analysis on a chiral stationary phase.

Table 3.6: Reaction 2-aminophenyl pyrroles and alkynols (C3→C2 cyclization)^a

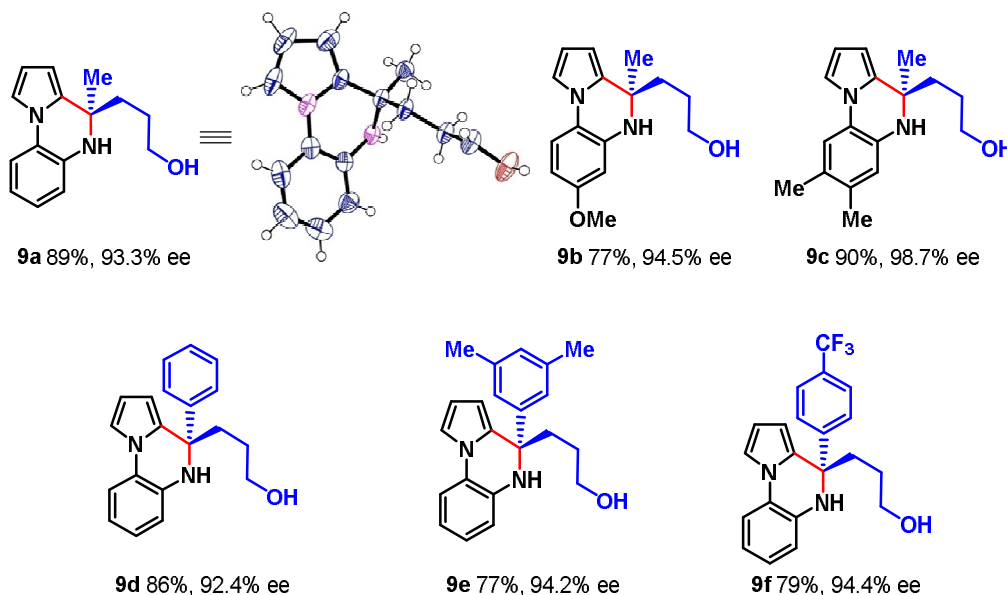
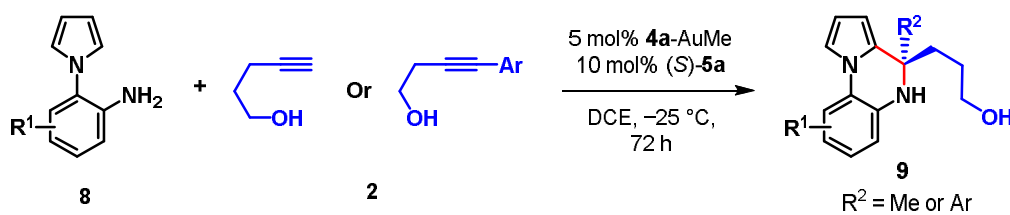
^aReaction conditions: 0.15 mmol 6, 0.15 mmol 2, 5 mol% 4a-AuMe, 10 mol% (S)-5a, DCE (2 mL), -25 °C, 72 h. All are isolated yields and ee's determined by HPLC analysis on a chiral stationary phase. ^bReaction performed at -15 °C.

Next, we endeavored to examine the applicability of 2-amino phenyl pyrroles for catalytic enantioselective hydroamination-hydroarylation reactions (Table 8). Even in this case also, lowering the temperature proved beneficial (Table 7) In all the cases examined, pyrrolo[1,2-*a*]quinoxalines (N-C2 cyclization) were obtained in good yields and with excellent ee's (>90%).

Table 3.7: Optimization of the temperature

Entry	Temperature (°C)	Yield (%)	ee (%)
1	rt	94	79
2	25	95	71
3	10	91	69
4	5	86	88
5	0	79	88
6	-10	88	92
7	-25	90	94

^aReaction conditions: 0.15 mmol **8a**, 0.15 mmol **2b**, 5 mol% **4a-AuMe**, 10 mol% (*S*)-**5a**, DCE (2 mL), 72 h. All are isolated yields and ee's determined by HPLC analysis on a chiral stationary phase.

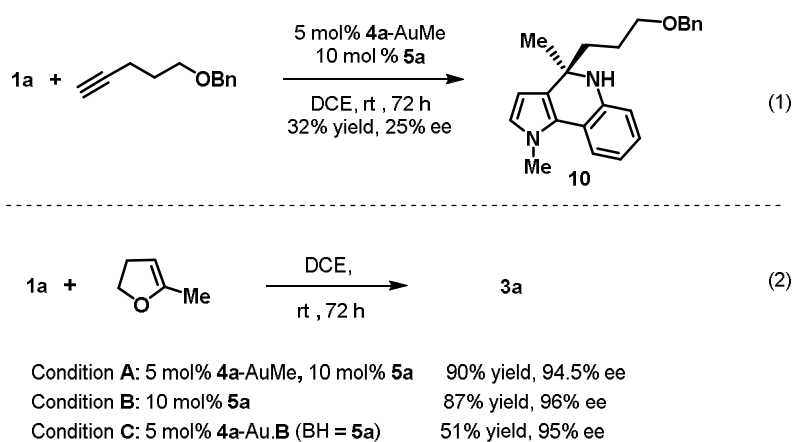
Table 3.8: Reaction of 2-aminophenylpyrroles and alkynols (*N*→C2 cyclization)^a

^aReaction conditions: 0.15 mmol **8**, 0.15 mmol **2**, 5 mol% **4a-AuMe**, 10 mol% (*S*)-**5a**, DCE (2 mL), -25 °C, 72 h. All are isolated yields and ee's determined by HPLC analysis on a chiral stationary phase.

3.3.3 Control Experiments

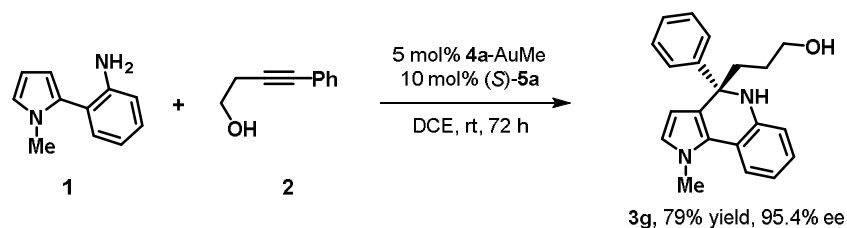
The absolute configuration of product **9a** (Table 4) and **3g** (after dehydrative cyclization) was determined by single crystal X-ray analysis and that of the rest of the products was assigned by analogy. The control experiments has been performed carefully which led us to conclude that the –OH group in alkyne is essential for the reaction to provide good yields and ee's (Scheme 2). The reaction of benzyl protected 4-pentyn-1-ol with **1a** under the optimized reaction condition, gave **10** only with 25% ee (Eq. 1). When commercially available 2-methylenetetrahydrofuran was treated with **1a** under conditions A and B; **3a** was obtained in almost identical yields and ees (Eq. 2, condition A and B). The use of pre-formed gold phosphate, generated insitu from **4a**-AuMe and (*S*)-**5a**, delivered **3a** only in 51% yield without causing detrimental effect on ee (95% ee) (Eq. 2, condition C). These all observations clearly indicates the importance of tethered hydroxyl group in the alkynes. It also can be concluded that the hydroalkoxylation is catalyzed by the insitu generated gold phosphate, while the condensation is promoted only by (*S*)-**5a**

Scheme 3.9: Control experiments

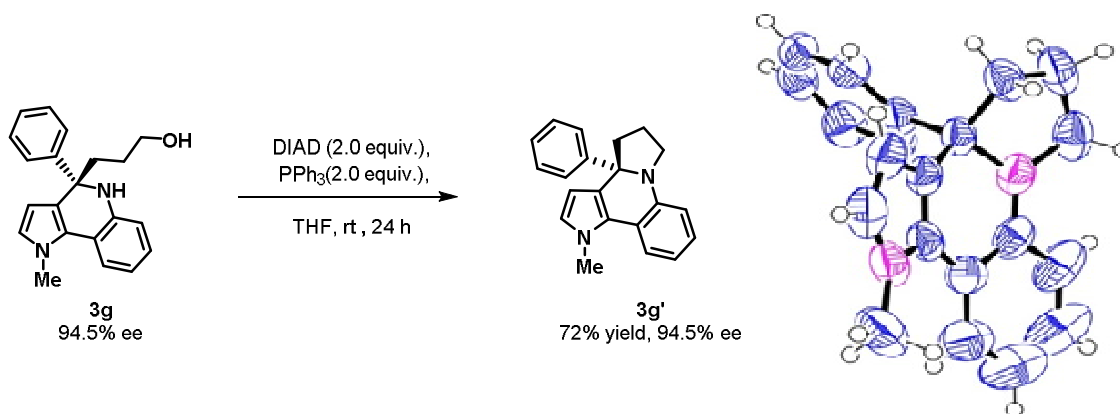


Study of Scalability and Practicality:

The scalability and practicality of the developed method is demonstrated by the gram-scale asymmetric synthesis of **3g** (82% yield, 94.5% ee) from **1a** and **2g**.

Scheme 3.9: Scalability study experiment

Literature analysis revealed that the organo-catalytic enantioselective condensation reaction between aminoaromatics with carbonyls (or equivalent) is an important method for accessing enantiopure scaffolds. However, all these methods leads to the generation of asymmetric *tertiary* carbon centers.²⁵ Since the formation of asymmetric *quaternary* carbon centers²⁶ is very important, a recent focus of many research groups is on the development of catalytic asymmetric variants that generates quaternary carbon centers. However, most of these reactions require either cyclic imines²⁷ or specially designed substrate.²⁸ In this regards, the newly developed method is valuable. Because of the importance of pyrrole containing heterocycles in the pharmaceutical field, the present reaction can provide an efficient means for generating such molecules in enantiomerically pure form. Moreover, the hydroxyl group in the product provides a versatile handle for further transformations to access additional molecular complexity.

Scheme 3.10: Transformation of **3g** to fused tetracyclic compound **3g'****3.4 Computational Studies:**

In order to understand clearly the role of tethered -OH group and mode of enantio-induction, DFT calculations were performed using the Turbomole 6.4 suite of programs, and the TZVP/PBE/B3LYP approach. The studies indicate that the "Re-face" attack of

nucleophile is kinetically preferred over the "Si-face" attack by 5.8 kcal/mol (ΔG) and 3.6 kcal/mol (ΔE) (Fig 4). Clearly, the highest level of enantio-induction can be accounted based on the transition state involving the H-bonding interaction between the transient imino-alcohol and B*-H. The bifunctional nature of chiral phosphoric acid 23 is responsible for concurrent activation of both imine nitrogen and tether hydroxyl group through hydrogen bonding interactions which creates chiral environment and exhibited product with very high ee.

All DFT calculations were performed using the Turbomole 6.4 suite of programs.¹ Geometry optimizations were performed using the Perdew, Burke, and Ernzerhof density functional (PBE).² The electronic configuration of the atoms was described by a triple- ζ basis set augmented by a polarization function (Turbomole basis set TZVP).³ The resolutions of identity (RI)⁴ along with the multipole accelerated resolution of identity (marij)⁵ approximations were employed for an accurate and efficient treatment of the electronic Coulomb term in the density functional calculations. Single point calculations were done with the hybrid B3-LYP functional⁶⁻⁷ in order to obtain more reliable energy values for the potential energy surfaces for the different investigated reactions. With regard to the transition-state, care was taken to make sure that the structures possessed only one imaginary frequency corresponding to the correct normal mode. The contributions of internal energy and entropy were obtained from frequency calculations done on the DFT structures at 298.15 K; thus, the energies reported in the figures are the ΔG values.

Figure 3.2: "Si-face" attack vs. "Re-face" attack: (*S*)-TRIP **5a** as catalyst

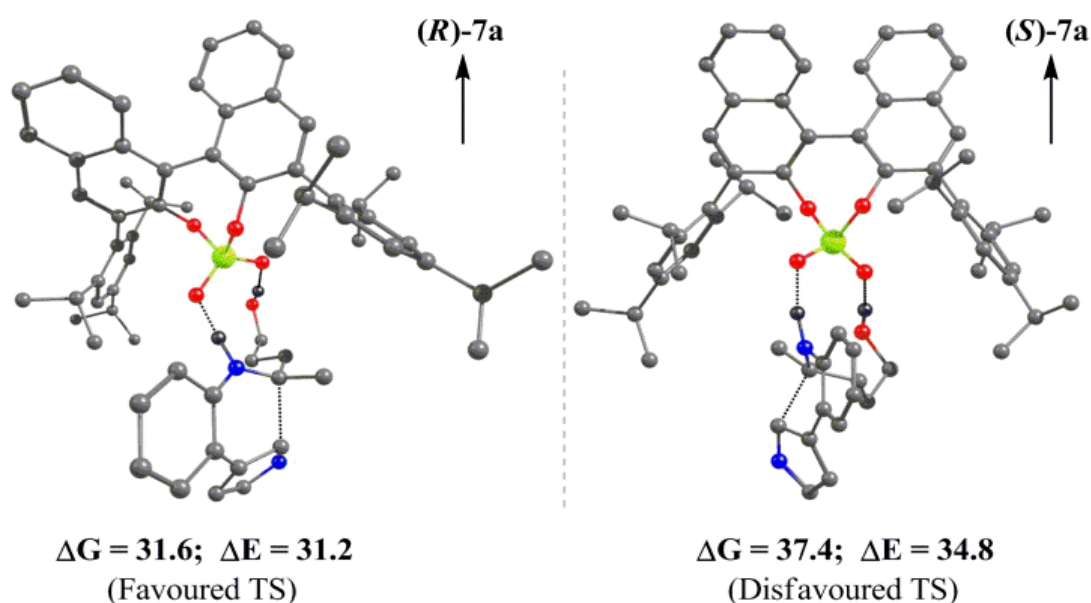
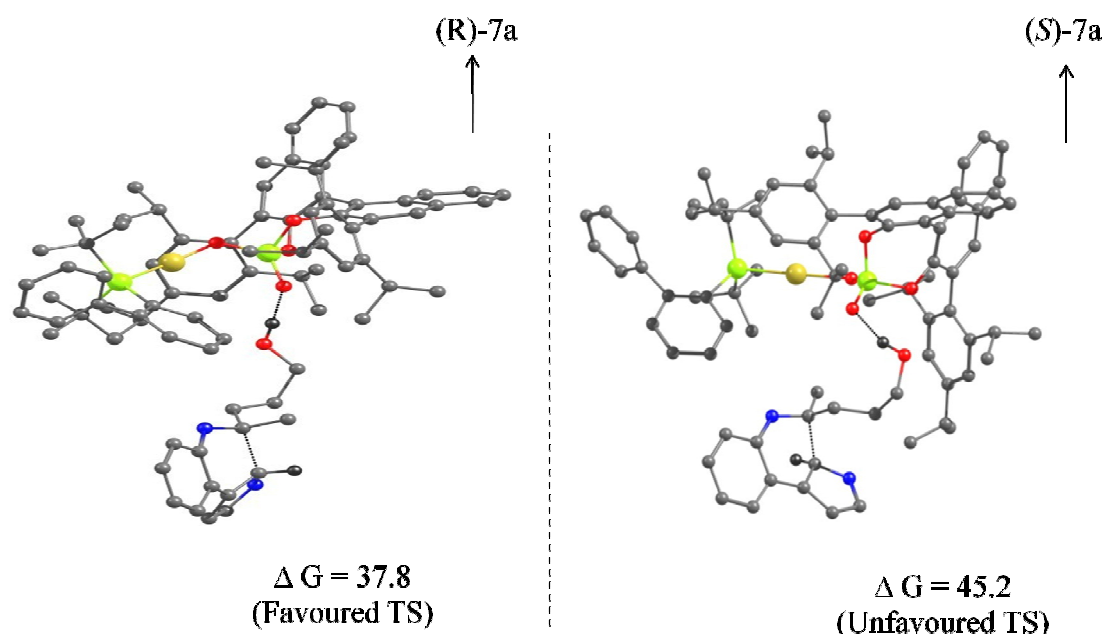


Figure 3.3: "Si-face" attack vs. "Re-face" attack: Au-phosphate as catalyst

3.5 Conclusions

In summary, we have realized the concept of enantioselective relay catalytic branching cascade (ERCBC) by catalytic enantioselective hydroamination-hydroarylation of alkynes under the catalysis of Au(I)/chiral Brønsted acid binary catalytic system. The method is very general and worked well over a range of three pyrrole-based amino-aromatics and therefore may open unprecedented opportunities in diversity oriented synthesis (DOS) for the development of enantioselective relay²⁹ catalytic branching cascade.³⁰ In addition, the work presented herein could be considered as an advanced complements to Pictet-Spengler reactions as the formation quaternary carbon through the condensation of aminoaromatics with carbonyls is highly challenging and mostly limited to tryptamines.³¹

3.6 Experimental Procedures

The gold catalysts **4a**-Au-Me and **4b**-Au-Me were prepared according to literature known procedures.¹ The Brønsted acid catalysts **5a**-**5f** were prepared following literature known procedures.²

¹ (a) Nieto-Oberhuber, C.; Lopez, S.; Echavarren, A. M.; *J. Am. Chem. Soc.* **2005**, *127*, 6178-6179; (b) Wang, C.; Han, Z-Y.; Luo, H-W.; Gong, L-Z. *Org. Lett.* **2010**, *12*, 2266-2269.

General Procedure for Enantioselective Synthesis of 3, 7 and 9:

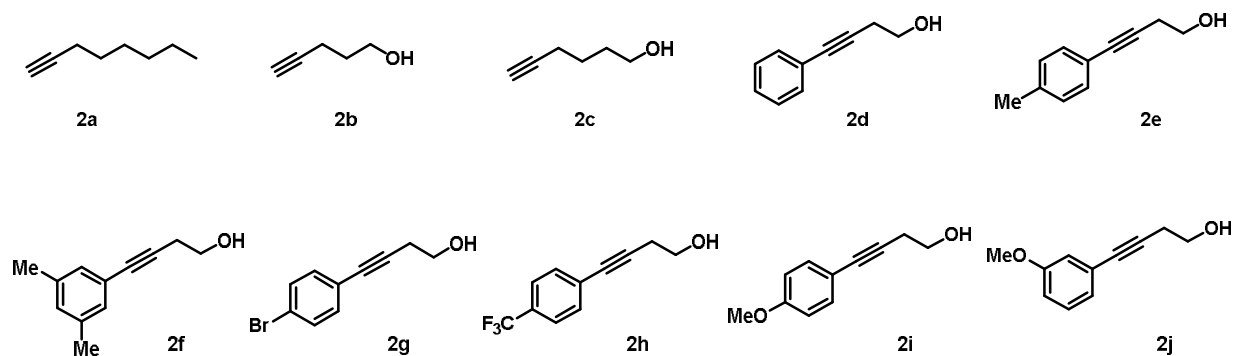
The procedure is representative. To a flame-dried screw-capped vial equipped with magnetic stir bar, were added (S)-TRIP (10 mol%) and Johnphos-Au-Me (5 mol%), in DCE (2 mL) at room temperature and the reaction mixture was stirred for 30 min. To this reaction mixture alkyne (0.15 mmol) was introduced followed by amino-aromatics (0.15 mmol) under argon atmosphere. The reaction vial was fitted with a cap, evacuated and back filled with argon and stirred for specified temperature for 72 h. The reaction mixture was diluted with ethyl acetate and filtered through plug of silica gel. The filtrate was concentrated and the residue thus obtained was purified by silica gel column chromatography using Pet. ether/EtOAc as an eluent to afford analytically pure final compounds.

All racemic compound were synthesized using Johnphos-Au-Cl (5 mol%), AgOTf (5 mol%), following same reaction conditions (Reaction time = 24 h).

General Procedures for Synthesis of Starting materials:

4.1 Preparation of Alkynols 2:

The alkyne **2a**, **2b** and **2c** were purchased from commercial sources and used as received whereas alkyne **2d**, **2e**, **2f**, **2g**, **2h** and **2i** were prepared according to literature known procedures.³



² (a) Romanov-Michailidis, F.; Guénée, L.; Alexakis, A. *Angew. Chem. Int. Ed.* **2013**, *52*, 9266–9270; (b) Rueping, M.; Nachtsheim, B. J.; Koenigs, R. M.; Ieawsuwan W. *Chem. Eur. J.* **2010**, *16*, 13116–13126; (c) Liu, W.-J.; Chen, X.-H.; L.-Z. Gong. *Org. Lett.* **2008**, *10*, 5357–5360. (d) Yamanaka, M.; Itoh, J.; Fuchibe, K.; Akiyama, T. *J. Am. Chem. Soc.*, **2007**, *129*, 6756–6764; (e) Storer, R. I.; Carrera, D. E.; Ni, Y.; MacMillan, D. W. C. *J. Am. Chem. Soc.* **2006**, *128*, 84–86; (f) Wu, T. R.; Shen, L.; Chong J. M. *Org. Lett.*, **2004**, *6*, 2701–2704.

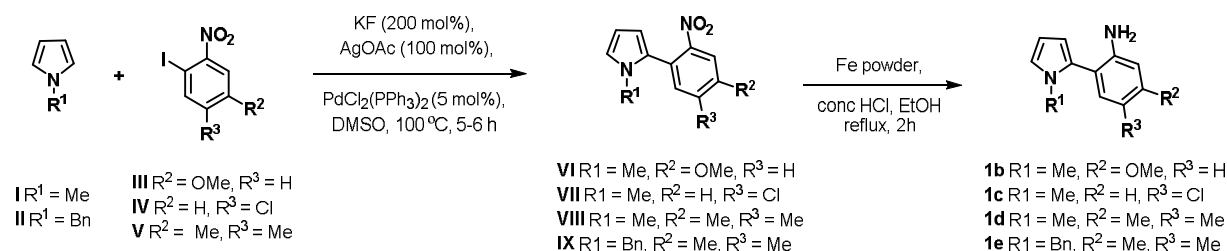
³ (a) Ueda, T.; Kanomata, N.; Machida, H. *Org. Lett.* **2005**, *7*, 2365–2368. (b) O'Rourke, N. F.; Davies, K. A.; Wulff, J. E. *J. Org. Chem.* **2012**, *77*, 8634–8647. (c) Mizukami, M.; Saito, H.; Higuchi, T.; Imai, M.; Bando, H.; Kawahara, N.; Nagumo, S. *Tetrahedron Lett.* **2007**, *48*, 7228–7231.

4.2 Preparation of 2-(1-alkyl-1H-pyrrol-2-yl)aniline 1:

The nitro compounds **VI**, **VII**, **VIII** and **IX** were synthesized by the procedure similar to that reported by Gryko *et al.*⁴

General Procedure for the Synthesis of 2-(1-methyl-1H-pyrrol-2-yl)aniline 1:

A solution of 1-methyl-2-(2-nitrophenyl)-1H-pyrroles [(**VI** to **IX**), 1.0 equiv.] and Fe powder (5.0 equiv.) in acidic ethanol (1:4 aq. HCl/EtOH,) was heated at reflux under nitrogen atmosphere for 2 h. The solution was cooled down to room temperature and then poured into ice. The pH was made basic (pH 8) by the addition of 10% aqueous NaHCO₃. The EtOAc (25 mL) was added to the mixture and filtered through a bed of Celite. The organic layer was finally washed with water (25 mL) and then brine (25 mL) and dried over anhydrous Na₂SO₄. The organic layer was evaporated under reduced pressure. The residue obtained was purified on a silica gel column using Pet ether/EtOAc (9:1, v/v) as eluent to afford corresponding amines **1**.



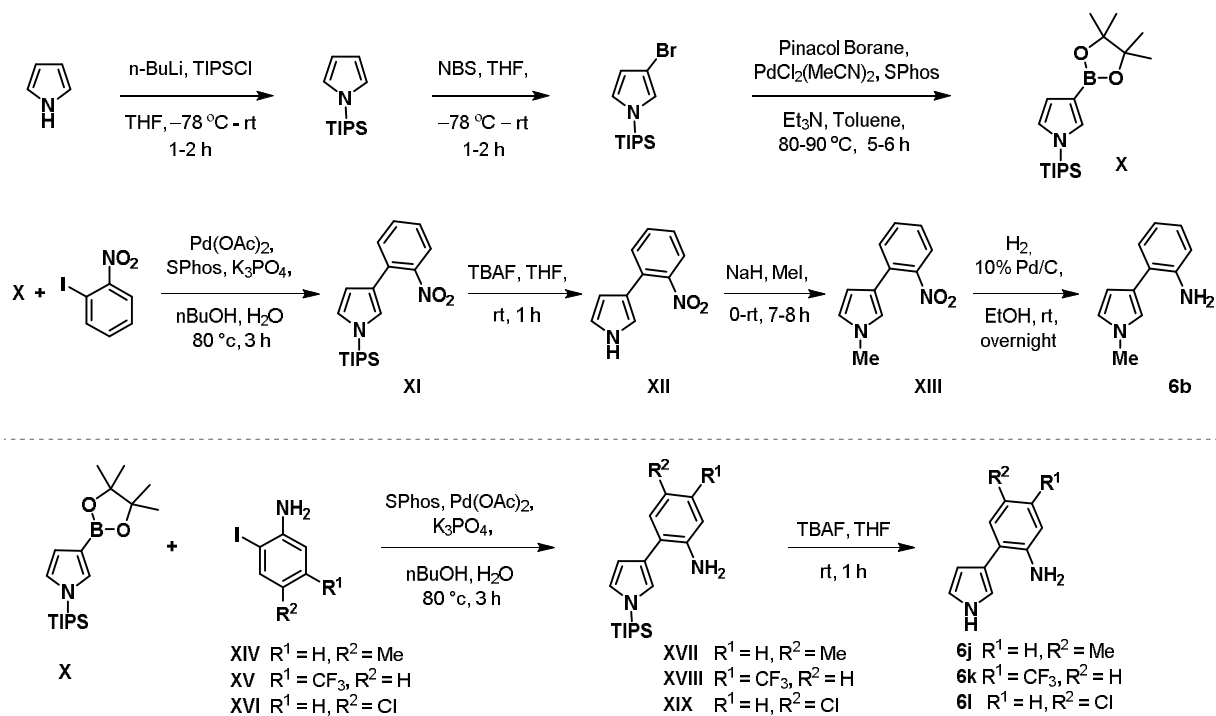
4.3 Preparation of 2-(1H-pyrrol-3-yl)anilines 6:

The pyrrolyl amine compounds **6a**, **6j**, **6k** and **6l** were synthesized by the procedure similar to that reported by Gu and Zakarian.⁵ The nitro compound **XII** was prepared from the procedure similar to that reported by Pratt and coworker.⁶ The compound **6b** was obtained from **XII** in two steps by N-methylation using NaH/MeI in DMF as solvent followed by catalytic hydrogenation with 10 % Pd/C in EtOH.

⁴ Gryko, D. T.; Vakuliuk, O.; Dorota G.; Koszarna B. *J. Org. Chem.* **2009**, *74*, 9517-9520.

⁵ Gu, Z.; Zakarian A. *Org. Lett.* **2010**, *12*, 4224-4227.

⁶ Morrison, M. D.; Hanthorn, J. J.; Pratt, D. A. *Org. Lett.* **2009**, *11*, 1051-1054.



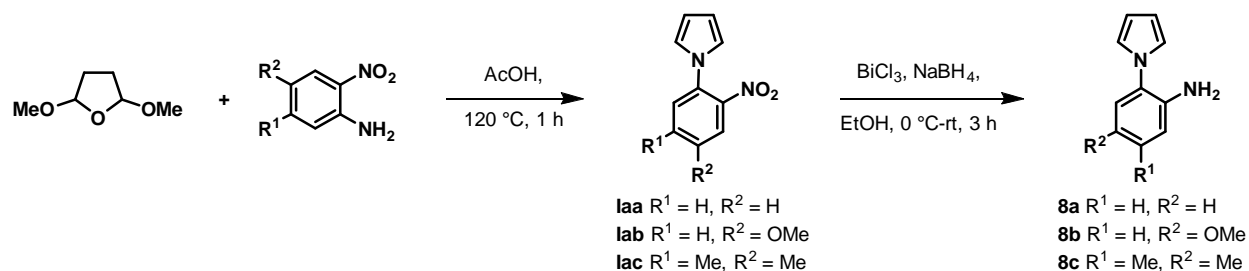
Procedure for the Synthesis of 2-(1-methyl-1H-pyrrol-3-yl)aniline:

The nitro compound **XII** (0.50 g, 2.66 mmol) was added at 0°C to a slurry of hexane-washed 60% sodium hydride (0.08 g, 3.20 mmol) in 5 mL DMF. The reaction mixture was slowly warm to room temperature and stirred for 30 minutes. After 30 min the reaction mixture was cool to 0°C and methyl iodide (0.57 g, 4.00 mmol) was added dropwise, and the reaction mixture was stirred at room temperature for 7-8 hours. After completion of reaction, reaction mixture was poured in water (25 mL) and extracted with EtOAc (2×25 mL). The EtOAc layer was washed with water (2×10 mL) and brine (1×10 mL). The combined organic layer was dried over anhydrous Na₂SO₄, evaporated under reduced pressure and to obtained yellow coloured oil which was subjected to catalytic hydrogenation with 10 % Pd/C in EtOH as a solvent afforded 2-(1-methyl-1H-pyrrol-3-yl)aniline **6b** as yellow oil in 81% over two step.

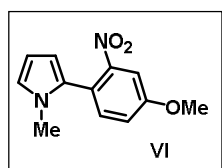
4.4 Preparation of 2-(1H-pyrrol-1-yl)anilines **8**:

The aminoaromatics **8a**, **8b** and **8c** were synthesized by the procedure similar to that reported by Jarry and coworkers.⁷

⁷ Guillon, J.; Grellier, P.; Labaied, M.; Sonnet, P.; Léger, J.-M.; Déprez-Poulain, R.; Forfar-Bares, I.; Dallemagne, P.; Lemaître, N.; Péhourcq, F.; Rochette, J.; Sergheraert, C.; Jarry, C. *J. Med. Chem.* **2004**, *47*, 1997–2009.



3.7 Characterization Data of Starting Materials and Products



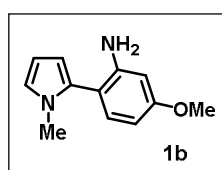
(VI): yellowish thick liquid,

Yield: 52% ; $R_f = 0.3$ (Pet. ether/EtOAc = 95/05)

$^1\text{H NMR}$ (200 MHz, CDCl_3) δ = 7.46 (d, $J = 2.7$ Hz, 1 H), 7.36 (d, $J = 8.6$ Hz, 1 H), 7.15 (dd, $J = 2.7, 8.5$ Hz, 1 H), 6.76 - 6.69 (m, 1 H), 6.21 - 6.13 (m, 1 H), 6.08 (dd, $J = 1.8, 3.6$ Hz, 1 H), 3.91 (s, 3 H), 3.42 (s, 3 H).

$^{13}\text{C NMR}$ (100 MHz, CDCl_3) δ = 159.6, 150.4, 134.4, 128.1, 123.0, 120.1, 118.7, 109.2, 108.9, 107.7, 55.9, 34.2.

HRMS (ESI): calcd for $\text{C}_{12}\text{H}_{13}\text{O}_3\text{N}_2$ ($\text{M}^+ + \text{H}$) 233.0919, found 233.0921.



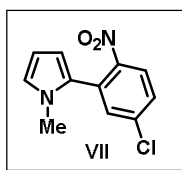
(1b): brownish solid

Yield: 67% ; $R_f = 0.45$ (Pet. ether/EtOAc = 90/10)

$^1\text{H NMR}$ (400 MHz, CDCl_3) δ = 7.04 - 6.99 (m, 1 H), 6.73 - 6.70 (m, 1 H), 6.38 - 6.33 (m, 1 H), 6.32 - 6.29 (m, 1 H), 6.20 (t, $J = 3.7$ Hz, 1 H), 6.13 - 6.10 (m, 1 H), 3.79 (s, 3 H), 3.46 (s, 3 H).

$^{13}\text{C NMR}$ (100 MHz, CDCl_3) δ = 160.6, 147.0, 132.6, 130.2, 122.3, 111.7, 108.7, 107.5, 103.6, 100.4, 55.1, 34.1.

HRMS (ESI): calcd for $C_{12}H_{15}N_2O$ ($M^+ + H$) 203.1179, found 203.1177.



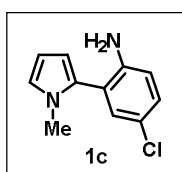
(VII): yellow oil

Yield: 57% $R_f = 0.4$ (Pet. ether/EtOAc = 95/05)

1H NMR (400 MHz, $CDCl_3$) $\delta = 7.97 - 7.82$ (m, 1 H), 7.55 - 7.35 (m, 2 H), 6.76 (d, $J = 2.3$ Hz, 1 H), 6.35 - 6.09 (m, 2 H), 3.44 (s, 3 H).

^{13}C NMR (100 MHz, $CDCl_3$) $\delta = 147.8, 138.6, 133.2, 129.8, 128.6, 127.2, 125.6, 124.2, 110.2, 108.3, 34.3$.

HRMS (ESI): calcd for $C_{11}H_{10}ClN_2O_2$ ($M^+ + H$) 237.0425, found 237.0423.



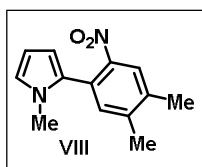
(1c): yellow viscous oil

Yield: 68%; $R_f = 0.4$ (Pet. ether/EtOAc = 90/10)

1H NMR (400 MHz, $CDCl_3$) $\delta = 7.14 - 7.05$ (m, 2 H), 6.76 - 6.71 (m, 1 H), 6.66 (d, $J = 8.2$ Hz, 1 H), 6.23 - 6.19 (m, 1 H), 6.16 (dd, $J = 1.8, 3.7$ Hz, 1 H), 3.77 (br. s., 2 H), 3.48 (s, 3 H).

^{13}C NMR (100 MHz, $CDCl_3$) $\delta = 144.4, 131.1, 129.1, 128.8, 123.0, 122.3, 120.0, 116.0, 109.1, 107.8, 34.2$.

HRMS (ESI): calcd for $C_{11}H_{12}ClN_2$ ($M^+ + H$) 207.0684, found 207.0683.



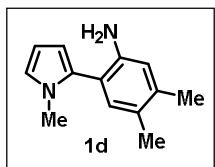
(VIII): yellowish oil

Yield: 62%; $R_f = 0.45$ (Pet. ether/EtOAc = 95/05)

1H NMR (400 MHz, $CDCl_3$) $\delta = 7.79$ (s, 1 H), 7.21 (s, 1 H), 6.72 (t, $J = 2.5$ Hz, 1 H), 6.18 (t, $J = 3.2$ Hz, 1 H), 6.08 (dd, $J = 1.8, 3.7$ Hz, 1 H), 3.40 (s, 3 H), 2.37 (s, 3 H), 2.34 (s, 3 H).

^{13}C NMR (50 MHz, CDCl_3) δ = 147.3, 142.3, 137.8, 134.5, 128.8, 125.5, 125.1, 123.1, 109.0, 107.8, 34.1, 19.7, 19.4.

HRMS (ESI): calcd for $\text{C}_{13}\text{H}_{15}\text{N}_2\text{O}_2$ ($\text{M}^+ + \text{H}$) 231.2570, found 231.2573.



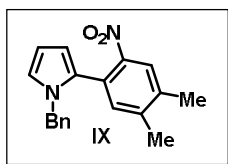
(1d): yellowish oil

Yield: 73%; R_f = 0.4 (Pet. ether/EtOAc = 95/05)

^1H NMR (200 MHz, CDCl_3) δ = 6.94 (s, 1H), 6.78 - 6.73 (m, 1 H), 6.69 (s, 1 H), 6.25 - 6.15 (m, 2 H), 4.08 (br. s., 2 H), 3.53 (s, 3 H), 2.27 (s, 3 H), 2.22 (s, 3 H).

^{13}C NMR (50 MHz, CDCl_3) δ = 142.5, 137.5, 132.5, 130.4, 126.5, 122.4, 117.2, 116.9, 108.7, 107.5, 34.1, 19.6, 18.6.

HRMS (ESI): calcd for $\text{C}_{13}\text{H}_{17}\text{N}_2$ ($\text{M}^+ + \text{H}$) 201.1386, found 201.1387.



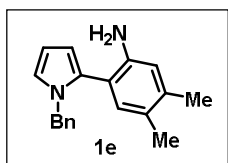
(IX): yellow viscous oil

Yield: 53%; R_f = 0.45 (Pet. ether/EtOAc = 90/10)

^1H NMR (400 MHz, CDCl_3) δ = 7.73 (s, 1 H), 7.27 - 7.17 (m, 3 H), 7.00 (s, 1 H), 6.99 - 6.92 (m, 2 H), 6.78 - 6.69 (m, 1 H), 6.22 (t, J = 3.2 Hz, 1 H), 6.15 - 6.07 (m, 1 H), 4.88 (s, 2 H), 2.33 (s, 3 H), 2.22 (s, 3 H).

^{13}C NMR (100 MHz, CDCl_3) δ = 147.5, 141.9, 138.0, 137.9, 134.8, 128.6, 128.4, 127.4, 127.1, 125.3, 125.0, 122.4, 109.4, 108.2, 51.1, 19.6, 19.4.

HRMS (ESI): calcd for $\text{C}_{19}\text{H}_{19}\text{N}_2\text{O}_2$ ($\text{M}^+ + \text{H}$) 307.3730, found 307.3730.



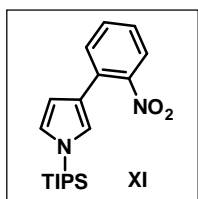
(1e): yellowish solid

Yield: 69%; R_f = 0.40 (Pet. ether/EtOAc = 90/10)

^1H NMR (400 MHz, CDCl_3) δ = 7.35 - 7.25 (m, 3 H), 7.13 - 7.00 (m, 2 H), 6.96 - 6.83 (m, 2 H), 6.83 - 6.72 (m, 1 H), 6.36 - 6.20 (m, 2 H), 5.33 (br. s., 2 H), 5.00 (s, 2 H), 2.28 (s, 3 H), 2.16 (s, 3 H).

^{13}C NMR (100 MHz, CDCl_3) δ = 140.2, 138.7, 137.7, 132.8, 129.8, 128.5, 128.4, 128.1, 127.2, 127.0, 122.0, 118.4, 117.9, 109.3, 108.2, 50.7, 19.6, 18.7.

HRMS (ESI): calcd for $\text{C}_{19}\text{H}_{21}\text{N}_2$ ($\text{M}^+ + \text{H}$) 277.3910, found 277.3911.



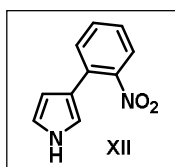
(XI): yellowish oil

Yield: 63%; R_f = 0.75 (Pet. ether/EtOAc = 90/10).

^1H NMR (200 MHz, CDCl_3) δ = 7.67 - 7.46 (m, 3 H), 7.38 - 7.24 (m, 1 H), 7.02 - 6.88 (m, 1 H), 6.87 - 6.77 (m, 1 H), 6.50 - 6.31 (m, 1 H), 1.59 - 1.40 (m, 3 H), 1.22 - 1.06 (m, 18 H).

^{13}C NMR (50 MHz, CDCl_3) δ = 131.3, 130.8, 126.0, 125.0, 123.2, 122.9, 120.8, 110.4, 110.0, 77.6, 76.4, 17.7, 11.6.

HRMS (ESI): calcd for $\text{C}_{19}\text{H}_{29}\text{N}_2\text{O}_2\text{Si}$ ($\text{M}^+ + \text{H}$) 345.5380, found 345.5355.



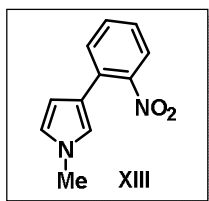
(XII): yellowish oil

Yield: 78%; R_f = 0.25 (Pet. ether/EtOAc = 80/20)

^1H NMR (400 MHz, CDCl_3) δ = 8.53 (br. s., 1 H), 7.60 (d, J = 7.8 Hz, 1 H), 7.55 - 7.42 (m, 2 H), 7.36 - 7.27 (m, 1 H), 7.00 - 6.90 (m, 1 H), 6.88 - 6.73 (m, 1 H), 6.37 - 6.26 (m, 1 H).

^{13}C NMR (100 MHz, CDCl_3) δ = 149.1, 131.5, 130.9, 129.7, 126.3, 123.2, 119.0, 118.9, 116.7, 108.2.

HRMS (ESI): calcd for $\text{C}_{10}\text{H}_9\text{N}_2\text{O}_2$ ($\text{M}^+ + \text{H}$) 189.1940, found 189.1943.



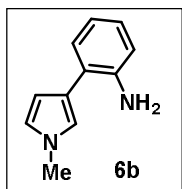
(XIII): yellowish oil

Yield: 92%; $R_f = 0.65$ (Pet. ether/EtOAc = 80/20)

$^1\text{H NMR}$ (500 MHz, CDCl_3) $\delta = 7.62 - 7.52$ (m, 1 H), $7.51 - 7.41$ (m, 2 H), $7.33 - 7.21$ (m, 1 H), 6.78 (t, $J = 2.0$ Hz, 1 H), 6.62 (t, $J = 2.6$ Hz, 1 H), $6.28 - 6.18$ (m, 1 H), 3.66 (s, 3 H).

$^{13}\text{C NMR}$ (125 MHz, CDCl_3) $\delta = 149.0, 131.4, 130.6, 129.7, 126.0, 123.2, 122.7, 120.5, 118.8, 108.2, 36.3$.

HRMS (ESI): calcd for $\text{C}_{11}\text{H}_{11}\text{N}_2\text{O}_2$ ($\text{M}^+ + \text{H}$) 203.0815, found 203.0814.



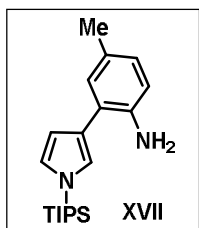
(6b): yellowish oil

Yield: 88%; $R_f = 0.55$ (Pet. ether/EtOAc = 80/20)

$^1\text{H NMR}$ (500 MHz, CDCl_3) $\delta = 7.23 - 7.17$ (m, 1 H), 7.03 (dt, $J = 1.7, 7.6$ Hz, 1 H), $6.81 - 6.69$ (m, 3 H), 6.65 (t, $J = 2.4$ Hz, 1 H), $6.35 - 6.29$ (m, 1 H), 3.93 (br. s., 2 H), 3.66 (s, 3 H).

$^{13}\text{C NMR}$ (125 MHz, CDCl_3) $\delta = 143.6, 129.6, 126.9, 122.4, 122.2, 122.0, 120.0, 118.5, 115.4, 108.4, 36.0$.

HRMS (ESI): calcd for $\text{C}_{11}\text{H}_{13}\text{N}_2\text{O}_2$ ($\text{M}^+ + \text{H}$) 173.1073, found 173.1071.



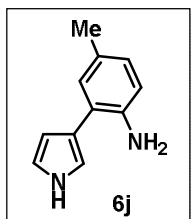
(XVII): yellowish oil

Yield: 58%; $R_f = 0.75$ (Pet. ether/EtOAc = 75/25)

¹H NMR (200 MHz, CDCl₃) δ = 7.20 - 7.04 (m, 2 H), 7.04 - 6.90 (m, 2 H), 6.84 (t, J = 2.3 Hz, 1 H), 6.56 (dd, J = 1.4, 2.4 Hz, 1 H), 6.09 - 5.52 (br. s., 2 H), 2.32 (s, 3 H), 1.58 - 1.38 (m, 3 H), 1.17 - 1.06 (m, 18 H).

¹³C NMR (50 MHz, CDCl₃) δ = 135.5, 131.4, 130.4, 127.6, 125.6, 125.1, 122.8, 122.7, 118.4, 110.9, 20.7, 17.8, 11.7.

HRMS (ESI): calcd for C₂₀H₃₃N₂Si (M⁺ + H) 329.2408, found 329.2402.



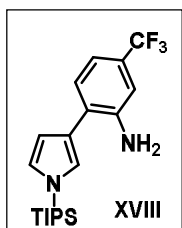
(6j): yellowish solid

Yield: 64%; mp = 74-76°C; R_f = 0.25 (Pet. ether/EtOAc = 75/25)

¹H NMR (400 MHz, CDCl₃) δ = 8.36 (br. s., 1 H), 7.13 - 7.03 (m, 1 H), 6.98 - 6.92 (m, 1 H), 6.91 - 6.86 (m, 1 H), 6.86 - 6.79 (m, 1 H), 6.71 - 6.64 (m, 1 H), 6.46 - 6.36 (m, 1 H), 3.77 (br. s., 2 H), 2.26 (s, 3 H).

¹³C NMR (50 MHz, CDCl₃) δ = 141.1, 130.4, 127.6, 122.3, 121.9, 118.3, 116.1, 115.7, 108.6, 102.8, 20.4.

HRMS (ESI): calcd for C₁₁H₁₃N₂ (M⁺ + H) 173.1073, found 173.1070.



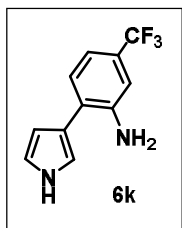
(XVIII): yellowish oil

Yield: 67%; R_f = 0.6 (Pet. ether/EtOAc = 80/20)

¹H NMR (400 MHz, CDCl₃) δ = 7.61 - 7.52 (m, 1 H), 7.51 - 7.30 (m, 2H), 7.04 - 6.97 (m, 1 H), 6.82 (dd, J = 3.0, 7.6 Hz, 1 H), 6.65 - 6.55 (m, 1 H), 1.53 - 1.39 (m, 3 H), 1.13 - 1.06 (m, 18 H).

¹³C NMR (100 MHz, CDCl₃) δ = 145.4, 126.8, 125.3, 124.0, 123.0, 122.6, 122.5, 122.4, 115.2, 110.5, 17.8, 11.6.

HRMS (ESI): calcd for C₂₀H₃₀N₂F₃Si (M⁺ + H) 383.2125, found 383.2116.



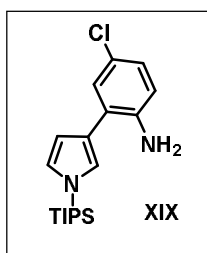
(**6k**): yellowish solid

Yield: 67%; mp = 85-87°C; R_f = 0.3 (Pet. ether/EtOAc = 70/30)

$^1\text{H NMR}$ (400 MHz, CDCl_3) δ = 8.41 (br. s., 1 H), 7.52 - 7.43 (m, 1 H), 7.37 - 7.28 (m, 1 H), 7.09 - 6.95 (m, 1 H), 6.92 (d, J = 2.3 Hz, 1 H), 6.77 (d, J = 8.2 Hz, 1 H), 6.52 - 6.36 (m, 1 H), 4.30 (br. s., 2 H).

$^{13}\text{C NMR}$ (100 MHz, CDCl_3) δ = 146.8, 127.0, 126.9, 124.3, 124.2, 121.8, 120.7, 118.8, 116.4, 114.6, 108.5.

HRMS (ESI): calcd for $\text{C}_{11}\text{H}_{10}\text{N}_2\text{F}_3$ ($\text{M}^+ + \text{H}$) 227.0791, found 227.0787.



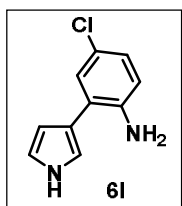
(**XIX**): yellowish oil

Yield: 67%; R_f = 0.6 (Pet. ether/EtOAc = 90/10)

$^1\text{H NMR}$ (200 MHz, CDCl_3) δ = 7.34 (d, J = 2.5 Hz, 1 H), 7.14 - 7.03 (m, 2 H), 6.99 - 6.92 (m, 1 H), 6.76 (d, J = 8.5 Hz, 1 H), 6.61 (dd, J = 1.5, 2.8 Hz, 1 H), 4.07 (s, 2 H), 1.70 - 1.46 (m, 3 H), 1.24 (d, J = 7.2 Hz, 18 H).

$^{13}\text{C NMR}$ (50 MHz, CDCl_3) δ = 142.1, 129.0, 126.3, 124.9, 124.1, 122.9, 122.4, 116.5, 110.4, 17.7, 11.6.

HRMS (ESI): calcd for $\text{C}_{19}\text{H}_{30}\text{N}_2\text{ClSi}$ ($\text{M}^+ + \text{H}$) 349.9980, found 349.9981.



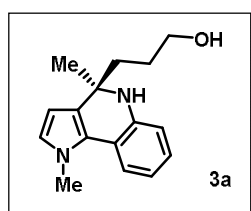
(6l): yellowish thick liquid

Yield: 73%; $R_f = 0.2$ (Pet. ether/EtOAc = 70/30)

$^1\text{H NMR}$ (200 MHz, CDCl_3) $\delta = 8.40$ (br. s., 1 H), 7.23 (d, $J = 2.5$ Hz, 1 H), 7.11 - 6.95 (m, 2 H), 6.93 - 6.82 (m, 1H), 6.68 (d, $J = 8.5$ Hz, 1 H), 6.44 (dt, $J = 1.5, 2.7$ Hz, 1 H), 3.82 (br. s., 2 H).

$^{13}\text{C NMR}$ (100 MHz, CDCl_3) $\delta = 142.3, 129.2, 126.7, 123.7, 123.0, 120.8, 118.7, 116.5, 116.3, 108.4$.

HRMS (ESI): calcd for $\text{C}_{10}\text{H}_{10}\text{N}_2\text{Cl}$ ($\text{M}^+ + \text{H}$) 193.0527, found 193.0524.



(3a): white solid

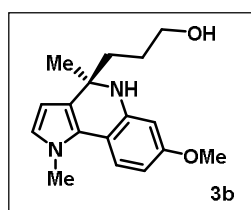
Yield: 81%; mp = 142-144°C; $R_f = 0.3$ (Pet. ether/EtOAc = 60/40)

98.8% ee, $[\alpha]_D^{25} = +2.02$ ($c = 0.95, \text{CHCl}_3$); **HPLC conditions:** Chiralcel OJ-H, 80:20 *n*-Hexane/IPA, Flow rate 1.0 mL/min; $\lambda = 254$ nm; tR = 18.15 min (minor), tR = 14.42 min (major).

$^1\text{H NMR}$ (500 MHz, CDCl_3) $\delta = 7.44 - 7.36$ (m, 1 H), 6.96 - 6.86 (m, 1 H), 6.74 - 6.62 (m, 1 H), 6.62 - 6.56 (m, 1H), 6.54 (d, $J = 2.7$ Hz, 1 H), 5.92 (d, $J = 2.7$ Hz, 1 H), 3.89 (s, 3 H), 3.57 (t, $J = 6.3$ Hz, 2 H), 1.83 - 1.76 (m, 1 H), 1.70 - 1.66 (m, 1 H), 1.61 - 1.53 (m, 2 H), 1.47 (s, 3 H).

$^{13}\text{C NMR}$ (100 MHz, CDCl_3) $\delta = 142.6, 126.1, 124.8, 124.6, 120.1, 117.5, 116.6, 114.1, 102.7, 63.3, 55.5, 40.1, 37.2, 29.9, 28.0$.

HRMS (ESI): calcd for $\text{C}_{16}\text{H}_{21}\text{N}_2\text{O}$ ($\text{M}^+ + \text{H}$) 257.1648, found 257.1643.



(3b): brownish thick liquid

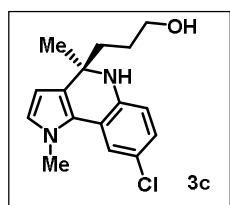
Yield: 77%; $R_f = 0.3$ (Pet. ether/EtOAc = 60/40)

98.7% ee, $[\alpha]_D^{27.2} = +0.39$ ($c = 1.0$, CHCl_3); **HPLC conditions:** Chiralcel OJ-H, 80:20 *n*-Hexane/IPA, Flow rate 1.0 mL/min; $\lambda = 254$ nm; $t_R = 30.77$ min (minor), $t_R = 27.71$ min (major).

^1H NMR (400 MHz, CDCl_3) $\delta = 7.31$ (d, $J = 8.2$ Hz, 1 H), 6.50 (d, $J = 3.2$ Hz, 1 H), 6.25 (dd, $J = 2.7, 8.7$ Hz, 1 H), 6.17 (d, $J = 2.7$ Hz, 1 H), 5.90 (d, $J = 3.2$ Hz, 1 H), 3.85 (s, 3 H), 3.76 (s, 3 H), 3.55 (t, $J = 6.2$ Hz, 2 H), 1.81 - 1.74 (m, 1 H), 1.72 - 1.62 (m, 2 H), 1.59-1.49 (m, 1 H), 1.47 (s, 3 H).

^{13}C NMR (100 MHz, CDCl_3) $\delta = 158.3, 144.2, 124.7, 123.8, 122.9, 121.0, 110.4, 102.6, 99.9, 63.3, 55.6, 55.1, 40.2, 37.1, 29.9, 28.0$.

HRMS (ESI): calcd for $\text{C}_{17}\text{H}_{23}\text{N}_2\text{O}$ ($\text{M}^+ + \text{H}$) 287.1754, found 287.1747.



(3c): yellowish thick liquid

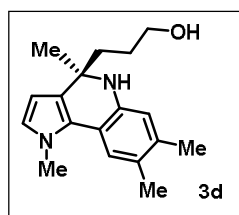
Yield: 73%; $R_f = 0.30$ (Pet. ether/EtOAc = 60/40)

95.0% ee, $[\alpha]_D^{26} = +2.40$ ($c = 0.55$, CHCl_3); **HPLC conditions:** Chiralcel OJ-H, 80:20 *n*-Hexane/IPA, Flow rate 1.0 mL/min; $\lambda = 254$ nm; $t_R = 23.87$ min (minor), $t_R = 16.40$ min (major).

^1H NMR (500 MHz, CDCl_3) $\delta = 7.32$ (d, $J = 2.4$ Hz, 1 H), 6.85 (dd, $J = 2.3, 8.4$ Hz, 1 H), 6.57 (d, $J = 2.7$ Hz, 1 H), 6.48 (d, $J = 8.2$ Hz, 1 H), 5.91 (d, $J = 2.7$ Hz, 1 H), 3.87 (s, 3 H), 3.56 (t, $J = 6.3$ Hz, 2H), 1.78 (dd, $J = 2.1, 4.9$ Hz, 1 H), 1.69 - 1.63 (m, 2 H), 1.58 - 1.54 (m, 2 H), 1.47 (s, 3 H).

^{13}C NMR (100 MHz, CDCl_3) $\delta = 141.1, 128.0, 125.5, 123.6, 122.0, 119.8, 117.8, 114.9, 102.9, 63.2, 55.6, 40.2, 37.2, 28.0$.

HRMS (ESI): calcd for $\text{C}_{16}\text{H}_{20}\text{ClN}_2\text{O}$ ($\text{M}^+ + \text{H}$) 291.1259, found 291.1254.



(3d): white solid

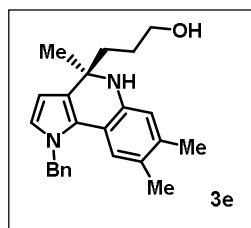
Yield: 83%; mp = 137-139°C; R_f = 0.37 (Pet. ether/EtOAc = 60/40)

99.0% ee, $[\alpha]_D^{26} = +2.39$ (c = 1.0, CHCl₃); **HPLC conditions:** Chiralcel OJ-H, 80:20 *n*-Hexane/IPA, Flow rate 1.0 mL/min; $\lambda = 254$ nm; tR = 22.57 min (minor), tR = 13.32 min (major).

¹H NMR (500 MHz, CDCl₃) δ = 7.17 (s, 1 H), 6.56 - 6.49 (m, 1 H), 6.43 (s, 1 H), 5.97 - 5.82 (m, 1 H), 3.89 (s, 3 H), 3.57 (t, $J = 6.1$ Hz, 2 H), 2.20-2.18 (s, 3 H), 2.17-2.15 (s, 3 H), 1.82 - 1.75 (m, 1 H), 1.71 - 1.59 (m, 3 H), 1.46 (s, 3 H).

¹³C NMR (100 MHz, CDCl₃) δ = 140.5, 134.2, 125.3, 124.8, 124.3, 124.1, 121.5, 115.9, 114.6, 102.7, 63.4, 55.3, 39.8, 37.1, 29.5, 28.2, 19.6, 19.0.

HRMS (ESI): calcd for C₁₈H₂₅N₂O (M⁺ + H) 285.1961, found 285.1956.



(3e): white solid

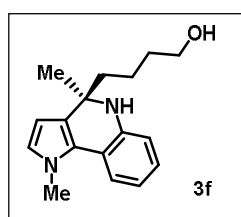
Yield: 67%; mp = 169-171°C; R_f = 0.45 (Pet. ether/EtOAc = 70/30)

55.3% ee, $[\alpha]_D^{26} = -0.68$ (c = 0.35, CHCl₃); **HPLC conditions:** Chiralcel OD-H, 90:10 *n*-Hexane/IPA, Flow rate 1.0 mL/min; $\lambda = 254$ nm; tR = 20.67 min (minor), tR = 26.40 min (major).

¹H NMR (400 MHz, CDCl₃) δ = 7.39 - 7.30 (m, 2 H), 7.29 - 7.25 (m, 1 H), 7.12 (d, $J = 7.3$ Hz, 2 H), 6.83 (s, 1 H), 6.69 - 6.50 (m, 1 H), 6.38 (s, 1 H), 6.01 (d, $J = 2.9$ Hz, 1 H), 5.37 (s, 2 H), 3.57 (t, $J = 6.1$ Hz, 2 H), 2.09 (s, 3 H), 2.01 (s, 3 H), 1.84 - 1.77 (m, 1 H), 1.74 - 1.59 (m, 3 H), 1.48 (s, 3 H).

¹³C NMR (100 MHz, CDCl₃) δ = 140.6, 138.4, 134.2, 128.9, 127.3, 126.2, 125.3, 124.7, 124.0, 121.8, 115.7, 114.0, 103.5, 63.4, 55.3, 52.4, 39.8, 29.5, 28.1, 19.5, 19.1.

HRMS (ESI): calcd for C₂₄H₂₉N₂O (M⁺ + H) 361.2274, found 361.2268.



(3f): thick liquid

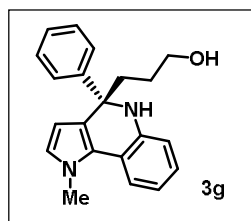
Yield: 67%; $R_f = 0.25$ (Pet. ether/EtOAc = 70/30)

30% ee; **HPLC conditions**: Chiralcel OJ-H, 80:20 *n*-Hexane/IPA, Flow rate 1.0 mL/min; $\lambda = 254$ nm; tR = 19.80 min (minor), tR = 15.32 min (major).

^1H NMR (400 MHz, CDCl_3) $\delta = 7.39$ (dd, $J = 1.6, 7.7$ Hz, 1 H), 6.96 - 6.87 (m, 1 H), 6.72 - 6.63 (m, 1 H), 6.60 - 6.50 (m, 2 H), 5.90 (d, $J = 2.9$ Hz, 1 H), 3.86 (s, 3 H), 3.59 - 3.50 (m, 2 H), 1.76 - 1.67 (m, 1 H), 1.67 - 1.56 (m, 1 H), 1.54 - 1.45 (m, 3 H), 1.45 - 1.42 (s, 3 H), 1.39 - 1.24 (m, 1 H).

^{13}C NMR (100 MHz, CDCl_3) $\delta = 142.7, 126.0, 125.2, 124.6, 124.5, 120.1, 117.3, 116.6, 114.1, 102.7, 62.8, 55.5, 43.3, 37.1, 33.0, 29.4, 20.7$.

HRMS (ESI): calcd for $\text{C}_{17}\text{H}_{23}\text{N}_2\text{O}$ ($\text{M}^+ + \text{H}$) 271.1805, found 271.1799.



(3g): white solid

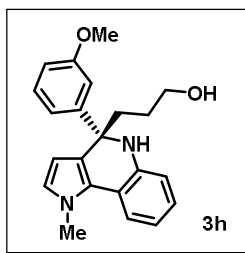
Yield: 79%; mp = 125-127°C; $R_f = 0.4$ (Pet. ether/EtOAc = 60/40)

94.5% ee, $[\alpha]_D^{27} = -77.31$ ($c = 2.0, \text{CHCl}_3$); **HPLC conditions**: Chiralcel OD-H, 70:30 *n*-Hexane/IPA, Flow rate 1.0 mL/min; $\lambda = 254$ nm; tR = 22.34 min (minor), tR = 14.64 min (major).

^1H NMR (400 MHz, CDCl_3) $\delta = 7.48 - 7.33$ (m, 3 H), 7.28 - 7.22 (m, 2 H), 7.18 - 7.06 (m, 1 H), 7.00 - 6.89 (m, 1 H), 6.77 - 6.62 (m, 2 H), 6.59 - 6.49 (m, 1 H), 6.02 - 5.90 (m, 1 H), 3.84 (s, 3 H), 3.66 - 3.59 (t, $J = 6.3$ Hz, 2 H), 2.36 - 2.28 (dd, $J = 6.0, 14.1$ Hz, 1 H), 2.1-2.16 (dd, $J = 13.9, 15.9$ Hz, 1 H), 1.81 - 1.62 (m, 2 H).

^{13}C NMR (100 MHz, CDCl_3) $\delta = 148.4, 142.3, 128.1, 126.3, 125.5, 124.9, 123.6, 120.3, 117.7, 116.6, 114.2, 103.9, 63.1, 61.1, 38.8, 37.3, 28.1$.

HRMS (ESI): calcd for $\text{C}_{21}\text{H}_{23}\text{N}_2\text{O}$ ($\text{M}^+ + \text{H}$) 319.1805, found 319.1799.



(3h): thick liquid

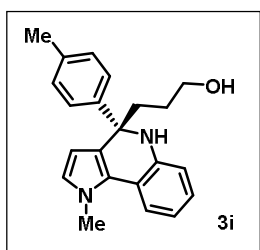
Yield: 63%; $R_f = 0.27$ (Pet. ether/EtOAc = 60/40)

93.7% ee, $[\alpha]_D^{25} = -2.06$ ($c = 1.7$, CHCl_3); **HPLC conditions:** Kromacil-5 Amycoat, 90:10 *n*-Hexane/IPA, Flow rate 1.0 mL/min; $\lambda = 254$ nm; $t_R = 47.57$ min (minor), $t_R = 39.32$ min (major).

^1H NMR (400 MHz, CDCl_3) $\delta = 7.38$ (dd, $J = 0.9, 8.2$ Hz, 1 H), 7.20 - 7.13 (m, 1 H), 7.04 - 6.92 (m, 3 H), 6.74 - 6.65 (m, 3 H), 6.54 (d, $J = 2.7$ Hz, 1 H), 5.99 (d, $J = 2.7$ Hz, 1 H), 3.84 (s, 3 H), 3.71 (s, 3 H), 3.62 (t, $J = 6.4$ Hz, 2 H), 2.35 - 2.26 (m, 1 H), 2.14 - 2.06 (m, 1 H), 1.79 - 1.63 (m, 2 H).

^{13}C NMR (100 MHz, CDCl_3) $\delta = 159.3, 150.2, 142.2, 129.0, 126.2, 124.9, 124.9, 123.4, 120.3, 117.9, 117.8, 116.6, 114.3, 112.1, 111.0, 103.8, 63.1, 61.1, 55.0, 38.8, 37.2, 28.1$.

HRMS (ESI): calcd for $\text{C}_{22}\text{H}_{25}\text{N}_2\text{O}_2$ ($\text{M}^+ + \text{H}$) 349.1902, found 349.1911.



(3i): white solid

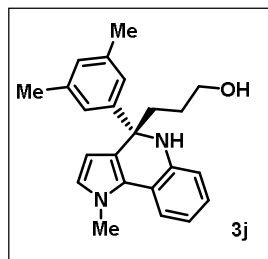
Yield: 73%; mp = 151-153°C; $R_f = 0.37$ (Pet. ether/EtOAc = 60/40)

95% ee, $[\alpha]_D^{27} = -7.92$ ($c = 1.0$, CHCl_3); **HPLC conditions:** Chiralcel OJ-H, 70:30 *n*-Hexane/IPA, Flow rate 1.0 mL/min; $\lambda = 254$ nm; $t_R = 16.27$ min (minor), $t_R = 23.38$ min (major).

^1H NMR (400 MHz, CDCl_3) $\delta = 7.45 - 7.38$ (m, 1 H), 7.38 - 7.31 (m, 2 H), 7.08 (d, $J = 8.3$ Hz, 2 H), 7.02 - 6.93 (m, 1 H), 6.76 - 6.62 (m, 2 H), 6.57 (d, $J = 2.7$ Hz, 1 H), 5.98 (d, $J = 2.9$ Hz, 1 H), 3.87 (s, 3 H), 3.65 (t, $J = 6.4$ Hz, 2 H), 2.34 (td, $J = 5.5, 8.6$ Hz, 1 H), 2.29 (s, 3 H), 2.16 - 2.08 (m, 1 H), 1.83 - 1.67 (m, 2 H).

^{13}C NMR (100 MHz, CDCl_3) δ = 145.4, 142.3, 135.5, 128.6, 126.0, 125.2, 124.7, 123.6, 120.1, 117.3, 116.3, 113.9, 103.6, 63.0, 60.7, 38.6, 37.0, 28.0, 20.6.

HRMS (ESI): calcd for $\text{C}_{22}\text{H}_{25}\text{N}_2\text{O}$ ($\text{M}^+ + \text{H}$) 333.1961, found 333.1954.



(3j): thick liquid

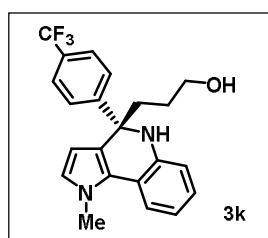
Yield: 82%; R_f = 0.42 (Pet. ether/EtOAc = 60/40)

92.2% ee, $[\alpha]_D^{25} = -1.51$ ($c = 1.2$, CHCl_3); **HPLC conditions:** Chiralcel OJ-H, 70:30 *n*-Hexane/IPA, Flow rate 1.0 mL/min; $\lambda = 254$ nm; $t_R = 15.66$ min (minor), $t_R = 10.92$ min (major).

^1H NMR (500 MHz, CDCl_3) δ = 7.43 (d, $J = 7.6$ Hz, 1 H), 7.07 (s, 2 H), 6.97 (t, $J = 7.6$ Hz, 1 H), 6.80 (s, 1 H), 6.73 - 6.65 (m, 2 H), 6.59 - 6.48 (m, 1 H), 5.99 - 5.89 (m, 1 H), 3.89 (s, 3 H), 3.65 (t, $J = 6.6$ Hz, 2 H), 2.35 - 2.30 (m, 1 H), 2.27 (s, 6 H), 2.11 - 2.04 (m, 1 H), 1.81 - 1.73 (m, 1 H), 1.70 - 1.64 (m, 1 H).

^{13}C NMR (100 MHz, CDCl_3) δ = 146.8, 140.2, 137.4, 128.3, 126.2, 125.1, 124.7, 123.7, 123.2, 120.4, 119.3, 117.7, 115.7, 104.4, 63.0, 62.0, 38.9, 37.2, 28.0, 21.5.

HRMS (ESI): calcd for $\text{C}_{23}\text{H}_{27}\text{N}_2\text{O}$ ($\text{M}^+ + \text{H}$) 347.2118, found 347.2113.



(3k): thick liquid

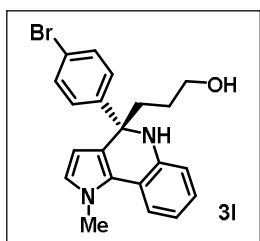
Yield: 60%; R_f = 0.35 (Pet. ether/EtOAc = 60/40)

94.6% ee, $[\alpha]_D^{27} = -7.52$ ($c = 0.53$, CHCl_3); **HPLC conditions:** Chiralcel OJ-H, 70:30 *n*-Hexane/IPA, Flow rate 1.0 mL/min; $\lambda = 254$ nm; $t_R = 9.80$ min (minor), $t_R = 16.03$ min (major).

^1H NMR (500 MHz, CDCl_3) δ = 7.55 - 7.52 (m, 2 H), 7.48-7.45 (m, 2 H), 7.41-7.37 (m, 1 H), 6.99-6.94 (td, J = 7.9 Hz, 1 H), 6.81-6.77 (d, J = 7.6 Hz, 1 H), 6.74 - 6.69 (m, 1 H), 6.60-6.57 (d, J = 2.4 Hz, 1 H), 6.02-5.99 (d, J = 2.7 Hz, 1 H), 3.86 (s, 3 H), 3.65 (t, J = 6.3 Hz, 2 H), 2.38 - 2.31 (m, 1 H), 2.15 (ddd, J = 5.2, 10.6, 14.1 Hz, 1 H), 1.79 - 1.68 (m, 2 H).

^{13}C NMR (125 MHz, CDCl_3) δ = 152.1, 141.4, 128.6, 128.3, 126.8, 126.4, 126.0, 125.3, 125.1, 125.1, 123.1, 122.6, 120.5, 118.5, 116.8, 114.7, 103.8, 62.9, 61.3, 38.6, 37.3, 27.9, 21.5.

HRMS (ESI): calcd for $\text{C}_{22}\text{H}_{22}\text{F}_3\text{N}_2\text{O}$ (M^+ + H) 387.1679, found 387.1673.



(31): thick liquid

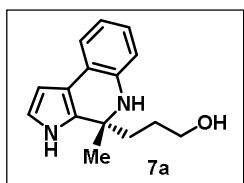
Yield: 77%; R_f = 0.40 (Pet. ether/EtOAc = 60/40)

95.3% ee, $[\alpha]_{\text{D}}^{25}$ = -0.64 (c = 1.2, CHCl_3); **HPLC conditions:** Chiralcel OJ-H, 80:20 *n*-Hexane/IPA, Flow rate 1.0 mL/min; λ = 254 nm; tR = 22.80 min (minor), tR = 40.46 min (major).

^1H NMR (400 MHz, CDCl_3) δ = 7.57 - 7.44-7.21 (m, 5 H), 7.01 - 6.92 (m, 1 H), 6.74 - 6.67 (m, 2 H), 6.57 (d, J = 2.7 Hz, 1 H), 5.99 (d, J = 3.2 Hz, 1 H), 3.85 (s, 3 H), 3.67 - 3.61 (m, 2 H), 2.39 - 2.27 (m, 1 H), 2.16 - 2.06 (m, 1 H), 1.81 - 1.64 (m, 2 H).

^{13}C NMR (100 MHz, CDCl_3) δ = 147.6, 142.1, 131.1, 127.5, 126.4, 125.1, 123.1, 120.4, 120.2, 117.9, 116.5, 114.2, 103.7, 63.1, 60.9, 38.6, 37.3, 28.1.

HRMS (ESI): calcd for $\text{C}_{21}\text{H}_{22}\text{N}_2\text{OBr}$ (M^+ + H) 397.0910, found 397.0905.



(7a): brownish thick liquid

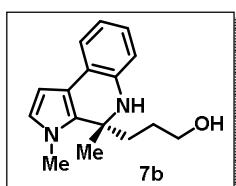
Yield: 79%; R_f = 0.3 (Pet. ether/EtOAc = 60/40)

86.9% ee, $[\alpha]_D^{27} = -0.42$ ($c = 1.9$, CHCl_3); **HPLC conditions:** Chiralcel OD-H, 80:20 *n*-Hexane/IPA, Flow rate 1.0 mL/min; $\lambda = 254$ nm; $t_R = 12.46$ min (minor), $t_R = 14.75$ min (major).

^1H NMR (500 MHz, CDCl_3) $\delta = 8.10$ (br. s., 1 H), 7.29 - 7.25 (m, 1 H), 6.93 - 6.84 (m, 1 H), 6.75 - 6.63 (m, 2 H), 6.51 (d, $J = 7.9$ Hz, 1 H), 6.42 - 6.35 (m, 1 H), 3.52 (t, $J = 5.0$ Hz, 2 H), 1.94 - 1.83 (m, 1 H), 1.73 - 1.62 (m, 2 H), 1.51 (s, 3 H), 1.45 - 1.37 (m, 1 H).

^{13}C NMR (125 MHz, CDCl_3) $\delta = 140.9$, 129.6, 125.6, 121.8, 119.0, 118.1, 117.8, 115.7, 112.9, 102.6, 62.8, 55.5, 40.0, 29.8, 27.7.

HRMS (ESI): calcd for $\text{C}_{15}\text{H}_{19}\text{N}_2\text{O}$ ($\text{M}^+ + \text{H}$) 243.1492, found 243.1490.



(7b): white solid

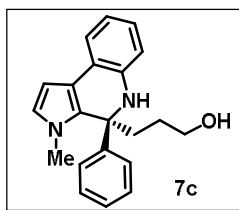
Yield: 82%; mp = 121-123°C; $R_f = 0.45$ (Pet. ether/EtOAc = 60/40)

87.1% ee, $[\alpha]_D^{25} = -0.64$ ($c = 0.5$, CHCl_3); **HPLC conditions:** Chiralcel OD-H, 80:20 *n*-Hexane/IPA, Flow rate 1.0 mL/min; $\lambda = 254$ nm; $t_R = 13.93$ min (minor), $t_R = 16.85$ min (major).

^1H NMR (400 MHz, CDCl_3) $\delta = 7.29$ - 7.24 (m, 1 H), 6.93 - 6.81 (m, 1H), 6.64 (t, $J = 7.5$ Hz, 1 H), 6.53 - 6.43 (m, 2 H), 6.37 - 6.29 (m, 1 H), 3.63 (s, 3 H), 3.58 - 3.51 (m, 2 H), 2.10 (ddd, $J = 4.9, 11.3, 13.9$ Hz, 1 H), 1.78 - 1.68 (m, 1 H), 1.65 - 1.58 (m, 1 H), 1.58 - 1.55 (m, 3 H), 1.43 - 1.33 (m, 1 H).

^{13}C NMR (100 MHz, CDCl_3) $\delta = 40.4$, 128.9, 125.5, 124.2, 121.3, 118.6, 117.5, 117.3, 112.1, 101.1, 62.8, 56.7, 40.4, 35.9, 30.6, 28.0.

HRMS (ESI): calcd for $\text{C}_{16}\text{H}_{21}\text{N}_2\text{O}$ ($\text{M}^+ + \text{H}$) 257.1648, found 257.1646.



(7c): yellowish thick liquid

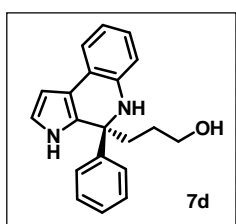
Yield: 73%; $R_f = 0.5$ (Pet. ether/EtOAc = 60/40)

91.5% ee, $[\alpha]_D^{25} = +0.39$ ($c = 3.1$, CHCl_3); **HPLC conditions:** Chiralcel OD-H, 80:20 *n*-Hexane/IPA, Flow rate 1.0 mL/min; $\lambda = 254$ nm; $t_R = 17.60$ min (minor), $t_R = 10.83$ min (major).

^1H NMR (500 MHz, CDCl_3) $\delta = 7.43 - 7.38$ (m, 1 H), 7.34 - 7.28 (m, 2 H), 7.24 - 7.19 (m, 1 H), 6.89 - 6.82 (m, 1 H), 6.68 - 6.61 (m, 1H), 6.50 (d, $J = 3.2$ Hz, 1 H), 6.41 (d, $J = 3.2$ Hz, 1 H), 6.37 (d, $J = 7.8$ Hz, 1 H), 3.67 - 3.61 (m, 2 H), 3.08 - 3.04 (s, 3 H), 2.57 - 2.48 (m, 1 H), 2.31 - 2.21 (m, 1 H), 1.92 - 1.81 (m, 1 H), 1.45 - 1.33 (m, 1 H).

^{13}C NMR (125 MHz, CDCl_3) $\delta = 147.2, 139.9, 128.5, 127.9, 127.2, 126.6, 125.6, 124.1, 121.4, 118.4, 117.5, 117.0, 111.5, 100.9, 62.8, 61.4, 37.4, 35.0, 28.0$.

HRMS (ESI): calcd for $\text{C}_{21}\text{H}_{23}\text{N}_2\text{O}$ ($\text{M}^+ + \text{H}$) 319.1805, found 319.1802.



(7d): yellowish thick liquid

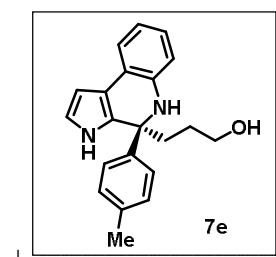
Yield: 84%; $R_f = 0.32$ (Pet. ether/EtOAc = 60/40)

96.4% ee, $[\alpha]_D^{23} = -5.49$ ($c = 1.0$, CHCl_3); **HPLC conditions:** Chiralcel OD-H, 80:20 *n*-Hexane/IPA, Flow rate 1.0 mL/min; $\lambda = 254$ nm; $t_R = 24.75$ min (minor), $t_R = 14.78$ min (major).

^1H NMR (400 MHz, CDCl_3) $\delta = 7.89$ (br. s., 1 H), 7.46 (d, $J = 8.2$ Hz, 2 H), 7.36 - 7.29 (m, 3 H), 7.26 - 7.19 (m, 1 H), 6.97 - 6.88 (m, 1 H), 6.75 - 6.65 (m, 2 H), 6.55 (d, $J = 7.8$ Hz, 1 H), 6.46 - 6.39 (m, 1 H), 3.63 (t, $J = 5.0$ Hz, 2 H), 2.47 - 2.37 (m, 1 H), 2.24 - 2.16 (m, 1 H), 1.86 - 1.76 (m, 1 H), 1.61 - 1.51 (m, 1 H).

^{13}C NMR (100 MHz, CDCl_3) $\delta = 146.6, 140.7, 128.6, 128.3, 127.2, 125.9, 125.8, 121.9, 118.6, 118.5, 117.8, 116.4, 112.7, 102.5, 62.7, 61.0, 37.2, 27.7$.

HRMS (ESI): calcd for $\text{C}_{20}\text{H}_{21}\text{N}_2\text{O}$ ($\text{M}^+ + \text{H}$) 305.1648, found 305.1644.



(7e): brownish thick liquid

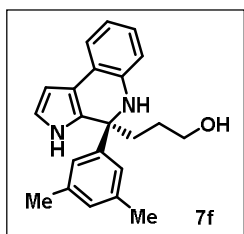
Yield: 78%; $R_f = 0.3$ (Pet. ether/EtOAc = 60/40)

95.9% ee, $[\alpha]_D^{23} = -2.06$ ($c = 0.8$, CHCl_3); **HPLC conditions:** Chiralcel OD-H, 80:20 *n*-Hexane/IPA, Flow rate 1.0 mL/min; $\lambda = 254$ nm; $t_R = 28.15$ min (minor), $t_R = 22.62$ min (major).

^1H NMR (400 MHz, CDCl_3) $\delta = 7.94$ (br. s., 1 H), 7.33 - 7.26 (m, 3 H), 7.12 - 7.05 (m, 2 H), 6.89 (dt, $J = 1.6, 7.7$ Hz, 1 H), 6.71 - 6.65 (m, 1 H), 6.62 (t, $J = 2.7$ Hz, 1 H), 6.51 (d, $J = 7.8$ Hz, 1 H), 6.39 (t, $J = 2.5$ Hz, 1 H), 3.57 (t, $J = 5.5$ Hz, 2 H), 2.39 - 2.32 (m, 1 H), 2.28 (s, 3 H), 2.17 - 2.08 (m, 1 H), 1.81 - 1.70 (m, 1 H), 1.55 - 1.44 (m, 1 H).

^{13}C NMR (100 MHz, CDCl_3) $\delta = 143.8, 140.7, 136.8, 129.2, 128.6, 125.8, 125.8, 121.9, 118.6, 117.7, 116.3, 112.7, 102.4, 62.7, 60.8, 37.2, 27.7, 20.9$.

HRMS (ESI): calcd for $\text{C}_{21}\text{H}_{23}\text{N}_2\text{O}$ ($\text{M}^+ + \text{H}$) 319.1805, found 319.1801.



(7f): thick liquid

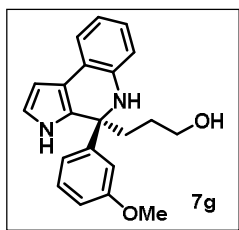
Yield: 63%; $R_f = 0.55$ (Pet. ether/EtOAc = 60/40)

91.4% ee, $[\alpha]_D^{25} = -4.62$ ($c = 1.2$, CHCl_3); **HPLC conditions:** Chiralcel OD-H, 90:10 *n*-Hexane/IPA, Flow rate 1.0 mL/min; $\lambda = 254$ nm; $t_R = 49.59$ min (minor), $t_R = 43.17$ min (major).

^1H NMR (500 MHz, CDCl_3) $\delta = 7.81$ (br. s., 1 H), 7.29 (dd, $J = 1.2, 7.3$ Hz, 1 H), 7.09 (s, 2 H), 6.93 - 6.88 (m, 1 H), 6.87 (s, 1 H), 6.71 - 6.66 (m, 1 H), 6.65 (t, $J = 2.6$ Hz, 1 H), 6.57 - 6.49 (m, 1 H), 6.40 (t, $J = 2.7$ Hz, 1 H), 3.59 (t, $J = 6.1$ Hz, 2 H), 2.40 - 2.33 (m, 1 H), 2.27 (s, 6 H), 2.18 - 2.10 (m, 1 H), 1.79 - 1.73 (m, 1 H), 1.54 - 1.47 (m, 1 H).

^{13}C NMR (125 MHz, CDCl_3) $\delta = 146.5, 140.8, 138.1, 128.9, 128.5, 125.8, 123.9, 121.9, 118.5, 117.6, 116.2, 112.6, 102.5, 62.8, 61.0, 37.6, 27.7, 21.5$.

HRMS (ESI): calcd for $\text{C}_{22}\text{H}_{25}\text{N}_2\text{O}$ ($\text{M}^+ + \text{H}$) 333.1961, found 333.1956.



(7g): thick liquid

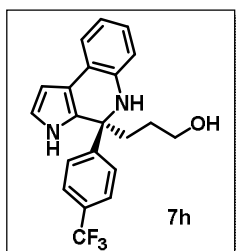
Yield: 59%; $R_f = 0.25$ (Pet. ether/EtOAc = 60/40)

94.7% ee, $[\alpha]_D^{23} = -4.04$ ($c = 1.35$, CHCl_3); **HPLC conditions:** Chiralcel OD-H, 80:20 *n*-Hexane/IPA, Flow rate 1.0 mL/min; $\lambda = 254$ nm; $t_R = 38.35$ min (minor), $t_R = 28.44$ min (major).

^1H NMR (400 MHz, CDCl_3) $\delta = 8.58$ (br. s., 1 H), 7.35 - 7.28 (m, 1 H), 7.24 - 7.13 (m, 1 H), 7.05 - 6.95 (m, 2 H), 6.95 - 6.88 (m, 1 H), 6.84 - 6.76 (m, 2 H), 6.75 - 6.70 (m, 1 H), 6.70 - 6.62 (m, 1 H), 6.43 - 6.37 (m, 1 H), 3.71 (s, 3 H), 3.57 (t, $J = 5.6$ Hz, 2 H), 2.55 - 2.43 (m, 1 H), 2.34 - 2.20 (m, 1 H), 1.84 - 1.71 (m, 1 H), 1.64 - 1.51 (m, 1 H).

^{13}C NMR (100 MHz, CDCl_3) $\delta = 159.6, 129.6, 128.0, 122.1, 120.5, 120.1, 119.0, 118.3, 116.3, 114.8, 112.4, 102.7, 62.5, 55.3, 36.8, 29.7, 27.6$.

HRMS (ESI): calcd for $\text{C}_{21}\text{H}_{23}\text{N}_2\text{O}_2$ ($\text{M}^+ + \text{H}$) 335.1754, found 335.1750.



(7h): thick liquid

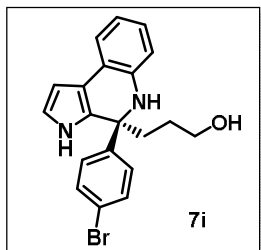
Yield: 56%; $R_f = 0.37$ (Pet. ether/EtOAc = 60/40)

96.0% ee, $[\alpha]_D^{27} = -0.88$ ($c = 0.5$, CHCl_3); **HPLC conditions:** Chiralcel OD-H, 80:20 *n*-Hexane/IPA, Flow rate 1.0 mL/min; $\lambda = 254$ nm; $t_R = 16.34$ min (minor), $t_R = 12.35$ min (major).

^1H NMR (400 MHz, CDCl_3) $\delta = 8.11$ (br. s., 1 H), 7.56 - 7.45 (m, 4 H), 7.30 (dd, $J = 1.1, 7.6$ Hz, 1 H), 6.92 (dt, $J = 1.1, 7.7$ Hz, 1 H), 6.77 - 6.66 (m, 2 H), 6.56 (d, $J = 7.8$ Hz, 1 H), 6.43 (t, $J = 2.5$ Hz, 1 H), 3.68 - 3.56 (m, 2 H), 2.48 - 2.38 (m, 1 H), 2.22 - 2.12 (m, 1 H), 1.88 - 1.76 (m, 1 H), 1.65 - 1.50 (m, 1H).

^{13}C NMR (100 MHz, CDCl_3) $\delta = 150.8, 140.3, 129.1, 127.2, 126.1, 126.0, 125.5, 125.5, 122.1, 119.0, 118.6, 118.3, 116.9, 112.9, 102.8, 62.5, 61.0, 36.9, 27.5$.

HRMS (ESI): calcd for $C_{21}H_{20}F_3N_2O$ ($M^+ + H$) 373.1522, found 373.1517.



(7i): thick liquid

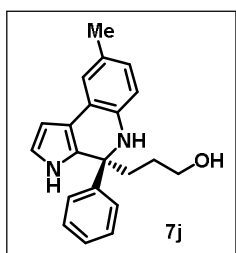
Yield: 69%; $R_f = 0.35$ (Pet. ether/EtOAc = 60/40)

97.5% ee, $[\alpha]_D^{26} = -2.39$ ($c = 1.6$, $CHCl_3$); **HPLC conditions:** Chiralcel OD-H, 90:10 *n*-Hexane/IPA, Flow rate 1.0 mL/min; $\lambda = 254$ nm; $t_R = 106.08$ min (minor), $t_R = 91.96$ min (major).

1H NMR (400 MHz, $CDCl_3$) $\delta = 7.96$ (br. s., 1 H), 7.39 (d, $J = 7.8$ Hz, 2 H), 7.32 - 7.26 (m, 3 H), 6.91 (t, $J = 7.6$ Hz, 1 H), 6.70 (t, $J = 7.3$ Hz, 2 H), 6.53 (d, $J = 7.8$ Hz, 1 H), 6.41 (t, $J = 2.5$ Hz, 1 H), 3.60 (t, $J = 5.3$ Hz, 2 H), 2.41 - 2.33 (m, 1 H), 2.18 - 2.09 (m, 1 H), 1.84 - 1.74 (m, 1 H), 1.58 - 1.49 (m, 1 H).

^{13}C NMR (100 MHz, $CDCl_3$) $\delta = 145.9, 140.4, 131.6, 127.6, 126.0, 122.0, 121.1, 118.9, 118.5, 118.1, 116.7, 112.8, 102.7, 62.6, 60.8, 36.9, 27.6$.

HRMS (ESI): calcd for $C_{20}H_{20}N_2OBr$ ($M^+ + H$) 383.0754, found 383.0747.



(7j): yellowish solid

Yield: 70%; mp = 149-151°C; $R_f = 0.35$ (Pet. ether/EtOAc = 60/40)

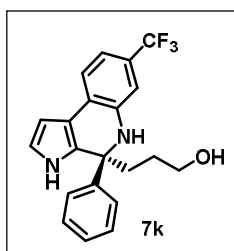
94.4% ee, $[\alpha]_D^{26} = -0.54$ ($c = 0.8$, $CHCl_3$); **HPLC conditions:** Chiralcel OD-H, 80:20 *n*-Hexane/IPA, Flow rate 1.0 mL/min; $\lambda = 254$ nm; $t_R = 19.15$ min (minor), $t_R = 22.98$ min (major).

1H NMR (500 MHz, $CDCl_3$) $\delta = 7.97$ (br. s., 1 H), 7.39 (d, $J = 9.2$ Hz, 2 H), 7.32 - 7.23 (m, 2 H), 7.22 - 7.15 (m, 1 H), 7.14 - 7.08 (m, 1 H), 6.76 - 6.67 (m, 1 H), 6.62 (t, $J = 2.6$ Hz, 1

H), 6.44 (d, $J = 7.9$ Hz, 1 H), 6.39 (t, $J = 2.6$ Hz, 1 H), 3.63 - 3.49 (m, 2 H), 2.40 - 2.31 (m, 1 H), 2.24 (s, 3 H), 2.16 - 2.09 (m, 1 H), 1.81 - 1.70 (m, 1 H), 1.56 - 1.46 (m, 1 H).

^{13}C NMR (125 MHz, CDCl_3) $\delta = 146.7, 138.3, 128.6, 128.5, 127.1, 126.9, 126.3, 125.8, 122.5, 118.7, 118.5, 116.4, 112.8, 102.5, 62.7, 61.0, 37.0, 27.7, 20.6$.

HRMS (ESI): calcd for $\text{C}_{21}\text{H}_{23}\text{N}_2\text{O}$ ($\text{M}^+ + \text{H}$) 319.1805, found 319.1800.



(7k): thick liquid

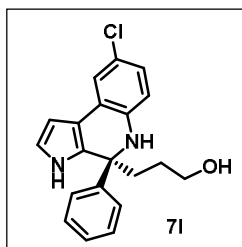
Yield: 84%; $R_f = 0.4$ (Pet. ether/EtOAc = 60/40);

94.5% ee, $[\alpha]_D^{25} = -0.98$ ($c = 1.05, \text{CHCl}_3$); **HPLC conditions:** Chiralcel OD-H, 80:20 *n*-Hexane/IPA, Flow rate 1.0 mL/min; $\lambda = 254$ nm; $t_R = 14.37$ min (minor), $t_R = 11.86$ min (major).

^1H NMR (400 MHz, CDCl_3) $\delta = 8.09$ (br. s., 1 H), 7.50 - 7.46 (m, 1 H), 7.40 - 7.33 (m, 2 H), 7.28 (t, $J = 7.6$ Hz, 2 H), 7.23 - 7.17 (m, 1 H), 7.14 - 7.07 (m, 1 H), 6.63 (t, $J = 2.9$ Hz, 1 H), 6.49 (d, $J = 8.5$ Hz, 1 H), 6.40 (t, $J = 2.7$ Hz, 1 H), 4.33 (br. s., 1 H), 3.60 - 3.51 (m, 2 H), 2.47 - 2.36 (m, 1 H), 2.20 - 2.10 (m, 1 H), 1.79 - 1.68 (m, 1 H), 1.51 - 1.39 (m, 1 H).

^{13}C NMR (100 MHz, CDCl_3) $\delta = 146.4, 143.3, 128.7, 128.3, 127.4, 125.8, 123.0, 122.9, 119.3, 118.8, 118.8, 118.0, 115.5, 111.8, 102.4, 62.5, 61.3, 37.4, 27.5$.

HRMS (ESI): calcd for $\text{C}_{21}\text{H}_{20}\text{N}_2\text{OF}_3$ ($\text{M}^+ + \text{H}$) 373.1522, found 373.1514.



(7l): yellow solid

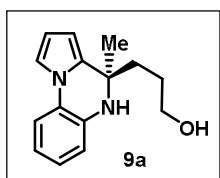
Yield: 76%; mp = 77-79°C; $R_f = 0.35$ (Pet. ether/EtOAc = 60/40)

93.5% ee, $[\alpha]_{\text{D}}^{25} = +2.15$ ($c = 0.95$, CHCl_3); **HPLC conditions:** Chiralcel OD-H, 80:20 *n*-Hexane/IPA, Flow rate 1.0 mL/min; $\lambda = 254$ nm; $t_{\text{R}} = 25.76$ min (minor), $t_{\text{R}} = 24.09$ min (major).

^1H NMR (400 MHz, CDCl_3) $\delta = 8.18$ (br. s., 1 H), 7.36 - 7.30 (m, 2 H), 7.28 - 7.15 (m, 4 H), 6.86 - 6.76 (m, 1 H), 6.59 (t, $J = 2.7$ Hz, 1 H), 6.40 (d, $J = 8.2$ Hz, 1 H), 6.35 - 6.27 (m, 1 H), 3.59 - 3.42 (m, 2 H), 2.39 - 2.27 (m, 1 H), 2.08 (ddd, $J = 4.8, 11.4, 14.0$ Hz, 1 H), 1.78 - 1.65 (m, 1 H), 1.51 - 1.39 (m, 1 H).

^{13}C NMR (100 MHz, CDCl_3) $\delta = 46.4, 139.2, 128.8, 128.6, 127.2, 125.7, 125.2, 122.3, 121.5, 120.2, 119.0, 115.5, 113.7, 102.4, 62.5, 61.1, 37.1, 27.5$.

HRMS (ESI): calcd for $\text{C}_{20}\text{H}_{20}\text{N}_2\text{OCl}$ ($\text{M}^+ + \text{H}$) 339.1259, found 339.1253.



(9a): white solid

Yield: 89%; mp = 142-144°C; $R_f = 0.3$ (Pet. ether/EtOAc = 60/40)

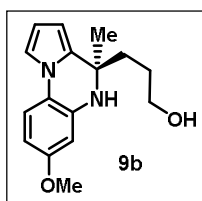
93.3% ee, $[\alpha]_{\text{D}}^{25} = +2.52$ ($c = 1.0$, CHCl_3); **HPLC conditions:** Chiralcel OJ-H, 80:20 *n*-Hexane/IPA, Flow rate 1.0 mL/min; $\lambda = 254$ nm; $t_{\text{R}} = 15.19$ min (minor), $t_{\text{R}} = 13.49$ min (major).

^1H NMR (500 MHz, CDCl_3) $\delta = 7.37 - 7.21$ (d, $J = 8.0$ Hz, 1H), 7.15 - 7.05 (m, 1 H), 6.97 - 6.84 (t, $J = 7.7$ Hz, 1H), 6.79 - 6.63 (m, 1 H), 6.29 - 6.16 (m, 1 H), 5.98 - 5.83 (m, 1 H), 3.53 - 3.33 (t, $J = 6.2$ Hz, 2H), 1.84 - 1.70 (m, 2H), 1.62 - 1.43 (m, 2 H), 1.46 (s, 3H).

^{13}C NMR (100 MHz, $\text{CDCl}_3 + \text{DMSO}$) $\delta = 135.2, 133.0, 124.5, 124.4, 118.1, 115.1, 114.0, 113.3, 109.6, 102.7, 62.1, 53.6, 38.2, 27.6, 27.3$.

IR (KBr): ν_{max} 3246, 3188, 2974, 2941, 2909, 1608, 1516, 1026 cm^{-1} .

HRMS (ESI): calcd for $\text{C}_{15}\text{H}_{19}\text{N}_2\text{O}$ ($\text{M}^+ + \text{H}$) 243.1497, found 243.1507.



(9b): white solid

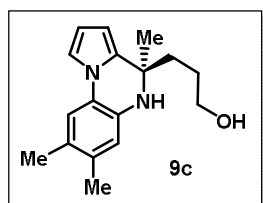
Yield: 77%; mp = 148-150°C; R_f = 0.35 (Pet. ether/EtOAc = 60/40)

94.5% ee, $[\alpha]_D^{25} = +34.03$ (c = 1.0, CHCl₃); **HPLC conditions:** Kromacil-5 Amycoat, 90:10 *n*-Hexane/IPA, Flow rate 1.0 mL/min; $\lambda = 254$ nm; tR = 31.42 min (minor), tR = 44.66 min (major).

¹H NMR (400 MHz, CDCl₃) δ = 7.17 (d, $J = 8.7$ Hz, 1 H), 7.10 - 7.02 (m, 1 H), 6.34 (dd, $J = 2.5, 8.5$ Hz, 1 H), 6.29 - 6.23 (m, 2 H), 5.94 (dd, $J = 1.1, 3.4$ Hz, 1 H), 3.76 (s, 3 H), 3.53 (t, $J = 6.2$ Hz, 2 H), 1.83 - 1.71 (m, 2H), 1.63 - 1.55 (m, 2 H), 1.51 (s, 3H).

¹³C NMR (100 MHz, CDCl₃) δ = 175.1, 157.2, 136.4, 132.4, 119.4, 115.2, 113.6, 109.5, 103.7, 102.8, 101.3, 63.0, 55.5, 54.2, 38.7, 27.8.

HRMS (ESI): calcd for C₁₆H₂₁N₂O₂ (M⁺ + H) 273.1598, found 273.1595.



(9c): white solid

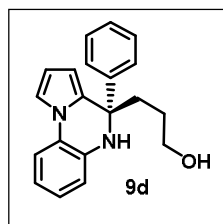
Yield: 90%; mp = 129-131°C; R_f = 0.45 (Pet. ether/EtOAc = 70/30)

99.3% ee, $[\alpha]_D^{25} = +3.09$ (c = 1.0, CHCl₃); **HPLC conditions:** Chiralcel OD-H, 75:25 *n*-Hexane/IPA, Flow rate 1.0 mL/min; $\lambda = 254$ nm; tR = 7.61 min (minor), tR = 9.35min (major).

¹H NMR (400 MHz, CDCl₃) δ = 7.14 - 6.95 (m, 2 H), 6.72 (br. s., 1 H), 6.25 (br. s., 1 H), 6.03 - 5.81 (m, 1 H), 3.59 - 3.51 (m, 2 H), 2.25 - 2.15 (m, 6 H), 1.84 - 1.75 (m, 1 H), 1.87 (s, 1 H), 1.83 - 1.76 (m, 1 H), 1.68 - 1.59 (td, $J = 7.1, 14.2$ Hz, 1H), 1.54 (s, 3 H).

¹³C NMR (100 MHz) δ = 133.1, 132.1, 130.1, 129.2, 124.0, 118.6, 116.0, 114.1, 109.8, 103.6, 62.9, 54.9, 37.8, 27.7, 26.8, 19.4.

HRMS (ESI): calcd for C₁₇H₂₃N₂O (M⁺ + H) 271.1805, found 271.1802.



(9d): white solid

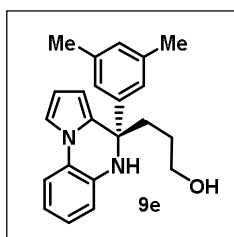
Yield: 86%; mp = 95-97°C; R_f = 0.35 (Pet. ether/EtOAc = 60/40)

91.7% ee, $[\alpha]_{\text{D}}^{25} = -4.61$ ($c = 1.0$, CHCl_3); **HPLC conditions:** Kromacil-5 Amycoat, 90:10 *n*-Hexane/IPA, Flow rate 1.0 mL/min; $\lambda = 254$ nm; $t_{\text{R}} = 21.31$ min (minor), $t_{\text{R}} = 27.48$ min (major).

^1H NMR (400 MHz, CDCl_3) $\delta = 7.34 - 7.27$ (m, 2 H), 7.27 - 7.19 (m, 3 H), 7.18 - 7.10 (m, 2 H), 6.98 - 6.89 (m, 1 H), 6.84 - 6.71 (m, 2 H), 6.32 (t, $J = 3.2$ Hz, 1 H), 6.08 (dd, $J = 1.4, 3.7$ Hz, 1 H), 3.69 - 3.60 (m, 2 H), 2.39 - 2.28 (m, 1 H), 2.24 - 2.12 (m, 1 H), 1.73 (qd, $J = 6.5, 8.9$ Hz, 2 H).

^{13}C NMR (100 MHz, CDCl_3) $\delta = 145.4, 135.1, 131.5, 128.2, 126.8, 126.0, 125.3, 124.7, 119.0, 115.6, 114.6, 114.2, 109.9, 105.0, 62.9, 60.0, 37.9, 27.6$.

HRMS (ESI): calcd for $\text{C}_{20}\text{H}_{20}\text{N}_2\text{O}$ ($\text{M}^+ + \text{H}$) 305.1648, found 305.1646.



(9e): white solid

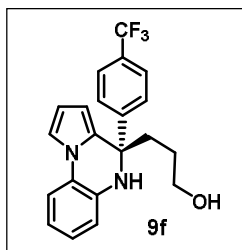
Yield: 77%; mp = 138-140°C; $R_f = 0.4$ (Pet. ether/EtOAc = 60/40)

94% ee, $[\alpha]_{\text{D}}^{25} = -3.56$ ($c = 1.0$, CHCl_3); **HPLC conditions:** Kromacil-5 Amycoat, 90:10 *n*-Hexane/IPA, Flow rate 1.0 mL/min; $\lambda = 254$ nm; $t_{\text{R}} = 10.23$ min (minor), $t_{\text{R}} = 13.13$ min (major).

^1H NMR (400 MHz, CDCl_3) $\delta = 7.29 - 7.19$ (m, 1 H), 7.18 - 7.09 (m, 1 H), 6.98 - 6.90 (m, 3 H), 6.84 - 6.72 (m, 3 H), 6.32 (t, $J = 3.4$ Hz, 1 H), 6.12 - 5.99 (m, 1 H), 3.72 - 3.52 (m, 2 H), 2.33 - 2.26 (m, 1 H), 2.23 (s, 6 H), 2.18 - 2.10 (m, 1 H), 1.80 - 1.63 (m, 2 H).

^{13}C NMR (100 MHz, CDCl_3) $\delta = 145.4, 137.6, 135.2, 131.6, 128.5, 125.2, 124.7, 123.8, 118.9, 115.5, 114.5, 114.0, 109.9, 105.1, 63.0, 59.9, 38.0, 27.7, 21.5$.

HRMS (ESI): calcd for $\text{C}_{22}\text{H}_{25}\text{N}_2\text{O}$ ($\text{M}^+ + \text{H}$) 333.1961, found 333.1960.



(9f): yellowish thick liquid

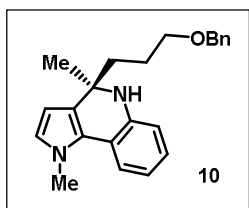
Yield: 79%; $R_f = 0.45$ (Pet. ether/EtOAc = 60/40)

94.4% ee, $[\alpha]_D^{25} = -1.97$ ($c = 1.0$, CHCl_3); **HPLC conditions:** Kromacil-5Amycoat, 90:10 *n*-Hexane/IPA, Flow rate 1.0 mL/min; $\lambda = 254$ nm; $t_R = 12.04$ min (minor), $t_R = 18.32$ min (major).

^1H NMR (400 MHz, CDCl_3) $\delta = 7.48$ (d, $J = 8.2$ Hz, 2 H), 7.41 (d, $J = 8.7$ Hz, 2 H), 7.30 - 7.20 (m, 2 H), 7.19 - 7.13 (m, 1 H), 7.01 - 6.93 (m, 1 H), 6.88 - 6.74 (m, 2 H), 6.39 - 6.31 (m, 1 H), 6.19 - 6.11 (m, 1 H), 3.74 - 3.62 (m, 2 H), 2.43 - 2.31 (m, 1 H), 2.26 - 2.15 (m, 1 H), 1.82 - 1.70 (m, 2 H).

^{13}C NMR (100 MHz, CDCl_3) $\delta = 149.7, 134.7, 130.6, 129.1, 128.8, 126.5, 125.3, 124.9, 122.7, 119.4, 115.7, 114.7, 114.5, 110.1, 105.1, 62.7, 60.0, 37.8, 27.3$.

HRMS (ESI): calcd for $\text{C}_{21}\text{H}_{20}\text{N}_2\text{OF}_3$ ($\text{M}^+ + \text{H}$) 373.1522, found 373.1519.



(10): brownish thick liquid

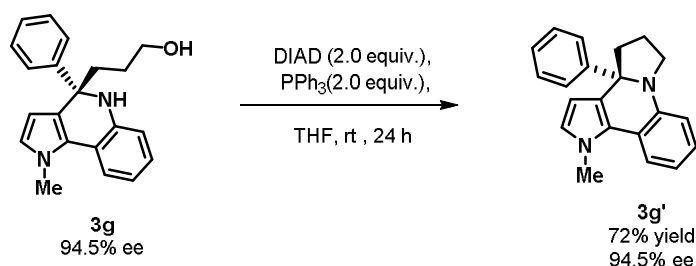
Yield: 32%; $R_f = 0.4$ (Pet. ether/EtOAc = 90/10)

20% ee, **HPLC conditions:** CHIRALPAK IF, 99:1 *n*-hexane/IPA, Flow rate 1.0 mL/min; $\lambda = 254$ nm; $t_R = 14.42$ min (minor), $t_R = 15.62$ min (major).

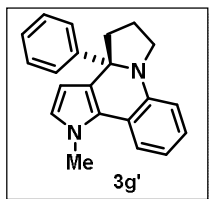
^1H NMR (400 MHz, CDCl_3) $\delta = 7.38$ (d, $J = 7.8$ Hz, 1 H), 7.35 - 7.24 (m, 5 H), 6.90 (t, $J = 8.0$ Hz, 1 H), 6.66 (t, $J = 7.6$ Hz, 1 H), 6.58 - 6.50 (m, 2 H), 5.91 (d, $J = 2.7$ Hz, 1 H), 4.43 (s, 2 H), 3.86 (s, 3 H), 3.40 (t, $J = 6.0$ Hz, 2 H), 1.83 - 1.58 (m, 4 H), 1.46 (s, 3 H). **^{13}C NMR (100 MHz, CDCl_3)** $\delta = 142.6, 138.5, 128.3, 127.6, 127.4, 126.0, 124.9, 124.7, 124.5, 120.1, 117.3, 116.5, 114.1, 102.7, 72.8, 70.7, 55.4, 40.3, 37.2, 29.6, 25.0$.

HRMS (ESI): calcd for $\text{C}_{23}\text{H}_{27}\text{N}_2\text{O}$ ($\text{M}^+ + \text{H}$) 347.2113, found 347.2118.

Transformation of **3g** to fused tetracyclic compound **3g'**



To a flame-dried screw-capped vial equipped with magnetic stir bar, were added compound **3g** (50 mg, 0.1 mmol), DIAD (64 mg, 0.2 mmol) and PPh₃ (82 mg, 0.2 mmol) in 3.0 mL THF at room temperature reaction vial was fitted with a cap, evacuated and back filled with argon. After 48 hours, the solvent was evaporated under reduced pressure and the residue was purified by column chromatography (Pet. ether/EtOAc = 90/10) to afford 34 mg (72 % yield) product **3g'** as white solid.



(3g'): white solid

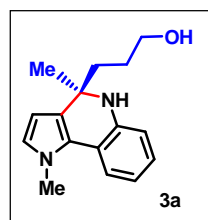
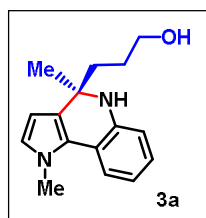
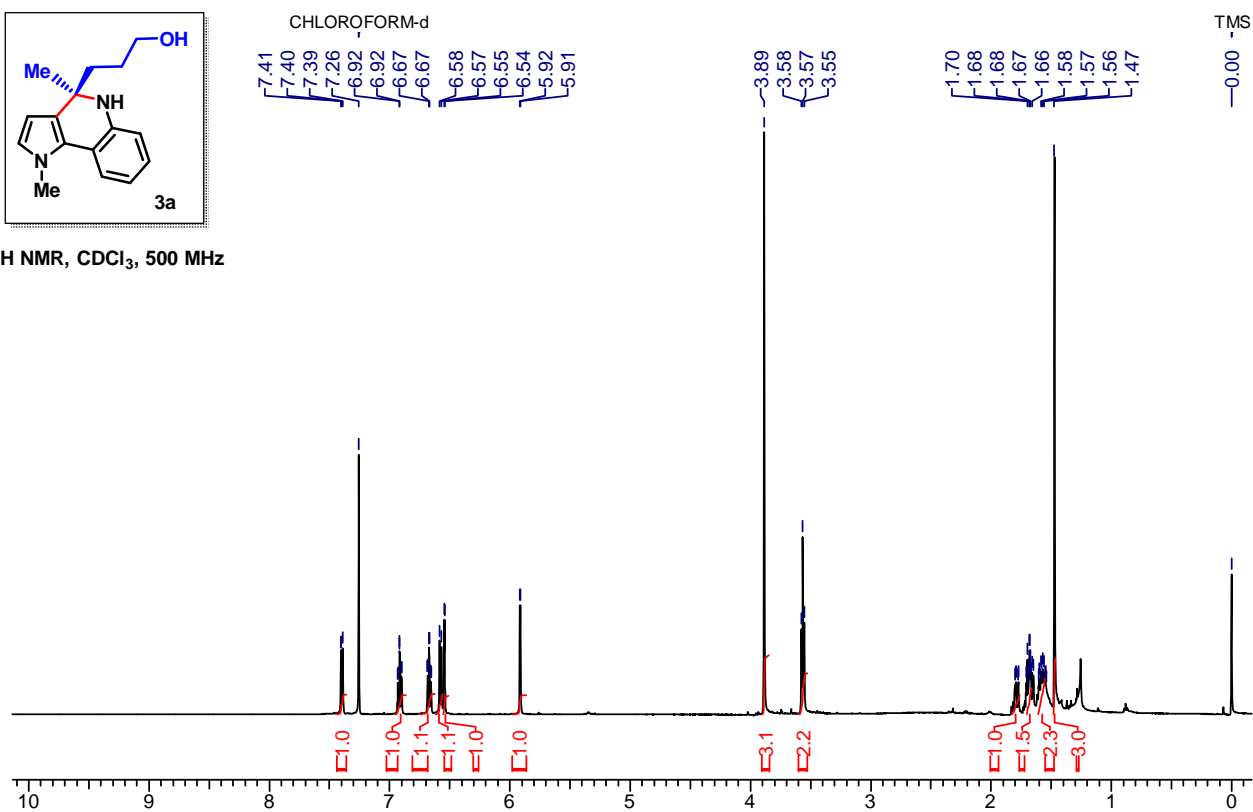
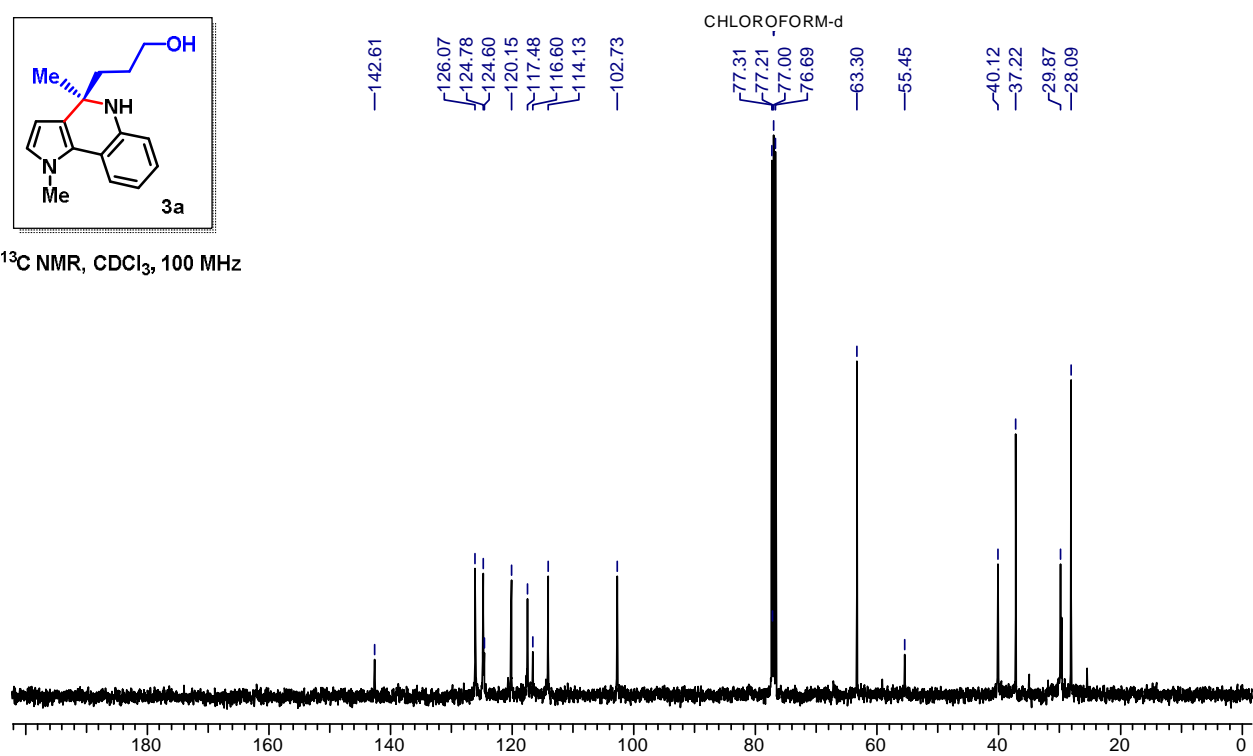
Yield: 72%; mp = 139-141°C; R_f = 0.75 (Pet. ether/EtOAc = 90/10)

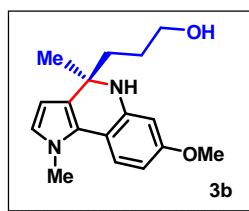
97.4% ee, $[\alpha]_D^{27} = -272.27$ (c = 0.5, CHCl₃); **HPLC conditions:** CHIRALPAK IF, 99:1 *n*-Hexane/IPA, Flow rate 1.0 mL/min; $\lambda = 254$ nm; tR = 6.33 min (minor), tR = 6.67 min (major).

¹H NMR (400 MHz, CDCl₃) δ = 7.41 (d, $J = 7.8$ Hz, 1 H), 7.22 - 7.11 (m, 5 H), 7.09 - 7.02 (m, 1 H), 6.72 (d, $J = 8.1$ Hz, 1 H), 6.67 (t, $J = 7.5$ Hz, 1 H), 6.59 (dd, $J = 0.6, 2.1$ Hz, 1 H), 6.27 - 6.08 (m, 1 H), 3.82 (s, 3 H), 3.77 - 3.63 (m, 1 H), 3.54 - 3.46 (m, 1 H), 2.73-2.68 (dd, $J = 6.6, 11.5$ Hz, 1 H), 2.58 - 2.38 (m, 1 H), 2.12 - 1.96 (m, 1 H), 1.88 - 1.69 (m, 1 H).

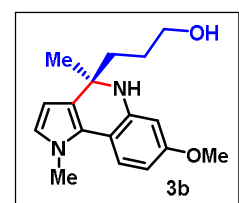
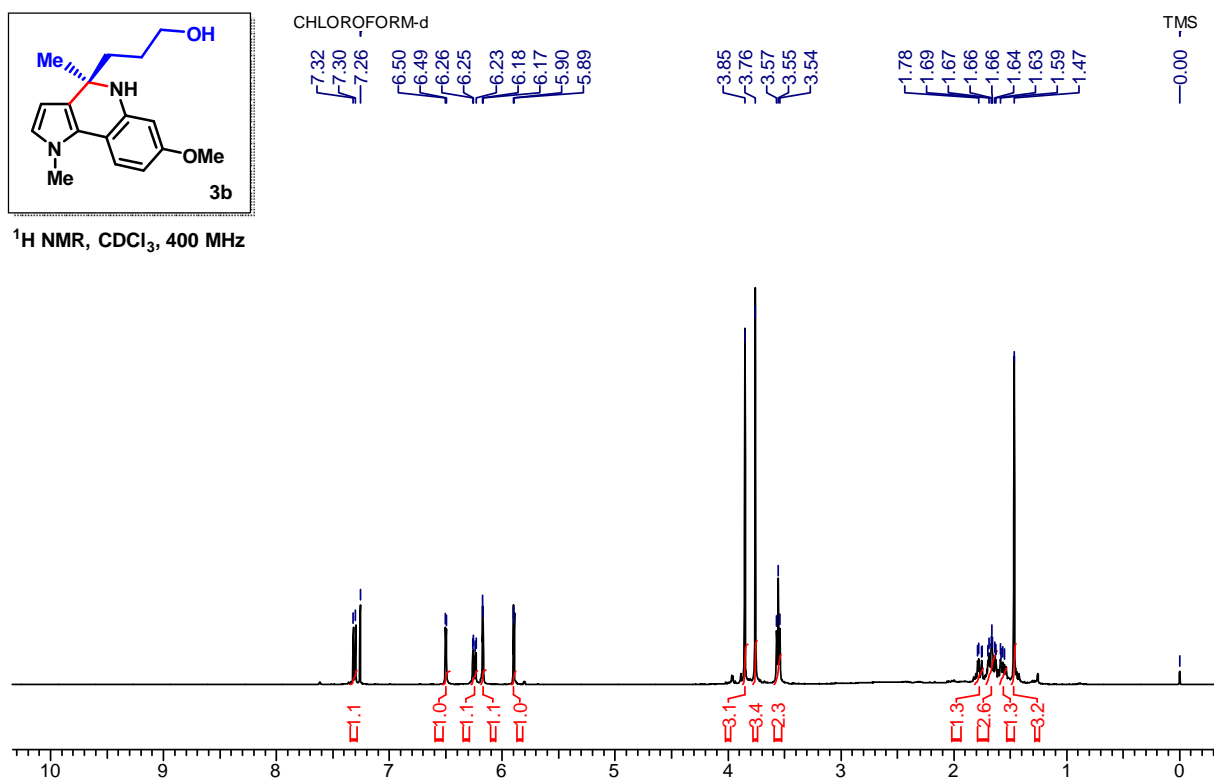
¹³C NMR (100 MHz, CDCl₃) δ = 147.9, 142.3, 128.1, 126.6, 126.0, 125.6, 124.9, 124.6, 120.5, 117.1, 115.8, 111.9, 102.0.

HRMS (ESI): calcd for C₂₁H₂₁N₂ (M⁺ + H) 301.1699, found 301.1694.

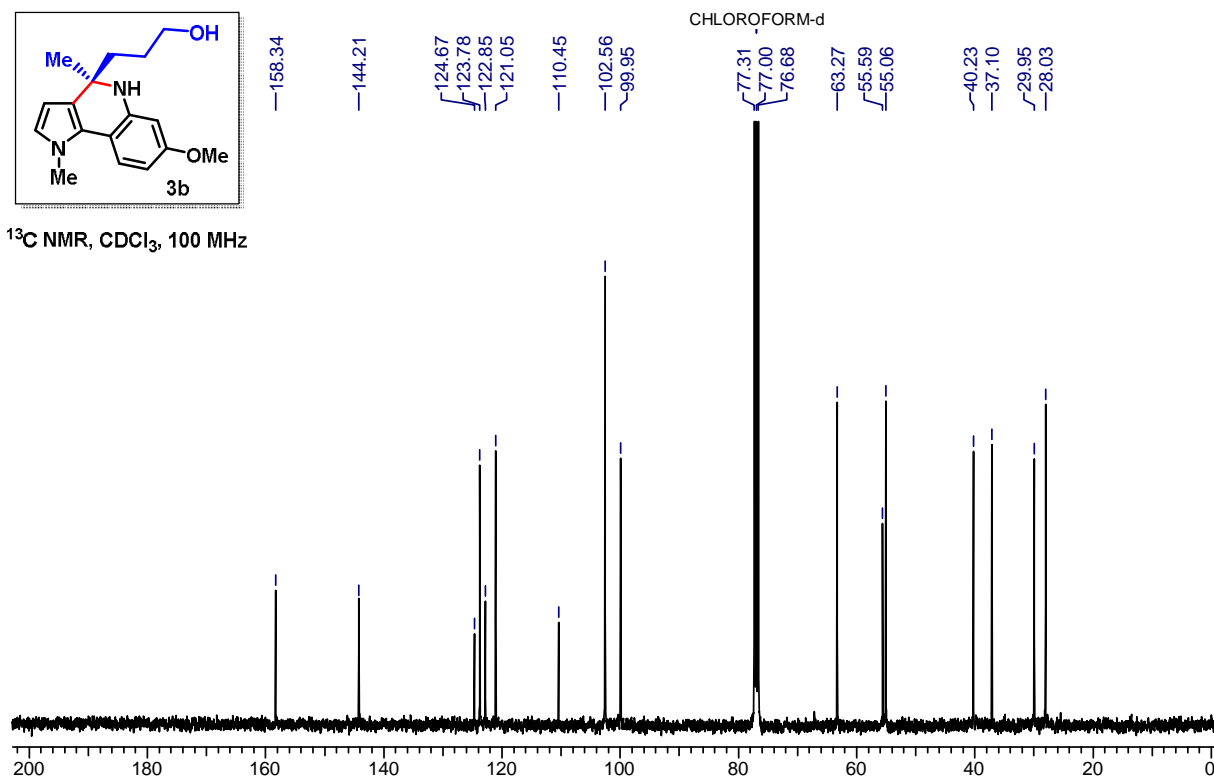
3.8 ^1H NMR and ^{13}C NMR Spectra ^1H NMR, CDCl_3 , 500 MHz ^{13}C NMR, CDCl_3 , 100 MHz

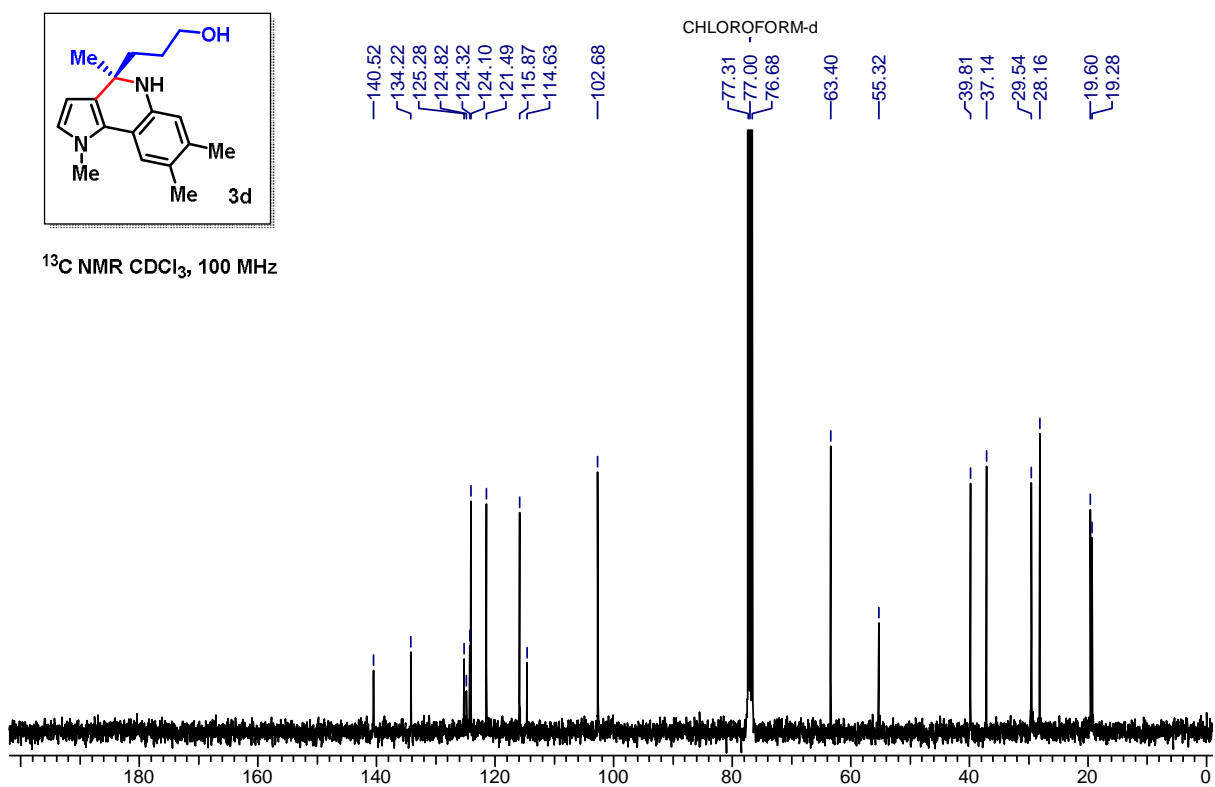
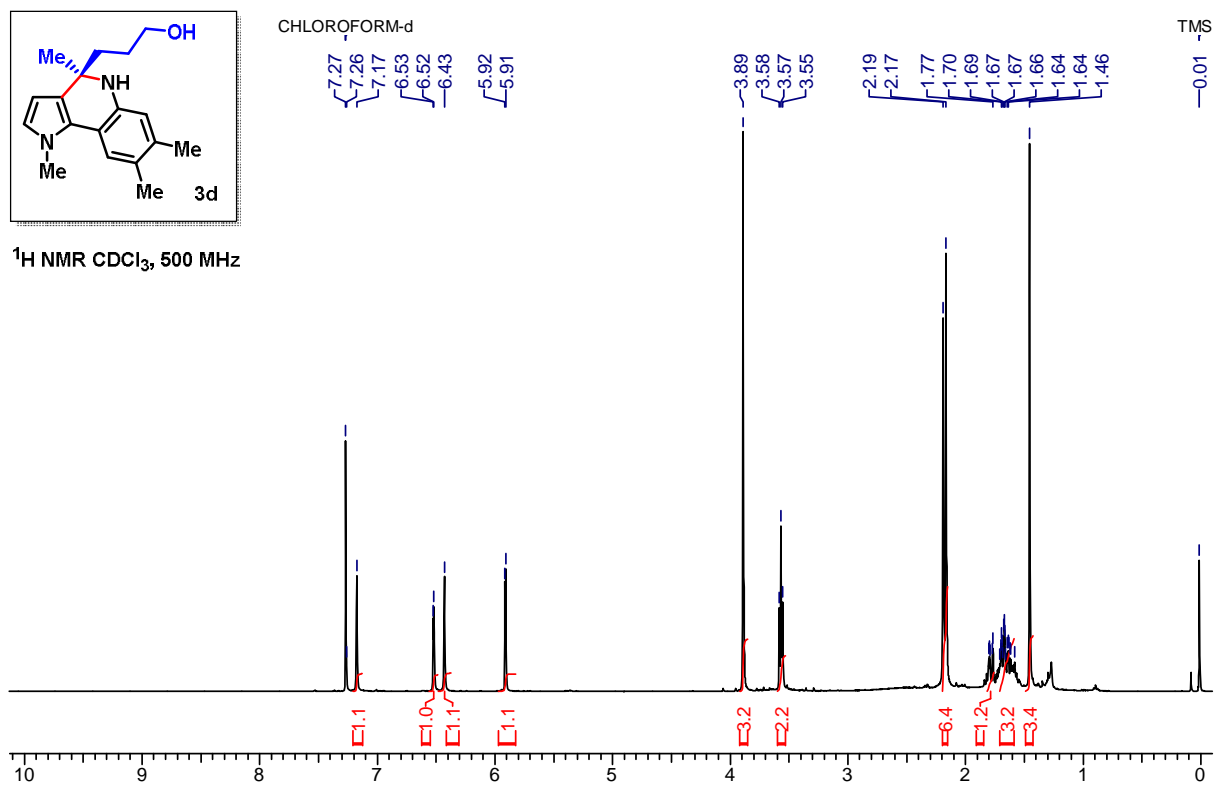


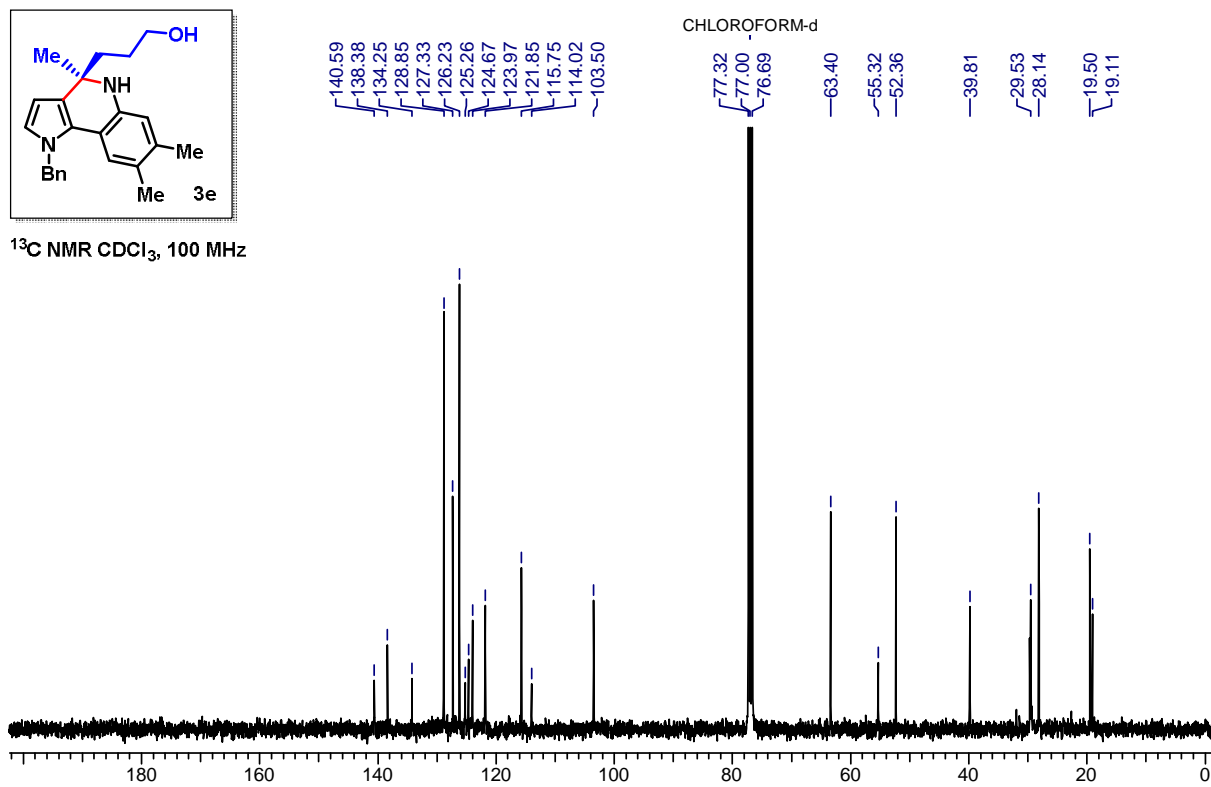
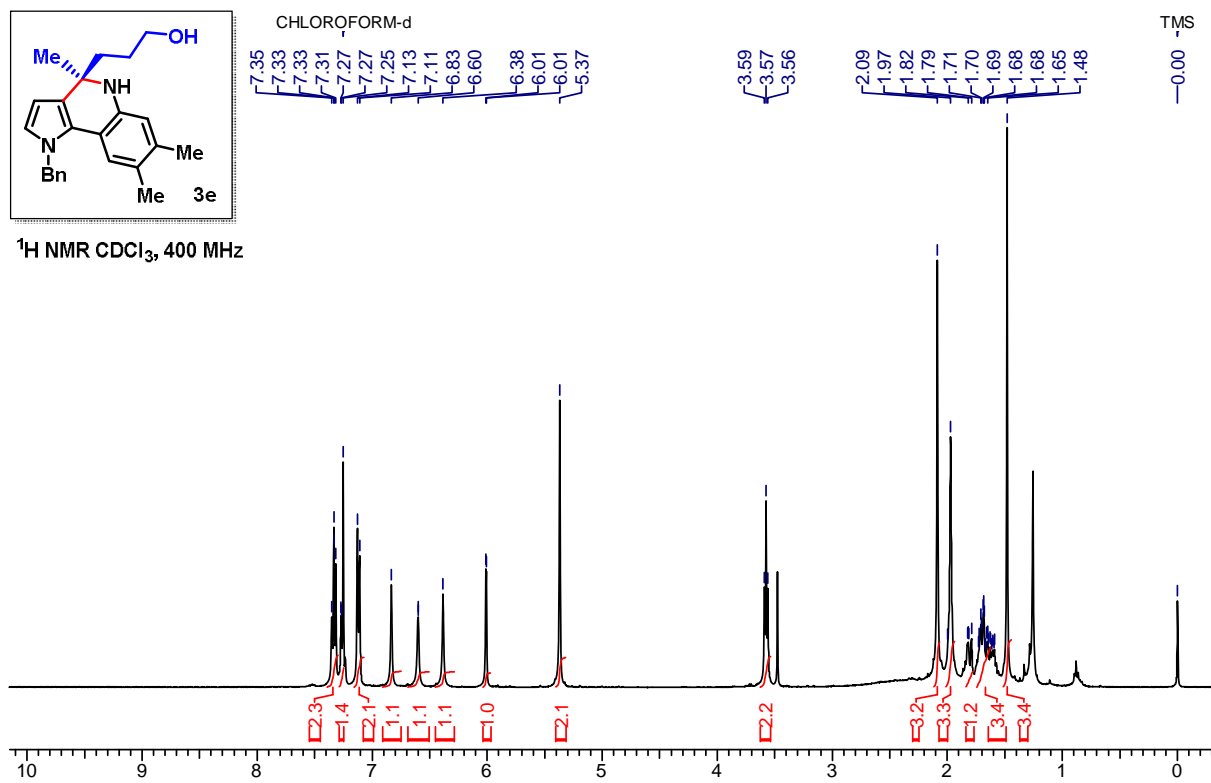
$^1\text{H NMR}$, CDCl_3 , 400 MHz

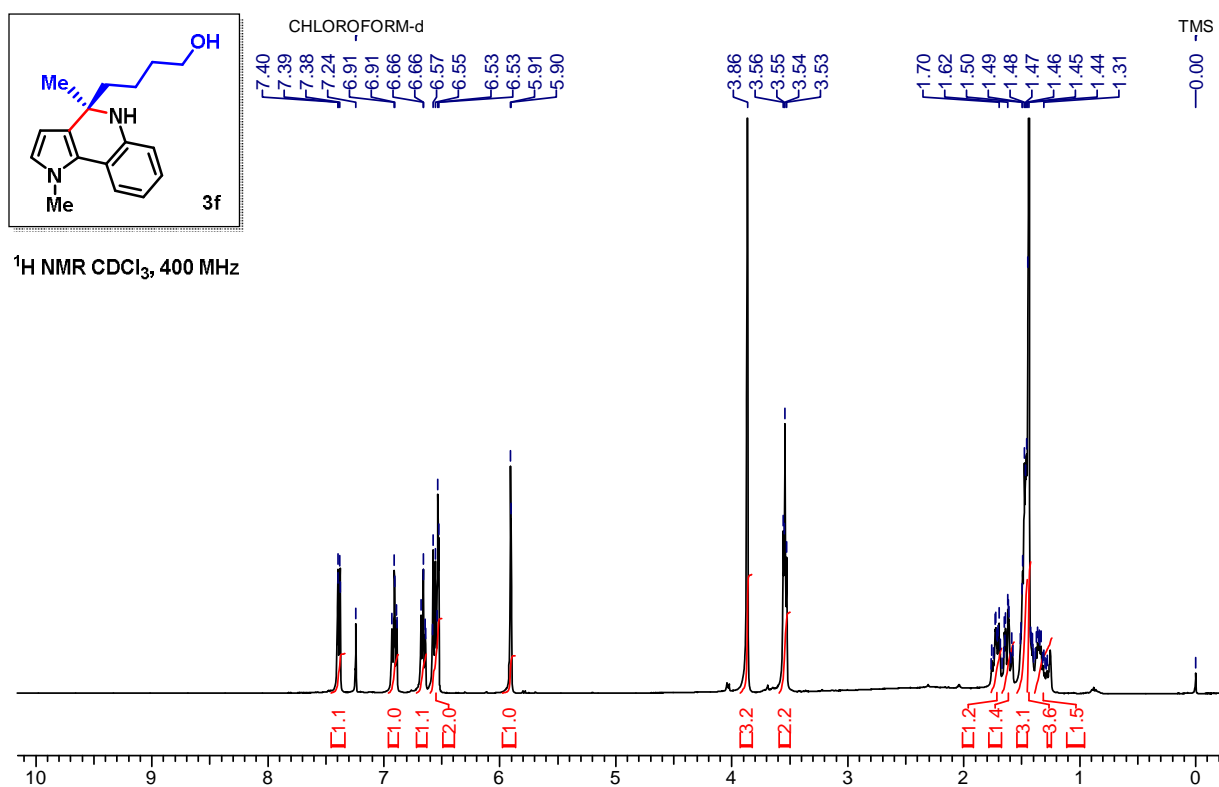
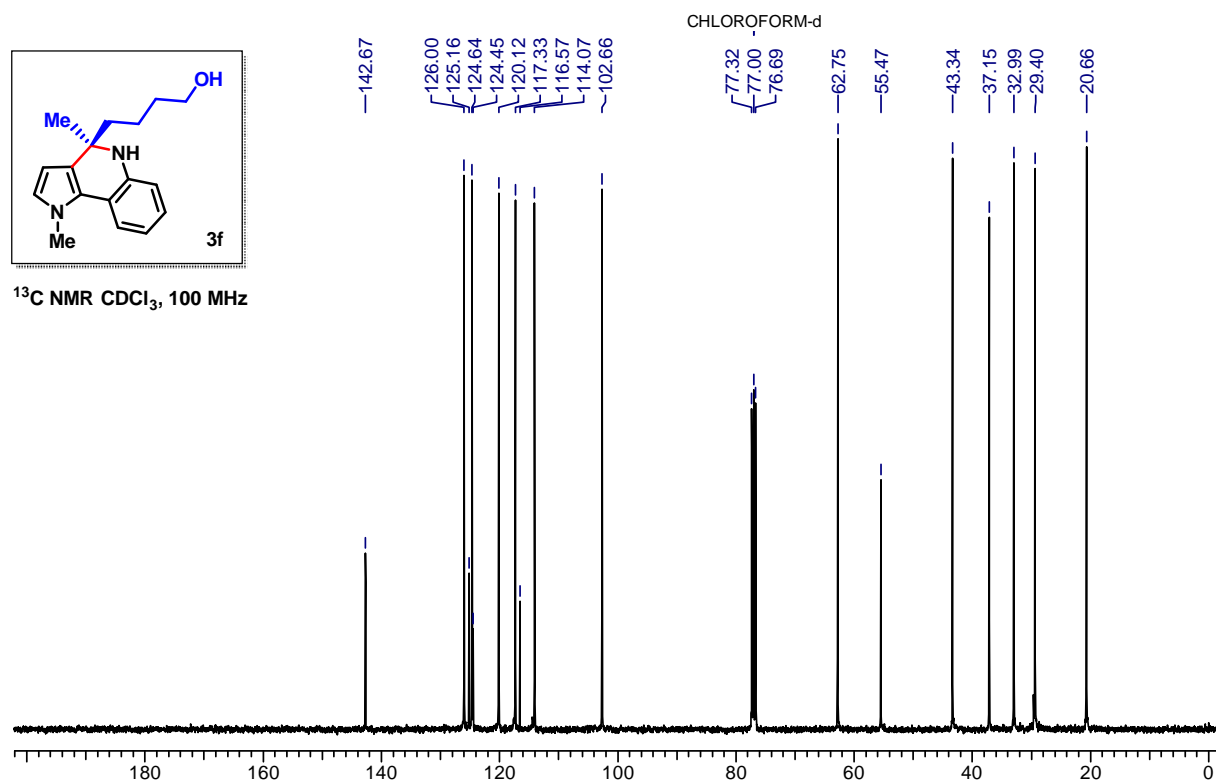


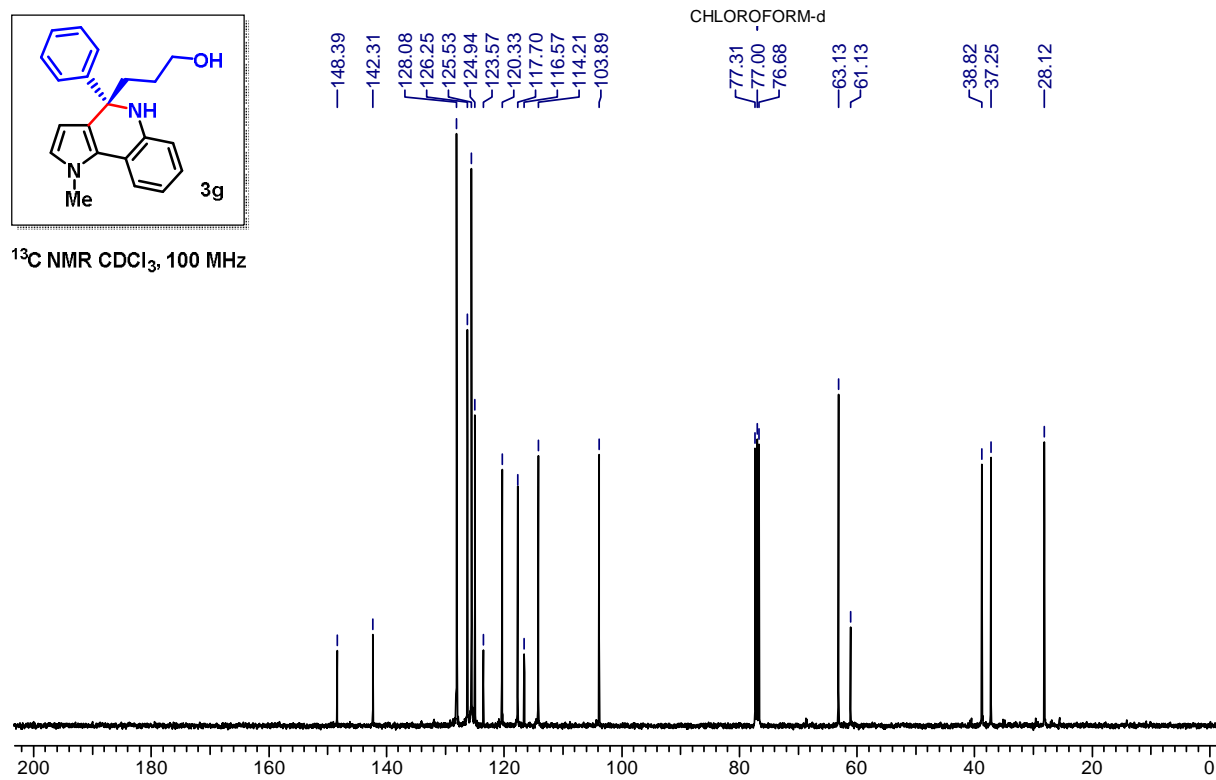
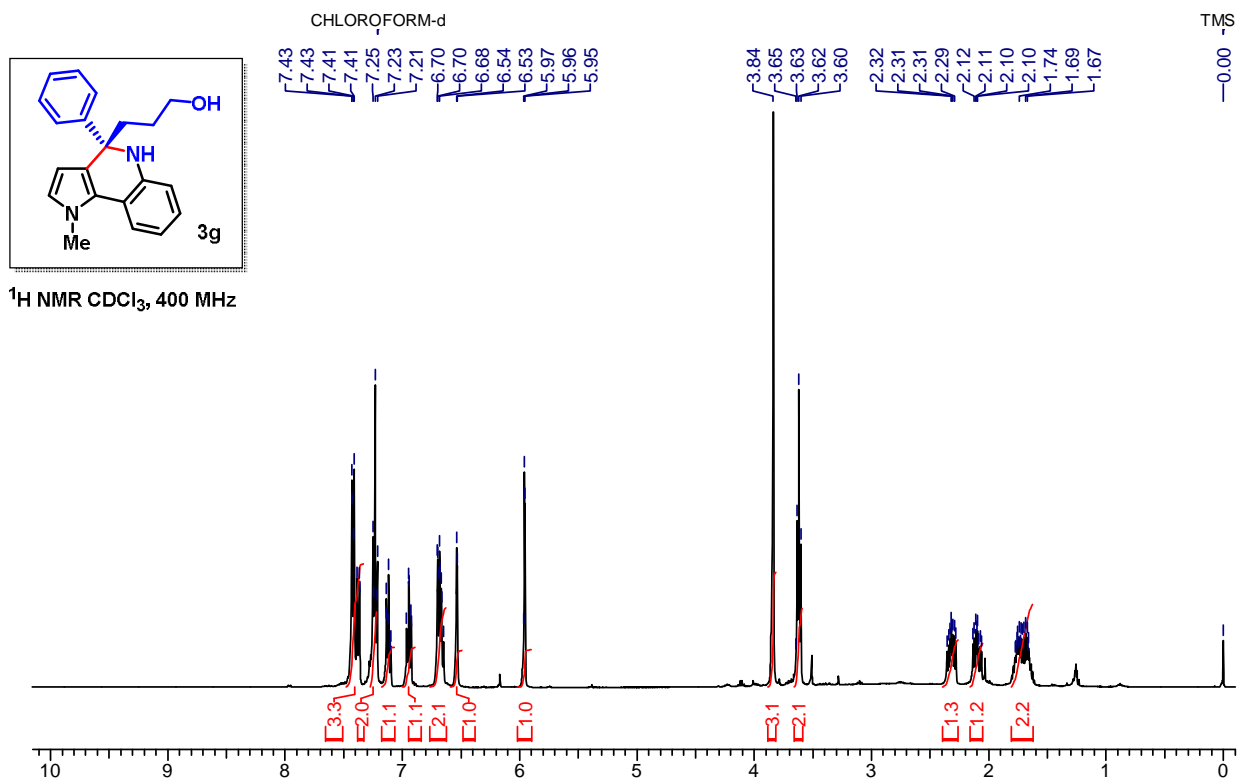
$^{13}\text{C NMR}$, CDCl_3 , 100 MHz

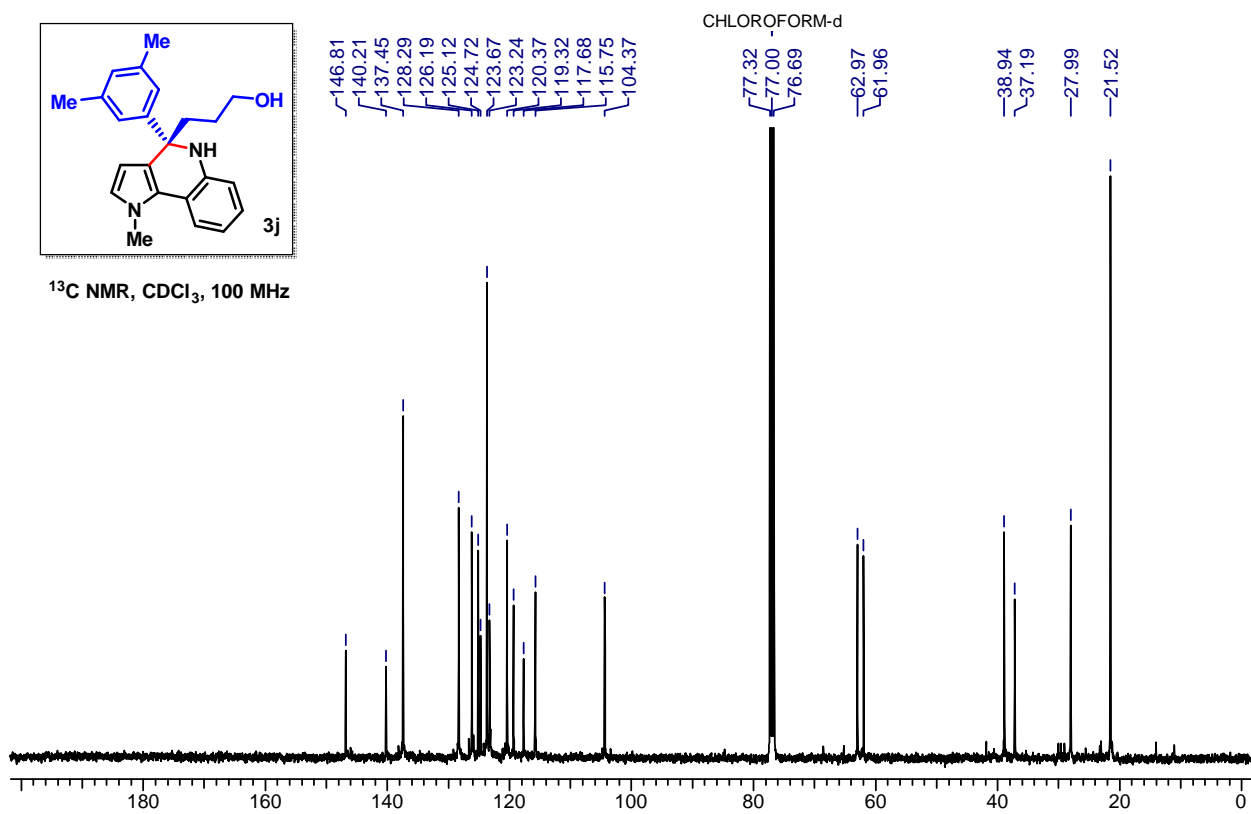
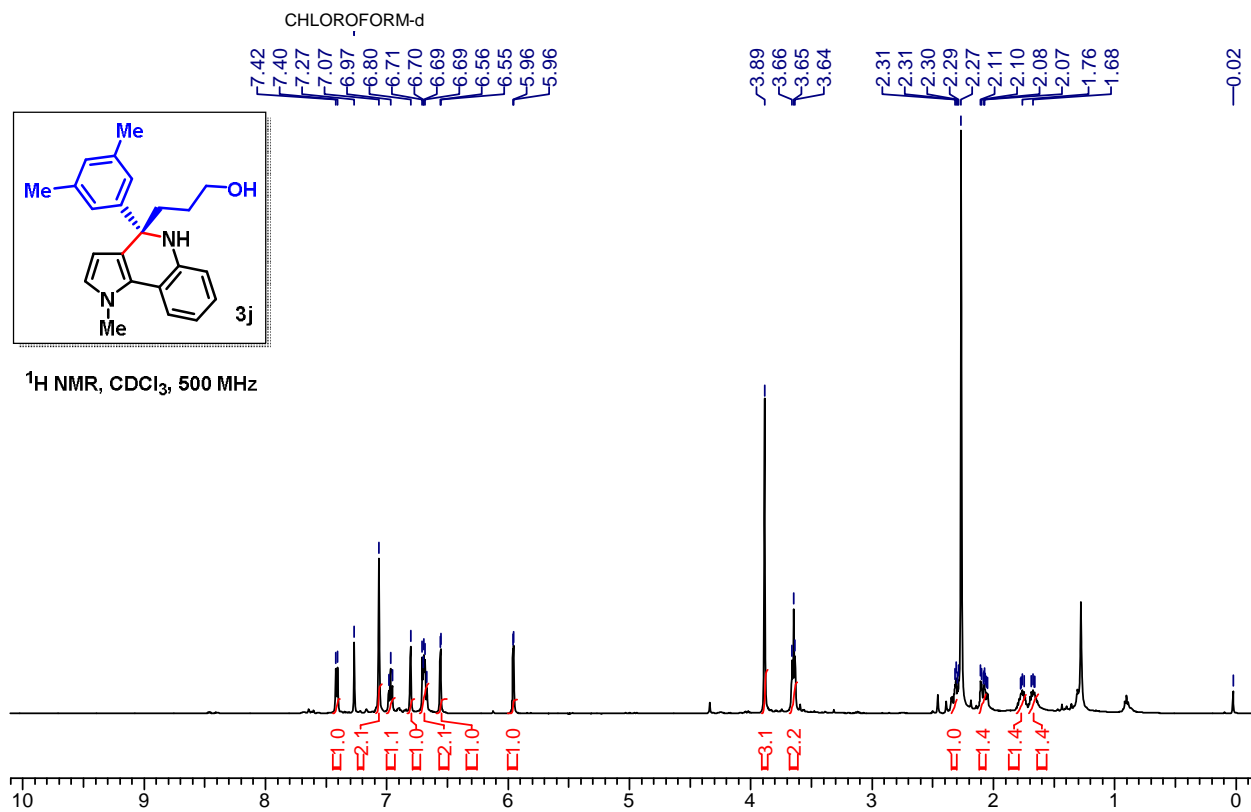


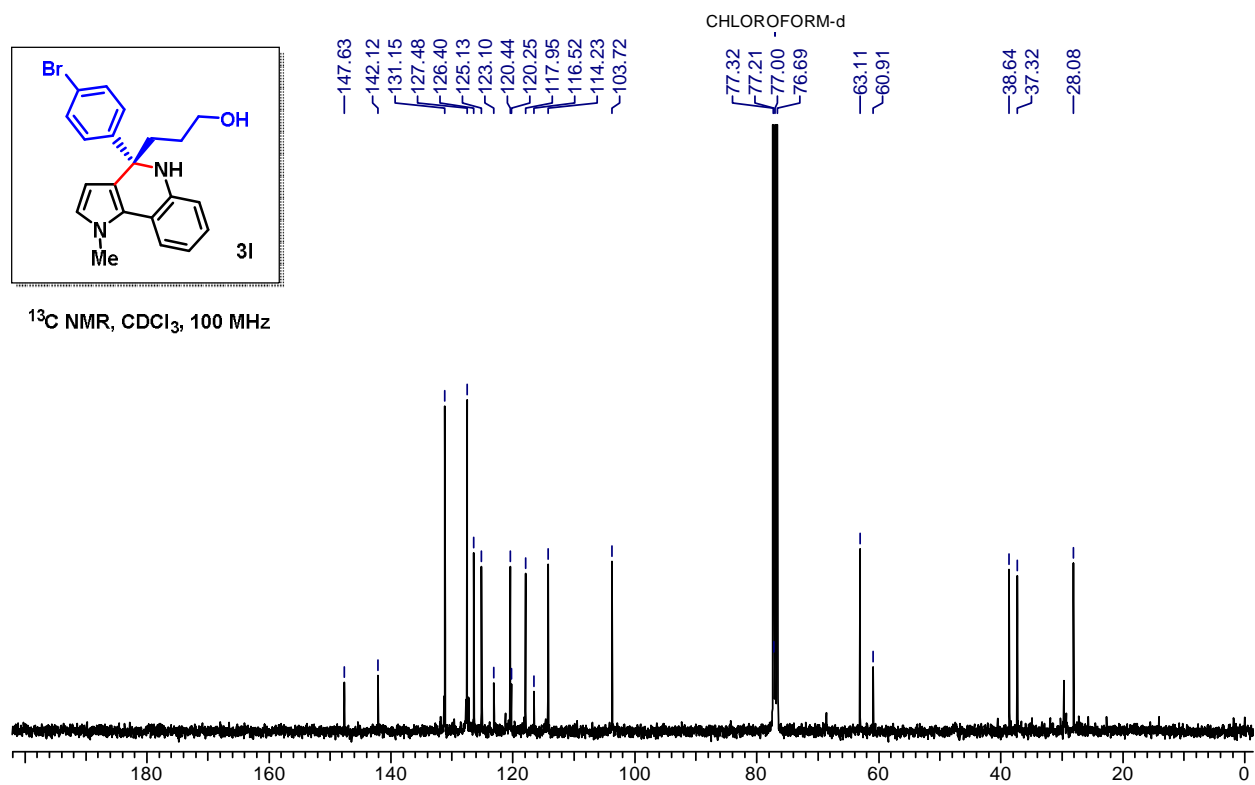
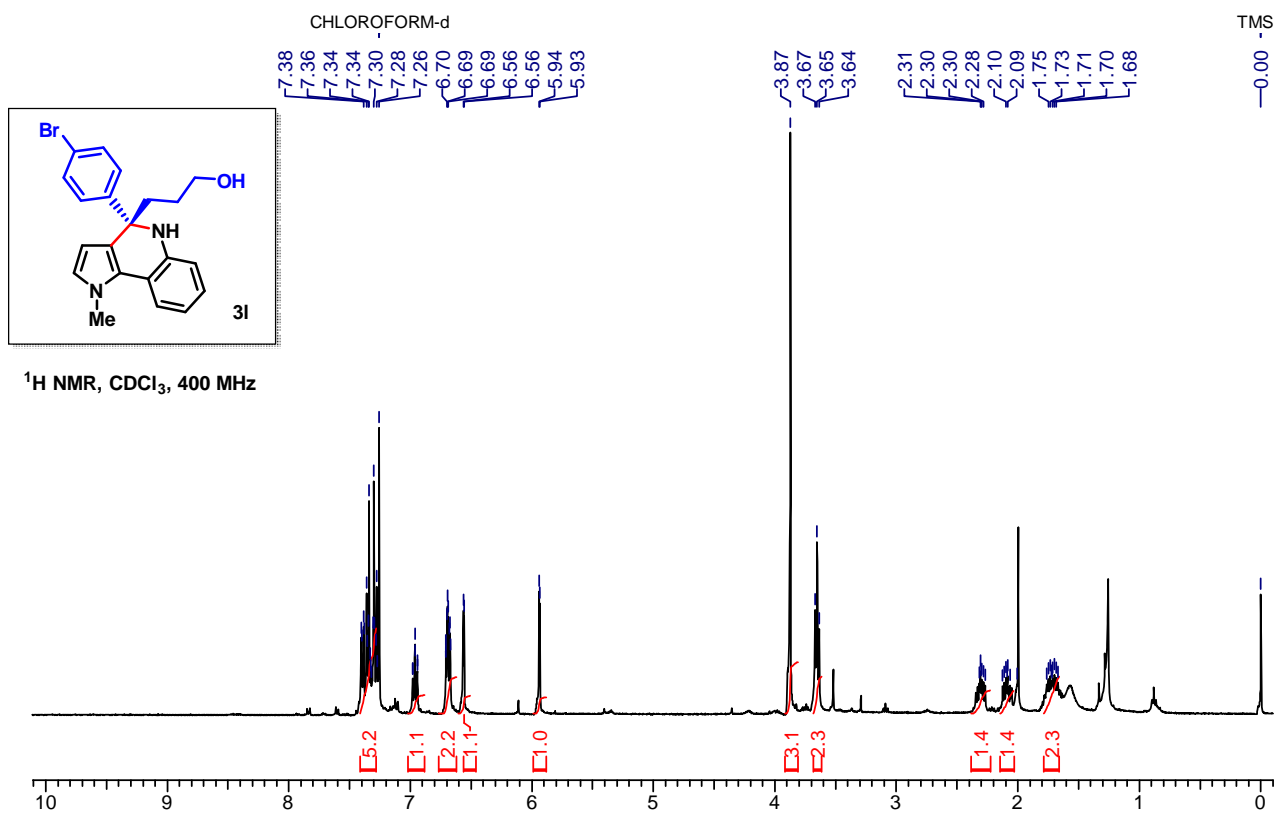


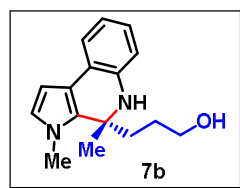


Fig. 00: ^1H and ^{13}C of compound 5a

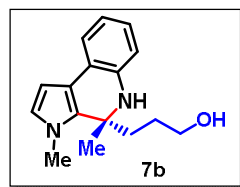
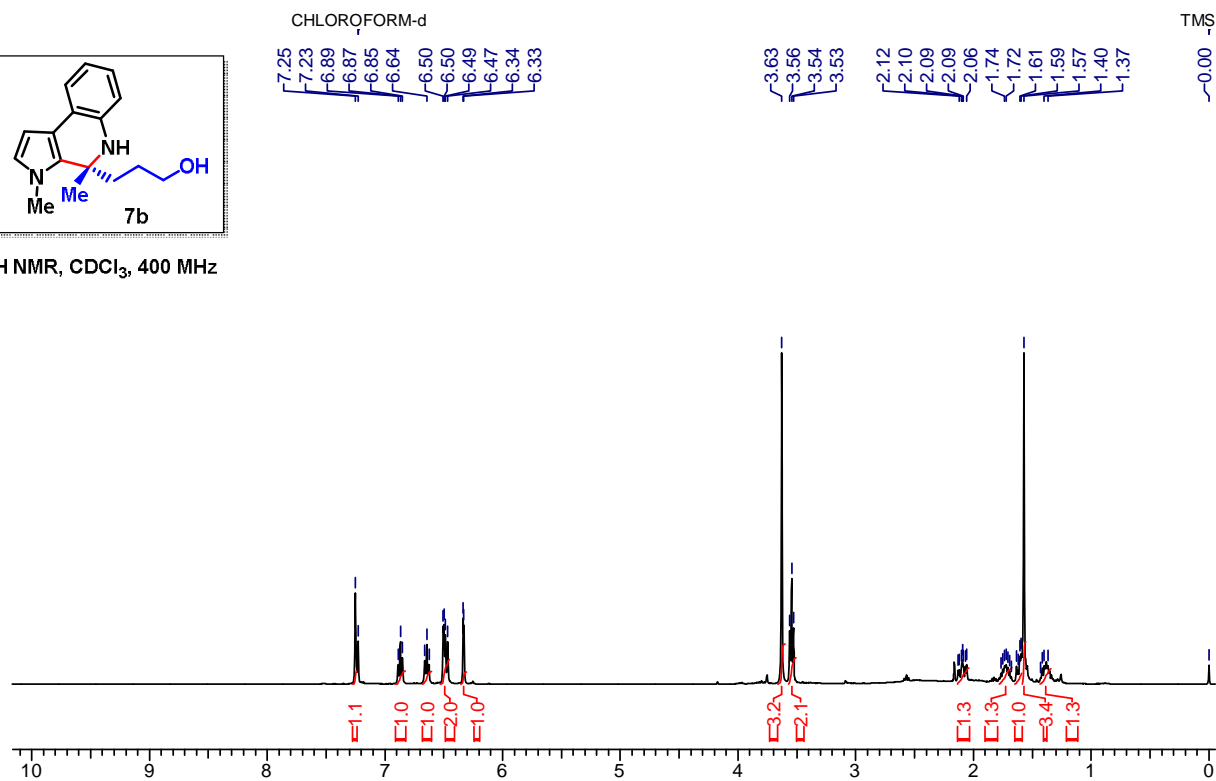




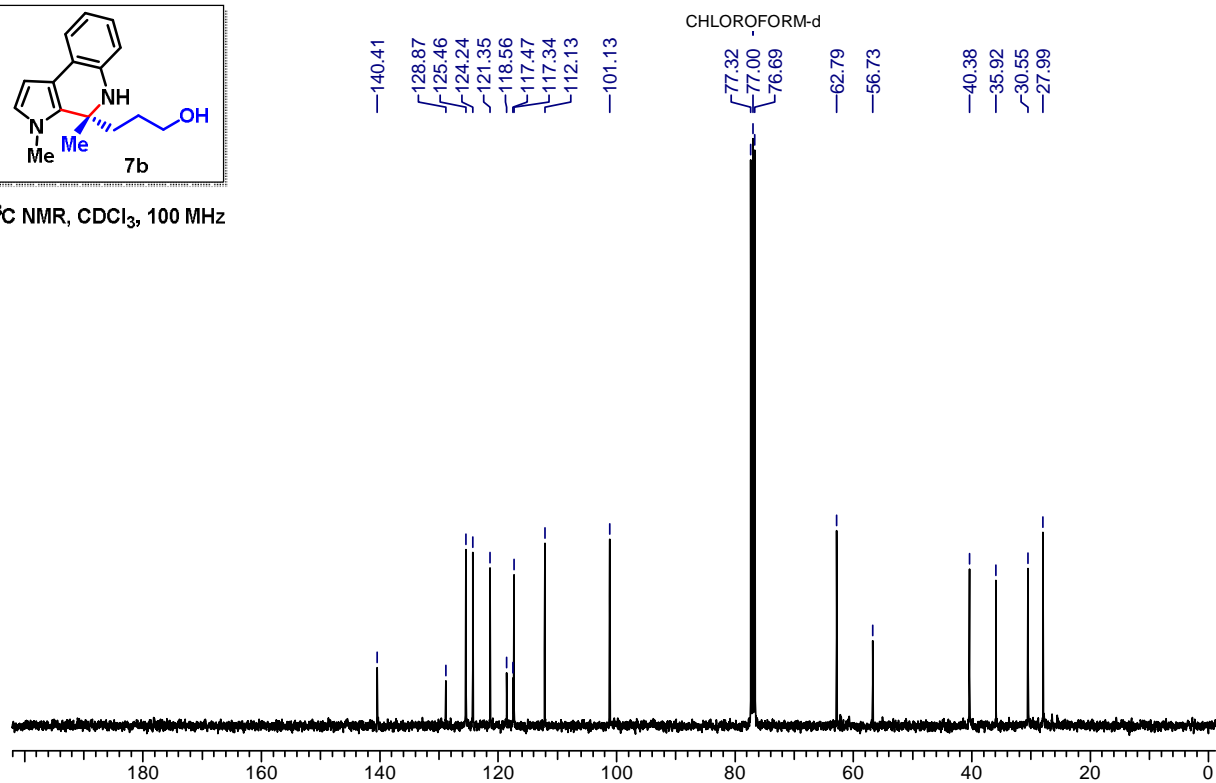


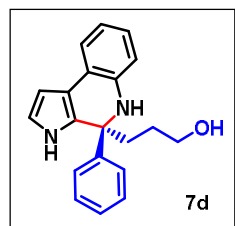


$^1\text{H NMR}$, CDCl_3 , 400 MHz

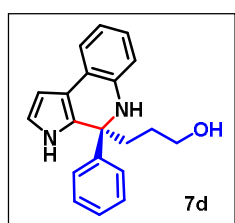
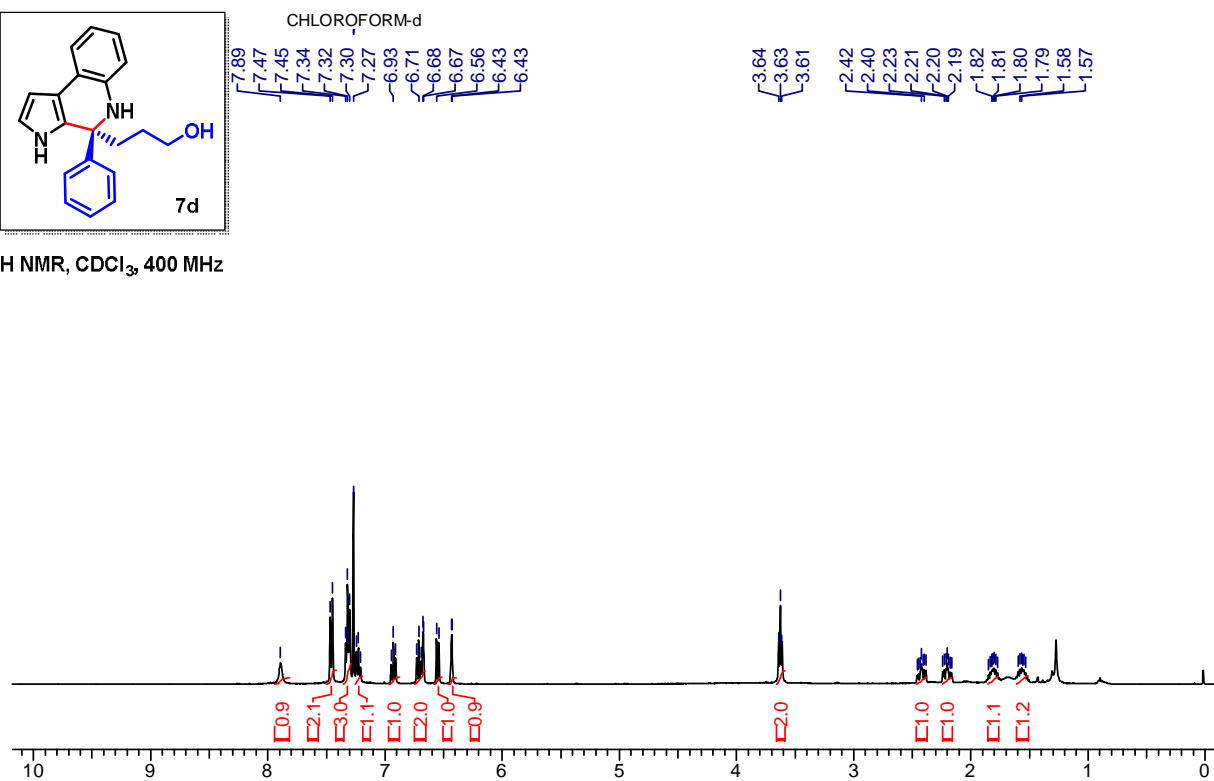


$^{13}\text{C NMR}$, CDCl_3 , 100 MHz

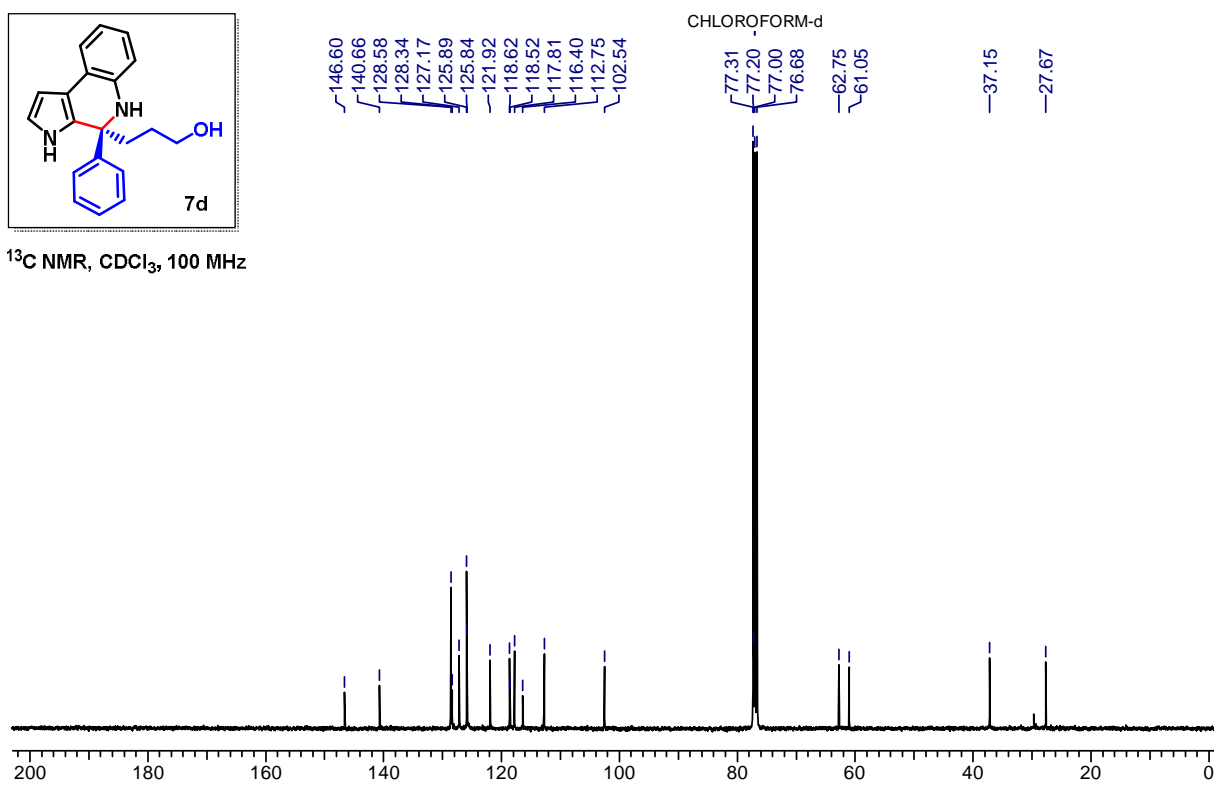


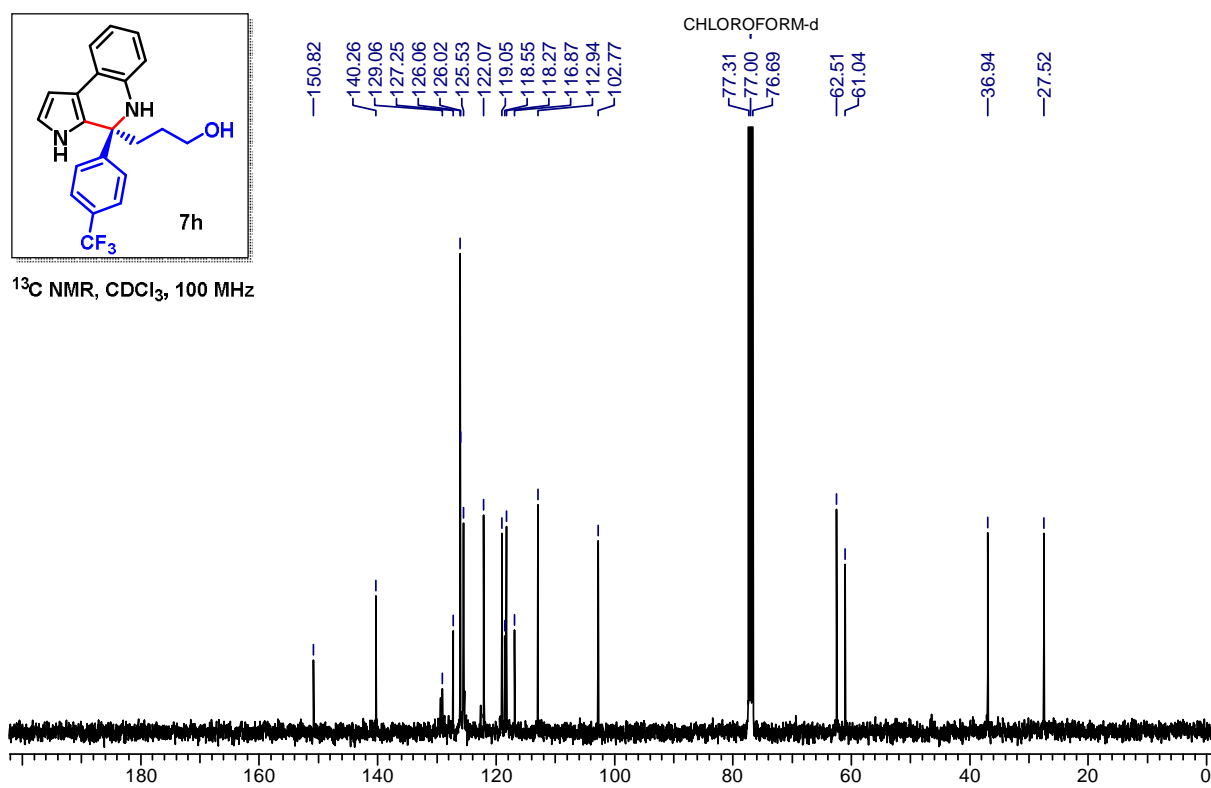
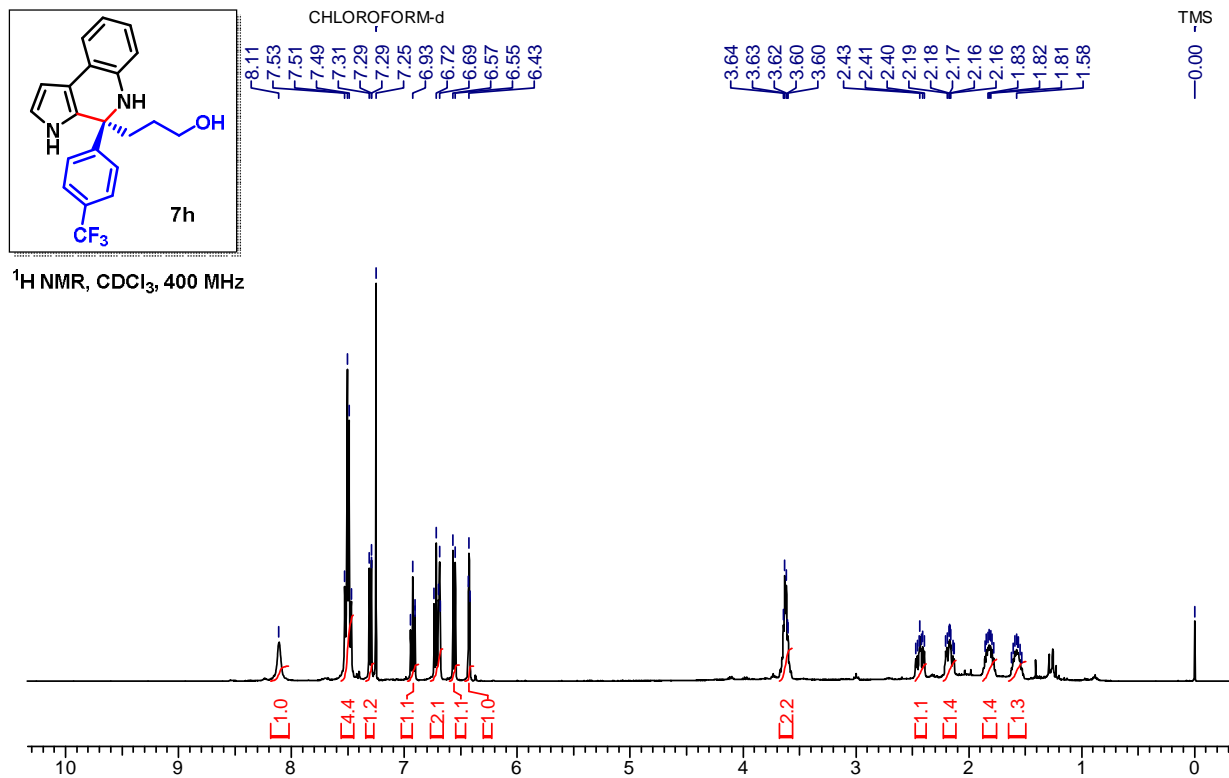


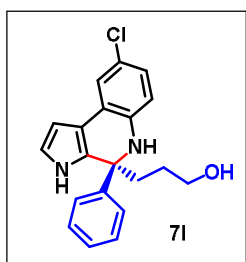
$^1\text{H NMR}$, CDCl_3 , 400 MHz



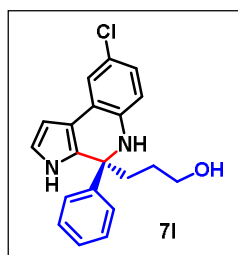
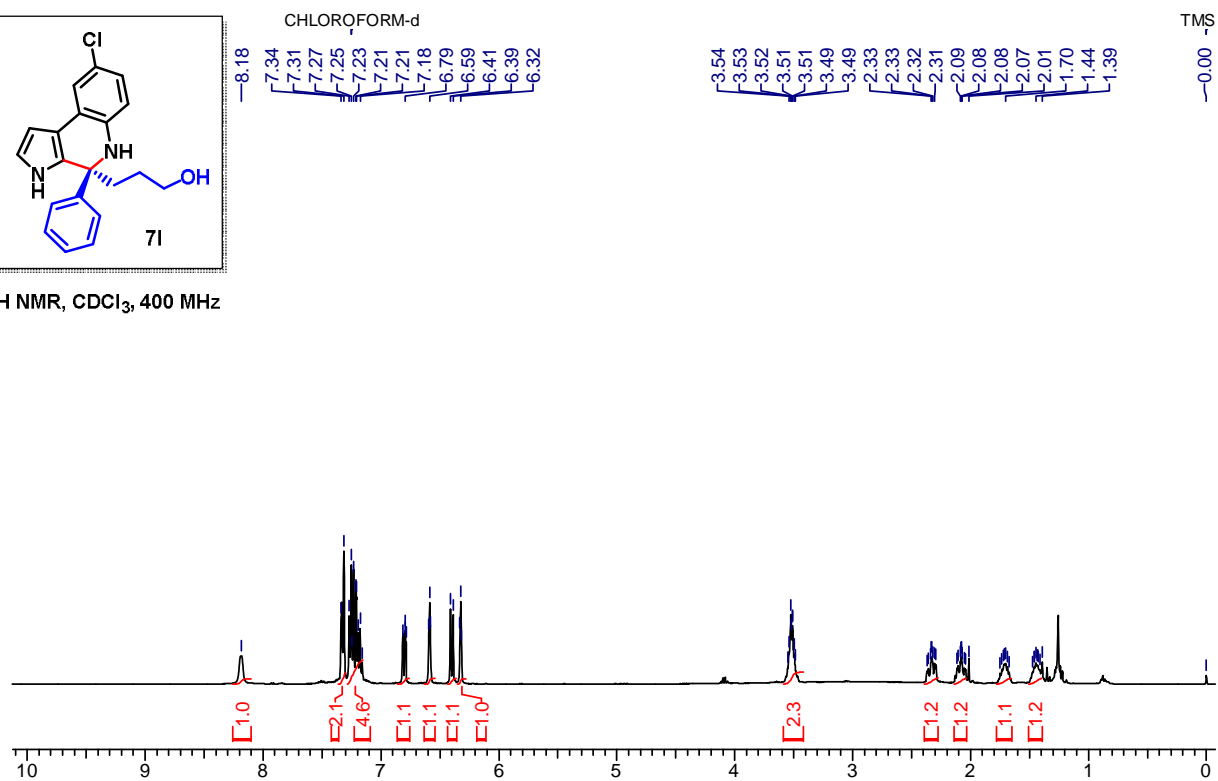
$^{13}\text{C NMR}$, CDCl_3 , 100 MHz



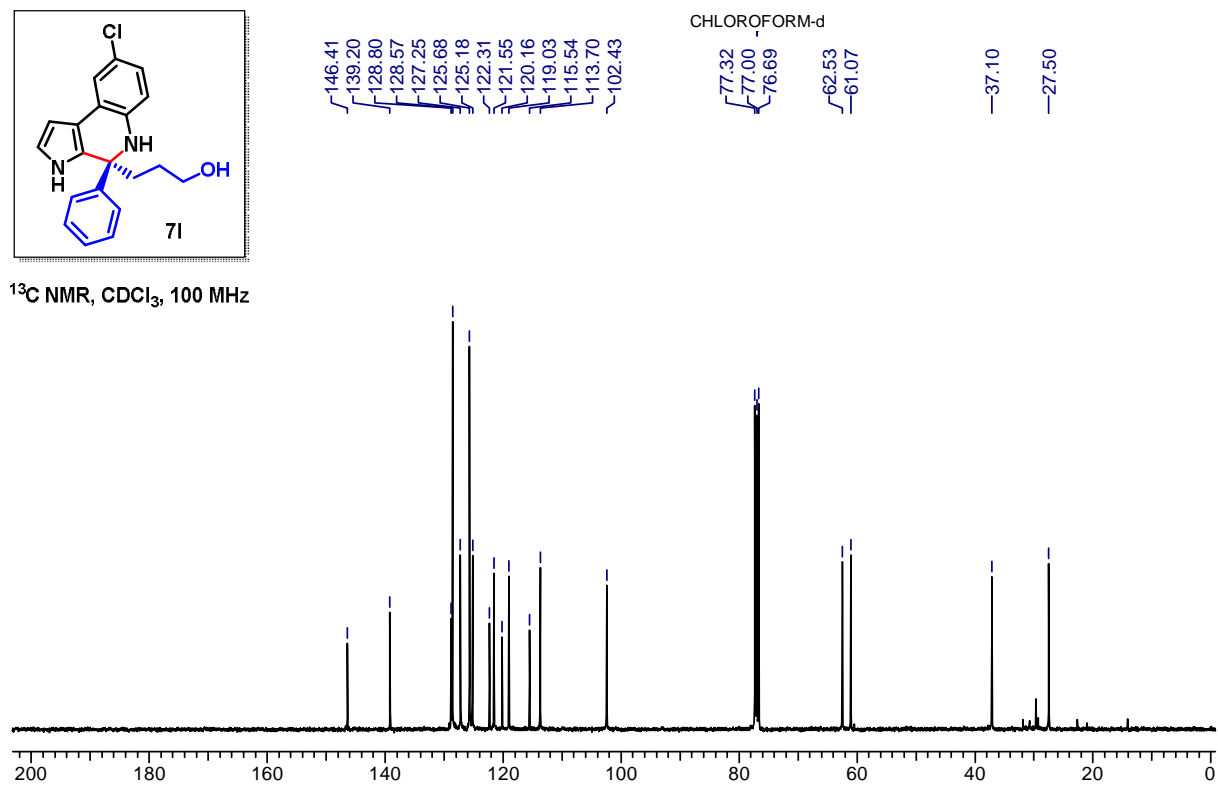


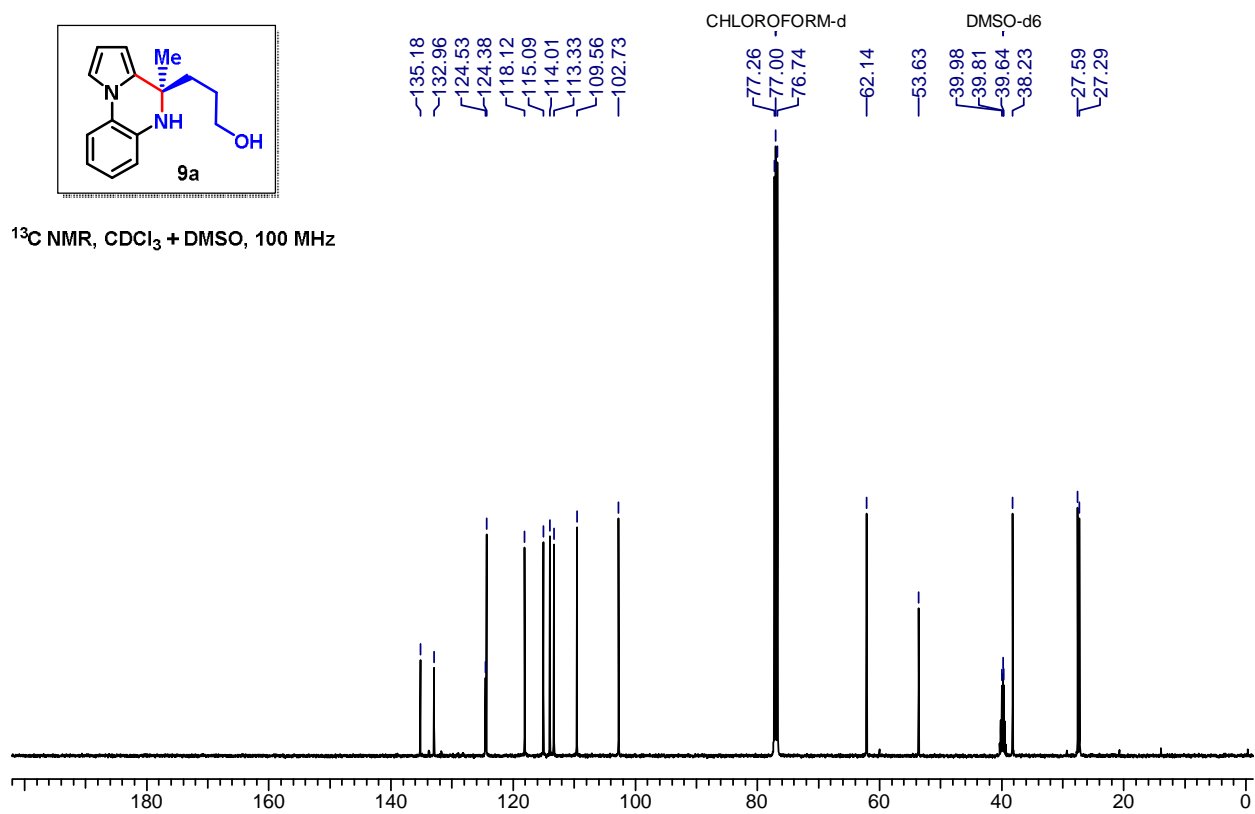
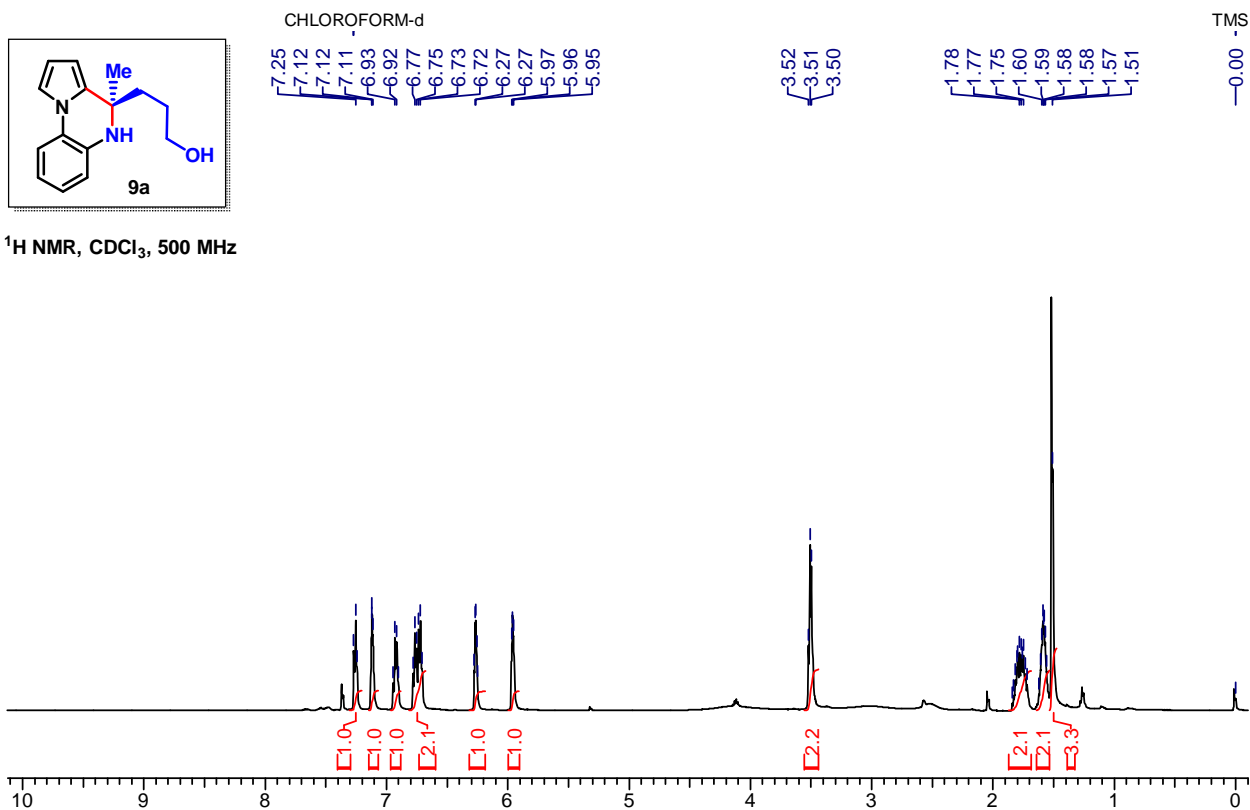


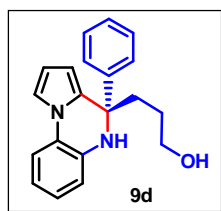
$^1\text{H NMR}$, CDCl_3 , 400 MHz



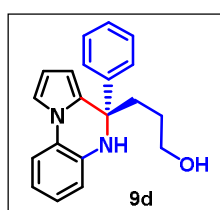
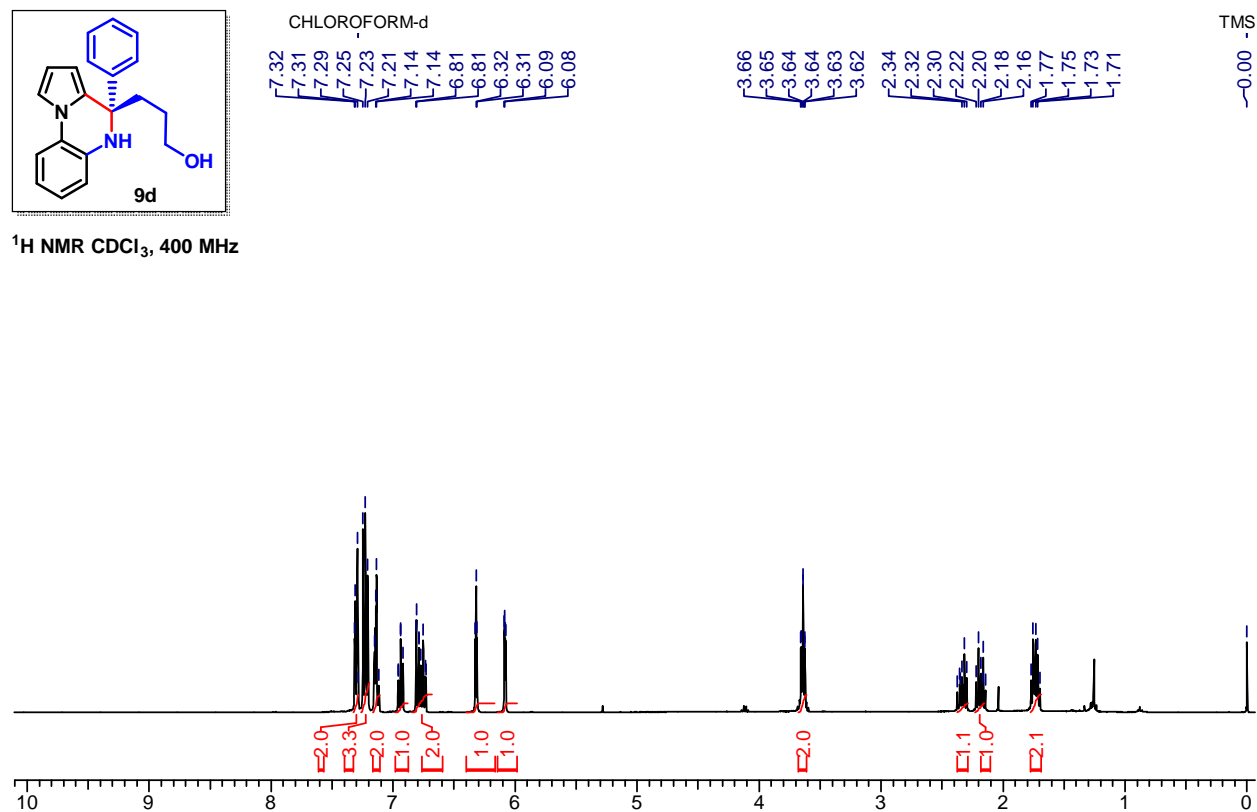
$^{13}\text{C NMR}$, CDCl_3 , 100 MHz



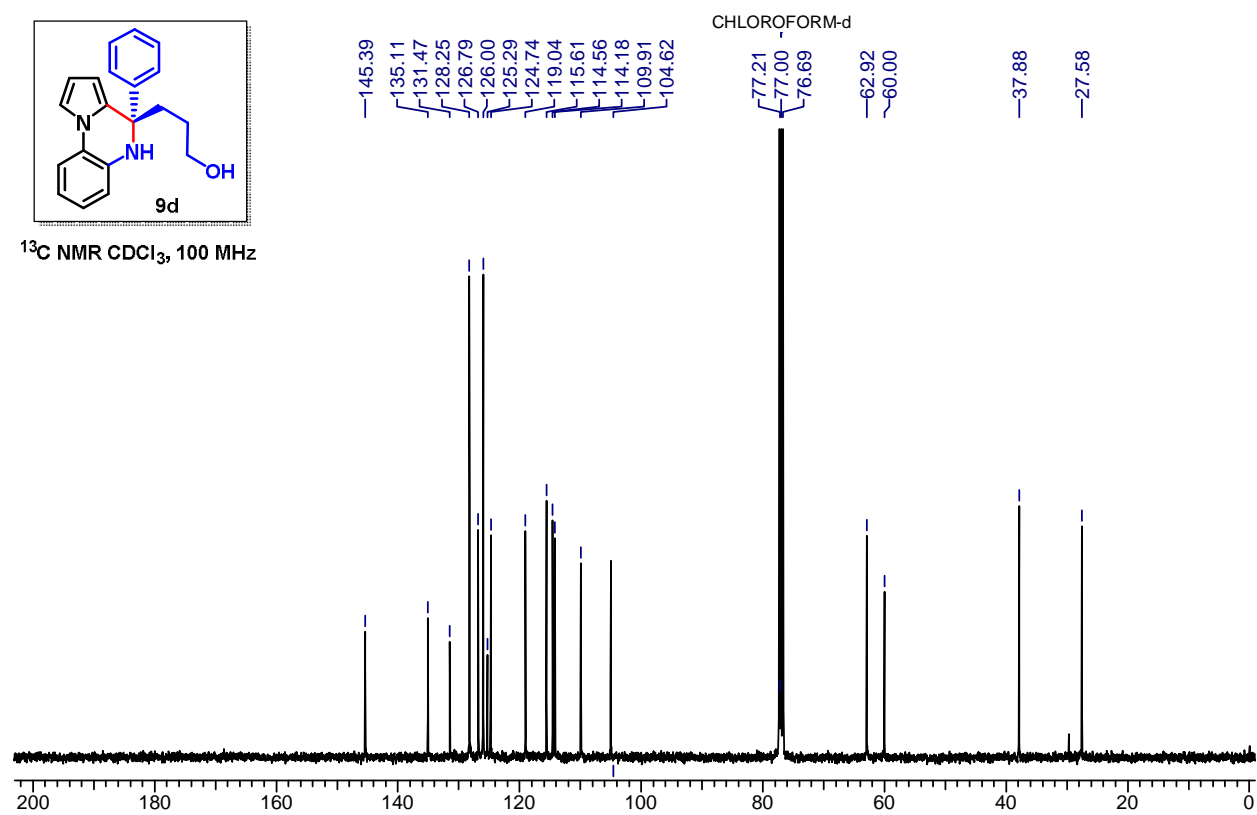


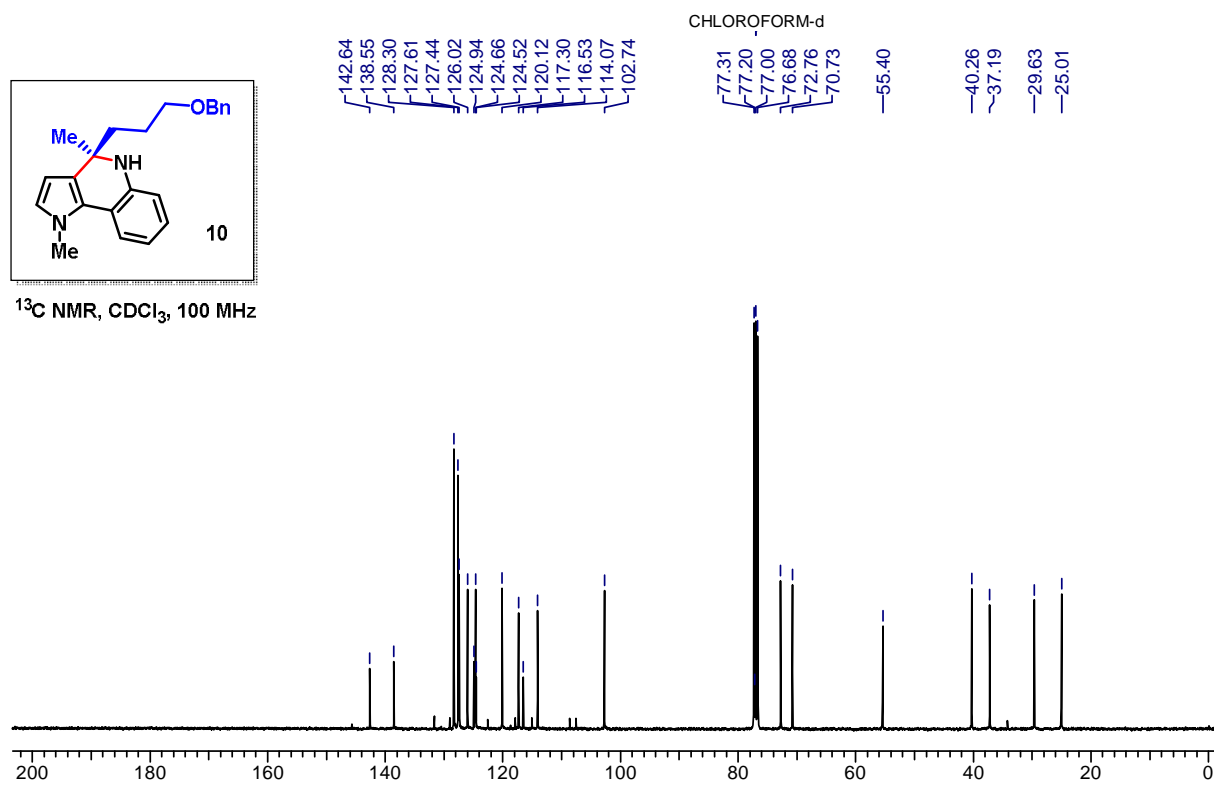
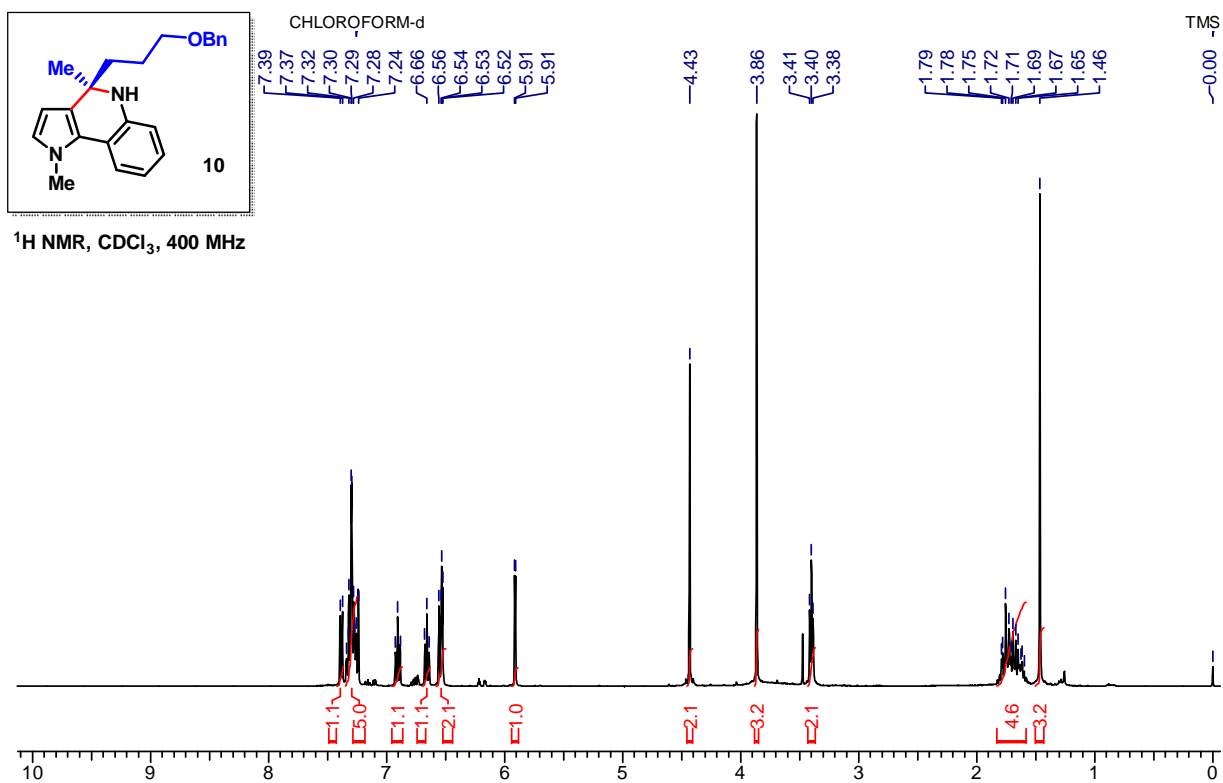


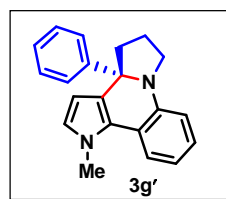
$^1\text{H NMR CDCl}_3$, 400 MHz



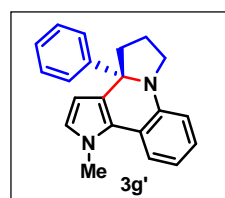
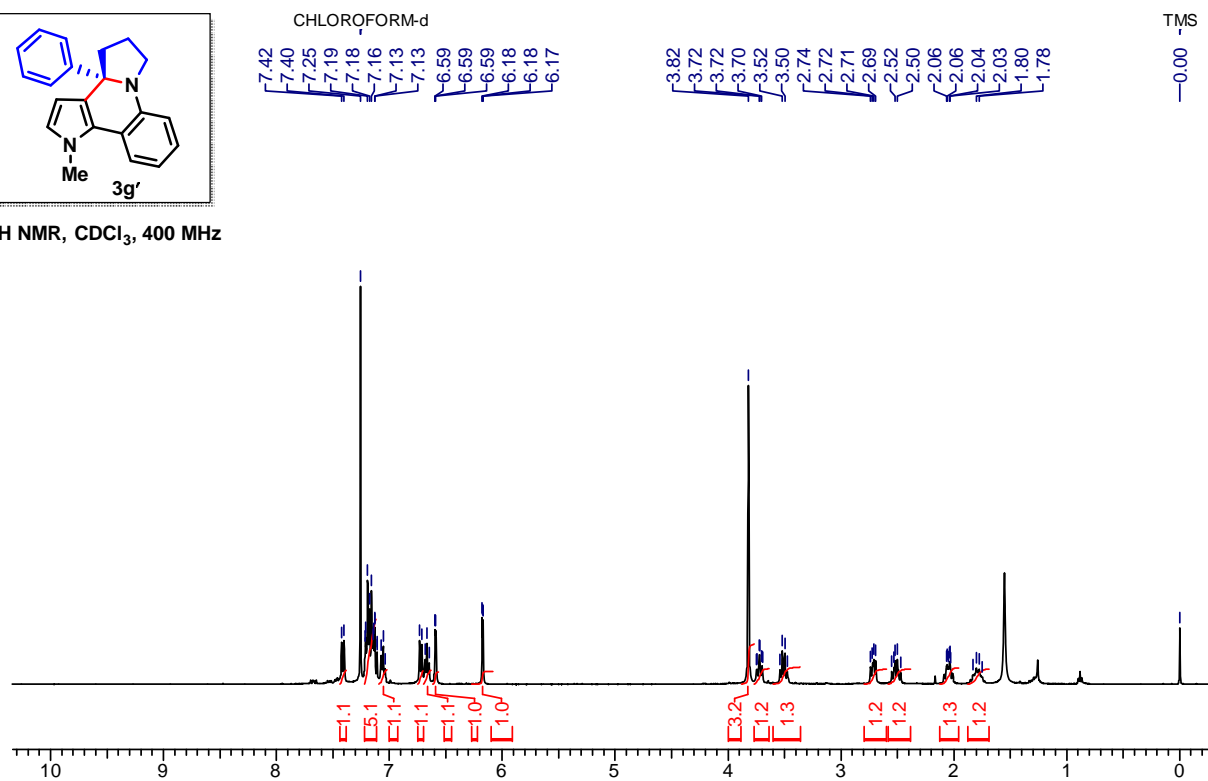
$^{13}\text{C NMR CDCl}_3$, 100 MHz



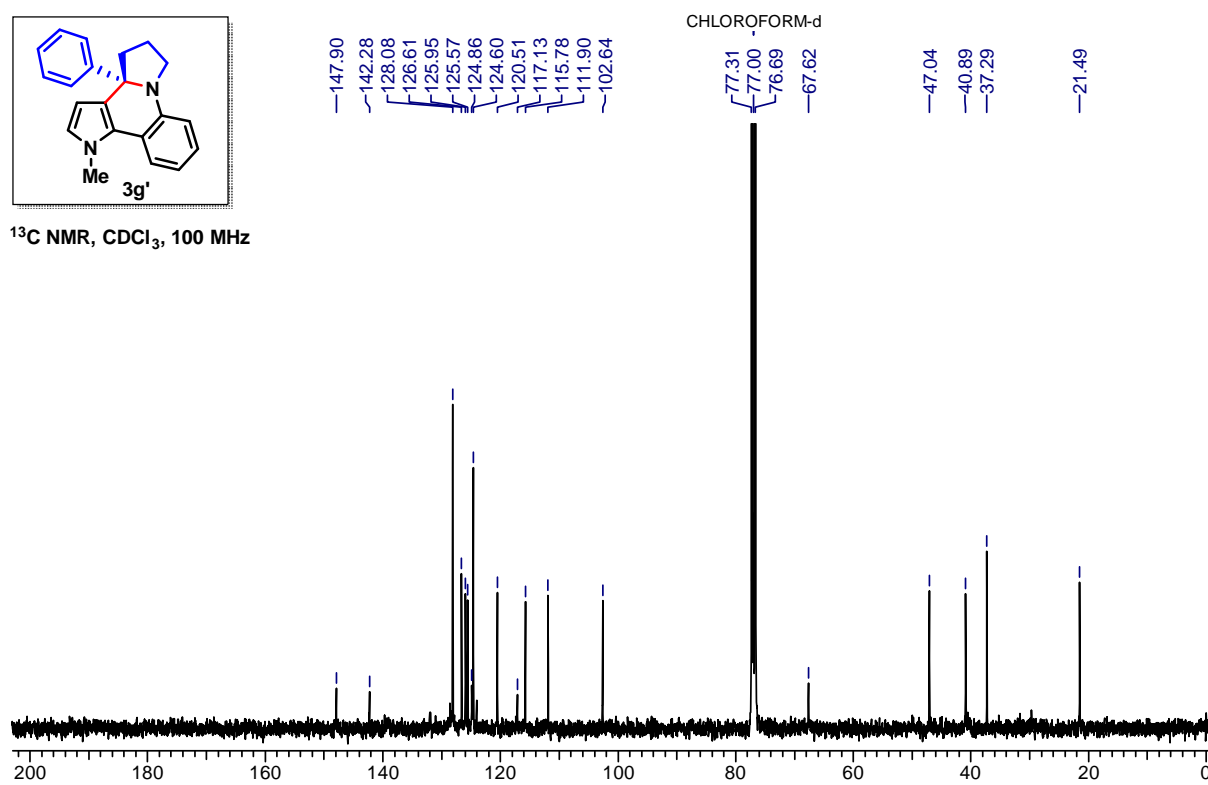




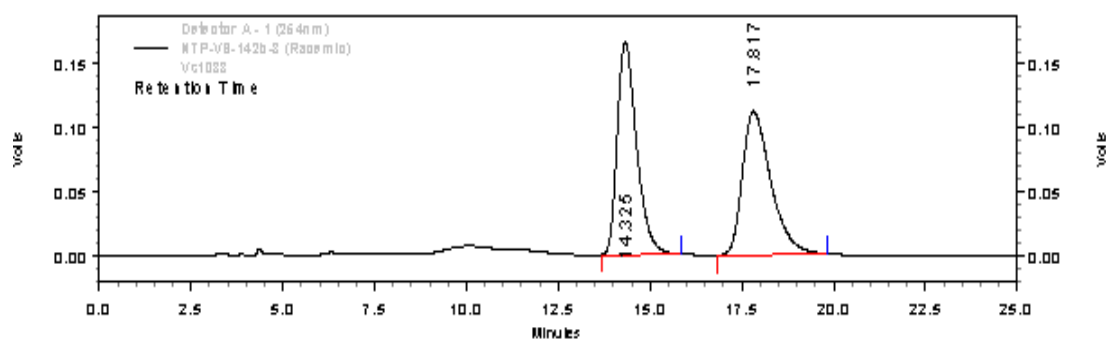
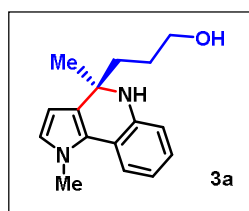
$^1\text{H NMR}$, CDCl_3 , 400 MHz



$^{13}\text{C NMR}$, CDCl_3 , 100 MHz

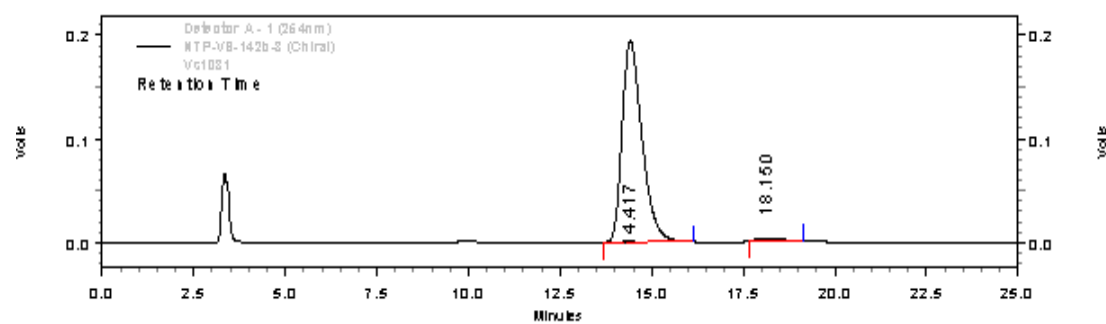


3.9 HPLC Chromatograms



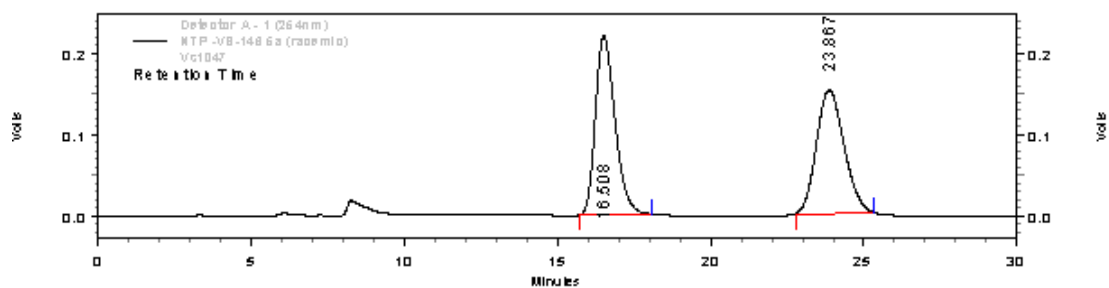
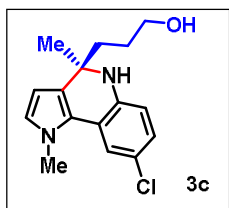
Retention Time	C Area	Area %
14.325	3074689	50.293
17.817	3038830	49.707

Totals	6113519	100.000
--------	---------	---------

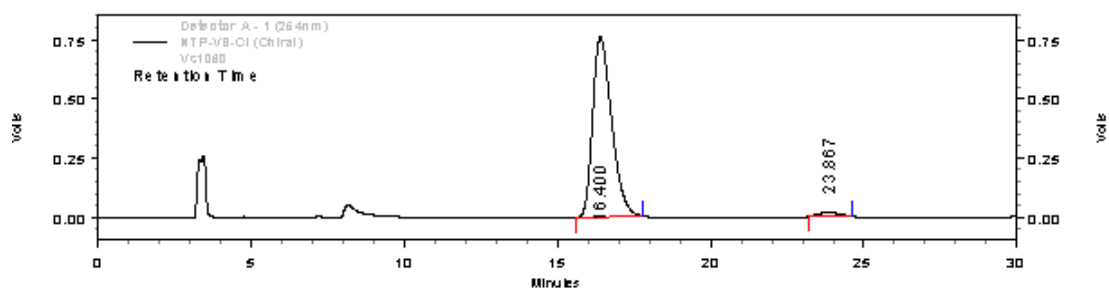


Retention Time	C Area	Area %
14.417	3714306	99.378
18.150	23235	0.622

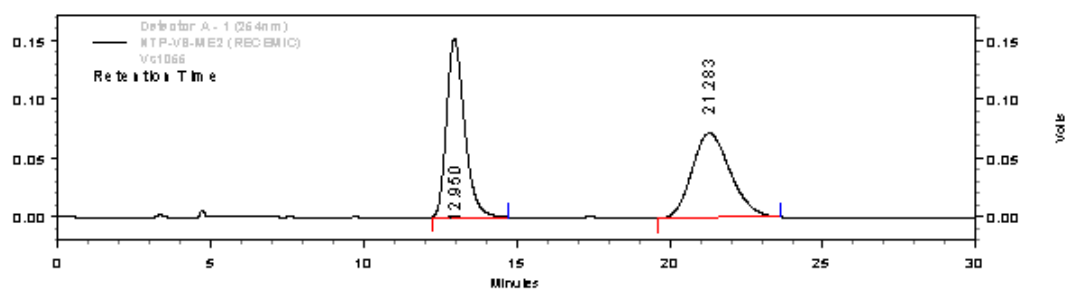
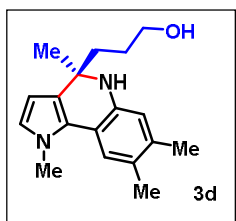
Totals	3737541	100.000
--------	---------	---------



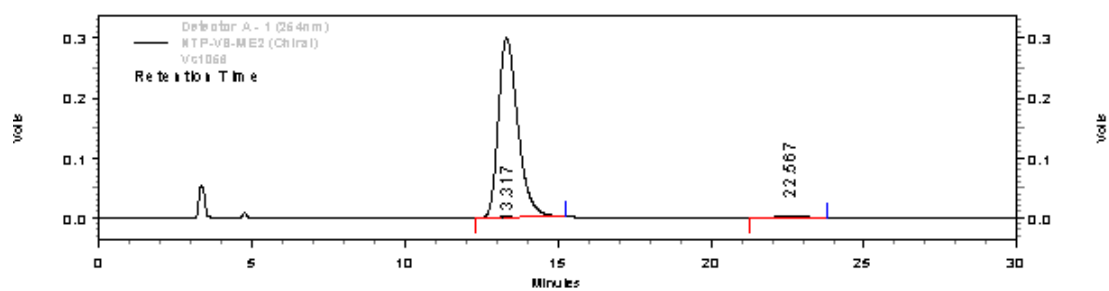
Detector A - 1 (254nm)		
Retention Time	C Area	Area %
16.508	4887388	50.617
23.867	4768207	49.383
Totals	9655595	100.000



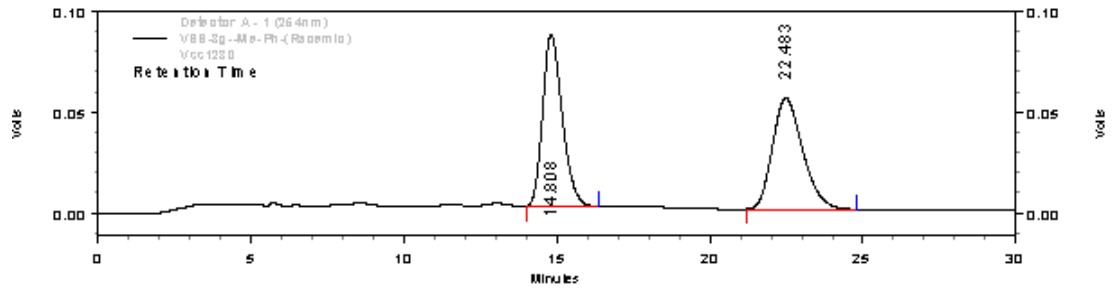
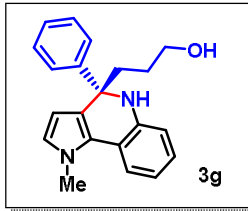
Detector A - 1 (254nm)		
Retention Time	C Area	Area %
16.400	16468617	97.507
23.867	420978	2.493
Totals	16889595	100.000



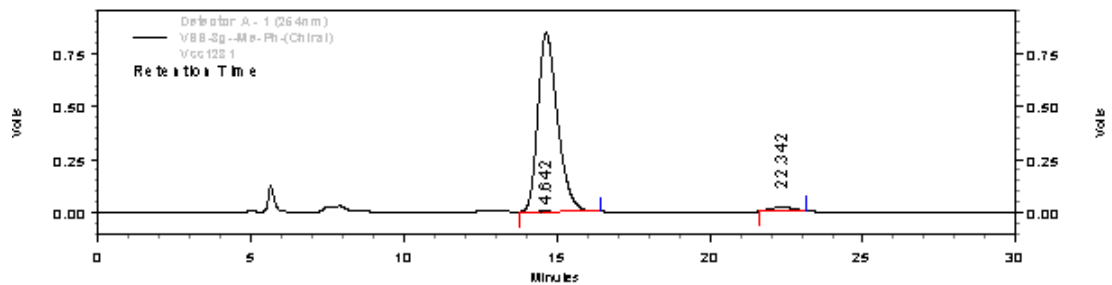
Detector A - 1 (254nm)		
Retention Time	C Area	Area %
12.950	3133470	49.925
21.283	3142887	50.075
Totals	6276357	100.000



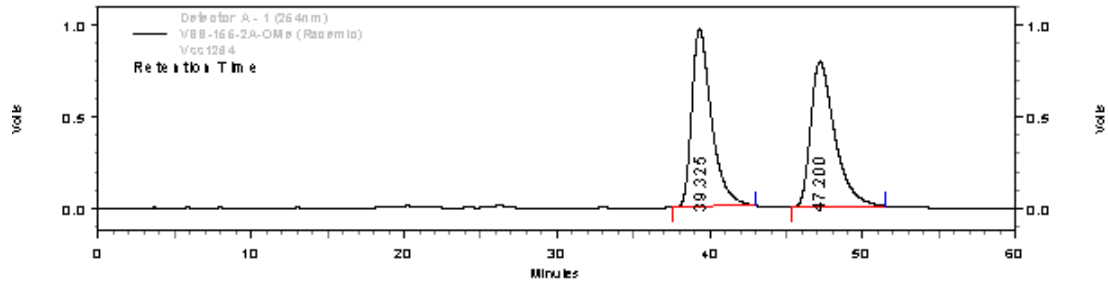
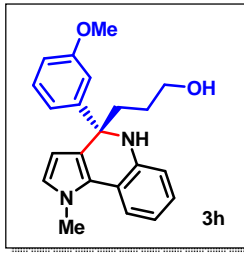
Detector A - 1 (254nm)		
Retention Time	C Area	Area %
13.317	6654305	99.478
22.567	34944	0.522
Totals	6689249	100.000



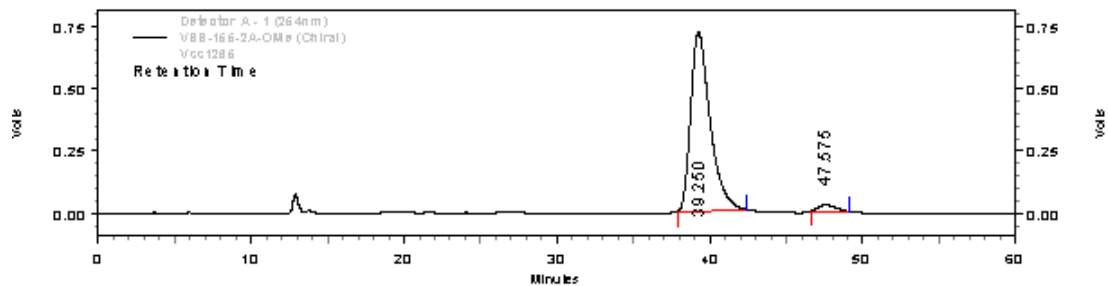
Detector A - 1 (254nm)			
Retention Time	C Area	Area %	
14.808	1905458	50.042	
22.483	1902289	49.958	
Totals	3807747	100.000	



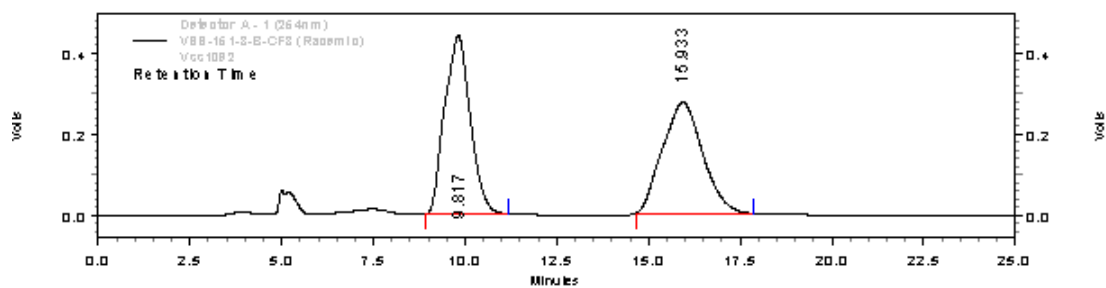
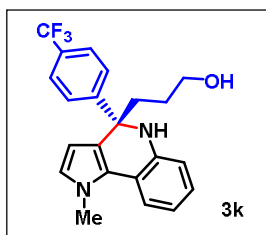
Detector A - 1 (254nm)			
Retention Time	C Area	Area %	
14.642	18930101	97.704	
22.342	444770	2.296	
Totals	19374871	100.000	



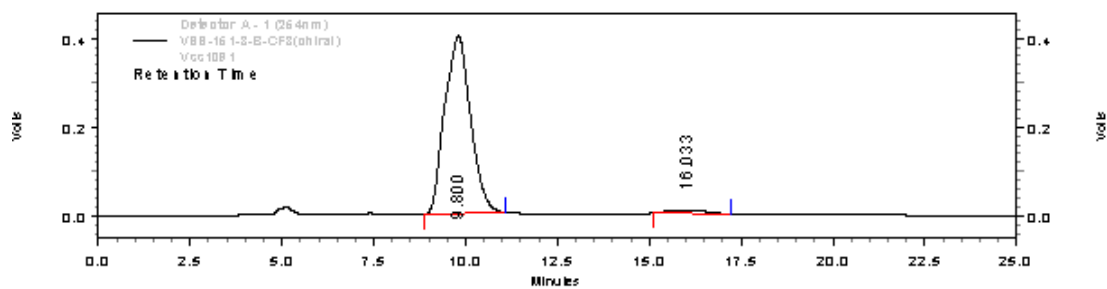
Detector A - 1 (254nm)			
Retention Time	C Area	Area %	
39.325	43505111	49.949	
47.200	43594672	50.051	
Totals		87099783	100.000



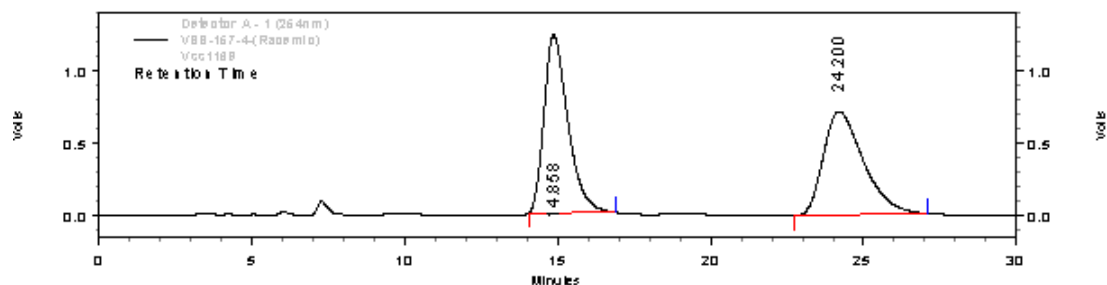
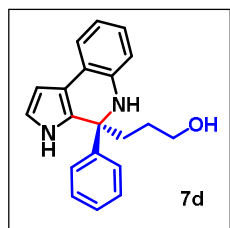
Detector A - 1 (254nm)			
Retention Time	C Area	Area %	
39.250	31630607	96.861	
47.575	1024928	3.139	
Totals		32655535	100.000



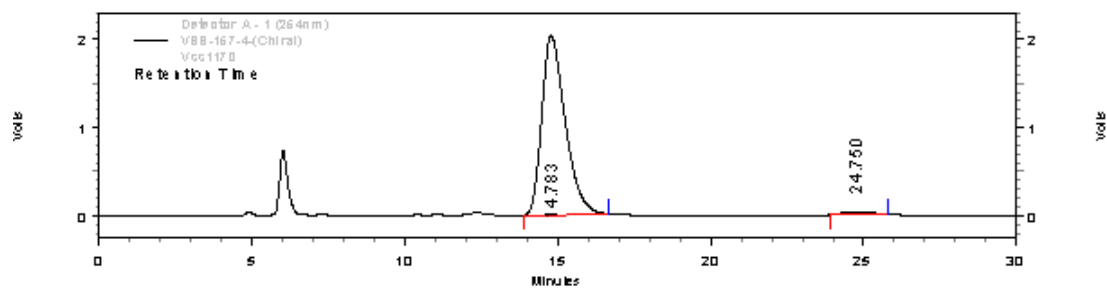
Detector A - 1 (254nm)		
Retention Time	C Area	Area %
9.817	10713527	50.565
15.933	10474056	49.435
Totals	21187583	100.000



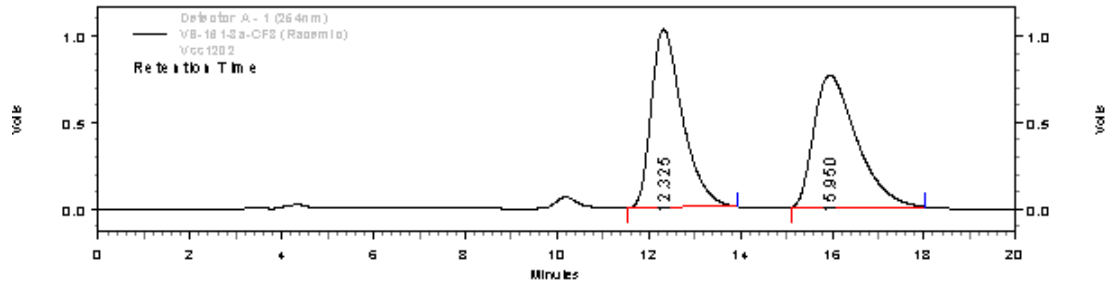
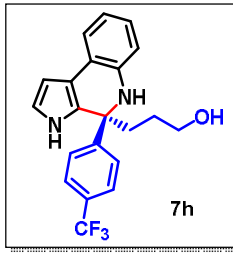
Detector A - 1 (254nm)		
Retention Time	C Area	Area %
9.800	9793184	97.285
16.033	273322	2.715
Totals	10066506	100.000



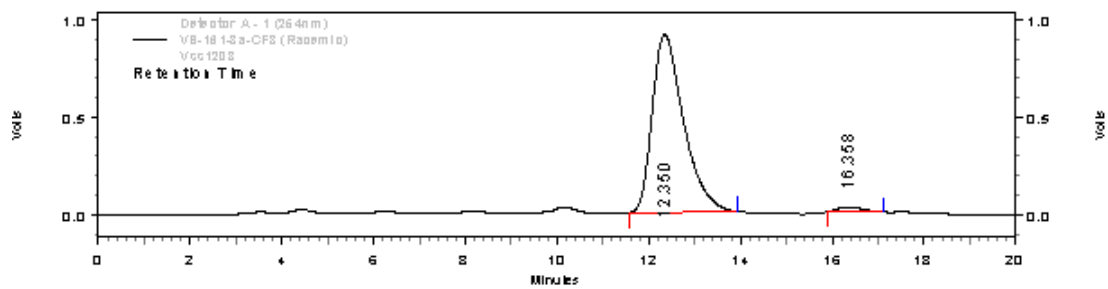
Detector A - 1 (254nm)		
Retention Time	C Area	Area %
14.858	33431941	50.537
24.200	32721000	49.463
Totals	66152941	100.000



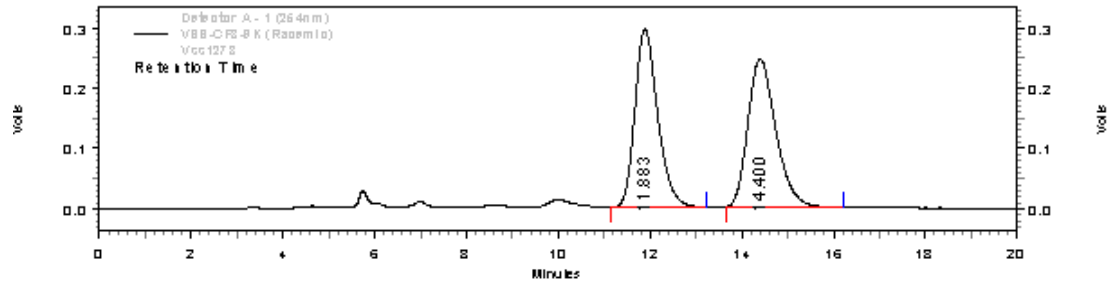
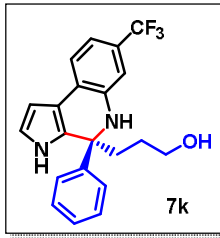
Detector A - 1 (254nm)		
Retention Time	C Area	Area %
14.783	54122881	98.219
24.750	981204	1.781
Totals	55104085	100.000



Detector A - 1 (254nm)		
Retention Time	C Area	Area %
12.325	24423586	49.681
15.950	24736765	50.319
Totals		49160351
		100.000

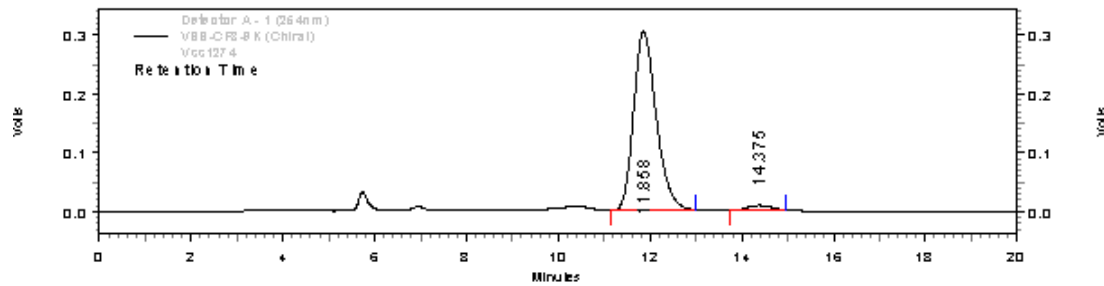


Detector A - 1 (254nm)		
Retention Time	C Area	Area %
12.350	21736488	98.011
16.358	441051	1.989
Totals		22177539
		100.000



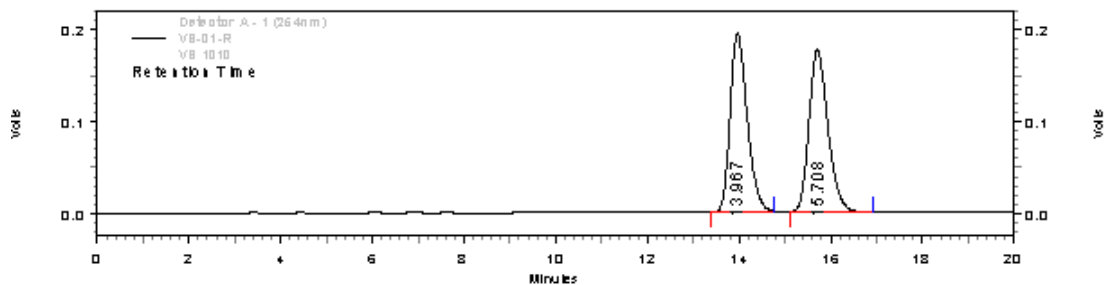
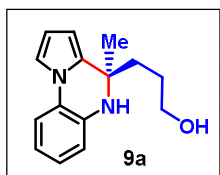
Detector A - 1 (254nm)		
Retention Time	C Area	Area %
11.883	5141355	49.639
14.400	5216204	50.361

Totals	10357559	100.000
--------	----------	---------

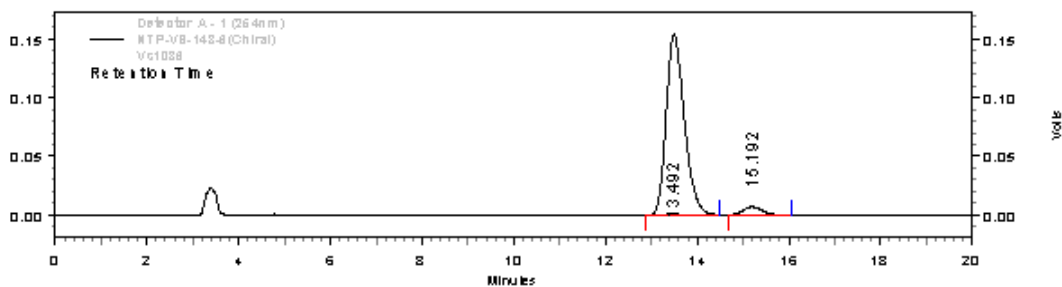


Detector A - 1 (254nm)		
Retention Time	C Area	Area %
11.858	5226463	97.244
14.375	148122	2.756

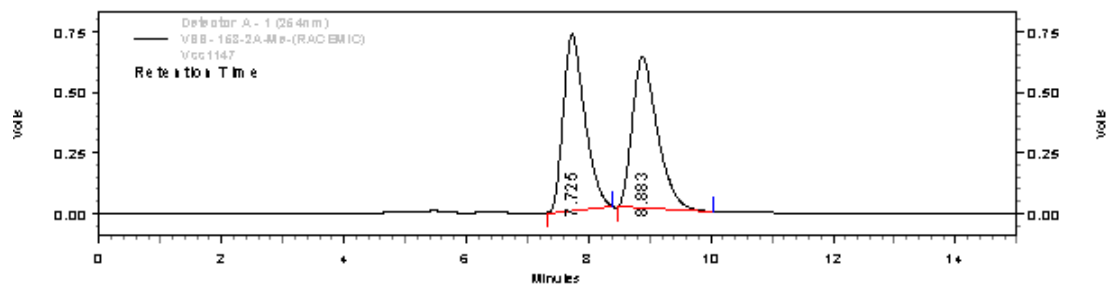
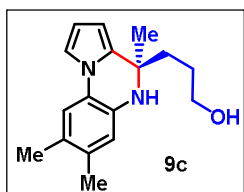
Totals	5374585	100.000
--------	---------	---------



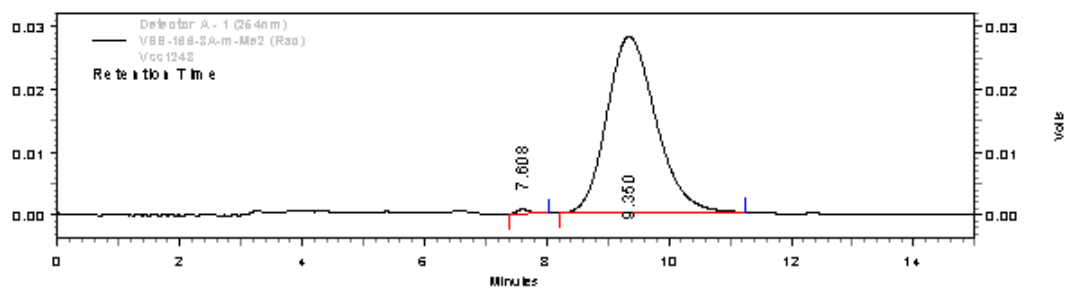
Detector A - 1 (254nm)		
Retention Time	C Area	Area %
13.967	2524193	49.872
15.708	2537148	50.128
Totals	5061341	100.000



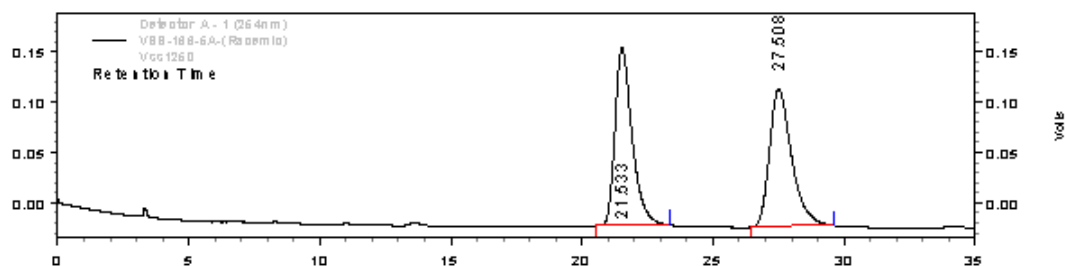
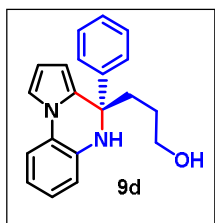
Detector A - 1 (254nm)		
Retention Time	C Area	Area %
13.492	2096921	96.653
15.192	72610	3.347
Totals	2169531	100.000



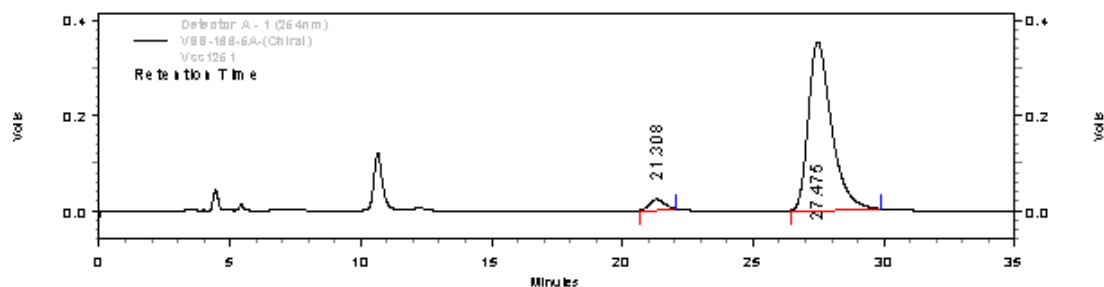
Detector A - 1 (254nm)		
Retention Time	C Area	Area %
7.725	8872057	49.919
8.883	8900994	50.081
Totals	17773051	100.000



Detector A - 1 (254nm)		
Retention Time	C Area	Area %
7.608	5162	0.657
9.350	781015	99.343
Totals	786177	100.000



Detector A - 1 (254nm)		
Retention Time	C Area	Area %
21.533	4012137	49.899
27.508	4028313	50.101
Totals	8040450	100.000



Detector A - 1 (254nm)		
Retention Time	C Area	Area %
21.308	431616	3.826
27.475	10848601	96.174
Totals	11280217	100.000

3.10 References

-
- [1] Grandberg, K. I.; Dyadchenko, V. P. *J. Organomet. Chem.* **1994**, *474*, 1.
- [2] Sengupta, S.; Shi, X. *ChemCatChem.* **2010**, *2*, 609–619.
- [3] Hamilton, G. L.; Kang, E. J.; Mba, M.; Toste, F. D. *Science*, **2007**, *317*, 496–499.
- [4] Han, Z.-Y.; Xiao, H.; Chen, X.-H.; Gong, L.-Z. *J. Am. Chem. Soc.* **2009**, *131*, 9182–9183.
- [5] Mizushima, E.; Hayashi, T.; Tanaka, M. *Org. Lett.* **2003**, *5*, 3349–3352.
- [6] Tamaki, A.; Magennis, S. A.; Kochi, J. K. *J. Am. Chem. Soc.* **1974**, *96*, 6140–6148.
- [7] Liu, X.-Y.; Che, C.-M. *Org. Lett.* **2009**, *11*, 4204–4207.
- [8] Muratore, M. E.; Holloway, C. A.; Pilling, A. W.; Storer, R. I.; Trevitt, G.; Dixon, D. J. *J. Am. Chem. Soc.* **2009**, *131*, 10796–10797.
- [9] Wang, C.; Han, Z.-Y.; Luo, H.-W.; Gong, L.-Z. *Org. Lett.* **2010**, *12*, 2266–2269.
- [10] Raducan, M.; Moreno, M.; Boura, C.; Echavarren, A. M. *Chem. Commun.* **2012**, *48*, 52–54.
- [11] Patil, N. T.; Mutyala, A. K.; Konala, A.; Tella, R. B. *Chem. Commun.* **2012**, *48*, 3094–3096.
- [12] (a) Rueping, M.; Antonchick, A. P.; Sugiono E.; Grenader, K. *Angew. Chem. Int. Ed.* **2009**, *48*, 908–910; (b) Cheng, X.; Vellalath, S.; Goddard R.; List, B. *J. Am. Chem. Soc.* **2008**, *130*, 15786–15787.
- [13] Patil, N. T.; Raut, V. S.; Tella, R. B. *Chem. Commun.* **2013**, *49*, 570–572.
- [14] Reviews: (a) Patil, N. T.; Kavthe R. D.; Shinde, V. S. *Tetrahedron* **2012**, *68*, 8079–8146; (b) Chemler, S. R. *Org. Biomol. Chem.* **2009**, *7*, 3009–3019; (c) Muller, T. E.; Hultsch, K. C.; Yus, M.; Foubelo F.; Tada, M. *Chem. Rev.* **2008**, *108*, 3795–3892; (d) Aillaud, I.; Collin, J.; Hannedouche J.; Schulz, E. *Dalton Trans.*, **2007**, 5105–5118; (e) Widenhoefer R. A.; Han, X. *Eur. J. Org. Chem.* **2006**, 4555–4563; (f) Hultsch, K. C. *Org. Biomol. Chem.* **2005**, *3*, 1819–1824; (g) Hultsch, K. C. *Adv. Synth. Catal.* **2005**, *347*, 367–391.
- [15] Selected papers: (a) Michon, C.; Medina, F.; Abadie M.-A.; Agbossou-Niedercorn, F. *Organometallics* **2013**, *32*, 5589–5600; (b) Teller, H.; Corbet, M.; Mantilli, L.; Gopakumar, G.; Goddard, R.; Thiel W.; Fürstner, A. *J. Am. Chem. Soc.* **2012**, *134*, 15331–15342; (c) Butler, K. L.; Tragni, M.; Widenhoefer, R. A. *Angew. Chem. Int. Ed.* **2012**, *51*, 5175–5178; (d) LaLonde, R. L.; Wang, Z. J.; Mba, M.; Lackner A. D.; Toste,

- F. D. *Angew. Chem. Int. Ed.* **2010**, *49*, 598–601; (e) Zhang, Z.; Lee S. D.; Widenhoefer, R. A. *J. Am. Chem. Soc.* **2009**, *131*, 5372–5373; (f) LaLonde, R. L.; Sherry, B. D.; Kang, E. J.; Toste, F. D. *J. Am. Chem. Soc.* **2007**, *129*, 2452–2453; (g) Hamilton, G. L.; Kang, E. J.; Mba M.; Toste, F. D. *Science*, 2007, **317**, 496–499.
- [16] (a) Patil, N. T.; Lakshmi, P. G. V. V.; Singh, V. *Eur. J. Org. Chem.* **2010**, 4719–4731; (b) Yi, C. S.; Yun, S. Y. *J. Am. Chem. Soc.* **2005**, *127*, 17000–17006.
- [17] Selected reviews on Au-catalysis: (a) Patil, N. T. *Chem. Asian J.* **2012**, *7*, 2186–2194; (b) Dudnik, A. S.; Chernyak, N.; Gevorgyan, V. *Aldrichimica Acta* **2010**, *43*, 37–46; (c) Gorin, D. J.; Sherry, B. D.; Toste, F. D. *Chem. Rev.* **2008**, *108*, 3351–3378; (d) Li, Z.; Brouwer C.; He, C. *Chem. Rev.* **2008**, *108*, 3239–3265; (e) Arcadi, A. *Chem. Rev.* **2008**, *108*, 3266–3325; (f) Jiménez-Núñez E.; Echavarren, A. M. *Chem. Rev.* **2008**, *108*, 3326–3350; (g) Hashmi A. S. K.; Rudolph, M. *Chem. Soc. Rev.* **2008**, *37*, 1766–1775; (h) Fürstner A.; Davies, P. W. *Angew. Chem. Int. Ed.* **2007**, *46*, 3410–3449.
- [18] (a) Pradal, A.; Toullec, P. Y.; Michelet, V. *Synthesis*, **2011**, 1501–1514; (b) Sengupta, S.; Shi, X. *ChemCatChem*, **2010**, *2*, 609–619; (c) Widenhoefer, R. A. *Chem. Eur. J.* **2008**, *14*, 5382–5391; (d) Bongers N.; Krause, N. *Angew. Chem. Int. Ed.* **2008**, *47*, 2178–2181.
- [19] Kojima, M.; Mikami, K. *Chem. Eur. J.* **2011**, *17*, 13950–13953.
- [20] (a) Gorin, D. J.; Toste, F. D. *Nature* **2007**, *446*, 395–403; (b) Yamamoto, Y. *J. Org. Chem.* **2007**, *72*, 7817–7831.
- [21] Reviews: (a) Loh, C. C. J.; Enders, D. *Chem.–Eur. J.* **2012**, *18*, 10212–10225; (b) Han, Z.-Y.; Wang, C.; Gong, L.-Z. In *Science of Synthesis, Asymmetric Organocatalysis*; List, B.; Maruoka, K. Eds.; Georg Thieme Verlag: Stuttgart, **2011**; section 2.3.6; (c) Hashmi A. S. K.; Hubbert, C. *Angew. Chem. Int. Ed.* **2010**, *49*, 1010–1012. Other Selected examples: (d) Han, Z.-Y.; Xiao, H.; Chen X.-H.; Gong, L.-Z. *J. Am. Chem. Soc.* **2009**, *131*, 9182–9183; (e) Han, Z.-Y.; Guo, R.; Wang, P.-S.; Chen, D.-F.; Xiao, H.; Gong, L.-Z. *Tetrahedron Lett.* **2011**, *52*, 5963–5967; (f) Wang, C.; Han, Z.-Y.; Luo H.-W.; Gong, L.-Z. *Org. Lett.* **2010**, *12*, 2266–2269; (g) Patil, N. T.; Mutyala, A. K.; Konala, A.; Tella, R. B. *Chem. Commun.* **2012**, *48*, 3094–3096; (h) Patil, N. T.; Raut, V. S.; Tella, R. B. *Chem. Commun.* **2013**, *49*, 570–572; (i) Wang, P.-S.; Li, K.-N.; Zhou, X.-L.; Wu, X.; Han, Z.-Y.; Guo, R.; Gong, L.-Z. *Chem. –Eur. J.* **2013**, *19*, 6234–6238.

- [20] Raducan, M.; Moreno, M.; Bour C.; Echavarren, A. M. *Chem. Commun.* **2012**, *48*, 52–54.
- [23] Reviews on enantioselective Brønsted acid catalysis, see: (a) Patil, N. T.; Mutyala, A. K. *Org. Chem. Front.* **2014**, *1*, 582–586; (b) Zamfir, A.; Schenker, S.; Freund, M.; Tsogoeva, S. B. *Org. Biomol. Chem.* **2010**, *8*, 5262–5276; (c) Akiyama, T. *Chem. Rev.* **2007**, *107*, 5744–5758; (d) Terada, M. *Chem. Commun.* **2008**, 4097–4112; (e) Terada, M. *Bull. Chem. Soc. Jpn.* **2010**, *83*, 101–119; (f) Kampen, D.; Reisinger, C. M.; List, B. *Top. Curr. Chem.* **2010**, *291*, 395–456.
- [24] (a) Patil, N. T.; Kavthe, R. D.; Shinde, V. S.; Sridhar, B. *J. Org. Chem.* **2010**, *75*, 3371–3380; (b) Patil, N. T.; Kavthe, R. D.; Raut, V. S.; Reddy, V. V. N. *J. Org. Chem.* **2009**, *74*, 6315–6318.
- [25] (a) Mittal, N.; Sun, D. X.; Seidel, D. *Org. Lett.* **2014**, *16*, 1012–1015; (b) Li, Y.; Su, Y.-H.; Dong, D.-J.; Wua, Z.; Tian, S.-K. *RSC Adv.* **2013**, *3*, 18275–18278; (c) Huang, D.; Xu, F.; Lin, X.; Wang, Y. *Chem. Eur. J.* **2012**, *18*, 3148–3152; (d) He, Y.; Lin, M.; Li, Z.; Liang, X.; Li, G.; Antilla, J. C. *Org. Lett.* **2011**, *13*, 4490–4493; (e) Cheng, D.-J.; Wu, H.-B.; Tian, S.-K. *Org. Lett.* **2011**, *13*, 5636–5639. (f) Klausen, R. S.; Jacobsen, E. N.; *Org. Lett.* **2009**, *11*, 887–889; (g) Sewgobind, N.; Wanner, M. J.; Ingemann, S.; de Gelder, R.; van Maarseveen, J. H.; Hiemstra, H. *J. Org. Chem.* **2008**, *73*, 6405–6408; (h) Wanner, M. J.; van der Haas, R. N. S.; de Cuba, K. R.; Van Maarseveen, J. H.; Hiemstra, H. *Angew. Chem., Int. Ed.* **2007**, *46*, 7485–7487; (i) Seayad, J.; Seayad, A. M.; List, B. *J. Am. Chem. Soc.* **2006**, *128*, 1086–1087; (j) Taylor, M. S.; Jacobsen, E. N. *J. Am. Chem. Soc.* **2004**, *126*, 10558–10559.
- [26] Trost, B. M.; Jiang, C. *Synthesis* **2006**, 369–396.
- [27] (a) Gregory, A. W.; Jakubec, P.; Turner, P.; Dixon, D. J. *Org. Lett.* **2013**, *15*, 4330–4333; (b) Aillaud, I.; Barber, D. M.; Thompson, A. L.; Dixon, D. J. *Org. Lett.* **2013**, *15*, 2946–2949; (c) Muratore, M. E.; Holloway, C. A.; Pilling, A. W.; Storer, R. I.; Trevitt, G.; Dixon, D. J. *J. Am. Chem. Soc.* **2009**, *131*, 10796–10797; (d) Muratore, M. E.; Shi, L.; Pilling, A. W.; Ian Storer, R.; Dixon, D. J. *Chem. Commun.* **2012**, *48*, 6351–6353; (e) Raheem, I. T.; Thiara, P. S.; Jacobsen, E. N. *Org. Lett.* **2008**, *10*, 1577–1580; (f) Raheem, I. T.; Thiara, P. S.; Peterson, E. A.; Jacobsen, E. N. *J. Am. Chem. Soc.* **2007**, *129*, 13404–13405.

-
- [28] (a) Li, X.; Chen, D.; Gu, H.; Lin, X. *Chem. Commun.* **2014**, *50*, 7538–7541; (b) Schönherr, H.; Leighton, J. L. *Org. Lett.* **2012**, *14*, 2610–2613; (c) Lee, Y.; Klausen, R. S.; Jacobsen, E. N.; *Org. Lett.* **2011**, *13*, 5564–5567; (d) Duce, S.; Pesciaioli, F.; Gramigna, L.; Bernardi, L.; Mazzanti, A.; Ricci, A.; Bartoli, G.; Bencivenni, G. *Adv. Synth. Catal.* **2011**, *353*, 860–864; (e) Badillo, J. J.; Silva-García, A.; Shupe, B. H.; Fettingner, J. C.; Franz, A. K. *Tetrahedron Lett.* **2011**, *52*, 5550–5553; (f) Holloway, C. A.; Muratore, M. E.; Storer, R. I.; Dixon, D. J. *Org. Lett.* **2010**, *12*, 4720–4723; (g) Bou Hamdan, F. R.; Leighton, J. L. *Angew. Chem. Int. Ed.* **2009**, *48*, 2403–2406.
- [29] Patil, N. T.; Shinde, V. S.; Gajula, B. *Org. Biomol. Chem.* **2012**, *10*, 211–224.
- [30] Patil, N. T.; Shinde, V. S.; Sridhar, B. *Angew. Chem. Int. Ed.* **2013**, *52*, 2251–2255.
- [31] Stöckigt, J.; Antonchick, A. P.; Wu, F.; Waldmann, H. *Angew. Chem. Int. Ed.* **2011**, *50*, 8538–8564.

Development of Highly Selective Fluorescent Probe (Chemosensor) for Detection of Gold Ions

Table of Contents

4.1 Introduction	208
4.2 Hypothesis	214
4.3 Results and Discussion.....	215
4.3.1 Studies of UV-Visible Absorption Changes.....	217
4.3.2 Studies of Fluorescence Spectrophotometric Changes	218
4.3.2 Studies of Specificity and Selectivity of Probe	220
4.4 Bioimaging Studies Using A549 Lung Cancer Cells.....	222
4.5 Conclusion.....	224
4.6 Experimental Procedures and Characterization Data.....	224
4.7 Spectra.....	230
4.8 References	235

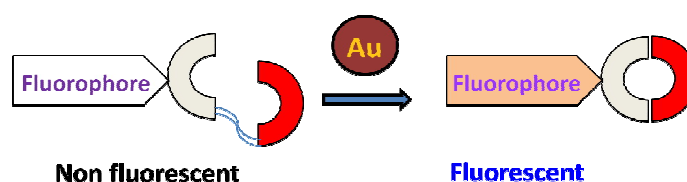
4.1 Introduction

The gold in elemental form is inert; however its salt exhibits some biological effects. For instance, gold ions have anti-inflammatory properties and are used as pharmaceuticals in the treatment of tuberculosis, arthritis, and cancer.¹ In addition, it is well established that gold ions are known as inhibitors of macrophages and polymorphonuclear leucocytes.² However, gold species may tightly bind to biomolecules such as enzymes and DNA, leading to toxicity to humans.³ Similarly, certain gold salts such as gold chloride are known to cause damage to the liver, kidneys, and the peripheral nervous system.⁴ Based on sharp increase in gold catalysis and toxicity associated with gold ions, it is essential to develop a chemosensor to monitor the presence of gold species both in the environment and under physiological conditions.

Chemosensors or chemical probes are valuable tools for the investigation of biochemical processes, diagnosis of disease markers, detection of hazardous compounds, and other purposes. Therefore, the development of chemical probes continues to grow through various approaches with different disciplines and designed strategies. Fluorescent probes have received much attention because they are sensitive and easy-to-operate, in general. To realize desired selectivity toward a given analytes, the recognition site of a fluorescent probe is designed in such a way to maximize the binding interactions, usually through weak molecular forces such as hydrogen bonding, toward the analyte over other competing ones or by functional group modifications by carrying our various chemical transformations. In general, the development of chemosensor for the detection of gold is based on two approaches.

(A) Reaction Based Approaches

Figure 4.1: Pictorial representation of reaction based approaches

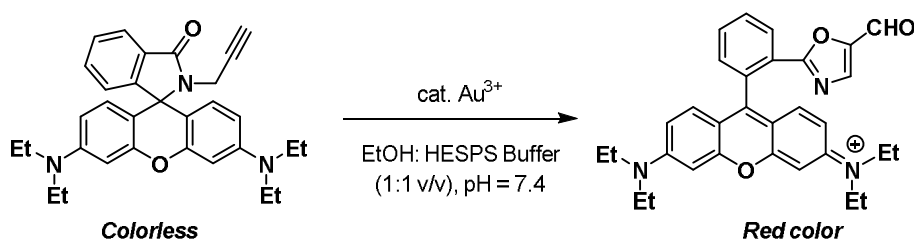


Various turn-on fluorescent probes or chemosensors have been developed recently based on the chemical reactions between the probes and gold ions. The reaction-based probes provide unique and versatile means for investigating a wide range of gold ions present in

chemical and biological systems. This approach enables the probes with superior selectivity when specific chemical transformations are creatively coupled with turn-on photophysical properties of fluorophores. A nonfluorescent probe, consisting of a fluorophore and organic molecule, on reaction with gold species generates a new structure resulting in a change in the fluorescence intensity (Figure 1). Various chemical reactions have been implemented in the development of many reactive chemosensors with very high selectivity and sensitivity toward gold ions.

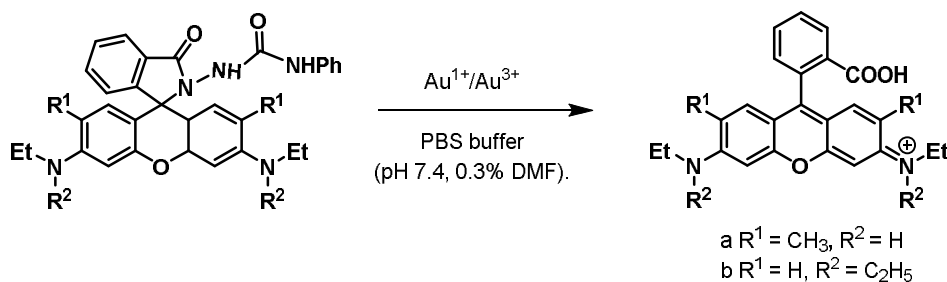
Concerning detection of gold ion Jou *et al.*, for the first time, reported Au^{3+} selective fluorescent probe based on cyclization of rhodamine-based propargylamide (Scheme 1).⁵ The probe displayed a high fluorescence enhancement and colorimetric change with Au^{3+} at pH 7.4, which is attributed to the transformation of propargylamide moiety to oxazolecarbaldehyde in the presence of Au^{3+} . The authors have also demonstrated its application in cell imaging for detection of Au^{3+} ions. Almost at the same time, Tae and coworkers disclosed rhodamine-based probe for detection of Au^{3+} species, based on intramolecular hydroamination.⁶ In the subsequent year, Ahn and coworkers⁷ suggested that major reaction product formylloxazole in this reaction was produced from a vinylgold intermediate.

Scheme 4.1: Detection of Au^{3+} ions based on cyclization of propargylamide



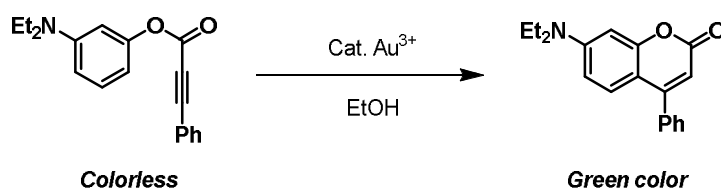
Lin and coworkers designed a fast responsive $\text{Au}^{1+}/\text{Au}^{3+}$ selective fluorescent probe based on hydrolysis of rhodamine-based acyl-semicarbazides to carboxylic acids at rt (Scheme 2).⁸ The probe has been applied for sensing gold ions in the living HeLa cells. Importantly, the authors have also demonstrated that residual Au^{3+} ions present in synthetic samples, that are prepared from gold-catalyzed reactions, can be rapidly detected by the fluorescent probe. In their subsequent paper, the authors have shown that not only gold ions but gold NPs can also be detected.⁹

Scheme 4.2: Detection of $\text{Au}^{1+}/\text{Au}^{3+}$ ions based on hydrolysis of rhodamine-based acyl-semicarbazides to carboxylic acids

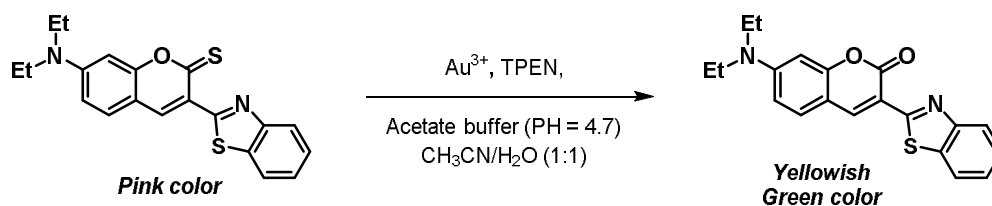


As shown in scheme 3, Do *et al.* developed Au^{3+} selective fluorescence turn-on probe based on intramolecular hydroarylation of phenyl alkynoates.¹⁰ The probe was designed in such a way that the dialkylamino group is located for the intramolecular hydroarylation reaction in the para position with a Michael acceptor, and the phenyl ester functionality is introduced to cause a proper push-pull electronic effect on the generated fluorophore.

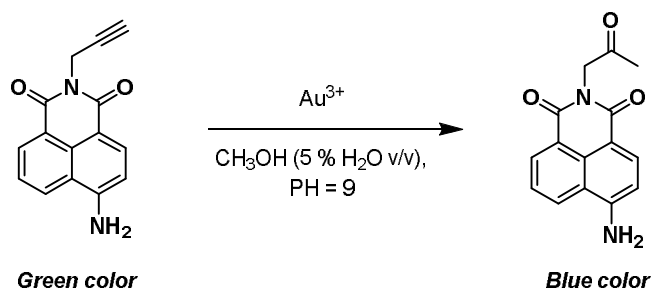
Scheme 4.3: Detection of Au^{3+} ions based on intramolecular hydroarylation of phenyl alkynoates



Chang and coworkers reported Au^{3+} selective probe based on desulfurization of thiocoumarin (Scheme 4).¹¹ In the presence of a heavy metal ion chelator *N,N,N,N*-tetrakis-(2-pyridylmethyl)ethylenediamine (TPEN), thiocoumarin was selectively converted to its oxo analogue by reaction with Au^{3+} , resulting in a pronounced chromogenic and fluorescent signalling. The colorimetric determination of Au^{3+} was possible by the color change from pink to yellowish green. The detection limit for the determination of Au^{3+} in 50% aq. acetonitrile was 1.1×10^{-7} M.

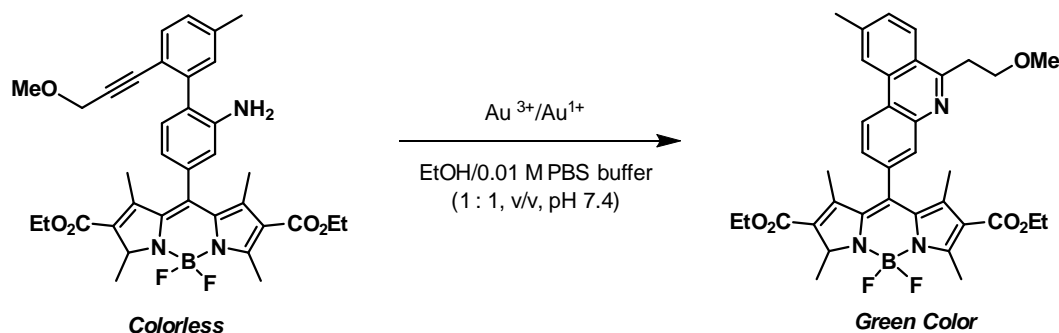
Scheme 4.4: Probe based on desulfurization of thiocoumarin

Peng and Wang developed highly selective ratiometric fluorescent probe for the selective recognition of Hg^{2+} and Au^{3+} ions.¹² The developed 1,8-naphthalimide based chemosensor tethered via an alkyne moiety underwent gold catalyzed alkyne hydration reaction. The ratiometric change from green to blue was also observed (Scheme 5).

Scheme 4.5: Ratiometric fluorescent probe for detection Au^{3+} ions based on hydration of alkyne

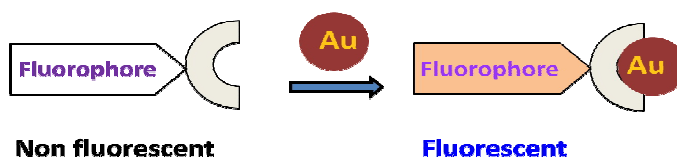
Song and coworkers disclosed fluorescent probe for $\text{Au}^{1+}/\text{Au}^{3+}$ ions based on intramolecular hydroamination of Bodipy-derived aminoalkynes (Scheme 6).¹³ The gold catalyzed hydroamination converts the electron donor aniline moiety, to phenanthridine, resulting in its loss of the electron-donating ability, thus blocking the intramolecular PET process to emit a strong green fluorescence.

Scheme 4.6: Au¹⁺/Au³⁺ ions Detection based on intramolecular hydroamination of Bodipy-derived aminoalkynes

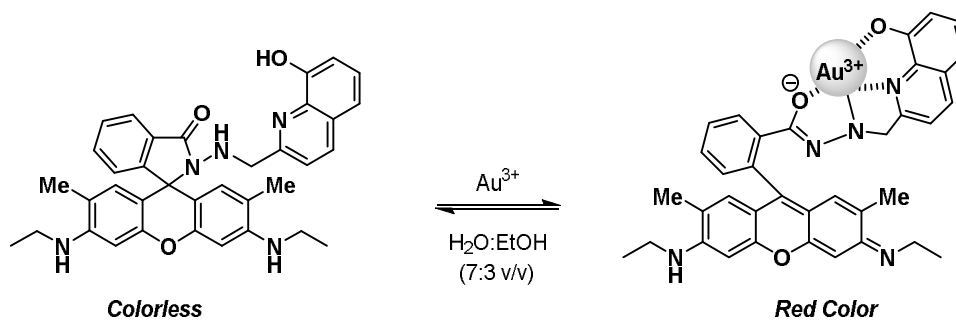


A) Complexation Based Approach

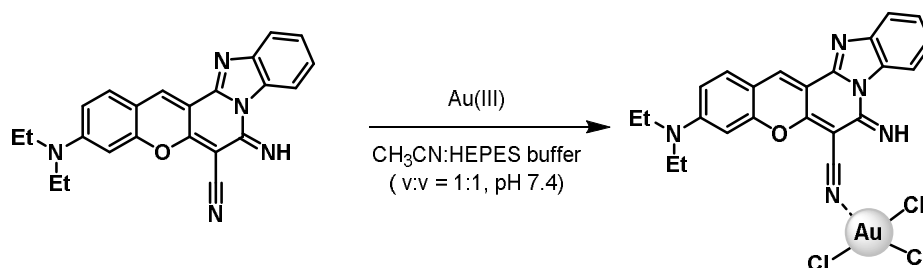
Figure 4.2: Pictorial representation of complexation based approach



The chemical reactions are driven by the host–guest interactions between receptor and analyte molecules, leading to the formation of supramolecular complexes. Such reactive probes provide higher selectivity with larger spectroscopic changes than chemical probes based on non-covalent interactions in most cases, owing to the structural changes from the chemical conversion. Thus complexation based approach wherein the nonfluorescent probe, containing a fluorophore and a gold ion receptor, binds with Au ions triggering change in the fluorescence intensity (Figure 2). For instance, Wang *et al.* developed selective and reversible rhodamine based fluorescent chemosensor for selective detection of Au³⁺ ions (Scheme 7).¹⁴ In addition, It demonstrated that developed chemosensor could be employed to image Au³⁺ in HeLa cells.

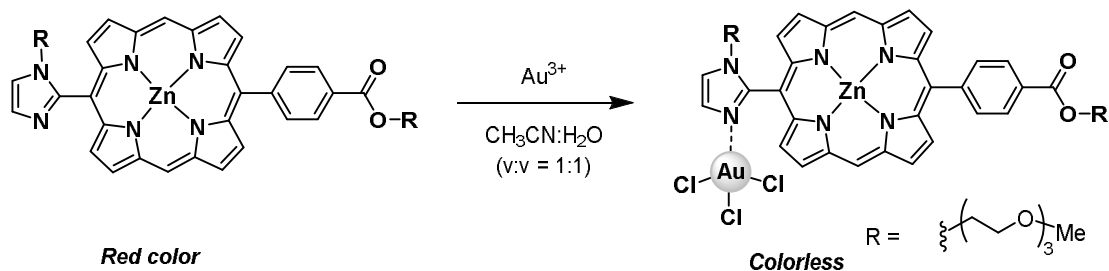
Scheme 4.7: Rhodamine based fluorescent chemosensor for selective detection of Au³⁺ ions

Yin and coworkers developed a highly selective fluorescence on-off fluorescent probe for Au³⁺ ion from commercially available luminescent Fluorol Red GK dye (Scheme 8).¹⁵ This approach was based on Au³⁺ coordination to cyano group of probe, resulting in fluorescence quenching in CH₃CN/HEPES buffer solution with good selectivity and sensitivity both fluorescence spectrophotometrically and visually. The FRGK-Au complex was confirmed by ESI-MS and also was successfully applied to fluorescence imaging in living cells.

Scheme 4.8: Fluorescent on-off probe based on Au³⁺ coordination with cyano group of FRGK dye.

Very recently, Campos, Jang and coworkers have designed an imidazole-bearing zinc porphyrin probe for the selective detection of Au³⁺. The probe was based on the coordination of Au³⁺ onto imidazole groups [(PZn-Au Au³⁺) complex] (Scheme 9).¹⁶ The zinc porphyrin and Au³⁺ complex further showed response to the addition of thiol-bearing compounds. This unique characteristic of the imidazole-bearing zinc porphyrin was exploited for the in vitro bioimaging, as well as for the detection of residual thiols in thiol-ene crosslinking hydrogels.

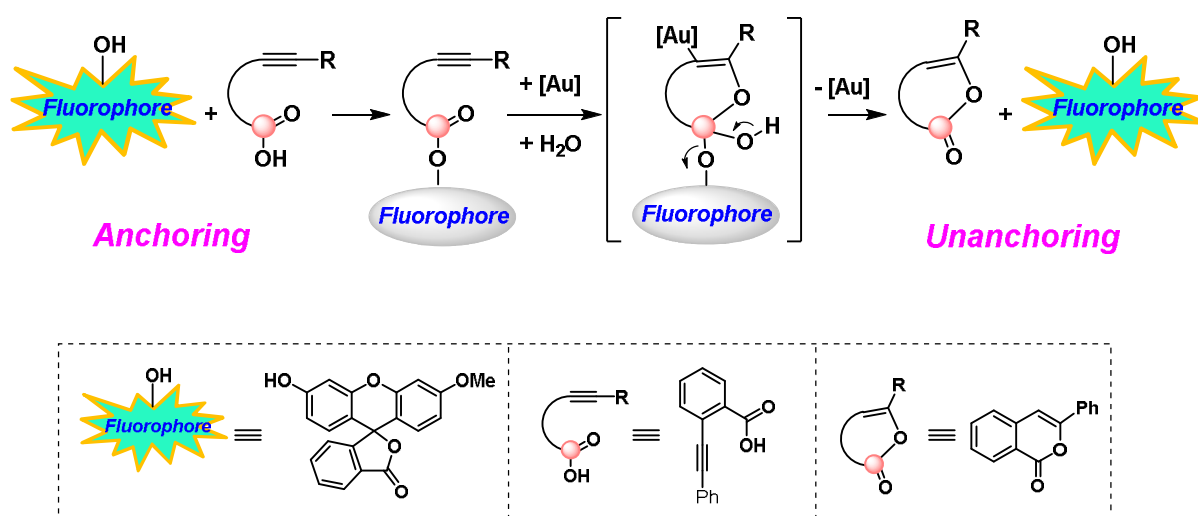
Scheme 4.9: Imidazole-bearing porphyrins based fluorescent chemosensor for selective detection of Au^{3+} ions



4.2 Hypothesis

With above literature background and our expertise in gold catalysis it was envisioned that an organic molecule of type **X** would be activated by gold ions which, in turn, trigger cascade as depicted in figure 3 (cf. **Y**).¹⁷ The reaction, thus envisaged, would liberate highly fluorescent fluorophore and therefore the designed molecules of type **X** would serve as a probe for sensing gold ions. Thus we hypothesized a new approach involving anchoring-unanchoring of the fluorophore. It can be judged from figure 3 the fluorescence of fluorophore is turned off by anchoring with organic substrate. Once the gold ions have been sensed, the probe would liberate highly fluorescent fluorophore with formation of organic product.

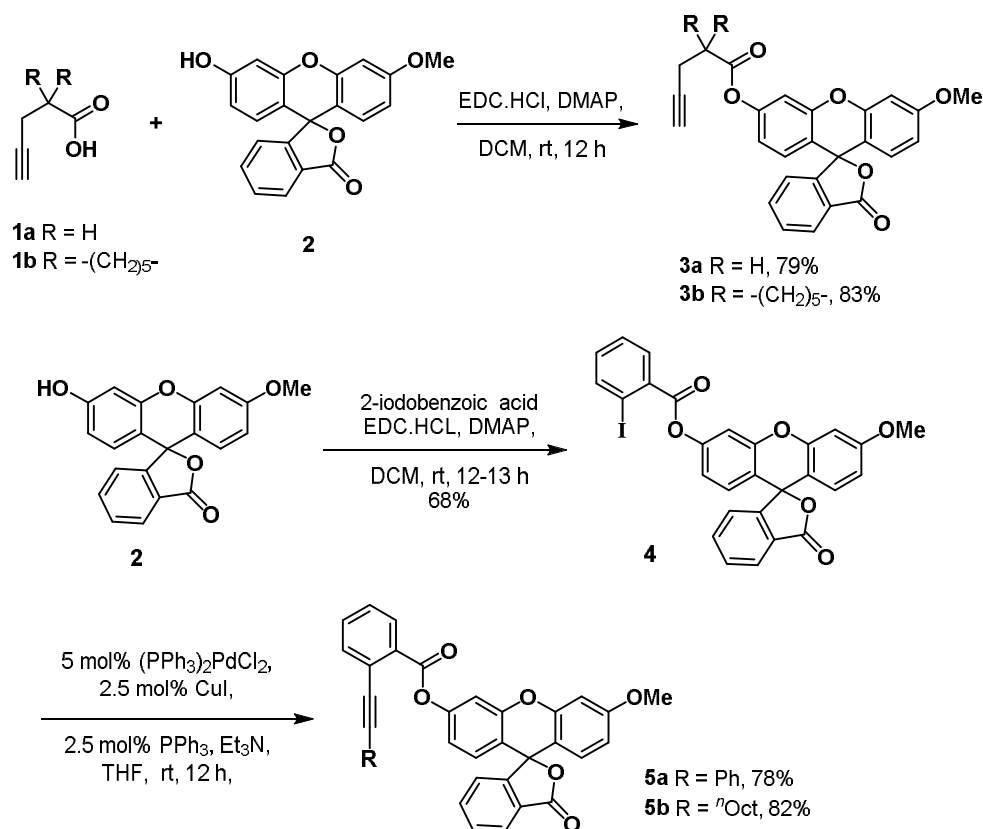
Figure 4.3: Approach involving anchoring-unanchoring of fluorophore



4.3 Results and Discussion

In order to test the hypothesis, probes **3a-b** and **5a-b** were synthesized from fluorescein as outlined in scheme 10. Fluorescein was chosen as a fluorophore because of its bright fluorescence combined with its non-toxicity.¹⁸ The probes **3a** and **3b** were obtained by the reaction of methoxyfluorescein **2** with alkynoic acids **1a** and **1b**, respectively. The synthesis of probes **5a** and **5b** was achieved in two steps from fluorescein **2**. The esterification of 2-iodobenzoic acid with **2** was achieved by a conventional procedure to obtain haloester **4** in 68% yield. The halo-ester **4**, thus obtained, reacted with phenyl acetylene and 1-octyne by Sonogashira coupling by to give the desired probes **5a** and **5b** in 78 and 82% yields, respectively.

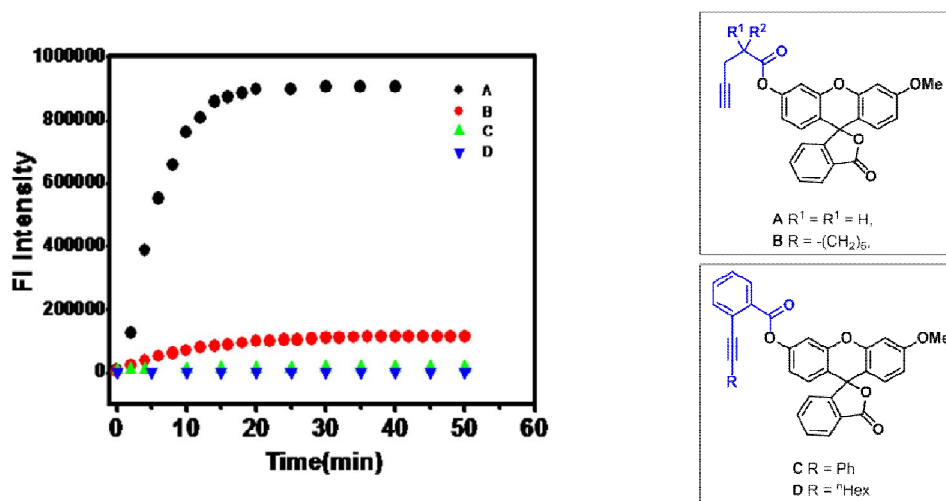
Scheme 4.10: Synthesis of various probes



As expected, all the chemosensors **3a-b** and **5a-b** showed negligible fluorescence and are colorless in $\text{H}_2\text{O}-\text{CH}_3\text{CN}$ buffer (pH = 7.4). The probes **5a-b** (30 μM) on treatment with 100 μM solution of HAuCl_4 exerted strong fluorescence at 515 nm. In addition, the solution changes from colorless to a yellow color. Since the probes **3a-b** did not give promising

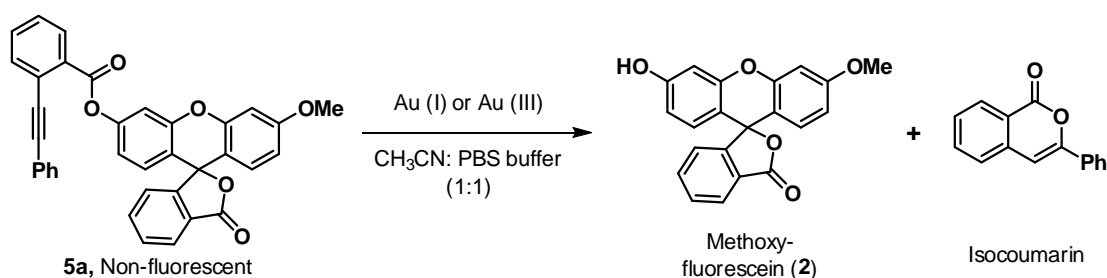
results (Figure 4), **5a** and **5b** were considered; out of which the **5a** was chosen for further studies because of its superiority over the other probes.

Figure 4.4: Fluorescence response of probes: Plot of fluorescence intensity at 515 nm against time for (A) Probe **5a**, (B) Probe **5b**, (C) Probe **3a**, (D) Probe **3b** (all Probes-10 μM) in the presence of Au^{1+} (100 μM) in $\text{CH}_3\text{CN}:\text{PBS}$ buffer (1:1, 0.1M, pH = 7.4). $\lambda_{\text{excit}} = 452 \text{ nm}$.



Probe **5a** in $\text{CH}_3\text{CN}/\text{PBS}$ buffer (1:1, pH = 7.4) has an absorption maxima centered at 313 nm with no absorption in the visible region. However, the addition of Au^{1+} or Au^{3+} ions to probe **5a** induces a colorimetric change from colorless to yellow which is visible to the naked eye.

Scheme 4.11: Model reaction for detection of gold ions



4.3.1 Studies of UV-Visible Absorption Changes

The study was initiated by recording normalized absorption spectrum of probe **5a** ($\lambda_{\text{max}} = 313 \text{ nm}$) and the fluorescein derivative **2** ($\lambda_{\text{max}} = 452 \text{ nm}$) using UV spectrophotometer (figure 5). The figure 6 shows the time dependent absorption change of **5a** (10 μM) upon addition of 10 equiv. of Au^{1+} ion. A new band appeared in the visible region ($\lambda_{\text{max}} = 452 \text{ nm}$) immediately after addition of the Au^{1+} ion and a large enhancement in absorption is observed with time. The increase in absorbance (at $\lambda_{\text{max}} = 452 \text{ nm}$) is rapid and it saturates after 40 min, indicating the reaction is very fast. Similar spectral behaviour has been observed to take place between **5a** with the Au^{3+} ion with much less enhancement in absorption (Figure 7).

Figure 4.5: Normalized absorption spectrum of probe **5a** and the fluorescein derivative **2**.

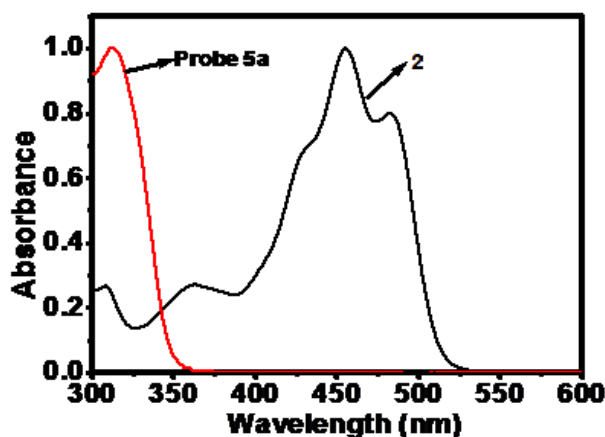


Figure 4.6: (A) Time dependent absorption change of **5a** (10 μM) upon addition of 10 equivalents of Au^{1+} in $\text{CH}_3\text{CN}:\text{PBS}$ buffer (1:1, 0.1M, pH = 7.4). (B) Absorption kinetics change upon addition of 10 equivalents of Au^{1+} to **5a** (10 μM) in $\text{CH}_3\text{CN}:\text{PBS}$ buffer (1:1, 0.1M, pH = 7.4).

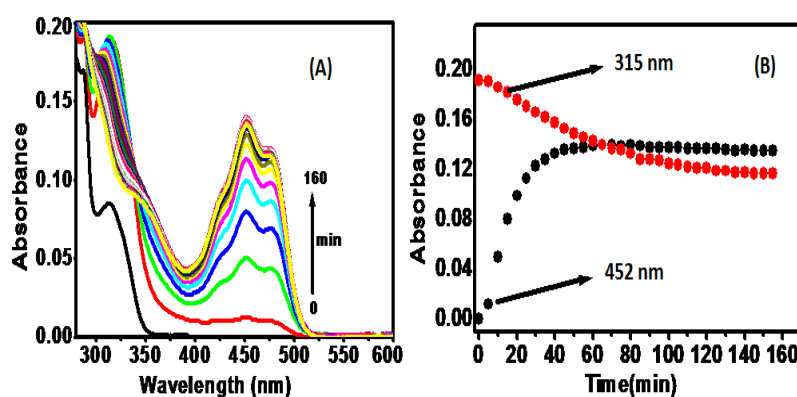
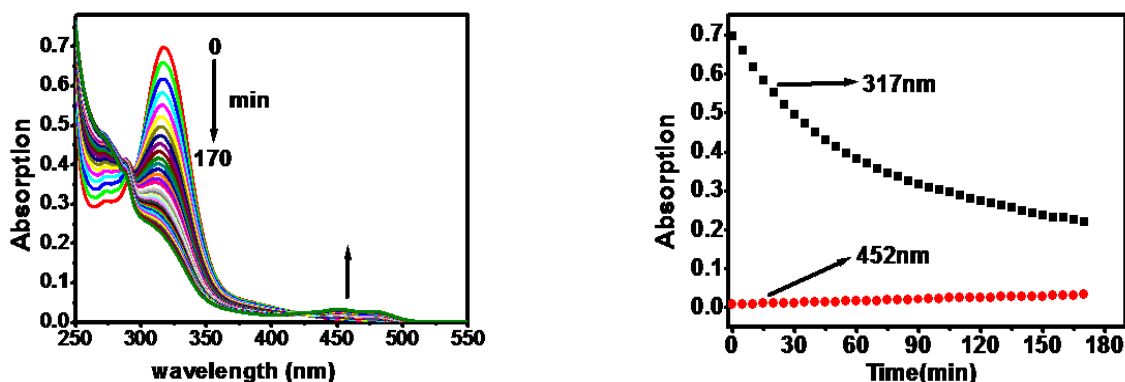


Figure 4.7: Time dependent absorption change and its kinetics upon addition of 10 equivalents of Au^{+3} to **5a** ($10\ \mu\text{M}$) in CH_3CN :PBS buffer (1:1, 0.1M, pH = 7.4). Isosbestic point at 424 nm.



4.3.2 Studies of Fluorescence Spectrophotometric Changes

Studies of time-dependent fluorescence change

The solution of probe **5a** in CH_3CN /PBS buffer (1:1, pH = 7.4) is colorless and exhibits negligible fluorescence. However, the addition of Au^{1+} ion to probe **5a** triggers a large enhancement in fluorescence ($\lambda_{\text{max}} = 515\ \text{nm}$). The time dependent fluorescence response of probe **5a** ($10\ \mu\text{M}$) with Au^{1+} ($100\ \mu\text{M}$) showed a rapid increase in intensity up to 30 min and then saturates (Figure 8). Similar behaviour has been found with Au^{3+} , but the rate at which intensity increases is less compared with Au^{1+} (Figure 9).

Figure 4.8: Time dependent fluorescence change obtained for a mixture of **5a** ($10\ \mu\text{M}$) and Au^{1+} ($100\ \mu\text{M}$) in CH_3CN :PBS buffer (1:1, 0.1M, pH = 7.4). $\lambda_{\text{excit}} = 452\ \text{nm}$. Inset: Plot of fluorescence intensity at 515 nm against time.

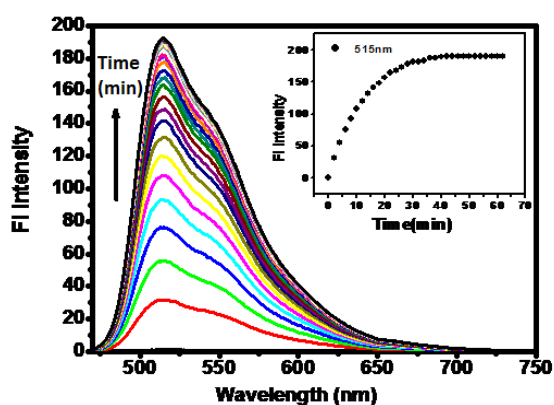
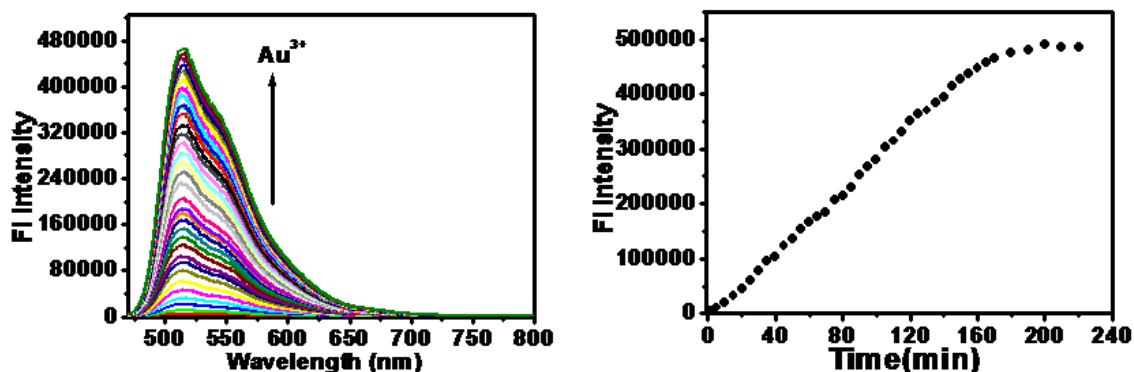


Figure 4.9: (a) Time dependent fluorescence change obtained for a mixture of **5a** (10 μM) and Au^{3+} (100 μM) in CH_3CN :PBS buffer (1:1, 0.1M, pH = 7.4). $\lambda_{\text{excit}} = 452 \text{ nm}$. (b) Plot of fluorescence intensity at 515nm against time.



A) The concentration dependent fluorescence change studies

Next, we studied concentration dependent study that is fluorescence titrations with chemosensor **5a** for Au (I) ions (Figure 10). Concentration dependent fluorescence change acquired for a mixture of **5a** (10 μM) upon addition of Au^{1+} (5 μM -80 μM) in CH_3CN :PBS buffer (1:1,0.1M, pH = 7.4). The Au(III) ions also showed similar profile on change in concentration (Figure 11)

Figure 4.10: (a) Concentration dependent fluorescence change acquired for a mixture of **5a** (10 μM) upon addition of Au^{1+} (5 μM -80 μM) in CH_3CN :PBS buffer (1:1,0.1M, pH = 7.4). $\lambda_{\text{excit}} = 452 \text{ nm}$. (b) Plot of fluorescence intensity at 515nm against Au^{1+} concentration. Each spectrum is taken after 2 min of Au^{1+} addition.

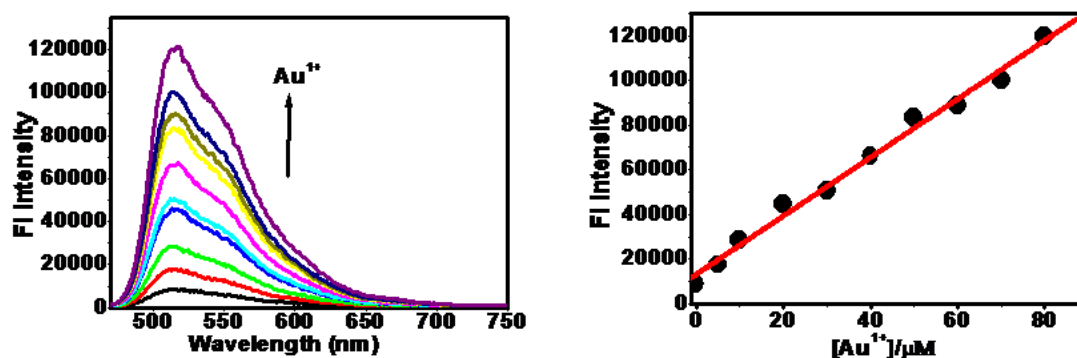
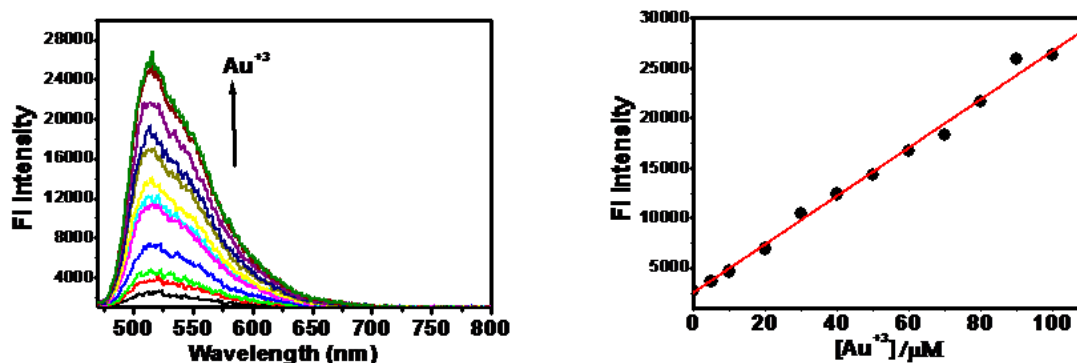


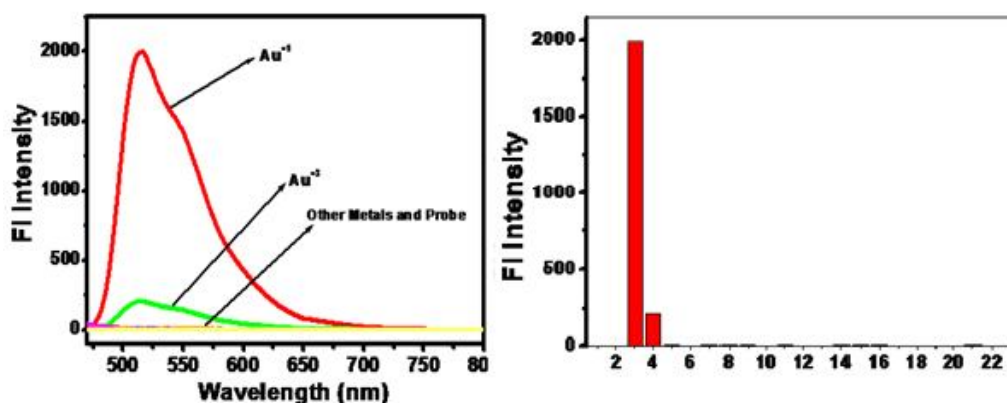
Figure 4.11: Concentration dependent fluorescence change acquired for a mixture of **1** (10 μM) and Au^{3+} (100 μM) in $\text{CH}_3\text{CN}:\text{PBS}$ buffer (1:1, $\text{pH} = 7.4$). $\lambda_{\text{excit}} = 452$ nm. (b) Plot of fluorescence intensity at 515nm against Au^{3+} concentrations. Each spectrum is taken after 5 min of Au^{3+} additions.



4.3.2 Studies of Specificity and Selectivity of Probe

Next task was to examine the selectivity of probe **5a** towards various other metal species. The Figure 12 reveals that probe **5a** showed special selectivity towards Au^{1+} and Au^{3+} metal ions only. Fluorescence response of other metals such as Ag^{1+} , Ba^{2+} , Bi^{3+} , Fe^{3+} , Hg^{2+} , Ir^{3+} , K^{1+} , La^{3+} , Mn^{2+} , Ni^{2+} , Pd^{2+} , Pt^{2+} , Pt^{4+} , Ru^{3+} , Sc^{3+} , Yb^{3+} , Zn^{2+} , Cd^{2+} , Cr^{3+} is negligible.

Figure 4.12: Fluorescence response of **5a** (10 μM) in the presence of various metals ions (100 μM). Excitation at 452 nm and emission monitoring at 515 nm. Metal ions: 1) probe **5a**, 2) Ag^{1+} , 3) Au^{1+} , 4) Au^{3+} , 5) Ba^{2+} , 6) Fe^{3+} , 7) Bi^{3+} , 8) Hg^{2+} , 9) Ir^{3+} , 10) K^{1+} , 11) La^{3+} , 12) Mn^{2+} , 13) Ni^{2+} , 14) Pd^{2+} , 15) Pt^{2+} , 16) Pt^{4+} , 17) Ru^{3+} , 18) Sc^{3+} , 19) Yb^{3+} , 20) Zn^{2+} , 21) Cd^{2+} , 22) Cr^{3+}



Further the selectivity of probe **5a** towards Au^{1+} in presence of other competing metal species have been tested (Figure 13). It is evident that the interference of other metal species is minimal, so this probe can be used as Au^{1+} sensor in presence of other metal species. The fluorescence response of probe shows excellent linear relationship towards Au^{1+} in the range

of 5 – 80 μM , indicating that probe can be used for quantitative determination of Au^{1+} . The developed probe **5a** can recognize $\text{Au}(\text{I})$ and $\text{Au}(\text{III})$ ions with good selectivity and sensitivity which can be detected both visually and fluorescence spectrophotometrically (Figure 14 and Figure 15).

Figure 4.13: Fluorescence response of **1** ($10\ \mu\text{M}$) in the presence of Au^{1+} ($100\ \mu\text{M}$) and other metals ions ($100\ \mu\text{M}$). Excitation at 452 nm and emission monitoring at 515 nm. Metals: 1) Ag^{1+} , 2) Au^{1+} , 3) Au^{3+} , 4) Ba^{2+} , 5) Fe^{3+} , 6) Bi^{3+} , 7) Hg^{2+} , 8) Ir^{3+} , 9) K^{+1} , 10) La^{3+} , 11) Mn^{2+} , 12) Ni^{2+} , 13) Pd^{2+} , 14) Pt^{2+} , 15) Pt^{4+} , 16) Ru^{3+} , 17) Sc^{3+} , 18) Yb^{3+} , 19) Zn^{2+} , 20) Cd^{2+} , 21) Cr^{3+} . Each spectrum is taken after 30 min of metal ion addition.

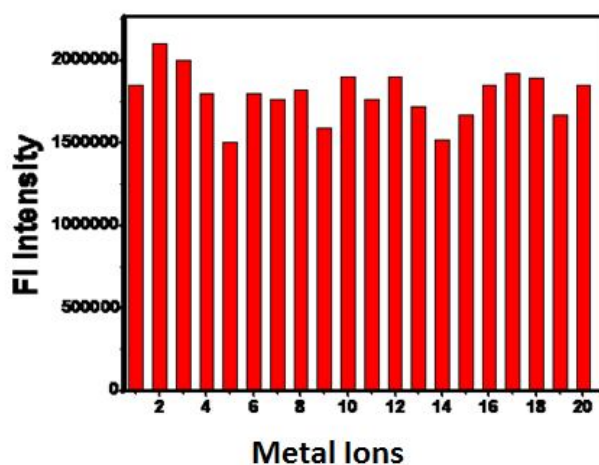
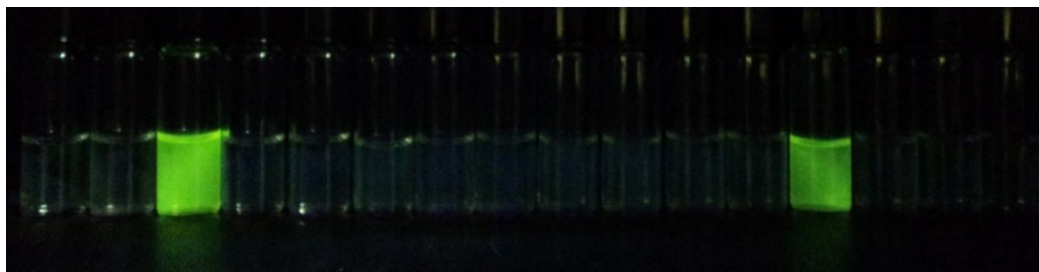


Figure 4.14: Naked eye detection of metal ions of **5a** ($50\ \mu\text{M}$), Au^{1+} and Au^{3+} $10\ \mu\text{M}$, ions were added whereas $100\ \mu\text{M}$ of other ions were added. From left to right, no metal ion, Pt^{2+} , Au^{1+} , Hg^{2+} , Ag^{1+} , Mn^{2+} , Pd^{2+} , Ni^{2+} , Sc^{3+} , Cd^{2+} , Ru^{3+} , Ba^{2+} , Au^{3+} , Zn^{2+} , Fe^{3+} and Cr^{3+} .



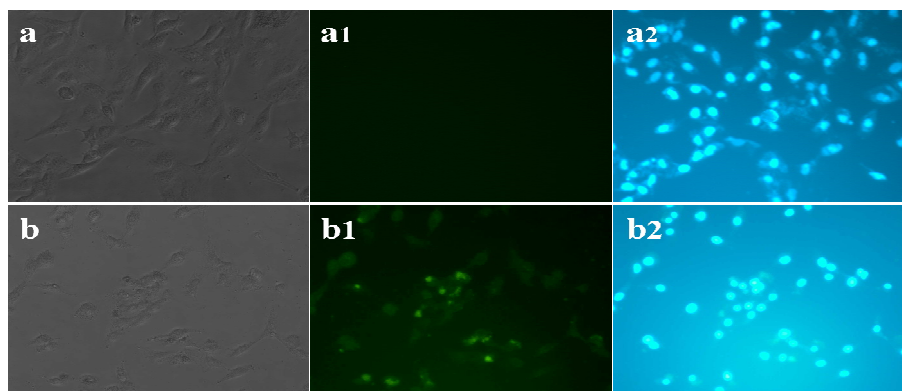
Figure 4.15: Fluorescence photographs of probe **5a** (50 μM), Au^{1+} and Au^{3+} 10 μM whereas 100 μM of different metal ions in CH_3CN / PBS buffer (1:1, v/v, pH = 7.4) recorded after 1 h at 25 $^\circ\text{C}$. From left to right, no metal ion, Pt^{2+} , Au^{1+} , Hg^{2+} , Ag^{1+} , Mn^{2+} , Pd^{2+} , Ni^{2+} , Sc^{3+} , Cd^{2+} , Ru^{3+} , Ba^{2+} , Au^{3+} , Zn^{2+} , Fe^{3+} , Cr^{3+} .



4.4 Bioimaging Studies Using A549 Lung Cancer Cells

The favourable features of **5a** such as fast response, high selectivity and strong fluorescence under physiological pH encouraged us to further examine the potential of the sensor for imaging Au^{1+} in living cell. The lung cancer cell A549 and Au^{1+} were chosen for studies. The bright field images of control untreated A549 cells are depicted in Figure 16. The corresponding fluorescence image and the blue color DAPI stained image of untreated control A549 cells are shown in Figure 16, a1 and Figure 16, a2 respectively. As can be judged, the green fluorescence of untreated A549 cells was not observed in the absence of **5a** and Au^{1+} (Figure 16, a1). However, the presence of green fluorescence noticed when the **5a** was treated with with Au^{1+} (Figure 16, b1) even after extensive washing with DPBS. These observations clearly indicate that the probe **5a** can sense Au^{1+} ion in living cells.

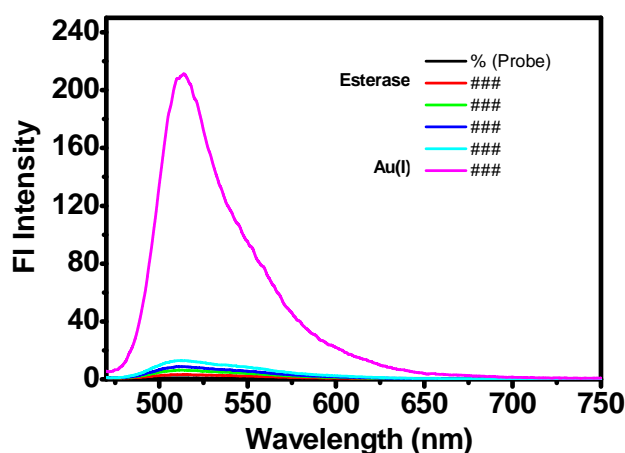
Figure 4.16: Fluorescence images of A549 cells: (a-b) bright field images, (a1-b1) fluorescence images and (a2-b2) DAPI stained images of A549 cells. The figures a, -a1 and -a2 indicate the bright field, fluorescent and DAPI stained images of control untreated A549 cells. Similarly, b, -b1 and -b2 indicate the bright field, fluorescent and DAPI stained images of A549 cells treated with 20 μM of Au^{1+} and 50 μM of probe 5a.



Ester Hydrolysis Studies in Cell by Esterase Enzyme

We recognized that probe **5a** which contains ester group which could potentially be hydrolyzed by cellular esterase. The probe **5a** was therefore tested for the stability in the presence of enzyme esterase (Porcine liver esterase source -Sigma Aldrich E3019-3.5 KU). The results suggested that the probe **5a** was quite stable toward esterase (Figure 17).

Figure 4.17: 6 μL of probe **5a** (5 μM) is mixed with 25 μL of esterase enzyme (0.013g/mL) stock solution. The resultant solution is made up to 2 mL with phosphate buffer (pH = 7.4, 0.1M). The fluorescent intensity was measured at different time intervals up to 1 h. Then 100 μM of Au^{1+} is added to the mixture and intensity was measured after 30 min. ($\lambda_{\text{excit}} = 452$ nm).



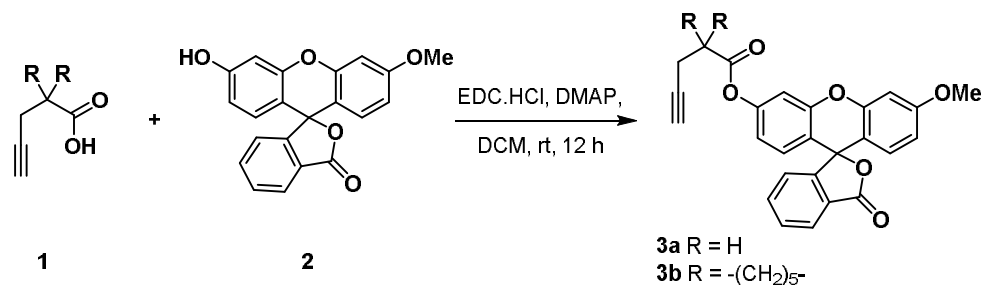
4.5 Conclusion

In summary, we have developed a new approach involving anchoring-unanchoring of fluorophore, for detection of gold ions. The developed probe can recognize Au(I) and Au(III) ions with good selectivity and sensitivity which can be detected both visually and fluorescence spectrophotometrically. The bioimaging studies have also been successfully demonstrated with A549 lung cancer cells.

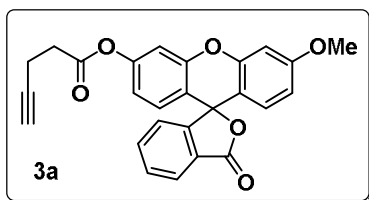
4.6 Experimental Procedures and Characterization Data

Unless otherwise stated, all reagents were purchased from commercial suppliers and used without further purification. Solvents used were purified and dried by standard methods prior to use. Twice-distilled water was used throughout all experiments. The solutions of metal ions were prepared from $\text{HAuCl}_4 \cdot 3\text{H}_2\text{O}$, AuCl , AgOTf , $\text{Ba}(\text{OH})_2 \cdot 8\text{H}_2\text{O}$, $\text{FeCl}_3 \cdot 8\text{H}_2\text{O}$, $\text{Bi}(\text{OTf})_3$, $\text{Hg}(\text{OTf})_2$, IrCl_3 , KI , $\text{La}(\text{OTf})_3$, $\text{MnSO}_4 \cdot \text{H}_2\text{O}$, $\text{NiCl}_2 \cdot 6\text{H}_2\text{O}$, CdCl_2 , PdCl_2 , PtCl_2 , PtCl_4 , RuCl_3 , CrCl_3 , $\text{Sc}(\text{OTf})_3$, $\text{Yb}(\text{OTf})_3$, ZnCl_2 .

General procedure for preparation compound 3a and 3b:



To a mixture of alkyne acid (1.0 equiv.), EDC (1.0 equiv.) and DMAP (0.1 equiv.) in DCM was added fluorescein **2** (1.0 equiv.) in DCM at rt. The mixture was stirred for additional 12 hrs. After completion of reaction the solvent was removed under reduced pressure and resulting residue was purified by flash column chromatography with 10/90 mixture of ethyl acetate and hexane as eluent to yield pure products.



(**3a**): white solid

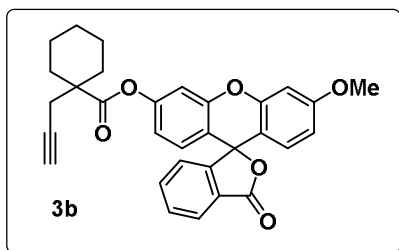
Yield: 79% yield; mp = 138-141°C; R_f 0.50 (hexane/EtOAc = 60/40)

^1H NMR (300 MHz, CDCl_3): δ 8.04-8.02 (d, $J = 7.5$ Hz, 1H), 7.71-7.60 (m, 2H) 7.18-7.16 (d, $J = 7.5$ Hz, 1H), 7.1 (s, 1H), 6.81 (m, 2H), 6.78-6.77 (d, $J = 2.3$ Hz, 1H), 6.72-6.69 (d, $J = 8.3$ Hz, 1H), 6.65-6.61 (dd, $J = 8.3$ & 2.3 Hz, 1H), 3.84 (s, 3H), 2.85-2.80 (t, $J = 7.5$ Hz, 2H), 2.66-2.60 (t, $J = 7.5$ Hz, 2H), 2.05-2.04 (t, $J = 2.3$ Hz, 1H).

^{13}C NMR (75 MHz, CDCl_3): δ 169.7, 169.2, 161.4, 152.9, 152.2, 151.8, 151.7, 135.1, 129.8, 129.0, 128.9, 126.4, 125.0, 117.3, 116.8, 111.9, 110.8, 110.2, 100.8, 82.3, 81.8, 69.5, 55.5, 33.4, 14.4.

IR (KBr): ν_{max} 2927, 1762, 1598, 1477, 1419, 1245, 1102, 835 cm^{-1} .

MS (ESI): m/z 427.0 ($\text{M}^+ + \text{H}$); HRMS calcd for $\text{C}_{26}\text{H}_{18}\text{O}_6$ ($\text{M}^+ + \text{H}$) 427.11816 found 427.11819.



(**3b**): white solid

Yield: 83%; mp = 179-182°C; R_f 0.45 (hexane/EtOAc = 60/40)

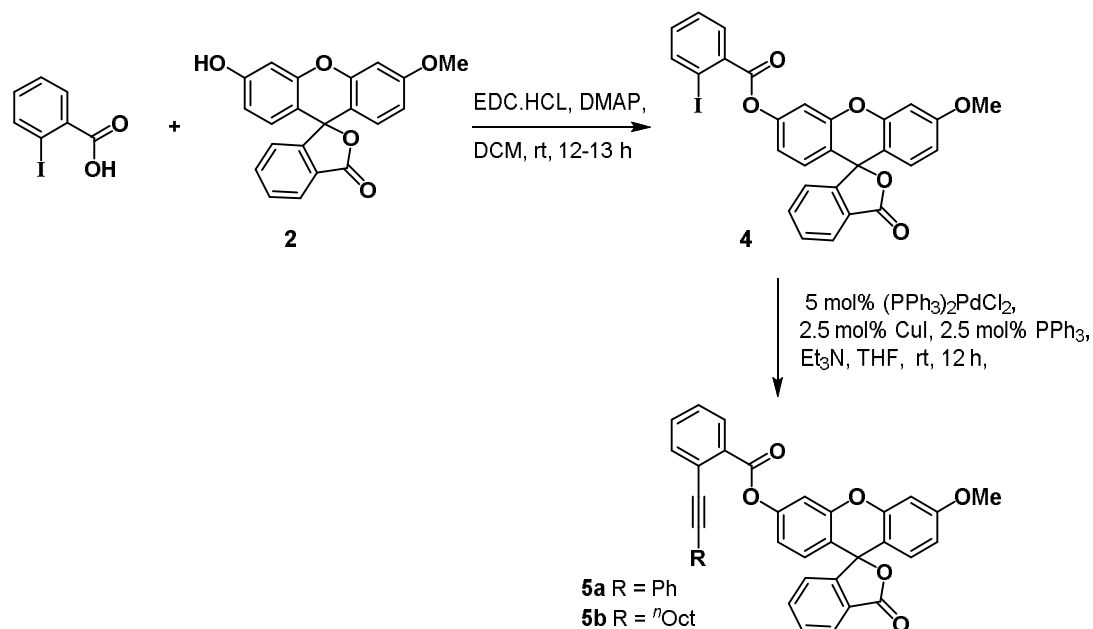
^1H NMR (300 MHz, CDCl_3): δ 8.04-8.02 (d, $J = 6.8$ Hz, 1H) 7.70-7.60 (m, 2H), 7.18-7.15 (d, $J = 7.5$ Hz, 1H), 7.07 (s, 1H), 6.80-6.77 (m, 3H), 6.72-6.70 (d, $J = 8.3$ Hz, 1H), 6.65-6.61 (dd, $J = 9.1$ & 2.3 Hz, 1H), 3.84 (s, 3H), 2.57-2.56 (d, $J = 2.3$ Hz, 2H), 2.26-2.22 (m, 2H), 2.1 (s, 1H), 1.65-1.49 (m, 6H), 1.39-1.24 (m, 2H).

^{13}C NMR (75 MHz, CDCl_3): δ 173.6, 169.3, 161.4, 153.0, 152.2, 151.8, 135.0, 129.8, 128.9, 126.4, 125.0, 123.9, 117.5, 116.6, 111.8, 110.8, 110.4, 100.8, 82.4, 79.7, 71.4, 55.5, 47.0, 33.2, 30.9, 29.6, 29.2, 25.4, 22.8.

IR (KBr): ν_{max} 2931, 1764, 1601, 1497, 1423, 1247, 1167, 1107, 884, 759 cm^{-1} .

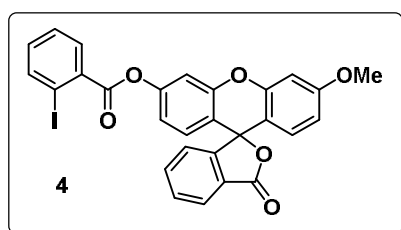
MS (ESI): m/z 495.0 ($M^+ + H$); HRMS calcd for $C_{31}H_{26}O_6$ ($M^+ + H$) 495.18076 found 495.18072.

General procedure for preparation compound 5a and 5b:



Procedure for synthesis of ester 4:

Ester 4 was prepared by following similar procedure mentioned for the preparation of 3a and 3b as described above.



(4): pale yellow solid

Yield: 68%; mp = 155-158°C; R_f 0.60 (hexane/EtOAc = 60/40)

1H NMR (300 MHz, $CDCl_3$): δ 8.08-8.00 (m, 3H), 7.69-7.58 (m, 3H) 7.50-7.47 (t, $J = 7.0$ Hz, 1H), 7.23-7.14 (m, 2H), 6.96-6.86 (dd, $J = 8.9$ & 2.0 Hz, 1H), 6.79-6.76 (dd, $J = 8.9$ & 2.0 Hz, 2H), 6.69-6.72 (d, $J = 8.9$ Hz, 1H), 6.61-6.59 (dd, $J = 8.9, 2.0$ Hz, 1H), 3.83 (s, 3H).

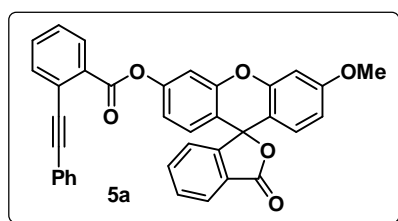
^{13}C NMR (75 MHz, CDCl_3): δ 169.2, 164.3, 161.2, 152.2, 151.8, 141.7, 135.1, 134.9, 133.5, 131.6, 129.8, 129.6, 129.1, 129.0, 128.1, 125.0, 124.9, 123.9, 123.8, 117.4, 11.9, 111.5, 110.4, 100.7, 94.7, 55.5.

IR (KBr): ν_{max} 2924, 1762, 1609, 1500, 1423, 1245, 1166, 1106, 878, 759 cm^{-1} .

MS (ESI): m/z 577.0 ($\text{M}^+ + \text{H}$); HRMS calcd for $\text{C}_{28}\text{H}_{17}\text{I O}_6$ ($\text{M}^+ + \text{H}$) 577.01481 found 577.01487.

General procedure for synthesis of probes **5a** and **5b**:

To a solution of ester **4** (1.0 equiv.) in anhydrous THF (5 mL) were added CuI (0.025 equiv) and PPh_3 (0.025 equiv) in a flame dried two neck flask with magnetic stirring bar and rubber septum. The mixture was degassed and filed with nitrogen three times and then $\text{PdCl}_2(\text{PPh}_3)_2$ (0.05 equiv), Et_3N (1.5 equiv), and phenylacetylene or octyne (1.5 equiv) were added to the solution. The reaction mixture was stirred for 12 h at rt and then filtered through a pad of silica and Celite. The solvents were removed under reduced pressure and the crude oil obtained was purified by chromatography on silica gel, using a 10/90 mixture of ethyl acetate/hexane as the eluent to yield corresponding product **5a** and **5b** in 78 and 82% yields, respectively.



(5a): brownish solid

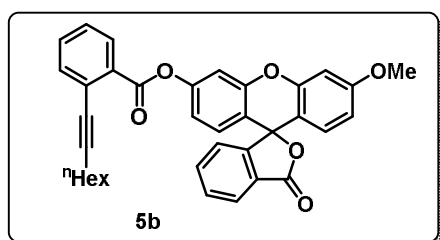
Yield: 78%; mp = 185-187°C; R_f 0.60 (hexane/EtOAc = 60/40)

^1H NMR (500 MHz, CDCl_3): δ 8.18-8.16 (d, $J = 7.7$ Hz, 1H), 8.05-8.03 (d, $J = 7.7$ Hz, 1H), 7.74-7.72 (d, $J = 7.7$ Hz, 1H), 7.71-7.68 (t, $J = 7.7$ Hz, 1H), 7.65-7.62 (t, $J = 7.7$ Hz, 1H), 7.61-7.58 (t, $J = 7.7$ Hz, 1H), 7.52-7.50 (m, 2H), 7.49-7.46 (t, $J = 7.7$ Hz, 1H), 7.52-7.50 (m, 2H), 7.49-7.46 (t, $J = 7.7$ Hz, 1H), 7.33-7.31 (m, 3H), 7.28-7.27 (d, $J = 2.2$ Hz, 1H), 7.22-7.20 (d, $J = 7.7$ Hz, 1H), 6.98-6.96 (dd, $J = 8.8$ & 2.2 Hz, 1H), 6.87-6.85 (d, $J = 8.8$ Hz, 1H), 6.80-6.79 (d, $J = 2.2$ Hz, 1H), 6.73-6.71 (d, $J = 8.8$ Hz, 1H), 6.66-6.63 (dd, $J = 8.8$ & 2.2 Hz, 1H), 3.85 (s, 3H).

^{13}C NMR (75 MHz, CDCl_3): δ 169.3, 161.4, 152.9, 152.2, 152.1, 135.1, 134.3, 132.6, 131.7, 131.0, 129.8, 129.1, 128.9, 128.6, 128.3, 128.0, 126.4, 125.0, 124.5, 124.0, 122.9, 117.5, 116.7, 111.9, 110.4, 100.8, 95.3, 82.5, 55.5.

IR (KBr): ν_{max} 2924, 1764, 1609, 1497, 1421, 1105, 1031, 756 cm^{-1} .

MS (ESI): m/z 551.0 ($\text{M}^+ + \text{H}$); HRMS calcd for $\text{C}_{36}\text{H}_{22}\text{O}_6$ ($\text{M}^+ + \text{H}$) 551.14946 found 551.14946.



(**5b**): white solid

Yield: 82%; mp = 169-171 $^\circ\text{C}$; R_f 0.65 (hexane/EtOAc = 60/40)

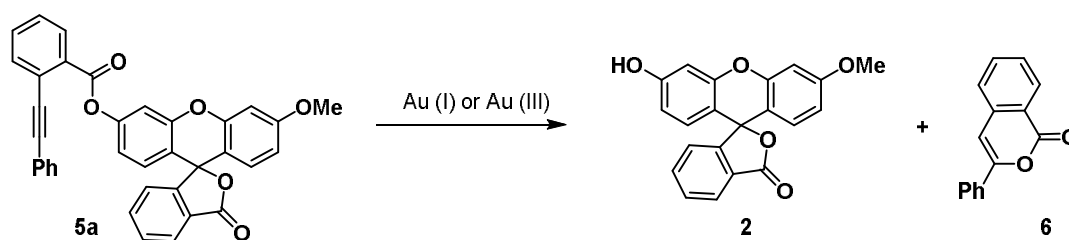
^1H NMR (300 MHz, CDCl_3): δ 8.10-8.03 (m, 3H), 7.72-7.61 (m, 3H), 7.53-7.48 (t, $J = 7.5$ Hz, 1H), 7.25-7.18 (m, 2H), 6.98-6.94 (dd, $J = 8.3$ & 2.3 Hz, 1H), 6.89-6.86 (d, $J = 8.3$ Hz, 1H), 6.80-6.79 (d, $J = 1.5$ Hz, 1H), 6.74-6.71 (d, $J = 8.9$ Hz, 1H), 6.66-6.62 (dd, $J = 8.9$ & 2.3 Hz, 1H), 3.85 (s, 3H), 3.77-3.73 (t, $J = 6.0$ Hz, 2H), 1.87-1.83 (m, 2H), 1.35-1.20 (m, 6H), 0.92-0.83 (m, 3H).

^{13}C NMR (75 MHz, CDCl_3): δ 161.4, 153.0, 152.2, 151.9, 151.8, 141.7, 135.1, 133.5, 131.6, 130.8, 129.9, 129.2, 129.0, 128.8, 128.1, 126.4, 125.1, 124.0, 117.4, 117.0, 112.0, 110.8, 110.4, 110.2, 100.8, 94.7, 68.1, 55.6, 30.3, 30.0, 23.7, 22.7, 14.0, 10.9.

IR (KBr): ν_{max} 3386.9, 2924, 1704, 1486, 1452, 1345, 1205, 1157, 942, 751 cm^{-1} .

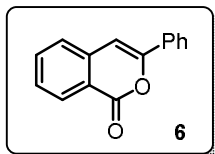
MS (ESI): m/z 559.0 ($\text{M}^+ + \text{H}$); HRMS calcd for $\text{C}_{36}\text{H}_{30}\text{O}_6$ ($\text{M}^+ + \text{H}$) 559.21206 found 559.21216.

Model reaction



To a screw-cap vial containing stir bar, were added probe **5a** (1.0 equiv.), and catalyst $\text{HAuCl}_4 \cdot 3\text{H}_2\text{O}$ or AuCl (0.01 equiv.) in aq. CH_3CN (2 mL/mmol). The reaction vial was fitted

with a cap and stirred at rt for 1 hr. The solvent was removed under reduced pressure and resulting residue was purified by flash column chromatography using hexane and ethyl acetate as eluent to obtain flurophore **2** and isochromene-1one **6**.



3-Phenyl-1H-isochromen-1-one: white solid

Yield: 94%; mp = 89-91°C; R_f 0.65 (hexane/EtOAc = 60/40)

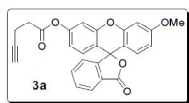
^1H NMR (300 MHz, CDCl_3): δ 8.33-8.30 (d, $J = 7.5$ Hz, 1H) 7.91-7.90 (d, $J = 7.5$ Hz, 1H), 7.88-7.87 (d, $J = 7.5$ Hz, 1H), 7.75-7.69 (dd, $J = 7.5$ & 1.5 Hz, 1H), 7.53-7.43 (m, 5H), 6.96 (s, 1H).

^{13}C NMR (75 MHz, CDCl_3): δ 162.3, 153.5, 137.4, 134.8, 131.9, 129.9, 129.5, 128.8, 128.1, 125.9, 125.2, 101.8.

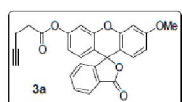
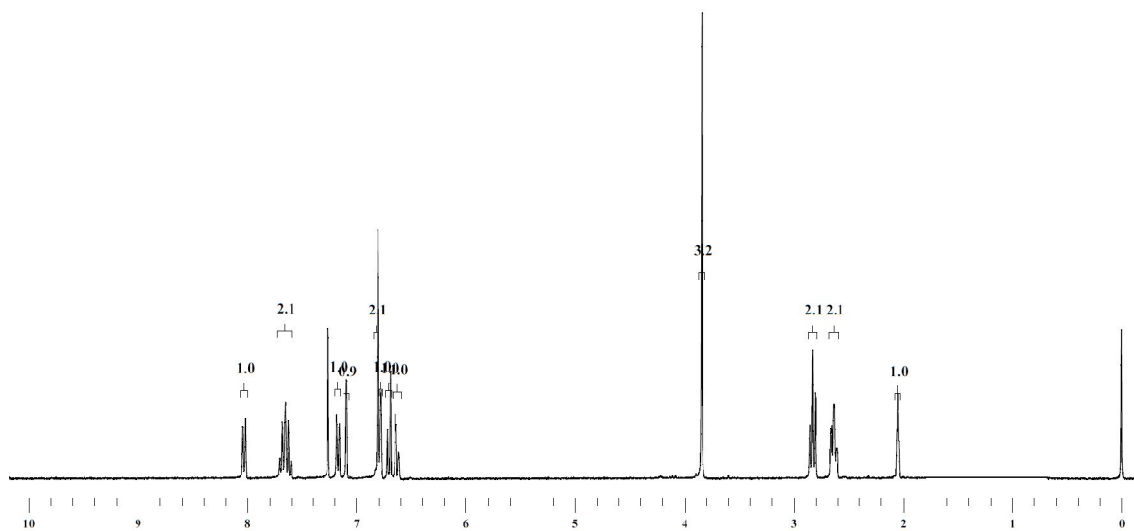
IR (KBr): ν_{max} 3069, 3027, 2962, 1732, 1631, 1483, 1234, 1069, 766 cm^{-1} .

MS (ESI): m/z 223.0 ($\text{M}^+ + \text{H}$); HRMS calcd for $\text{C}_{15}\text{H}_{10}\text{O}_2$ ($\text{M}^+ + \text{H}$) 223.07542 found 223.07561.

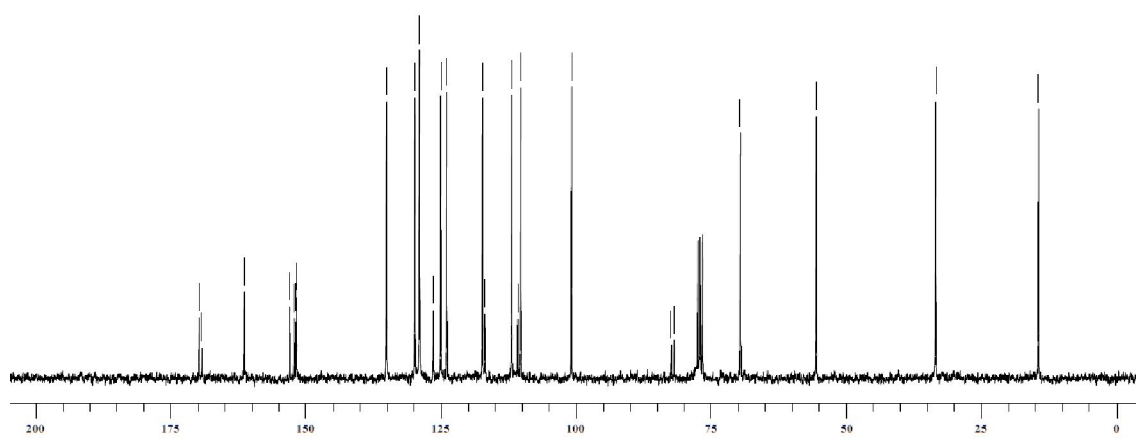
4.7 Spectra

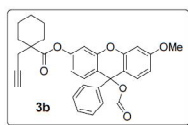


$^1\text{H NMR}$ (300 MHz, CDCl_3)

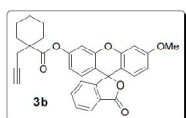
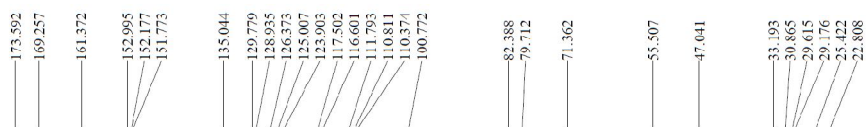
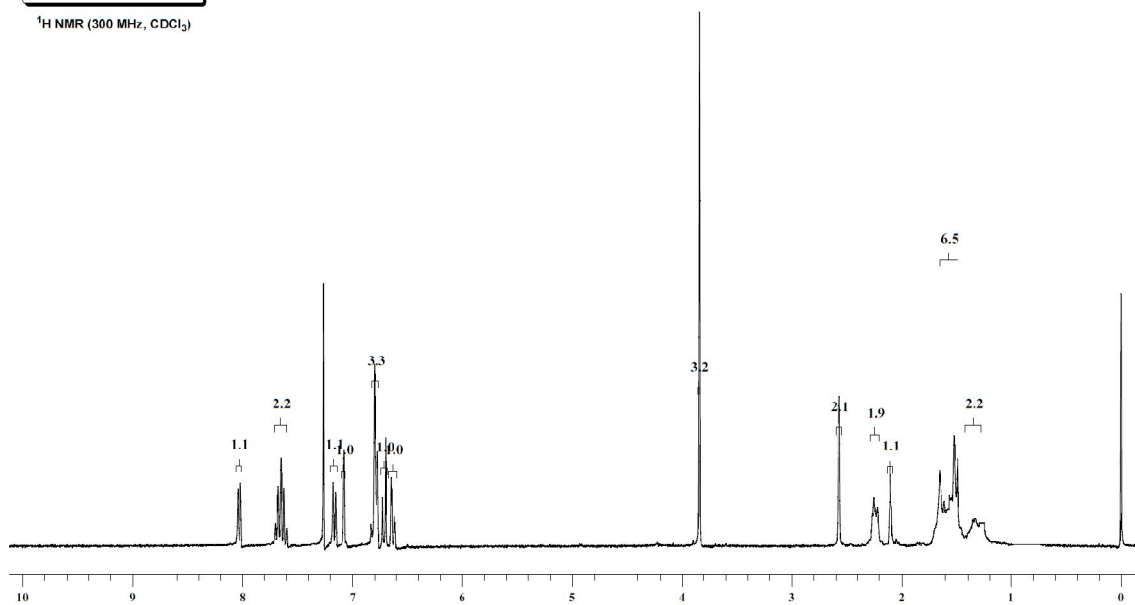


$^{13}\text{C NMR}$ (75 MHz, CDCl_3)

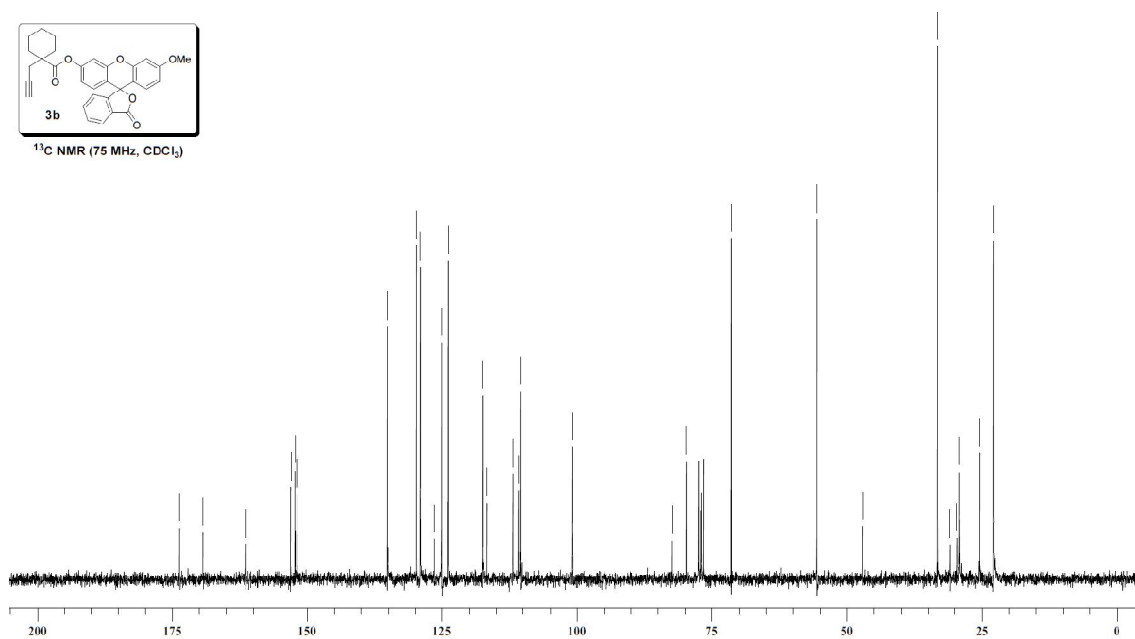


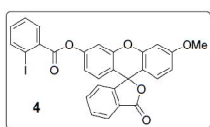


$^1\text{H NMR}$ (300 MHz, CDCl_3)

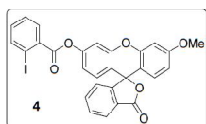
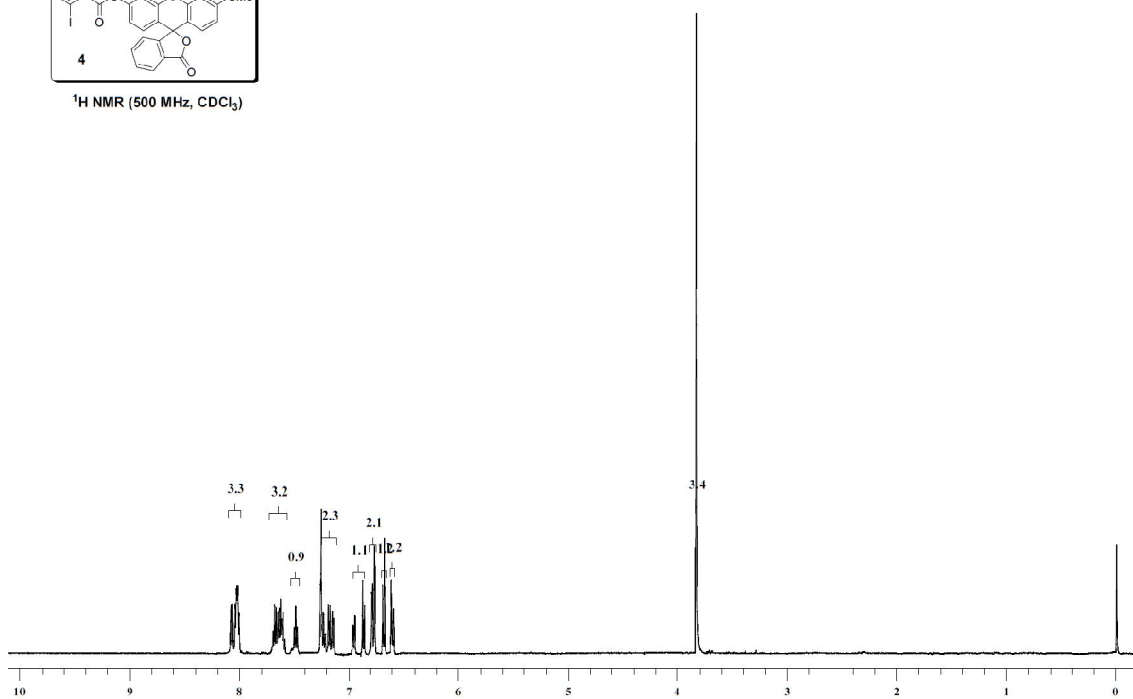


$^{13}\text{C NMR}$ (75 MHz, CDCl_3)

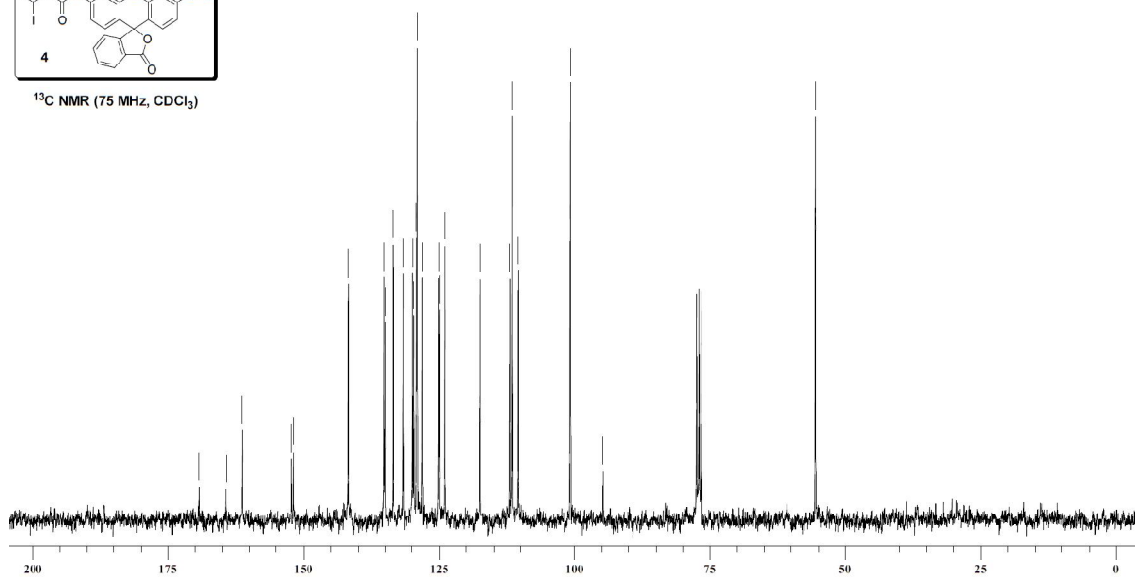


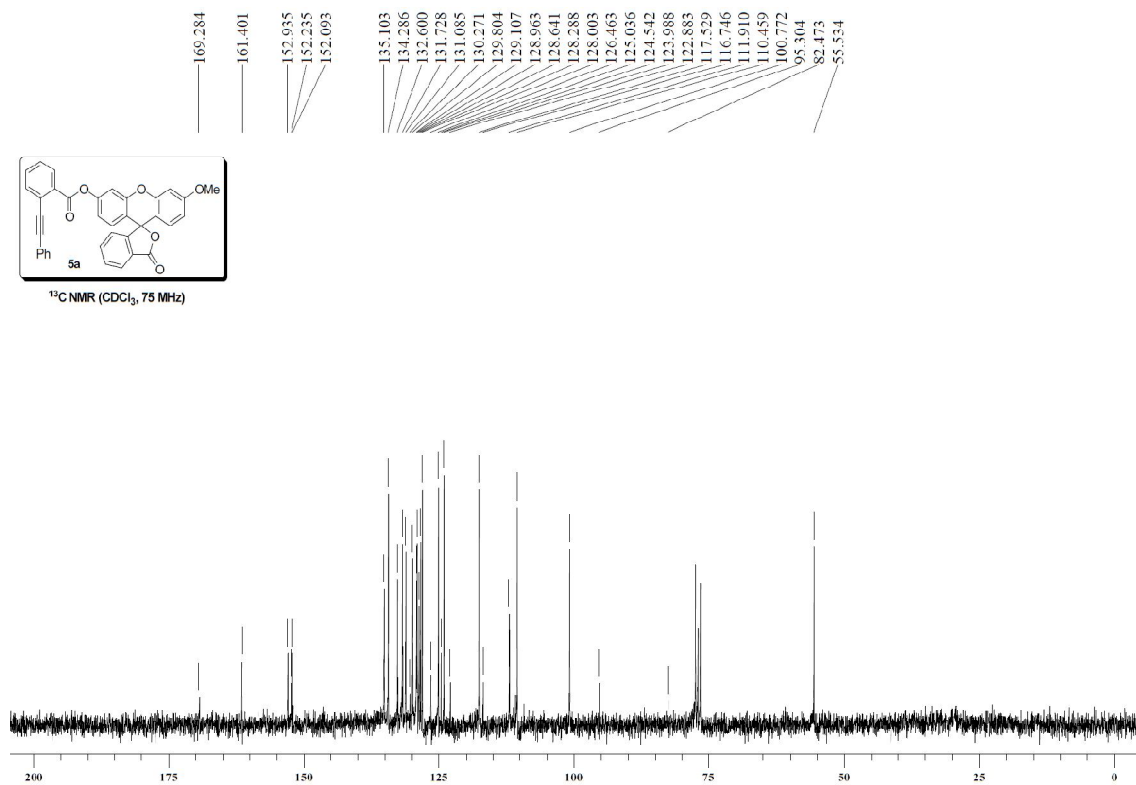
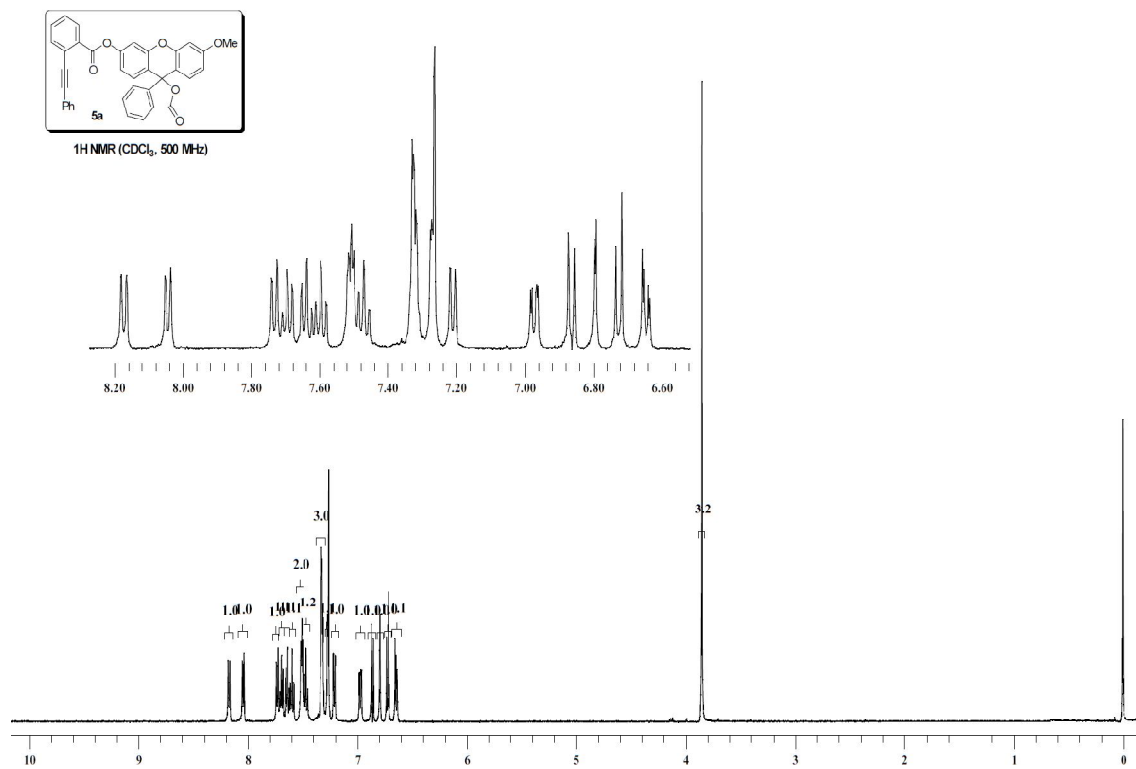


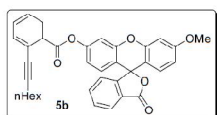
$^1\text{H NMR}$ (500 MHz, CDCl_3)



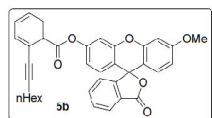
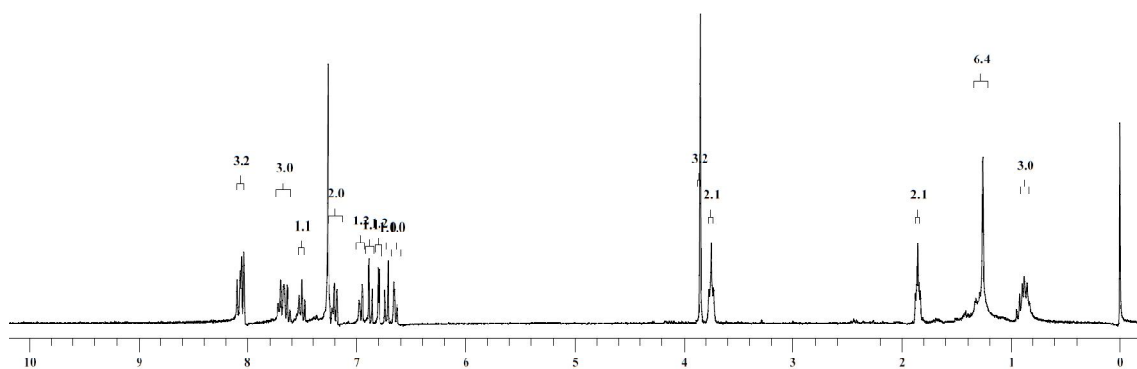
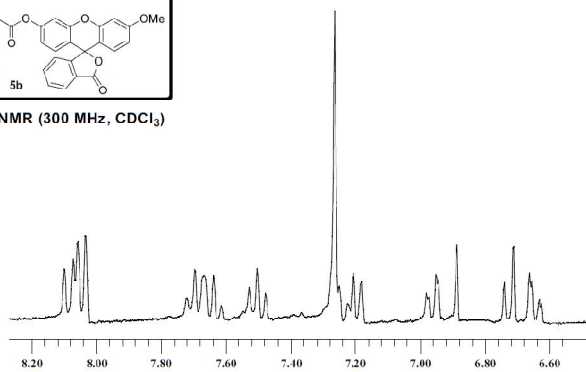
$^{13}\text{C NMR}$ (75 MHz, CDCl_3)



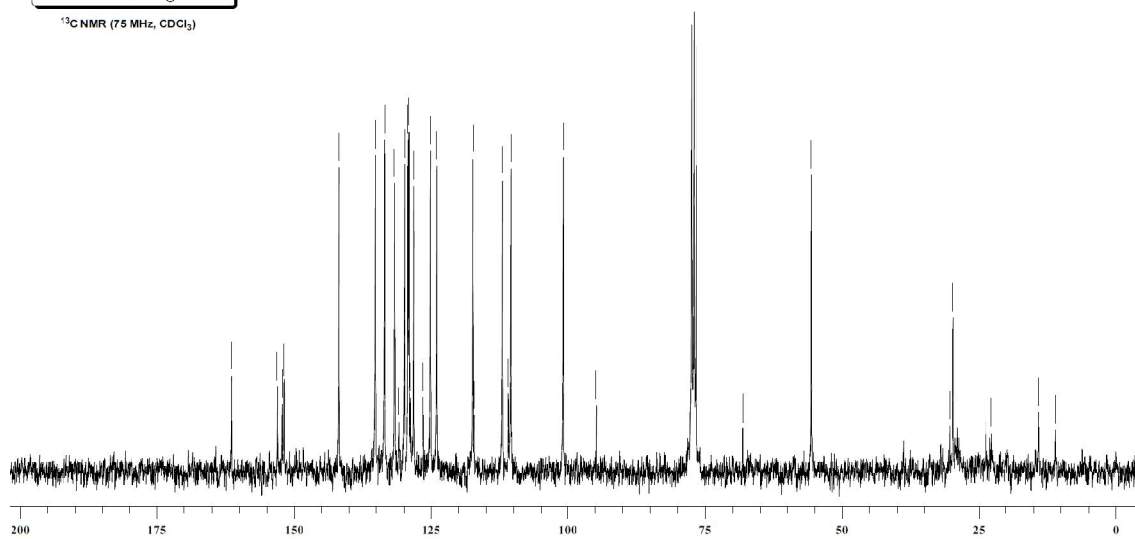




$^1\text{H NMR}$ (300 MHz, CDCl_3)



$^{13}\text{C NMR}$ (75 MHz, CDCl_3)



4.8 References

-
- [1] (a) Ott, I. *Coord. Chem. Rev.* **2009**, *253*, 1670–1681; (b) Navarro, M. *Coord. Chem. Rev.* **2009**, *253*, 1619–1626. (c) Messori L.; Marcon, G.; Metal ions and their complexes in medication, ed. Sigel A. and Sigel, H. CRC Press, New York, **2004**, pp. 279–304; (d) Shaw, C. F. *Chem. Rev.* **1999**, *99*, 2589–2600; (e) American Rheumatism Association (The Cooperating Clinics Committee), *Arthritis Rheum.* **1973**, *16*, 353–358; (f) Locke A.; Main, E. R. *J. Am. Med. Assoc.* **1928**, *90*, 259–260; (g) Mishulow A.; C. Krumwiede, *J. Immunol.* **1927**, *14*, 77–80.
- [2] Fleming, C. J.; Salisbury, E. L.; Kirwan, P.; Painter D. M.; Barnetson, R. S. *J. Am. Acad. Dermatol.* **1996**, *34*, 349–351.
- [3] (a) Jones, J. R. E. *J. Exp. Biol.* **1940**, *17*, 408–415; (b) Lee, M.-T.; Ahmed T.; Friedman, M. E *J. Enzyme Inhibition*, **1989**, *3*, 23–33; (c) Habib A.; Tabata, M. *J. Inorg. Biochem.* **2004**, *98*, 1696–1702; (d) Nyarko, E.; Hara, T.; Grab, D. J.; Habib, A.; Kim, Y.; Nikolskaia, O.; Fukuma T.; Tabata, M. *Chem.-Biol. Interact.*, **2004**, *148*, 19–25; (e) Connor, E. E. Mwamuka, J.; Gole, A.; Murphy C. J.; Wyatt, M. D. *Small*, **2005**, *1*, 325–327.
- [4] Block W. D.; Knapp E. L. *J. Pharm. Exp. Therap.*, **1945**, *83*, 275–278.
- [5] Jou, M. J.; Chen, X.; Swamy, K. M. K.; Kim, H. N.; Kim, H. J.; Lee, S. G.; Yoon, J. *Chem. Commun.* **2009**, 7218–7220.
- [6] Yang, Y. K.; Lee, S.; Tae, J. *Org. Lett.* **2009**, *11*, 5610–5613.
- [7] Egorova, O. A.; Seo, H.; Chatterjee, A.; Ahn, K. H. *Org. Lett.* **2010**, *12*, 401–403.
- [8] Yuan, L.; Lin, W.; Yang, Y.; Song, J. *Chem. Commun.* **2011**, *47*, 4703–4705.
- [9] Cao, X.; Lin, W.; Ding Y. *Chem. Eur. J.* **2011**, *17*, 9066–9069.
- [10] Do, J. H.; Kim, H. N.; Yoon, J.; Kim, J. S.; Kim, H. J. *Org. Lett.* **2010**, *12*, 932–934.
- [11] Park, J. E.; Choi, M. G.; Chang, S.-K. *Inorg. Chem.* **2012**, *51*, 2880–2884.
- [12] Dong, M.; Wang, Y. W.; Peng, Y. *Org. Lett.* **2010**, *12*, 5310–5313.
- [13] Wang, J. B.; Wu, Q. Q.; Min, Y. Z.; Liu Y. Z.; Song, Q. H. *Chem. Commun.* **2012**, *48*, 744–746.
- [14] Wang, J.; Lin, W.; Yuan, L.; Song, J.; Gao, W. *Chem. Commun.* **2011**, *47*, 12506–12508.

-
- [15] Yang, Y.; Yin, C.; Huo, F.; Chao J. *RSC Adv.* **2013**, *3*, 9637–9640.
- [16] Kim, J.-H.; Jeong, Y.-H.; Yoon, H.-J.; Tran, H.; Campos, L. M.; Jang, W.-D. *Chem. Commun.* **2014**, *50*, 11500–11503.
- [17] (a) Zhu, Y.; Yu, B. *Angew. Chem. Int. Ed.* **2011**, *50*, 8329–8332; (b) Marchal, E.; Uriac, P.; Legouin, B.; Toupet L.; van de Weghe, P. *Tetrahedron*, **2007**, *63*, 9979–9990.
- [18] (a) Thielbeer F. *Synlett*, **2012**, *23*, 1703–1704; (b) McQueen, P. D.; Sagoo, S.; Yao H.; Jockusch, R. A. *Angew. Chem. Int. Ed.* **2010**, *49*, 9193–9196.